"Anthrapyrazole Cysteinyl Peptides as Inhibitors of AP-1 Transcription Factor Binding"

By Phuong My Tran

Thesis submitted to De Montfort University for
the degree of Doctor of Philosophy, October 1998.

Contents

List of Figures and Tables.

The work reported in this thesis is original except where due reference is made and has not been submitted in whole or in part for any other degree at De Montfort University or other institute of higher education.

Phuong Tran

Abbreviations

The abbreviations used for amino acids and peptides are those recommended by the IUPAC-IUB Commission on Biochemical Nomenclature (*J. Biol. Chem.*, 1972, **247**, 977).

Å	Ångström
AP-1	Activator protein - 1
APZ	Anthrapyrazole
ATF	Activating transcription factor
ASV	Avian sarcoma virus
Boc	*tert*-Butoxycarbonyl
BZLF	EBV immediate early protein
bZIP	Basic region leucine zipper
°C	Celsius
cAMP	Cyclic adenosine monophosphate
C/EBP	CAAT/enhancer binding protein
CRE	cAMP responsive element
CREB	CRE-binding protein
COSY	Correlation spectroscopy
CPC1	Cross pathway control protein 1
2D	Two dimensional
DIEA	Diisopropylethylamine
DMF	Dimethylformamide
DNA	Deoxyribonuleic acid
EBV	Epstein barr virus
EDT	1,2-Ethanedithiol
EMSA	Electrophoretic mobility shift assay
FAB	Fast atom bombardment
Fmoc	9-Fluorenylmethoxycarbonyl
GCN4	General control protein 4 (yeast)
HBP	Histone DNA-binding protein
HPLC	High performance liquid chromatography
hr	Hour
IR	Infra red
lzip	Leucine zipper
M	Molar
MALDI	Matrix assisted laser desorption ionisation
min	Minute
mM	Milimolar
MS	Mass spectrometry
Mtr	4-Methoxy-2,3,6-trimethylbenzene-sulfonyl
NADP	Nicotinamide adenine dinucleotide phosphate
nm	Nanometer
NMR	Nuclear magnetic resonance
NOESY	Nuclear overhauser enhancement spectroscopy

Abbreviations continued.

O2	Opaque 2
PKA	Protein kinase C
Pmc	2,2,5,7,8-Pentamethylchroman-6-sulphonyl
PyBOP	Benzotrizolyloxy-tris(pyrrolidino)-phosphonium hexafluoro-phosphate
Ref-1	Redox factor
RNA	Ribonucleic acid
SPPS	Solid phase peptide synthesis
TFA	Trifluoroacetic acid
TGA	TGACG-sequence specific binding proteins
TIS	Triisopropylsilane
Tm	Melting point of DNA
TPA	12-*O*-Tetradecanoyl-phorbol-13-acetate
TRE	TPA responsive element
Trt	Trityl
v/v	Volume for volume
w/v	Weight for volume
YAP1	Yeast AP-1 binding factor

Nomenclature for Amino Acids

The protein codes used in this thesis are those from the IUPAC definitions. These are summarised below. 'X' is frequently used in a consensus or the definition of a motif and refers to any amino acids.

Codes for amino acids.		
A	Ala	Alanine
C	Cys	Cystine
D	Asp	Aspartic acid
E	Glu	Glutamic acid
F	Phe	Phenylalanine
G	Gly	Glycine
H	His	Histidine
I	Ile	Isoleucine
K	Lys	Lysine
L	Leu	Leucine
M	Met	Methionine
N	Asn	Asparagine
P	Pro	Proline
Q	Gln	Glutamine
R	Arg	Arginine
S	Ser	Serine
T	Thr	Threonine
V	Val	Valine
W	Trp	Tryptophan
Y	Tyr	Tyrosine
X		Any amino acid

Anthrapyrazole Cysteinly Peptides as Inhibitor of AP-1 Transcription Factor Binding.

Phuong Tran.

Abstract

Synthesis of peptides anchored to DNA by intercalating chromophores can incorporate the design principle of the naturally occurring peptide based antibiotics. This work is concerned with the synthesis of DNA anchored cysteinyl peptides designed to be potentially nucleotide sequence specific with possible affinity for the AP-1 transcription site. Previous work has shown that anthraquinones and anthrapyrazoles (APZs) substituted with cationic side groups are excellent DNA intercalating agents. In this work a series of APZ analogues has been synthesised which are coupled onto the amino terminus of varying peptide sequences. Three derivatives of APZs were prepared namely 2-, 2,5- and 2,7-substituted. Eight short polypeptides (see below), all varying slightly in sequence but all containing the KCR motif (with one exception where a Cys was replaced with Ser) were combined with the APZ chromophore to give a series of intercalator-peptide molecules. Peptides were synthesised using the Fmoc strategy on a solid phase peptide synthesizer (SPPS). The peptides were then isolated by reversed-phase HPLC using a water:acetonitrile gradient. Characterisation of the peptides was carried out by matrix assisted laser desorption ionisation (MALDI) mass spectrometry and two dimensional nmr (i.e. COSY and NOESY). Anthraquinone linked peptide ligands were also synthesised using similar synthetic routes, and tested for their activity. Coupling of the two components was achieved via activation of the carboxylic acid group using PyBOP or via formation of a reactive aziridinium ion. All intercalator-peptides prepared were examined for their DNA binding properties. The methods included the effect of intercalator-peptides on the thermal denaturation of DNA and the competitive displacement of ethidium by fluorimetry. It was shown that the APZ binds to DNA by intercalation. Peptides prepared were: H_2N-A-K-C-R-A-CO_2H; H_2N-A-K-C-R-A-$CONH_2$; H_2N-A-K-S-R-A-$CONH_2$; H_2N-A-K-C-R-N-A-$CONH_2$; H_2N-A-K-C-R-K-A-$CONH_2$; H_2N-A-K-C-R-N-R-A-$CONH_2$; H_2N-A-K-C-R-K-R-A-$CONH_2$; H_2N-A-A-K-C-R-A-A-$CONH_2$. The biological activities of the intercalator-peptides were then investigated using an electrophoretic mobility shift assay (EMSA), making use of cell nuclear extracts rich in AP-1 and also c-Jun homodimer recombinant proteins. It was shown that most of the intercalator-peptides were capable of inhibiting AP-1 (fos/jun) heterodimer protein from binding to the AP-1 DNA consensus sequence. Importantly, the intercalator-peptides showed superior activity over the intercalator or peptide moieties alone. The order of binding affinity was intercalator-peptide > intercalator >> peptide.

Acknowledgments

I wish to express my thanks to my supervisors, Dr. P. H. Teesdale-Spittle and Professor L. H. Patterson for their continual advice, guidance and encouragement throughout the course of this work. I also wish to thank Professor F. S. Guzeic (New Mexico State University), Dr. L. Mur (University of Leicester), Professor J. Draper (University of Leicester) and Ketan Ruparelia (De Montfort University) for their advice and contribution to this work.

I also wish to thank the technical staff for their assistance. Thanks also to my post graduate colleagues for their friendship over the three years. I also wish to thank my parents for their patience, encouragement and interest throughout the duration of this work.

I wish to express my gratitude to De Montfort University for financial support for the duration of this study.

Chapter 1

Introduction

The principle goal of this investigation is the inhibition of transcription factor binding by intercalator-peptide complexes. The introduction to this thesis focuses on transcription factors mainly concentrating on the bZIP proteins, particularly the AP-1 protein, and the mechanism by which they interact with DNA. A brief description of the transcription process is also provided, since this is the underlying process which we hope to selectively inhibit.

1.1 DNA-Binding Proteins and the Process of Protein:DNA Recognition.

Proteins are associated with many biological processes involving the recognition and manipulation of DNA. These processes include maintenance of the structure of chromatin (whether transcriptionally active or inactive), DNA replication, transcription, and the control of DNA replication and transcription. More specifically we can identify a variety of biological activities that DNA binding proteins are involved in. Classified by their biological activity, DNA binding proteins include; isomerases, nucleases, ligases, primases, helicases, gyrases, integrases (for viral and transposon integration), DNA repair enzymes (glycosylases), polymerases, exo/endonucleases, DNA packing proteins (e.g. histones), chromosomal attachment proteins (e.g. membrane attachment, nuclear spindle attachment), recombinases and both positive and negative transcription factors.

Consideration of all these classes is beyond the scope of this work, thus attention is restricted to transcription factors, especially fos/jun, which are required for the accurate and controlled expression of genes.

Many transcription factors share common protein sequence motifs. As these are small motifs shared between otherwise different DNA binding factors, these motifs convey a role common to these proteins. They can be DNA recognition elements, multimerisation elements, transcriptional activation motifs or other protein:protein interaction motifs. The common ground for most DNA binding associated motifs is that they are involved in the association of nuclear factors (some motifs might be involved in binding co-factors or in protein modification (e.g. phosphorylation, glycosylation)).

1.1.1 General Biology of Transcription Factors.

The transcription process uses a variety of proteins besides the RNA polymerases itself, in particular the *transcription factors*. Broadly speaking we can divide transcription factors into *activators* (which "activate" or promote transcription) and *repressors* (which repress or inhibit transcription). Activators and repressors can respond to the changes in the cellular "state" (e.g. the concentration of

chemicals and proteins within and around the cell) in various ways, enabling the formation of feedback loops. Both positive (increased transcription in response to the stimulus) and negative (decreased transcription in response to the stimulus) control is possible. More complex competing schemes are also commonplace. Combinatorial control of gene expression is also present, as are "cascades" of transcriptional control (for example those used in dividing the cells into developmental categories). Activation of a transcription factor can result in "committing" the cell to a particular state.

Transcription factors provide a means of converting a "signal" into a change in gene expression. The original signal (nutrients, toxins, other metabolic products) can be extracellular or intracellular. Extracellular signals include the steroid and thyroid hormones, which activate gene expression by binding to a membrane-bound receptor, which in turn initiates a signal transduction pathway that ultimately results in altered gene expression. Intracellular signals include feedback from biosynthetic pathways and other cellular events.

Autoregulation is commonly observed in transcription factors; some proteins bind to control regions in their own genes either activating or repressing their own synthesis (for a review see Serfling, 1989). This can provide tight feedback on a gene's expression and allow a brief burst of expression following an initial stimulation (e.g. in the Jun/Fos family of proteins). Alternatively a basal level of expression of a gene can be maintained by autorepression (one way a higher level of expression could be invoked is by a protein binding onto the repression site, derepressing the expression of the original transcription factor).

The complexity of gene regulation can be appreciated when one thinks of a single gene being controlled by several (upstream) control elements which are the binding sites for various transcription factors. The several transcription factors can all, simultaneously, affect the gene, furthermore their actions on the gene are often not independent; they might act cooperatively or antagonistically.

1.1.2. Recognition of DNA by Proteins.

There are two motifs associated with transcription factors, the leucine zipper (lzip) and CC/HH zinc finger motifs. The leucine zipper (lzip), associated with the Jun and Fos proteins, is a portion of the bZIP motif, which is composed of a 'basic region' immediately followed by the leucine zipper motif. The basic region is the protein:DNA interaction motif; the leucine zipper is a dimerisation motif involved in the formation of homo- and heterodimers of this family of transcription factors. The monomers are unable to bind DNA. Different homo- and heterodimers can form, possibly allowing complex gene regulation mechanisms to develop. The bZIP proteins are reviewed in more detail later in this chapter. Before this, an outline of DNA recognition by DNA binding proteins and resulting conformational rearrangements is presented.

DNA binding motifs can be viewed from a variety of perspectives (reviewed in Steitz, 1990; Freemont *et al*, 1991; von Hippel and Berg, 1989; Schlief, 1988). Thus binding can be considered at the level of motif recognition of DNA - both its target and non-target DNA. The reorganisation of both protein and DNA structure on forming the complex can be investigated, as well as the role of these alternations in recognition of the desired target site and the function of the complex.

There are two main components in site-specific recognition of DNA by proteins; (a) direct hydrogen bonding and van der Waals interactions with the edges of the bases and (b) the sequence-dependent conformation and flexibility of the DNA (Steitz, 1990). Proteins recognise DNA much in the way that they recognise other proteins; the basic principles are the same (e.g. Johnson and McKnight, 1989).

1.1.2.1 DNA Conformational Changes upon Binding and in Recognition.

The details of DNA conformations will not be discussed here, as there are numerous reviews on this subject (e.g. Seanger, 1984). More pertinent to this work are the conformational changes in DNA as part of the recognition and

binding process. This has been well reviewed see: Travers, 1988, 1989, 1990; Widom, 1985.

An additional level of recognition is the sequence dependent conformation of the DNA, as well as deformations of the conformation of both the DNA and the protein from their uncomplexed structures in solution. Steitz (1990) notes that (a) proteins often bind DNA in a conformation that is different from the conformation observed in solution and (b) different DNA sequences have different free energies for distortions in the manner required for binding of a particular protein. Broadly speaking, the DNA conformation can be altered in two ways:

-a locally-induced change caused by the "binding unit" (e.g. local twisting or kinking of the DNA).

-a globally-induced change caused via the association of two (or more) different binding units. The protein complex need not be homomeric.

(The term "binding unit" - is used to mean the smallest protein unit(s) that is able to form a stable DNA complex on its own). An example of a local induced change is the CAP repressor, which bends the DNA by about 90° upon binding. The Lac repressor system is an example of a globally induced change.

One could postulate a two step scheme for recognising an altered conformation of DNA where in the first step the protein binds loosely to the DNA, electrostatically trying to bend the DNA to roughly the conformation it desires. Most sequences will not be able to bind the protein appropriately within the energy limits of the positive interactions (e.g. hydrogen bonds) provided. For these sites the protein will then either fall off or "slide" to an adjacent site (note this step is a thermodynamic process). A second step occurs if the DNA is able to take up the appropriate conformation; a closer interaction forms which "tests" the exact sequence of the site. If the protein is capable of sliding, this interaction will arrest the sliding. If the protein has no particular specificity it can continue to slide. We could also consider alterations in protein conformation on DNA binding in the same manner, since protein conformation is also part of

the process. In this way protein-DNA binding is a balance between conformational isomerisation and association energies.

1.1.2.2 Protein Conformation Changes upon Binding and in Recognition.

As indicated above, proteins can also be altered on DNA binding (see Freemont *et al*, 1991). In particular, regions which are flexible in solution can become ordered in the DNA bound complex. This might be more true of proteins which are able to slide along the DNA, or otherwise non-specifically recognise DNA. Just as DNA distortions cost energy, so do protein alterations in conformation. So both DNA and protein "isomerisation" can contribute to DNA binding.

More attention has been paid recently to amino acids flanking the binding motif (see Freemont *et al*, 1991). These are often flexible in solution, but become structured upon interaction with the DNA and can play an important part in recognition. This can increase the affinity for certain sites, which can have important biological effects.

von Hippel and Berg (1989) suggest that DNA distortions can enhance specificity, whereas protein reorganisation/distortions will reduce specificity. Thus cooperative distortions from both the protein and DNA partners of the interaction are possible and could both contribute to the specificity of the interaction.

Cofactors can also be used to regulate the binding affinity of a protein. They can alter either the protein's geometry (through an allosteric rearrangement of the protein structure upon ligand binding) or the electrostatic nature of the protein.

1.1.2.3 Whole Proteins and Recognition of DNA.

Generally protein recognition of DNA can be divided into specific and non-specific. Proteins that recognise DNA non-specifically, recognise DNA in general, but do not favour any particular base sequence(s). This definition should be

viewed with some caution. Many so-called non-specific DNA-binding proteins that recognise structural features of the DNA can be *indirectly* sequence specific in that the conformation recognised can only be easily adopted by certain base sequences. In a sense this can be thought of as a shape complementary process. Non-specific single-stranded DNA binding proteins might be thought of as the most "pure" of non-specific DNA proteins in that they require neither global structure nor sequence.

Site-specific DNA binding proteins only bind DNA containing a specified target sequence or "site", or close variations thereof. Recognition of the sequence involves (usually direct) contact with the bases in their interaction with the DNA. These proteins go beyond recognising merely the shape of the DNA they interact with, and also recognise the *character* of the DNA surface. They still recognise the conformation of the DNA they bind, but additionally also recognise the base sequence. Many site specific DNA binding proteins are essentially unable to make stable interactions with non-target DNA (this is true of most of the transcription factors identified to date). Conversely, some site specific proteins are also able to recognise DNA non-specifically, in the process of "sliding" along DNA, scanning DNA for a binding site. All proteins that could be shown to "slide" along DNA must have some non-specific recognition component (Kim, 1983). EcoRI and EcoRV are good examples of this type of proteins.

Although the energies involved with specific recognition are small, the cost of an incorrect association is high. Inappropriate juxtaposition of atoms can result in an up to ~5 kcal/mole loss of energy in the association (see Tronrud *et al*, 1987; Fersht, 1987). Thus poorly matching sites are efficiently distinguished from correct binding sites (note this assumes that the DNA and the protein are unable to alter their conformation to recover from the inappropriate positioning of the atoms). In this way, we can view specificity as a kind of negative selection procedure. Loss of too many specific interactions quickly excludes a binding site from consideration.

1.1.3 Multimerisation of DNA Binding Proteins and DNA binding.

Many DNA binding proteins can associate with DNA only as dimers. This has the advantage that a smaller protein can recognise a large site (as in this case of homodimers) reducing the "genetic cost" of coding for proteins that can recognise large binding sites. The dimerisation process can also provide an additional level of control of binding affinity and specificity. Common dimerisation interfaces can increase the combinatorial power of a given set of DNA binding proteins, bringing together monomers of different binding affinities, specificities and biological functions. Differential splicing can be (and is) used to create different functional isoforms of DNA binding proteins.

The importance of dimerisation in generating a wider variety of transcriptional factors from common family of proteins has become clear from studies on the bZIP family of transcriptional activators (for a review see Jones, 1990). This family of proteins can form both homodimers and heterodimers within members of the family. In addition there are differentially spliced proteins with opposite roles; one product being an activator and the other a repressor. Interactions with the dimerisation region of these proteins have been observed with other families of DNA binding proteins. Clearly the combinatorial possibilities afforded by all these interactions is enormous (Ransone *et al*, 1990). These interactions are strengthened by the fact that the monomers are unable to bind specifically and certain members of the family are unable to homodimerise (and hence cannot bind DNA alone) (Kouzarides and Ziff, 1989). One possible advantage is fast and efficient response to change in stimuli.

Protein binding sites on DNA are frequently symmetrical, and this symmetry is reflected in the bound complex; the proteins from dimeric or tetrameric associations (Gentz *et al*, 1989; Pu and Struhl, 1991). Most often these higher-order protein units are homodimeric (Laughton, 1991), but, as indicated above, heteromeric units are also known (O'Shea *et al*, 1989b). One advantage of this is to create a larger binding surface than found in a smaller protein. Dimers can bind better than the two monomers separately; part of this effect is probably due

to the favourable energy change upon dimerisation and on binding of the protein specifically to the DNA sequence (Weiss, 1990).

Dimerisation can occur either in solution (Saudek *et al*, 1991a) (usually in this case dimerisation is required for DNA binding) or once on the DNA (i.e. bound monomers associate once on the DNA) (Saudek *et al*, 1991b). An example of the former are the bZIP proteins, typified by the Jun and Fos proteins. The latter has been shown to be the case for the LexA repressor (Kim and Little, 1992), for example. The second monomer can have enhanced binding, or "cooperativity" due to the presence of the first monomer bound to one half-site, as is the case for the LexA protein.

1.1.4 Sequence-Specific DNA binding by Pseudopeptides.

Talanian *et al* (1992) have reported efforts to minimise the size of the GCN4 (a member of the bZIP family) while retaining sequence-specific DNA binding activity. They used three criteria to evaluate the shorter peptides: DNase I footprinting, NMR analysis, and stability measurements using CD spectroscopy. Their study shows that DNA binding activity of GCN4, containing only 20 residues from the basic region of the GCN4, is capable of binding DNA in a sequence-specific manner. Circular dichroism experiments suggest that specific binding involves only 15 residues in an ∝-helical conformation. Thus it appears that most or all of the GCN4 residues that make specific DNA contact lie within the 15-residue region from GCN4 residues 231 to 245 (see below). Further reduction in the number of residues and its effect on DNA recognition still remains to be explored.

PESSDPAAL**KRARNTEAARRSRAR**KLQRMKQ

1.2 bZIP Proteins.

Table 1 shows a list of some of the leucine zipper proteins known, the sub-family they belong in, and the sequence reference. In the interests of brevity literature citations for these sequences are not given in the text below.

Table 1: Leucine zipper proteins known to date

Family (if any)	Name	Species	Reference	Function/Features (putative)
	C/EBP (also known as EBP1)	rat	Landschulz *et al*, 1988a	Binds either CAATT or enhancer core sites. C/EBP is known to promote growth arrest and terminal differentiation in adipocyctes. C/EBP has also been suggested to be involved in the control of polysaccharide and carbohydrate metabolism.
Jun	c-Jun	human	Bohmann *et al*, 1987; Hattori *et al*, 1988	phorbol ester inducible, probably via the protein kinase C pathway; (signal transduction).
Jun	v-Jun	ASV17	Maki *et al*, 1987	"
Jun	Jun-B	mouse	Ryder *et al*, 1988	"
Jun	Jun-D	mouse	Ryder *et al*, 1989	"
Jun	c-Jun	mouse	Ryseck *et al*, 1988; Lamph *et al*, 1988	"
Jun	c-Jun	chicken	Nishimura and Vogt, 1988	"
Jun	c-Jun	rat		"
Fos	c-Fos	human	Van Straaten *et al*, 1983	serum responsive nuclear phosphoproteins, probably via protein kinase C pathway.
Fos	c-Fos	mouse	Van Beveren *et al*, 1983	"
Fos	c-Fos	rat	Curran *et al*, 1987	"
Fos	Fos-B	mouse	Zerial *et al*, 1989	"
Fos	c-Fos	chicken	Molders *et al*, 1987	"

Table 1 continued.

Family (if any)	Name	Species	Reference	Function (putative)
Fos	fra-1	rat	Cohen and Curran, 1988	serum responsive nuclear phosphoproteins, probably via protein kinase C pathway.
Fos	v-Fos	MuSV	Van Beveren *et al*, 1983	"
	BZLF1	EBV	Farrell, *et al*, 1989	Required for the switch from latent to productive infection.
	GCN4	yeast	Hinnebusch, 1986; Thireos *et al*, 1984	general control of amino acid biosynthesis
	cpc-1	N.crassa	Paluh *et al*, 1988	general control of amino acid biosynthesis
	cys-3	N.crassa	Fu *et al*, 1989	sulfur metabolism pathway control
	yAP1	yeast	Moye-Rowley *et al*, 1989	
	O2 (Opaque 2)	Zea mays (peas)		Opaque-2 locus zein regulatory gene
	HBP-1	wheat		transcriptional regulator
	OTF-2	mouse		wide variety of promoters and enhancers may determine B-cell specificity.
CREB	CRE-BP1	human	Maekawa *et al*, 1991	binds CRE; cAMP possible mediated enhancer.
CREB	CREB	human	Hoeffler *et al*, 1988	CRE binder, activated by cAMP, prob. via protein kinase A; may have a role in signal transduction pathway.
CREB	TGA1a	tobacco	Katagiri *et al*, 1989	root gene expression control; Possible transcriptional regulator CaMV 35S promoter. Possible analogue of HBP1
CREB	TGA1b	tobacco	Katagiri *et al*, 1989	Potential transcriptional regulator; CaMV 35S promoter. Possible analogue of HBP1
CREB	CREB	rat	Gonzalez *et al*, 1989	"

1.2.1 Binding Sites of bZIP Proteins.

In general these can be divided into two classes; the AP-1 sites and CRE (ATF) sites, which differ by a single base in the centre of the dyad (see table 2). Some proteins (e.g. GCN4) are able to bind to both AP-1 and CRE sites. The addition/loss of one base would cause a rotation of 34° and translation of about 3.4Å of the half-sites along the DNA principal axis. Studies suggest the protein, rather than the DNA, adapts to the different sites (Chothia, 1984; Chothia and Finkelstein, 1990).

Table 2: Some leucine zipper protein DNA sites

Site name	Site family	Binding site
AP-1	AP-1	TGAC-TCA
GCN4	AP-1	GTGAC-TCAC
CRE	CRE/ATF	TGACGTCA
HBP-1	CRE/ATF	ACGTCA
TGA-repeat	CRE/ATF	TGACGTGACG
SV40 enhancer	-	TGTGGAAAG
G-box	G-box	CCACGTGG

1.2.2 Subfamilies of bZIP Proteins.

This section has been used to elaborate on some of the biology of these proteins referred to in table 1 and some that have not been mentioned above.

The Jun family. Jun, like Fos (see below), was originally identified as a viral oncogene (Maki *et al*, 1987) and was one of the first oncogenes to be shown to be directly involved in transcription.

The mammalian transcription complex AP-1 has a consensus binding site (Vogt *et al*, 1987; Lee, 1987; Piette and Yaniv, 1987) very similar to that of GCN4, which suggested that a Jun-like protein might be the mammalian AP-1 complex. Several lines of evidence supported this theory. When anti-sera of two v-jun

peptides (Bos *et al*, 1988) were immunoblotted against AP-1, both anti-sera recognised a single major polypeptide species; c-Jun (Bohmann *et al*, 1987) and several tryptic peptides of the AP-1 complex were identical to the predicted sequence of v-jun. This was followed by the demonstration that Jun (expressed in *E.coli*) could bind to an AP-1 site (Bohmann *et al*, 1987).

Several cellular homologues to v-Jun have now been identified (see table 1) and more than one Jun-related protein has been identified in the AP-1 complex (e.g. Jun-B, Jun-D).

The Fos family. The viral forms of Fos are found in the FBJ and FBR murine sarcoma viruses (MSV or MuSV), where they are responsible for the induction of osteogenic sarcomas. Like v-Jun, v-Fos is rapidly and transiently stimulated by the presence of growth factors, including the tumour inducing phorbol esters (e.g. 12-*O*-tetradecanoyl-phorbol-13 acetate (TPA), for review see Jones, 1988).

The cellular and viral forms of Fos had long been suspected to be directly involved in transcription (Muller, 1986; Verma, 1986; Setoyama *et al*, 1986a, b; Sambucetti and Curran, 1986; Renz *et al*, 1987) and were later observed in a complex interacting with a fat-specific element of the promoter of the adipocyteprotein 2 (aP2) gene (Distel *et al*, 1987). An AP-1 site was found to be present in the aP2 promoter element (see above), suggesting Fos might, too, be part of the AP-1 complex. Fos was shown to bind (in a complex) to AP-1 sites (Rauscher *et al*, 1988a, b; Franza *et al*, 1988, Lucibello *et al*, 1988; Chui *et al*, 1988), *trans*-activate AP-1 dependent transcription (Schonthal *et al*, 1988; Lucibello *et al*, 1988; Sassone-Corsi *et al*, 1988a; Chiu *et al*, 1988) and also *trans* repress it's own (c-fos) promoter (Schonthal *et al*, 1988; Sassone-Corsi *et al*, 1988b).

v-Fos and c-Fos were known to be associated with a nuclear phosphoprotein complex termed p39 (Curran and Teich 1982; Curran *et al*, 1985; Franza *et al*, 1987), with a similar molecular mass to AP-1. This and Fos transcriptional

regulation of AP-1 transcription suggested that p39 and Jun/AP-1 were the same proteins, which was subsequently shown to be the case (Rauscher *et al*, 1988c; Sassone-Corsi *et al*, 1988a,b; Chiu *et al*, 1988).

GCN4. GCN4 regulates most of the amino acid biosynthetic pathways in the yeast *Saccharomyces cerevisae.* Amino acid starvation of almost any amino acid results in the synthesis of GCN4 which binds upstream of many amino acid biosynthesis genes, inducing their transcription (Hinnebusch, 1986). This is a 'general control' mechanism; (negative) feedback from any one of the pathways stimulates the whole collection of pathways via some common control mechanism (usually a transcription activator, as in this case).

The CREB family. These binds the c-AMP responsive element (CRE) whose consensus differs from the AP-1 consensus in having one more base pair in the centre of the dyad (see table 2). The first known member of this family was C/EBP. CRE-BP1, which shows strong similarity to other CREB proteins found, is unusual in that it contains a consensus CC/HH zinc finger at the amino terminus.

CREB proteins' function has been reviewed by Brindle and Montiminy (1992). The CREB family activate/repress gene expression in response to extracellular stimuli. A common secondary messager is cAMP, which can in turn activate cAMP-dependent protein kinase A (PKA). In mammals the best studied response to cAMP is via the control of CREs by CREB. PKA activates CREB via phosphorylation of Ser 133. This does not alter DNA binding affinity. The CREB subfamily differs from the ATF family in having a conserved phosphorylation/activation domain and a kinase inducible domain (the latter consists of consensus sites for a variety of protein kinases).

γAP1. The transcriptional activator γAP1 recognises an AP-1 site, but has an amino acid sequence strikingly at odds with other members of the family. At 650 amino acids long it is much longer than either Jun or GCN4 (figure 1 &

table 3), and the lzip is located at the N-terminal, rather than C-terminal end of the protein. In addition position *3d* of the proposed lzip is held by Asn rather than Leu residue. γAP1 appears to be essential for yeast AP-1 element-dependent transcription. However, it should be noted that *both* GCN4 and γAP1, among other proteins, are present in immunoblots of yeast AP-1 binding proteins.

Figure 1: Helical wheel diagram of GNC4 leucine zipper (Hope and Struhl, 1987), viewed down the helix axis.

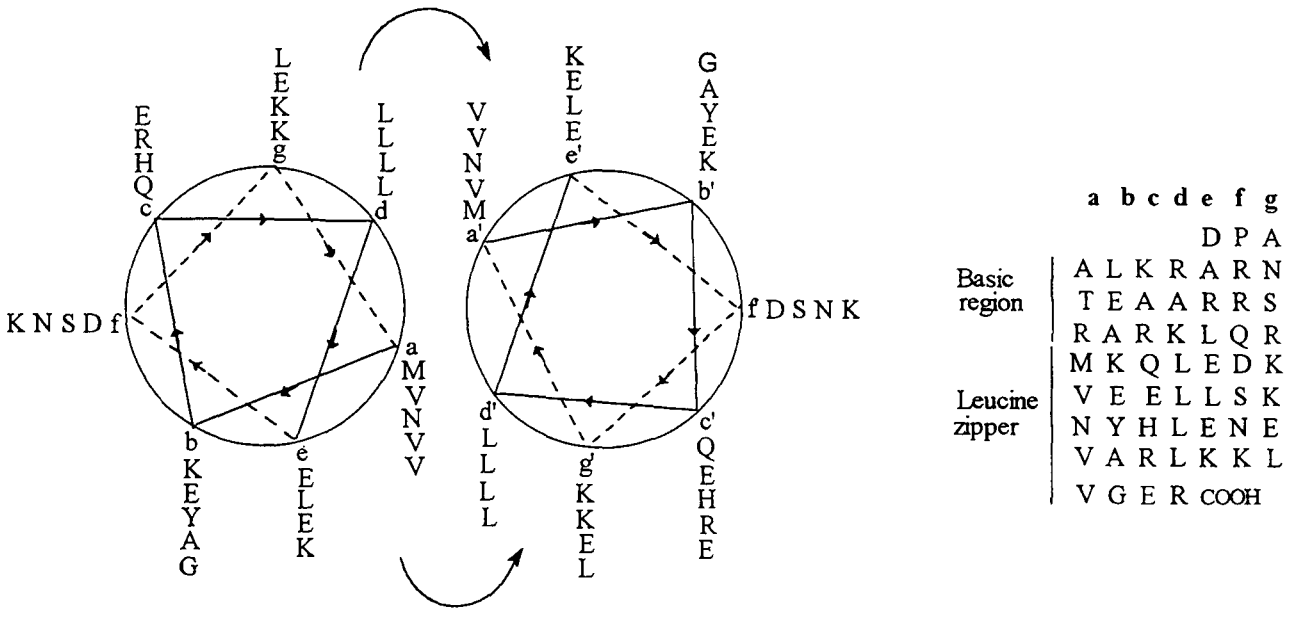

Table 3: Referring to positions in the leucine zipper

Heptad number	1	2	3	4	5
Position	*a b c d e f g*	*a b c d e f g*	*a b c d e f g*	*a b c d e f g*	*a b c d e f g*
Yeast GCN4	MKQ**L**EDKVE	H**LL**S KNYH**L**	ENEVAR**L**KKL	VGE	
human c-Jun	I AR**L**E EKVKT**L**	KAQN S E**L**	ASTANM**L**	REQVAQ	
Human c-Fos	T DT **L**QAETDQ**L**	EDE K S A**L**	QTEI AN**L**	LKE KEK	

CYS-3. The sulphur metabolic genes of *Neurospora crassa* (encoding for the enyzmes of the sulphur metabolism pathway) have two major regulatory genes; *cys-3* and *scon*, which are, respectively, activators and repressors of this set of genes. Cys-3 has been shown to have some similiarity to Fos and GCN4 in the bZIP regions of these proteins. The *2d* (table 3) position of the putative *cys*-3 leucine zipper is a methionine.

CPC-1. Another *N. crassa* protein, CPC-1, has a region with similarity to the DNA binding regions of GCN4 and v-Jun, which suggested that this protein was analogous to GCN4. CPC-1 is required for cross-pathway (i.e. general control) mediated regulation of amino acid biosynthesis, like GCN4, and is also transcriptionally regulated in response to amino acid starvation. However whereas yeast has a complex pathway leading to GCN4, so far in *N. crassa* only CPC-1 has been identified. CPC-1 has one of the most diverged of the lzips found thus far; only two of the *d* positions hold leucine. The *3d* and *4d* positions are Trp and His, respectively. The first heptad of the lzip is similar to GCN4's, but diverges after that. CPC1 contains a region rich in Gln, Thr and Pro, like Jun, but unlike GCN4. CPC1 cannot heterodimerise with GCN4, even though they are otherwise functionally equivalent.

BZLF1. Biochemical studies indicated BZLF1 had the functional characteristics of a bZIP protein, including dimerisation and binding an AP-1 site as a dimer. The sequence of BZLF1 was found to have a basic region, but (essentially) no leucine repeat. Only one of the *d* positions holds a Leu and two of the *a* positions have Leu.

1.2.3 The Role of bZIP Proteins.

Its has been considered that the bZIP proteins are the regulators of metabolic processes, but in a more general manner than envisaged by McKnight *et al* (1989). Most of the better characterised bZIP proteins are regulators of biosynthetic pathways (see table 1). Another common feature of these proteins is that they all act in response to extracellular stimuli. Those characterised are quick-acting, short-lived activators (or repressors). All these proteins share related target sites and general characteristics of activity.

Schena and Davis (1992) have suggested that the common molecular role of the bZIP proteins may be to mediate the transfer of an external (or possibly also intracellular, but extranuclear) signal to the nucleus and thus alter gene expression. However, its possible that these proteins may also transfer the signals

required to control metabolism into the intranuclear signals (activation, repression) required to control the genes that govern metabolism.

The Jun and Fos proteins are stimulated by growth factors implying that they are somehow involved in control of cell growth or differentiation. Recent work has illustrated the tissue and cell-cycle specifc expression of these proteins. Fos is activated in response to a very wide range of factors so Fos itself must have a very general function, such as activation of cellular growth, division or proliferation, etc.

1.3 Structure-Function Relationships in bZIP Proteins -
The Basic Region.

The basic region has been shown to be required for DNA binding by three lines of evidence: a. deletion mutagenesis, b. domain swops and c. point mutagenesis.

Deletion mutagenesis has shown that of the 281 amino acids in GCN4, the 60 carboxyl terminal amino acids containing the bZIP region are required and sufficient for DNA binding (Hope and Struhl, 1986; Vogt *et al*, 1987). GCN4 shows similarity to Jun, and this similarity is restricted to the carboxyl-terminal 70 amino acids of GCN4, which show 44% identity. In addition, functional similarity has been shown by domain exchange with v-Jun (Struhl, 1987). Here a modified (chimeric) GCN4 protein, with a Jun bZIP region was shown to bind the same site as GCN4, and be functionally similar *in vivo*. Likewise, a Lex A-Jun fusion protein can replace GCN4 in an apparently fully functional manner. This work strongly suggests that the structure of this region is similar in Jun and GCN4. Furthermore, a fusion protein with the proposed GCN4 DNA binding region substituted with the corresponding region from Jun (a Lex A-GCN4-Jun construct) functioned *in vivo* as a GCN4 analogue. More direct 'domain swop' experiments have been done since, and convincingly show that the basic and lzip regions can functionally replace one another (Cohen and Curran, 1990; Ransone *et al*, 1990).

Mutations that alter the basic domain affect DNA binding (see Neuberg *et al*, 1989). A single basic to Glu substitution (Gentz *et al*, 1989) abolished DNA binding. Gentz *et al* (1989) found deletions within the basic region affected DNA binding but not dimerisation. A single R→K substitution within the basic region of opaque-2 was able to abolish DNA binding (Aukerman *et al*, 1991).

Pu and Struhl (1991) have shown that a seven amino acid insertion between the basic and lzip regions of GCN4 preserves function, whereas 2, 4 and 6 amino acid insertions eliminate function. This shows that the phase of the basic region with respect to the lzip region is important for DNA binding.

1.3.1 Dimerisation is Required for DNA Binding.

Hope and Struhl (1987) used the band-shift assay to show that GCN4 is bound to its target site as a dimer. This method has been taken up by other authors to illustrate some of the features of the bZIP proteins: That they all bind their target sites as dimers, that a functional lzip is required for this dimerisation, and that this leucine zipper mediated dimerisation in turn is required for DNA binding. Using the band-shift assay, Hill *et al* (1986) demonstrated that the carboxyl terminal 60 amino acids of GCN4 alone can both dimerize and bind to DNA; the last 37 amino acids can only dimerise (see also Kouzarides and Ziff, 1989a), but not bind DNA, and that stable dimers form in the absence of DNA. The ability to form stable dimers in the absence of DNA is characteristic of these proteins, and strongly suggests they bind their target sites as a preformed dimer, as discussed in section 1.1.3. This is consistent with the monomers being unable to bind DNA.

1.3.2 The Lzip is Required for Dimerisation.

The lzip has been shown to be required for dimerisation by deletion and point mutagenesis. Several workers have found that only very short regions corresponding to the lzip are needed for wild-type dimerisation. Kouzarides and Ziff (1989a) have demonstrated that about 37 amino acids are required for heterodimerisation of Jun and Fos. Turner and Tjian (1989) also demonstrated

this using a protein cross-linking band shift assay, as did Landschulz *et al* (1989), using glutaraldehyde cross-linking, both in solution and bound to the target site. A detailed mutagenesis study can be found in Ransone *et al* (1989).

Gentz *et al* (1989) found replacement of individual Leu residue with Gly in Fos reduced, but did not block, dimerisation with Jun. Amino acid deletions within the lzip abolished dimerisation. Deletion within the basic region affected DNA binding but not dimerisation. Mutation of the three Ala's between the basic and lzip region reduced dimerisation and blocked DNA binding. One curious result was that the first 199 amino acids of Fos (which contains the complete lzip and 5 amino acids after the fifth Leu) could not bind DNA efficiently, suggesting a requirement for the conserved histidine 7 amino acids after the last Leu for efficient dimerisation.

1.3.3 The Basic and lzip Regions are Functionally Independent.

The basic and lzip regions of different proteins can be functionally exchanged (Struhl, 1987; Kouzarides and Ziff, 1988; Agre *et al*, 1989; O'Neil *et al*, 1990; Cohen and Curran, 1990), suggesting they are independent structurally and functionally. Some workers do note that the basic regions can be affected by adjacent sequences (Cohen and Curran, 1990; Kerpolla and Curran, 1991).

1.3.4 Homo- and Heterodimerisation of bZIP Proteins.

There have been many reports that Jun and Fos bind their target site either as a Jun-Fos heterodimer or a Jun homodimer (but never as a Fos homodimer; see section 1.2.2 above).

The Jun-Fos heterodimer forms in preference to a Jun homodimer (Nakabeppu *et al*, 1988; Turner and Tjian, 1989), and Fos is able to displace a Jun monomer from the homodimeric complex to form a Jun-Fos heterodimer (Nakabeppu *et al*, 1988). Likewise Fos can stabilise the Jun/AP1 association (Rauscher *et al*, 1988a). Elsewhere it has been shown that the major species present *in vivo* is the heterodimer. This raises the question of whether the Jun homodimer is

actually present and/or functional in the *in vivo* situation, but it is at least clear that in the presence of equimolar or excess Fos it is a minority species.

The Jun-Fos heterodimer has been shown to be very stable, capable of resisting high salt and detergent concentrations. This suggests that both hydrophilic and ionic interactions are crucial to the formation of dimers.

Various authors report little or no DNA binding of the Jun homodimer (Kouzarides and Ziff, 1988; Nakabeppu *et al*, 1988; Sassone-Corsi *et al*, 1988a, b) to the TPA-responsive element (TRE). This is likely to reflect the weaker and more stringent homodimerisation of Jun rather than a lack of DNA binding, as the Jun and Fos (and GCN4) basic regions have been shown to be functionally equivalent (it is known that the Jun basic regions are capable of binding to DNA strongly in proteins with the lzip substituted with either a Fos or GCN4 lzip). On the other hand weaker association might be expected to be more sensitive to the conditions used. Since Jun-Jun has been shown to efficiently form homodimers in solution (e.g. Turner and Tjian, 1989) and the basic regions of Jun and Fos are functionally equivalent, it would be expected that Jun might be capable of binding DNA, albeit at lower efficiency due to its lower degree of dimerisation.

The AP-1 and ATF/CREB families can form selective cross-family heterodimers (Hai and Curran, 1991). The DNA binding specificities of these heterodimers differ from the homodimers which they are derived from, and the different heterodimers show different DNA binding specificities. There seems to be an overall preference for the CRE, however.

Brindle and Montiminy (1992) report that ATF2, ATF3 and ATF4 can heterodimerise with Fos, Jun or Fra-1 *in vitro*. ATF1 would not heterodimerise with these proteins (Hai and Curran, 1991). Similarity Hoeffler *et al* (1991) found ATF2 could heterodimerise with either Fos or Jun, whereas CREB or

ATF1 could not. ATF1, but not ATF2 has been shown to heterodimerise with CREB both *in vitro* and *in vivo* (Hurst *et al*, 1990).

1.3.5 The Lzip Determines which Dimers are present.

Different lzips have differing affinities to associate as dimers with one-another. This raises the suggestion that the role of the lzip is to determine the dimer species available at any one time. This could affect either the DNA binding specificity of these dimers (via the different DNA binding abilities of the DNA binding regions) or other functions associated with the proteins, or both.

Kouzarides and Ziff (1988) analysed the relative contributions of the basic and lzip regions to DNA binding by domain exchange experiments, using Jun, Fos and GCN4. They constructed chimeric proteins with either the lzip or basic region domains swopped with those of one of the other two proteins used, and assayed the dimerisation and DNA activity of these chimeras. The Jun, Fos and GCN4 basic regions appear to be functionally equivalent; it is the differing dimerisation capacities of the different lzips that determine the relative affinities of the interactions with the TRE. They drew two conclusions:

i) The dimerisation abilities of the chimeric proteins are a reflection of the dimerisation ability of the protein the lzip concerned came from.

ii) An argument to explain the relative affinity of a lzip protein to its site is that the strength of the dimerisation determines the concentration of available dimers in solution. By controlling the amount of complexes able to bind DNA, the lzip determines the amount of DNA binding activity.

Other workers have found similar results. O'Shea *et al* (1989b) calculate that their Jun-Fos leucine zipper-based peptide heterodimer forms over 1000-fold preferentially to the Jun-based peptide homodimer. This parallels reasonably well with the >10-100 fold stronger binding of Jun-Fos to the same site as to Jun-Jun (Halazonetis *et al*, 1988; Kouzarides and Ziff, 1988; Nakabeppu *et al*, 1988; Sassone-Corsi *et al*, 1988a). Neuberg *et al* (1989) found that more than a one thousand-fold increase in the concentration of random oligonucleotide was required to abolish the band-shift of the Jun-Fos complex over that of Jun-Jun.

They observe that the ability of a dimer to bind to DNA correlates well with its ability to dimerise.

There are several members of the Fos and Jun family from the same organism, and it is known from experimental studies that several different related protein species are found in the AP-1 complex. The distinct dimerisation capacities of the different monomers may control the types of complexes that can associate, and hence bind DNA and thus control gene expression in some way. That is, while the general rules of what monomers could associate would remain the same (e.g. any Jun can dimerise with any Fos), the actual *affinities* of each monomer for the others would slightly vary, controlling the relative amounts of each complex available to bind DNA.

1.4 Activation of the AP-1 Protein by a Redox Mechanism.

It has been demonstrated (Abate *et al*, 1990a, b) that the *in vitro* DNA-binding activity of Fos and Jun is regulated by a redox mechanism involving a cysteine residue located at the basic region of both protein monomers. The biochemical attributes of Cys residues are often essential for functional and structural properties of proteins (Xanthoudakis and Curran, 1992a). Indeed, their presence and relative distribution are often used to define characteristic protein domains such as the zinc finger (Berg, 1990). For these reasons, Cys residues are often conserved across phylogenetic boundaries and among gene families.

A highly conserved Cys residue, flanked by two invariant basic amino acids, lysine-cysteine-arginine (KCR), is present in the DNA binding domain of the Fos and Jun family members. As well as facilitating DNA base contact it is likely that the positively charged lysine and arginine residues increase the oxidisability of the cysteine making it more susceptible to redox control (Abate *et al*, 1990a; Xanthoudakis *et al*, 1992b), hence, the oxidation constant (K_{ox}) of a sulfhydryl group is influenced by its local environment and is subject to change caused by alterations in protein conformation. However, this residue does not participate in disulfide bond formation between Fos and Jun *in vivo* and it is not part of a

zinc finger motif. In the proposed model of protein-DNA complexes involving basic region-leucine zipper proteins, the Cys is in close proximity to DNA, and as mentioned before this regulatory cysteine acts as a "sulfhydryl switch" that reversibly modulates binding of Fos and Jun to the AP-1 site. The exact chemical nature of the redox change in Fos and Jun has yet to be defined, but it is clear that oxidation of the Cys is not permissive for DNA binding, while reduction to a sulfhydryl state promotes the protein-DNA interaction. It is suggested that DNA binding of Fos/Jun is prevented by conversion of the critical cysteine residue (Fos-C154 and Jun-C272) of the KCR motif to the reversible oxidation products sulphenic (RSOH) or sulphonic (RSO_2H) acids, as in Oxy R proteins.

Furthermore, DNA-binding activity of Fos and Jun can be enhanced or permanently activated by mutation of Cys to Ser (Fos-C154S and Jun-C262S) or by treatment with high concentrations of reducing agents. This is indicative of the significant role of the cysteine residue in redox binding regulation.

1.4.1 Ref-1 a Ubiquitous Nuclear Protein.

A cellular nuclear protein can activate the DNA-binding activity of Fos and Jun in the absence of high levels of reducing agents. This protein does not appear to participate in the DNA-protein complex, and it does not affect the specificity of the interaction with DNA. These results suggest that a nuclear protein regulates the DNA-binding activity of Fos and Jun indirectly; perhaps by post-translational modification (Xanthoudakis and Curran, 1992c).

The activity of this nuclear factor, designated Ref-1 (Redox Factor-1) can be increased in the presence of thioredoxin, thioredoxin reductase and NADPH, implying that it may participate in a redox cycle by acting as an electron donor for AP-1 proteins (Xanthoudakis *et al*, 1992a, b). It is possible that the AP-1 redox signaling pathway comprises several components that are responsible for reducing Ref-1. Whether thioredoxin itself acts to regenerate active Ref-1 *in vivo* is not known, but it is clear that thioredoxin alone, as well as glutathione and glutathione transferase, failed to substitute for Ref-1 activity *in vitro*. This

protein, Ref-1 (a 37kDa protein), is identical to the human apurinic-apyrimidinic endonuclease HAP1 (Xanthoudakis *et al*, 1992b). Ref-1 is therefore a bifunctional protein possessing AP-1 redox and DNA repair activities (Xanthoudakis *et al*, 1994). Biochemical characterisation has revealed that only reduced Ref-1 is capable of stimulating Fos-Jun binding activity, whereas either reduced or oxidised Ref-1 functions as a endonuclease.

So to summarise, maintenance of the cysteinyl residue in a reduced and therefore DNA binding state is mediated by Ref-1 which is elevated when hypoxia is induced (Ausserer *et al*, 1994). The importance of Ref-1 in control of AP-1 binding is evident from hypoxia induced transcription of Ref-1 mRNA and increased stability of Ref-1 protein (Yao *et al*, 1994). However other reducing agents including thioredoxin as well as small molecular weight thiols also promote AP-1 binding of Fos/Jun (Abate *et al*, 1990a; Xanthoudakis *et al*, 1992b).

1.5 3D Model(s) for DNA Binding bZIP Proteins.

Binding sites on DNA impose several constraints on the proteins that must recognise them: a. The DNA contact surface of a protein must be capable of penetrating either the major or minor groove (Oakley *et al*, 1992) of the DNA in order to interact with the functional groups that distinguish one binding site form another. b. Dyad-symmetric binding sites (Risse *et al*, 1989) further demand that the two contact surfaces of the binding protein be assembled so that they can simultaneously interact with both halves of the recognition site.

An evaluation of the properties of conserved amino acids within the basic region of these bZIP protein sequences, coupled with the observation that they are located at an invariant distance from the leucine zipper, has led to the formulation of the "scissors-grip" model for DNA binding (Vinson *et al*, 1989). The architectural features of this model are well suited for interaction with directly abutted, dyad-symmetric DNA sequences. This model proposes that two polypeptide chains join to form a Y-shaped molecule. The stem of the Y

corresponds to a coiled pair of α -helices. Therefore its proposed that the cleft of the Y would be the point where the protein contact the DNA-binding site at the center of the dyad. The two arms of the Y, representing the two basic regions, are then proposed to wrap around the DNA so as to sit in the major groove and contact the two half sites of the dyad. To achieve this, it is thought that a sharp kink would be necessary in the basic region helix, probably at the conserved asparagine residue and this would facilitate protein contacts with the outer bases of the binding site.

Although the scissors-grip model provides a plausible architectural scheme for stable interaction between protein and DNA (Neuberg *et al*, 1991), it raises the question as to how bZIP proteins engage and disengage from their substrates. A variation on this model was proposed after further peptide studies (circular dichroism and nmr) revealed that in solution the GCN4 bZIP domain was only 30-70% ∝-helical (Gartenberg, 1990), but became almost completely ∝-helical on binding to DNA (O'Neil *et al*, 1991). Studies on fos/jun peptides also indicated a conformational change on binding to DNA (Patel *et al*, 1990). Consequently, the Induced Helical Fork model was proposed whereby a partially helical conformation allows the protein to efficiently "search" the DNA before it interacts with the DNA-binding site producing a true α-helix stabilised by specific protein DNA contacts (O'Neil *et al*, 1991). Thus preferential stabilisation of the DNA-binding conformation provides an attractive mechanism for the regulation of DNA binding by bZIP proteins. It also appears that DNA recognition by bZIP proteins is a dynamic process that involves changes in both protein and DNA conformation (Suzuki *et al*, 1996). Whether sequence recognition depends on the formation of specific hydrogen bonds with functional groups on the bases (direct read-out) or on a particular helix geometry induced primarily by contacts with the phosphodiester backbone (indirect read-out) remains to be determined.

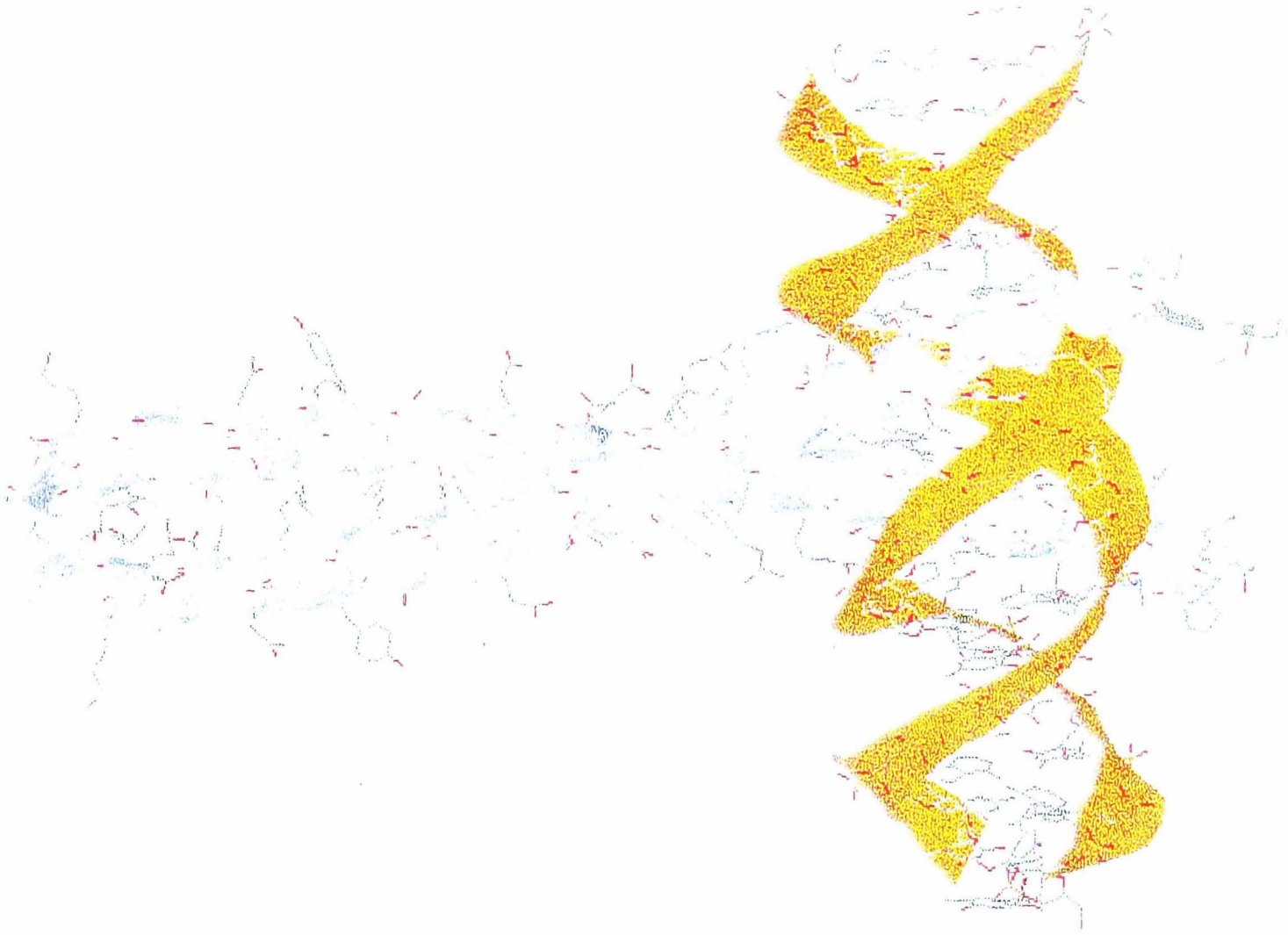

Figure 2: The Y-shaped scissors grip model for the GCN4 bound to the GTGACATCAC

1.6 Summary of the bZIP Proteins.

Cell growth and differentiation are controlled, to a large extent, through the selective regulation of gene expression by extracellular signals. In the past several years, a large number of sequence-specific DNA-binding proteins have been identified that function as regulators of gene transcription.

The product of two cellular proto-oncogenes, Fos and Jun (Talanian *et al*, 1990; 1992) (figure 3) appear to play a central role in the regulation of cell growth. They are thought to function in coupling short-term signals, elicited at the cell surface, to long-term changes in cellular phenotype by regulating expression of specific target genes. These proteins belong to a growing family of transcriptional regulators that include the cyclic AMP response element-binding protein (CREB) (Hoeffler *et al*, 1988), the yeast GNC4 protein (Hope and Struhl, 1987), and C/EBP enhancer-binding protein (Landschulz *et al*, 1988a). These transcriptional factors form dimeric complexes which recognise and bind to specific cognate DNA sequences.

Figure 3: Schematic diagram and nomenclature of protein domains.

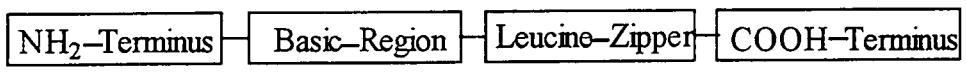

Jun	J_{1-255}	$J_{256-282}$	$J_{283-311}$	$J_{312-333}$	333 aa
Fos	F_{1-137}	$F_{138-164}$	$F_{194-380}$	$F_{194-380}$	380 aa

Two domains of these proteins are required for the combined functions of protein-protein and protein-DNA complex formation. The leucine zipper domain mediates protein dimerisation (Talanian *et al*, 1990) through the formation of parallel α-helical dimers as in the two-stranded coiled-coils of fibrous proteins (O'Shea *et al*, 1989a). The dimerisation interface in proteins consists of a 4-3 heptad repeat of hydrophobic amino acids that are almost exclusively leucines. Substitutions that change one or more of the residues in the leucine zipper can

abolish dimer formation and DNA binding; this demonstrates that dimerisation is required for DNA binding.

1.7. DNA Recognition by Hybrid Molecules -
Naturally Occuring Hybrid Molecules.

Nature provides examples of drugs whose binding to DNA simultaneously implicates various processes. Such is the case for actinomycin D, a natural antitumour agent which consists of a phenoxazone disubstituted with a cyclic pentapeptide. Intercalation of actinomycin (Takusagawa *et al*, 1982) occurs preferentially at some, but not at all, GpC sequences with the cyclic peptides fitting above and below the intercalating ring in the minor groove, each covering three base pairs.

Actinomycin D

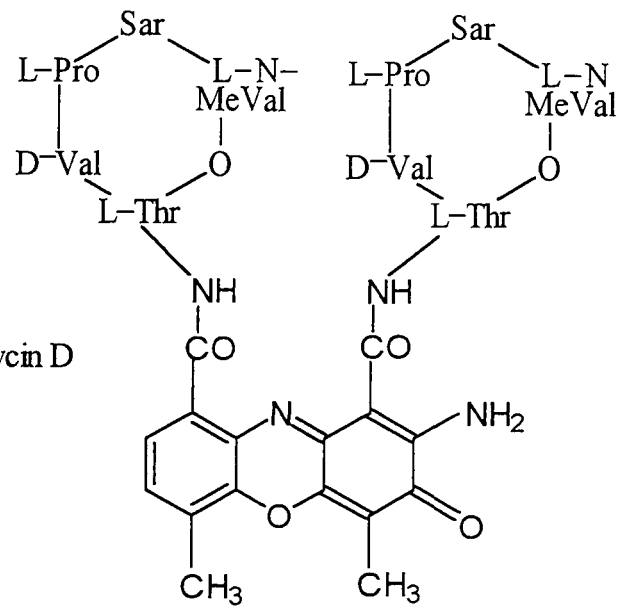

Other such bimodal binding process has been found in the intercalation with DNA of different natural antitumour anthracyclines, typified by daunorubicin (daunomycin) and doxorubicin (adriamycin).

X-ray diffraction analysis (Quigley *et al*, 1980; Frederick *et al*, 1990) has definitely demonstrated that while the chromophore intercalates CpG steps, the glycan moiety lies in the minor groove. The sugar forms several bonds with DNA and so greatly contributes to the stability of the complex.

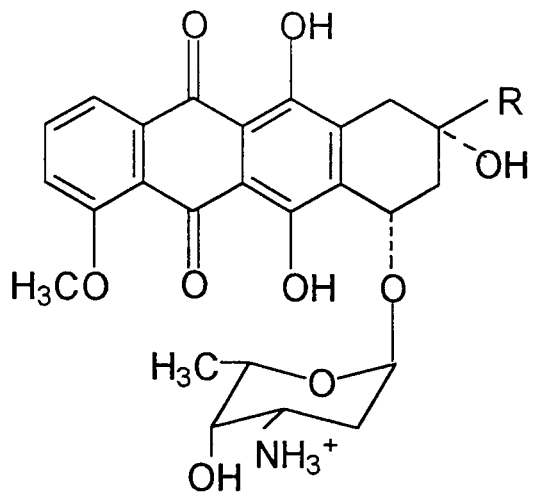

Daunorubicin R = $COCH_3$

Doxorubicin R = $COCH_2OH$

A considerable number of DNA-binding natural products contain carbohydrate residues that are likely to serve as DNA recognition elements. The molecular architecture is even more complicated with another natural anthracycline, nogalamycin, which differs from daunomycin and doxorubicin in that it contains two sugars moieties attached to the chromophore. The binding of nogalamycin to DNA consists of intercalation of the anthracycline ring and groove binding of the sugar moieties (Liaw *et al*, 1989). The nogalose is lying in the minor groove, and the positively charged aminoglucose is lying in the major groove, with the two sugars pointing on the same side of the aglycon ring.

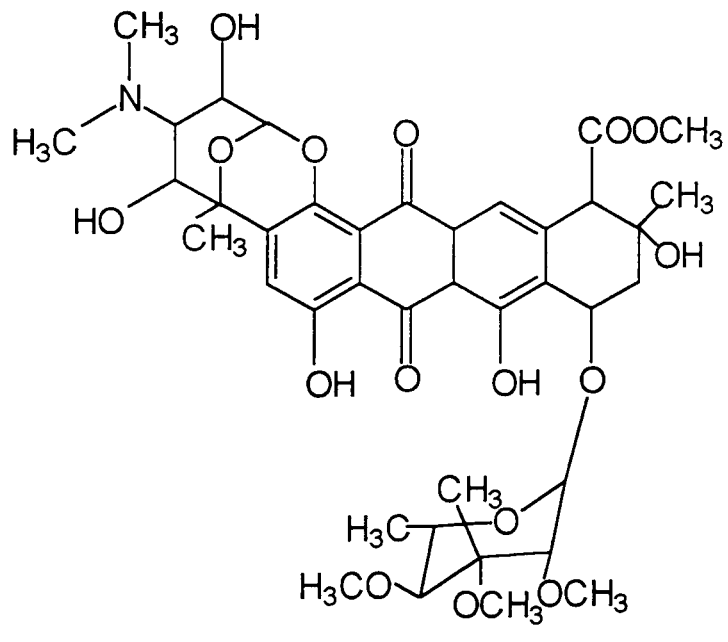

Nogalamycin

Other examples of natural drugs presenting these binding characteristics are the quinoxaline antibiotics. Quinoxaline antibiotics are a family of antitumour drugs, of which echinomycin is the best-known member, and in which two quinoxaline-2-carboylic acid chromophores are attached to a cross-bridged cyclic octapeptide dilactone containing both L- and D-amino acids. This group of compounds include triostin (Wang *et al*, 1984), which has the common properties with echinomycin (Ughetto *et al*, 1985) to bisintercalate with DNA placing the peptide ring into the minor groove.

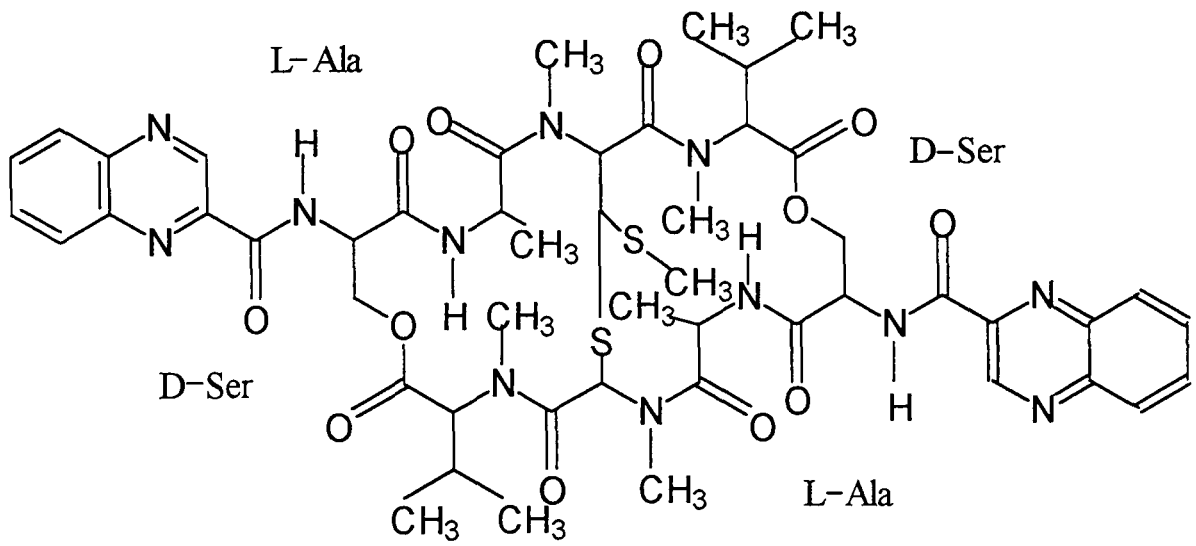

Echinomycin

Thus actinomycin, doxorubicin, daunomycin, nogalamycin, and the quinoxaline antibiotics are all examples of drugs whose binding to short DNA sequences implicates two processes, intercalation and groove-binding simultaneously and in close proximity. Both processes contribute to the affinity and sequence-specific recognition. All these natural compounds could provide models for the rational design of ligand exhibiting mixed modes of binding.

1.8 Aims

The purpose of this study is to investigate a minimalist approach to inhibition of redox sensitive transcription factors involved in malignant transformation and growth of tumour cells. This should assist the development of agents that are active specifically under reducing conditions and with specificity for the DNA binding domain of redox sensitive transcription factors.

The two main objectives are (a) to synthesise novel intercalator-cysteinyl peptides designed to interact with the DNA recognition sequence of redox sensitive proteins that bind to the AP-1 transcription site. It is anticipated that subsequent binding will inhibit binding of the relevant upregulating transcription factors and hence inhibit cell growth and promote cell death. (b) To correlate binding of the agents developed in (a) with the DNA binding domain of AP-1 using cell free nuclear extracts and then with free DNA constructs in binding assays.

In this work, the synthesis of Fos-Jun basic region-intercalator hybrid peptide (figure 4, see next page) will be described. This molecule has been designed to investigate the combination of minimum features of the peptide necessary for recognition of the consensus site with the known binding enhancement of an intercalating anthrapyrazole (APZ) moiety. In this way, it is hoped to achieve both tight binding and high degree of molecular recognition with a comparatively small peptide.

Chapter 2 of this thesis will be devoted to the synthesis of the anthrapyrazole derivatives. Chapter 3 will then discuss the synthesis, characterisation and isolation of the peptides. Chapter 4 will then outline the coupling of the intercalator (APZ) to the peptide sequence to yield the target hybrid ligand. Cell free biological evaluation of these hybrid ligands will be investigated in chapter 5. DNA binding assays will also be used in investigating the nature and the affinity of the binding.

Figure 4: Fos-Jun region-intercalator hybrid peptide construct.

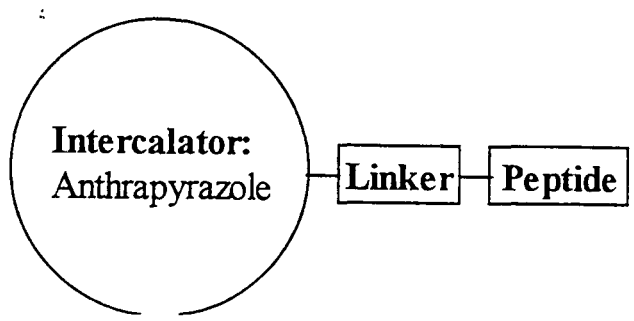

Intercalator = Anthraprazole

Linker = Alkylamines and alkylamides

Peptide = Short polypeptide containing the KCR motif:

H_2N-A-**K-C-R**-A-CO_2H; H_2N-A-**K-C-R**-A-$CONH_2$;

H_2N-A-**K-S-R**-A-$CONH_2$; H_2N-A-**K-C-R**-N-A-$CONH_2$;

H_2N-A-**K-C-R**-K-A-$CONH_2$; H_2N-A-**K-C-R**-N-R-A-

$CONH_2$; H_2N-A-**K-C-R**-K-R-A-$CONH_2$;H_2N-A-A-**K-C-R**-A-A-$CONH_2$.

Chapter 2

Synthesis of the Anthrapyrazole Derivatives

The first part of this Chapter outlines the Lerman model of intercalation. The synthesis of the different anthrapyrazole (APZ) intercalator derivatives are discussed together with the mechanisms for each reaction. The experimental procedure for the synthesis of the APZ derivatives can be found in chapter 6.

In this work a series of intercalators based on the anthrapyrazole compounds have been synthesised. It is important to begin this chapter by briefly describing the mechanisms underlying intercalation, and also the structural requirements for intercalating agents.

2.1 Lerman Model for Intercalation.

Lerman (1961) proposed that the planar aromatic proflavin molecule becomes inserted between adjacent base pairs of double helix of DNA (figure 5). The base pairs remain perpendicular to the helix axis, but they are moved apart, by 3.4Å, to accommodate the acridine molecule which lies in van der Waals contact between the base pairs. The intimate contact between the π-orbitals of the drug molecule and the base pairs would help to stabilise the complex via hydrophobic and charge-transfer forces. Local distortion of the helix occurs since it has to unwind in order to accommodate the drug molecule (Neidle *et al*, 1987). Distortion of the helix due to local unwinding at intercalation sites would destroy the long-range regularity of the helix, as observed by X-ray diffraction studies. Lerman (1961) proposed an unwinding angle of 45° in his original model which he subsequently revised to 36°.

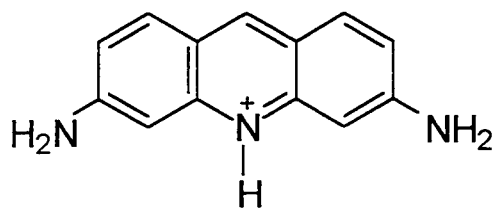

Proflavin

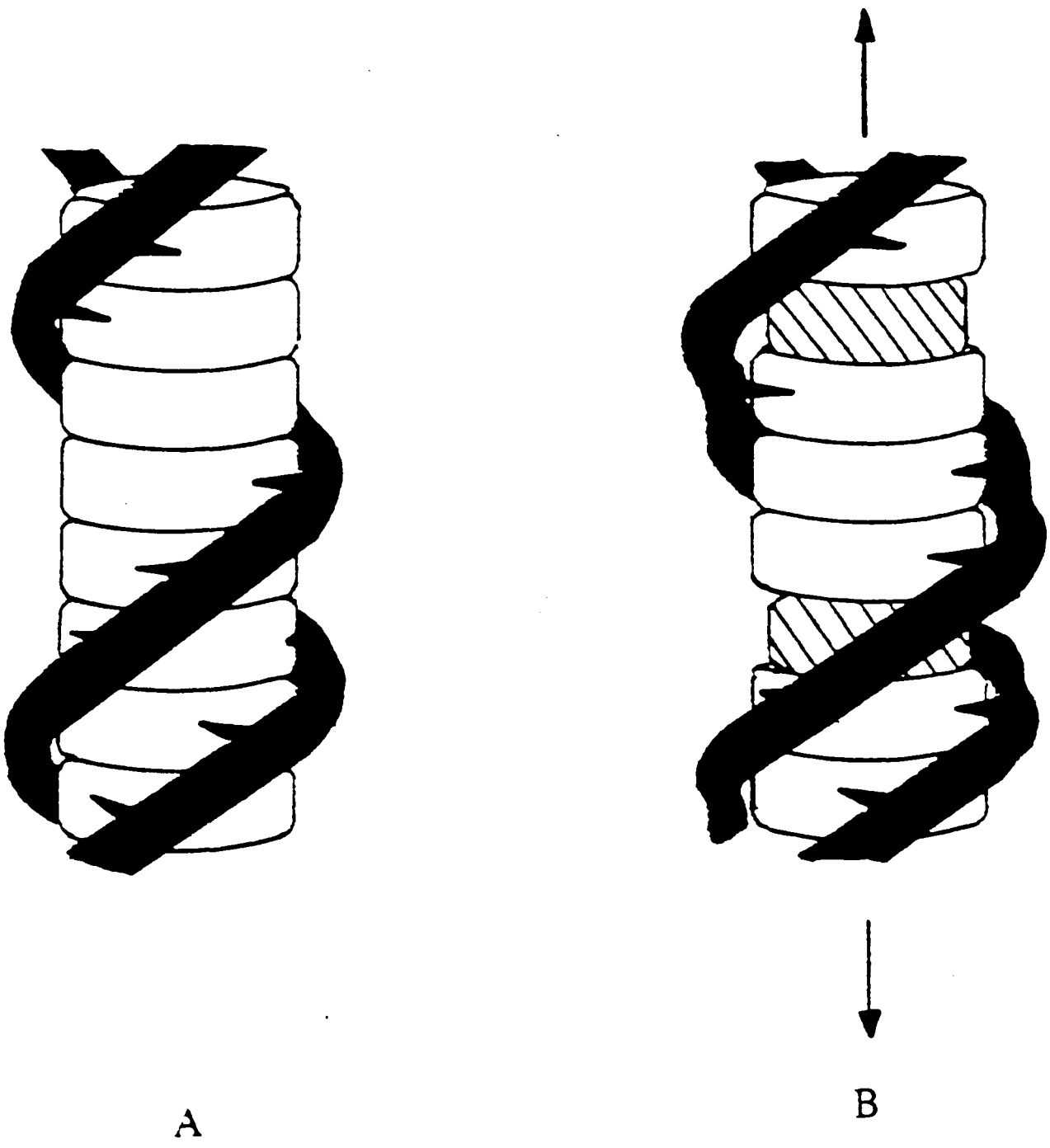

Figure 5: The Lerman intercalation model, in schematic form. (a) Illustrates the double-stranded DNA helix: (b) shows DNA with bound-drug molecules as shaded discs intercalated between base pairs, shown as unshaded discs.

2.1.1 Anthrapyrazoles as Intercalators.

The binding of various anthrapyrazoles to double stranded oligonucleotides, using computer assisted modelling techniques, indicate an intercalative mode of binding (Chen *et al*, 1987). This intercalative binding hypothesis has been verified by Hartley and colleagues who characterised the structural requirements for DNA binding using phage PM2 plasmid DNA (Hartley *et al*, 1988) and various A-ring modified anthrapyrazoles (figure 6). The 7,10 unsubstituted APZ was found to be an efficient intercalator, similar in magnitude to ethidium, but that the hydroxyl groups on the A-ring of the chromophore, resulted in a decrease of the unwinding angle, indicative of a decrease in the intercalative ability (Hartley *et al*, 1988). The trihydroxy anthrapyrazoles did not cause any significant unwinding of the DNA but were still strongly bound, presumably to the surface of the DNA helix.

Figure 6: Structures of various A-ring modified anthrapyrazoles

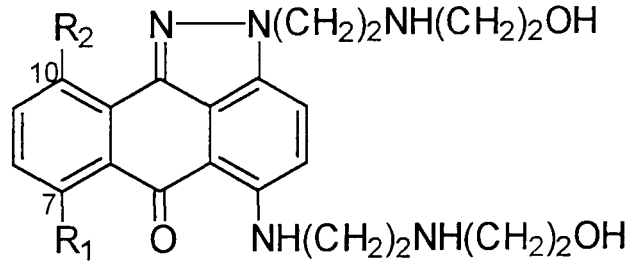

Compound	A-ring substituent
PD 110095	7,10-H
CI-941	7-OH
PD 114057	10-OH
PD 111707	7,10-OH

2.2 Synthesis of the Anthrapyrazole derivatives.

The rationale behind the synthesis of the anthrapyrazoles (Showalter *et al*, 1986a; Showalter *et al*, 1984), stems from the observation that the quinoneimine anthracycline, 5-iminodaunorubicin, has proved less cardiotoxic than doxorubicin in experimental systems (Tong *et al*, 1979). By analogy to 5-iminodaunorubicin, the anthrapyrazoles as modified quinoneimines are theoretically poor candidates for metabolic reduction and drug free radical formation. Electrochemical studies by Showalter *et al* (1986a) on the anthrapyrazoles have confirmed that these compounds are very difficult to reduce.

The first report of anthrapyrazole synthesis materials was that of Mohlau in 1912 in conjunction with the synthesis of the dyestuff pyrazoloanthrone yellow derived from 9,10-anthracenedione starting materials. Since then there have been numerous reports in both the patent and journal literature of the synthesis and chemistry of this commerically important class of compounds (Showalter *et al*, 1986b; Beylin *et al*, 1989).

2.3 Discussion and Mechanisms.

In general the synthesis of N-substituted APZ has required separate synthesis of the substituted hydrazine side chain, which was then reacted with the chloroanthraquinone. Further side chain functionalities were introduced subsequently to form the pyrazole ring. The overall synthetic strategies utilised in the preparation of target APZ derivatives are outlined in figure 7-9.

Figure 7: General synthetic route to 2-substituted APZ derivative.

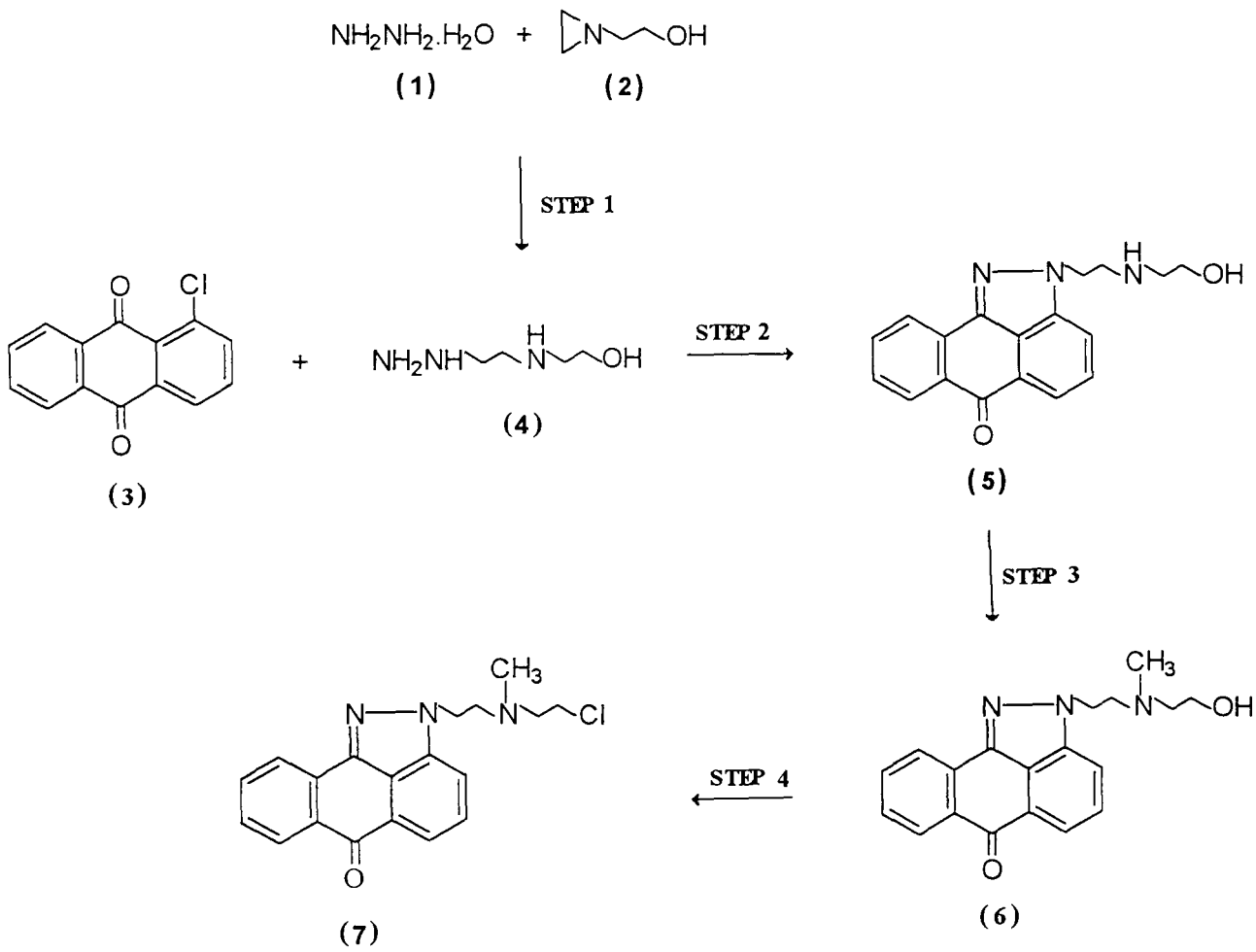

Figure 8: General synthetic route to 2,7-disubstituted APZ derivative.

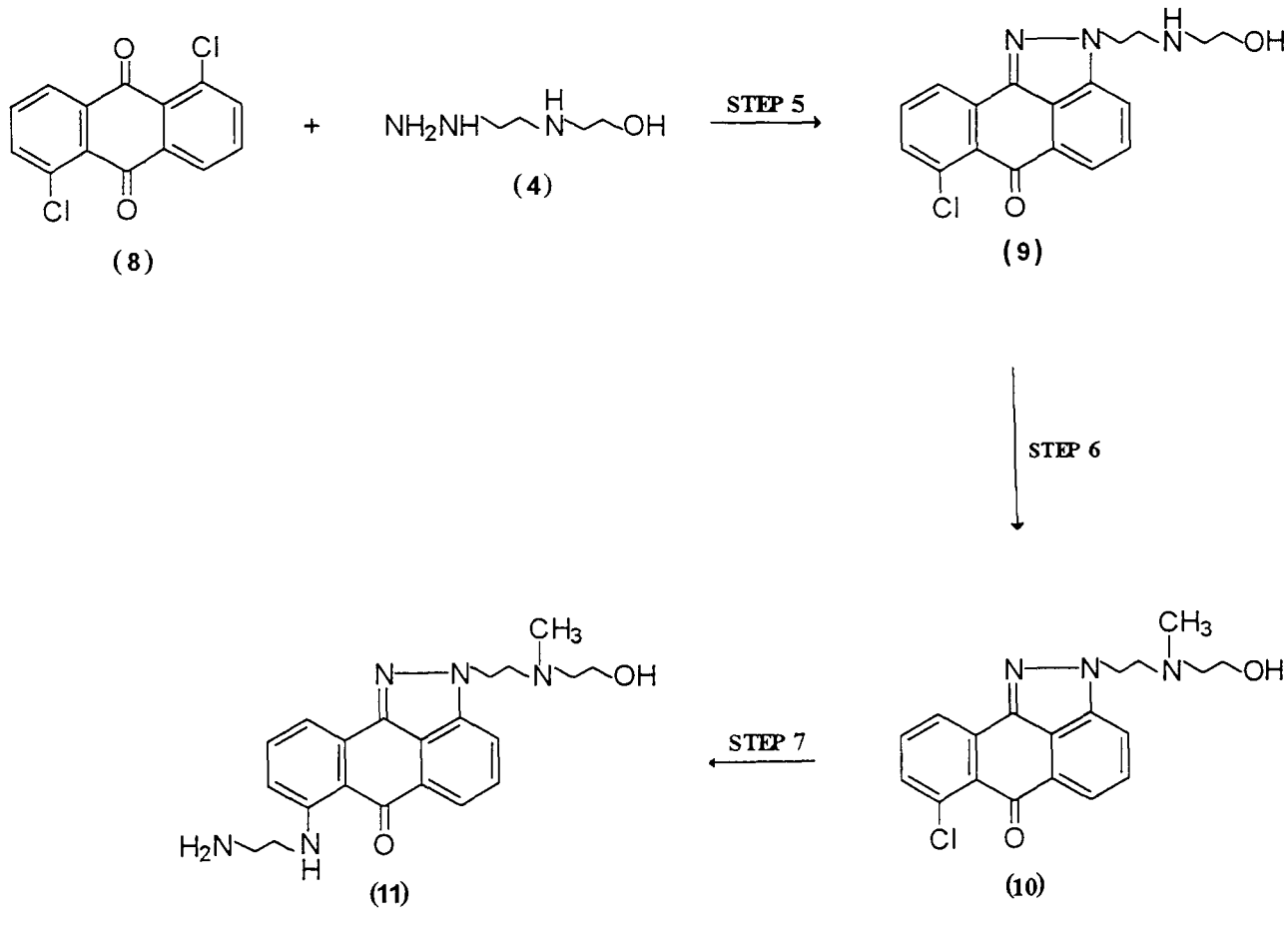

P.T.O

Continued... Synthetic route to 2,7-disubstituted APZ.

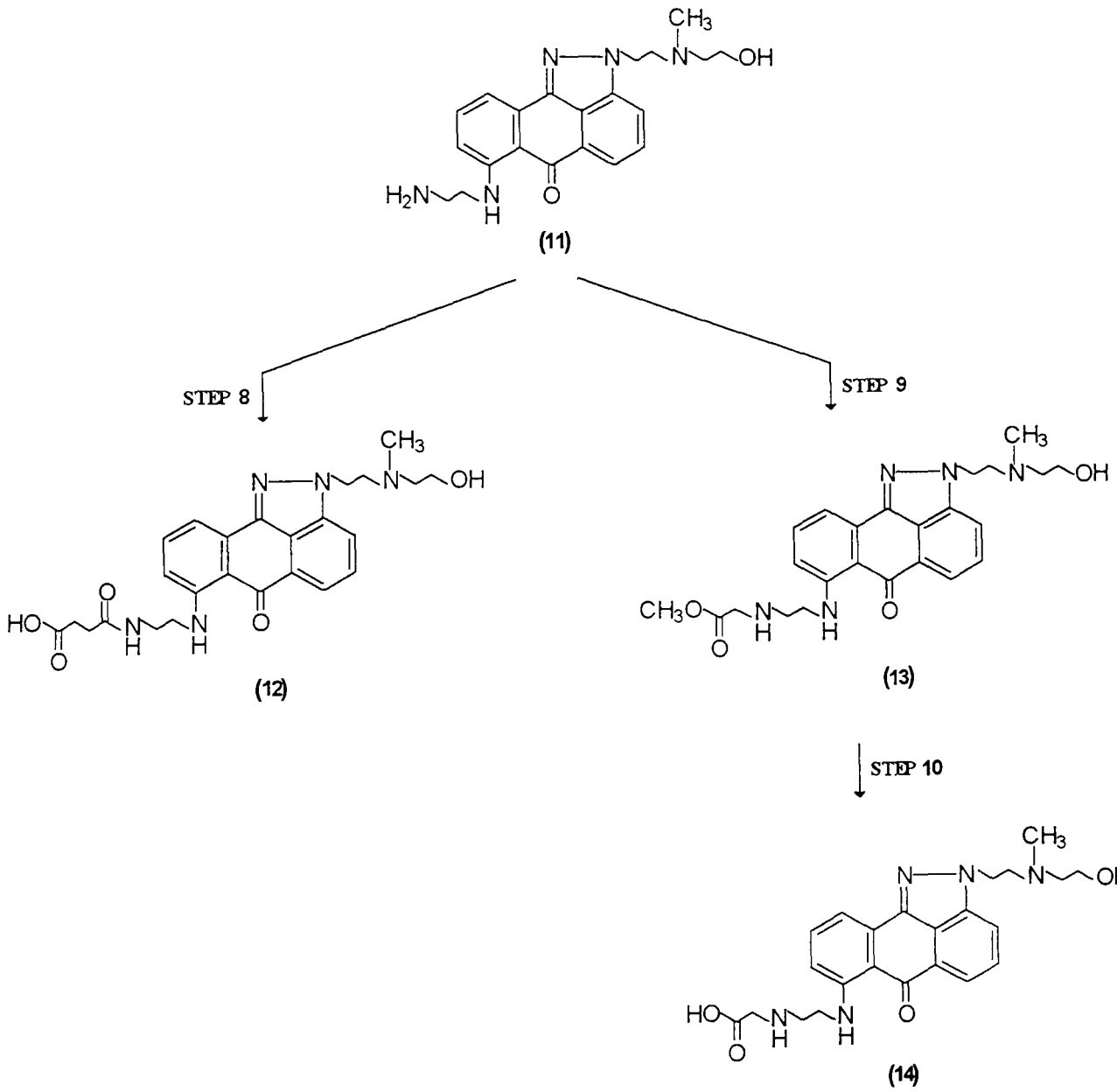

Figure 9: General synthetic route to 2,5-disubstituted APZ derivative.

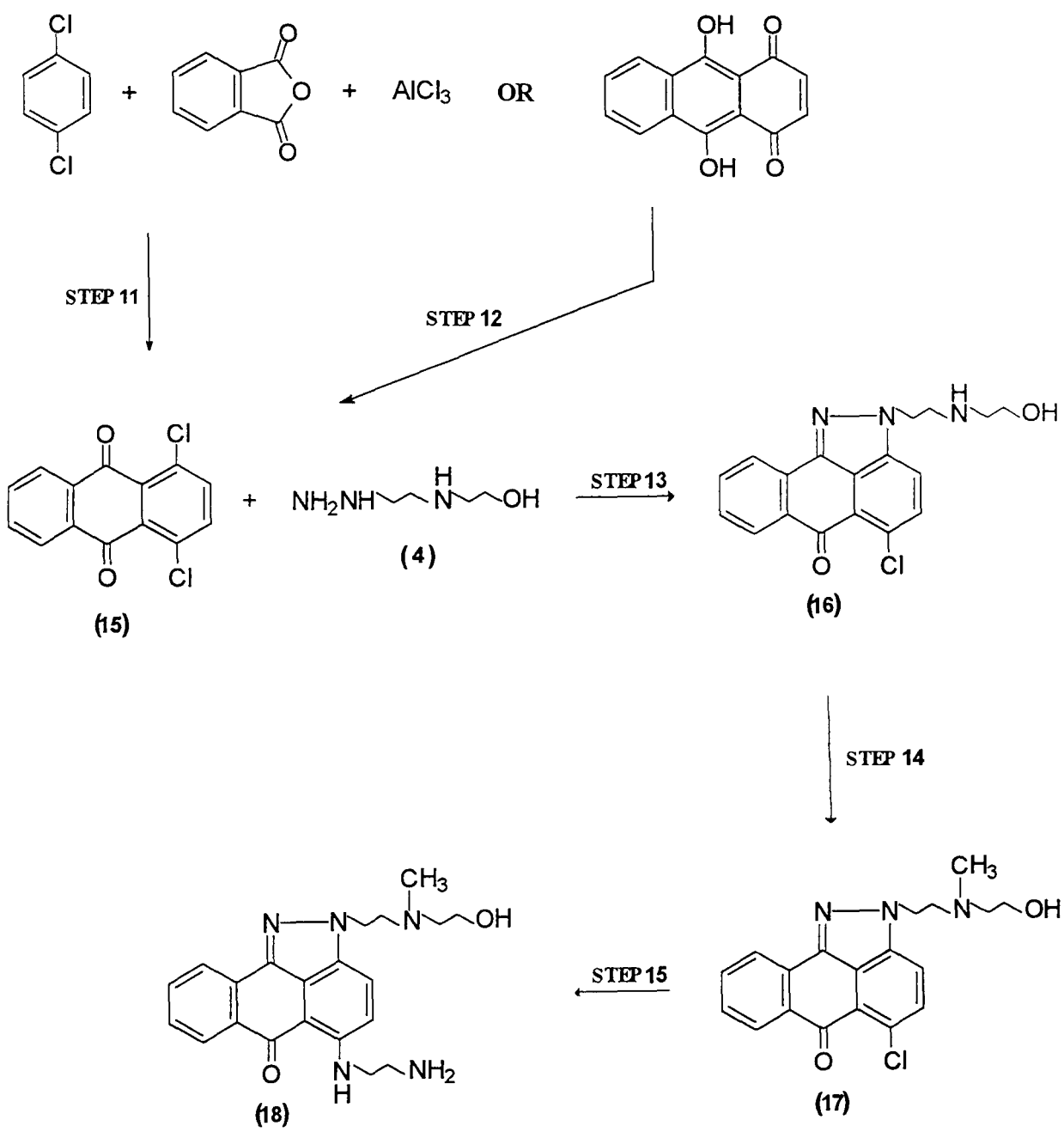

2.3.1. Synthesis of 2-[(2-Hydrazinoethyl)amino]ethanol (4) (Step 1).

The initial synthetic procedure involving the formation of side chain **(4)** was readily achieved using a literature procedure (Showalter *et al*, 1986b). This product was extremely hygroscopic and decomposed on prolonged heating, and was therefore stored under inert conditions at 5°C. Figure 10 shows a direct nucleophilic attack by the monohydrazine hydrate **(1)** on the strained 3-membered ring of 1-aziridine ethanol **(2)**, to afford an energetically more stable dipolar intermediate **(4i)**.

Bis-substituted hydrazine **(4ii)** produced as a by-product was separated from the desired monosubstitued hydrazine **(4)** by Kugelrohr distillation. The monosubstituted hydrazine of lower boiling point was collected in the first fraction.

Figure 10: Synthesis of the side chain 2-[(2-hydrazinoethyl)amino]ethanol

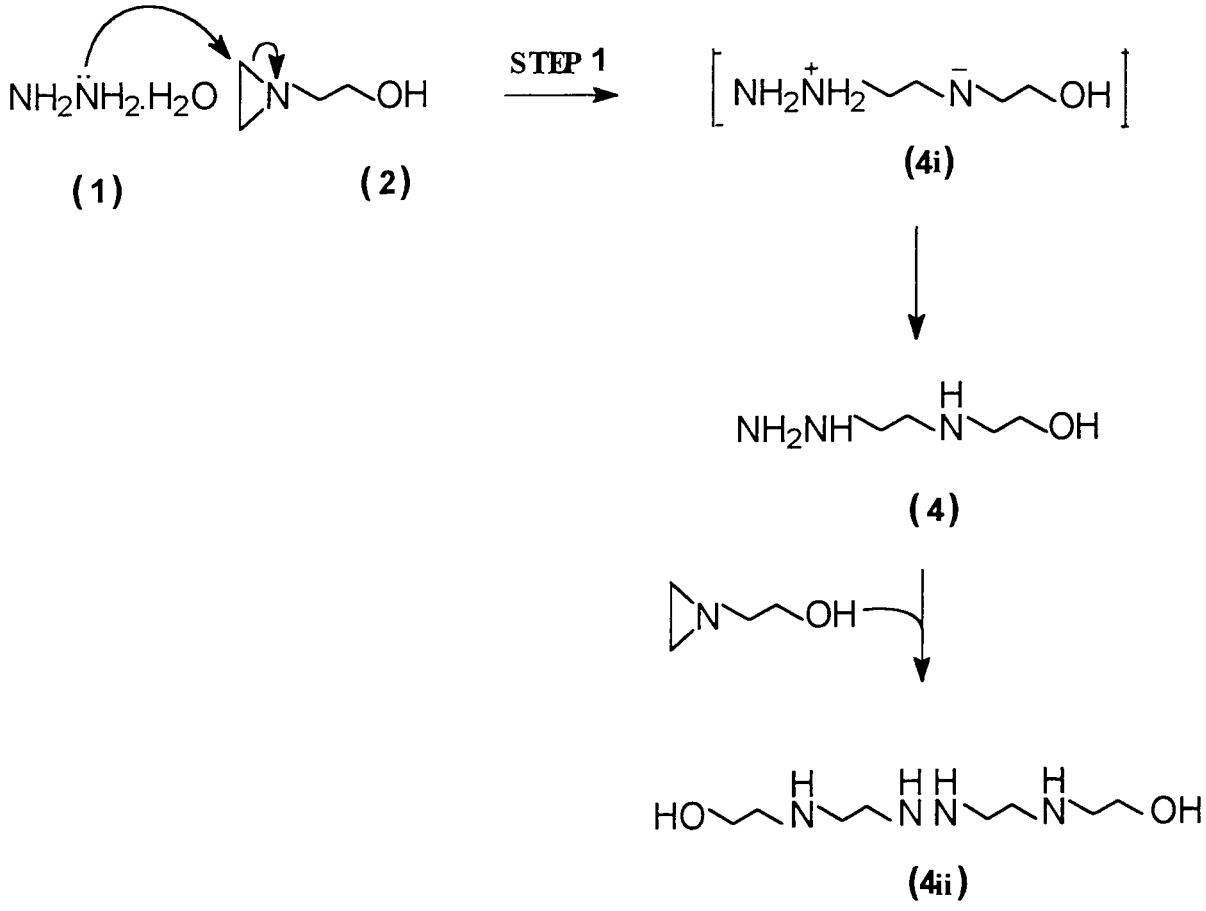

2.3.2 Synthesis of 2-{2-[*N*-(-2-Hydroxyethyl)amino]ethyl}anthra[1,9-*c*,*d*]pyrazol -6(*2H*)-one (5) (Step 2).

Coupling of 1-chloroanthraquinone **(3)** to side-chain **(4)** was carried out using a literature procedure (Showalter *et al*, 1986c), however by reducing the amount of solvent (dimethylformamide:acetonitrile) used in the reaction mixture, the yield was increased by at least 10%. An outline mechanism for the coupling step is shown in figure 11.

Figure 11: Mechanism of reaction of 1-chloroanthraquinone with side-chain **4**.

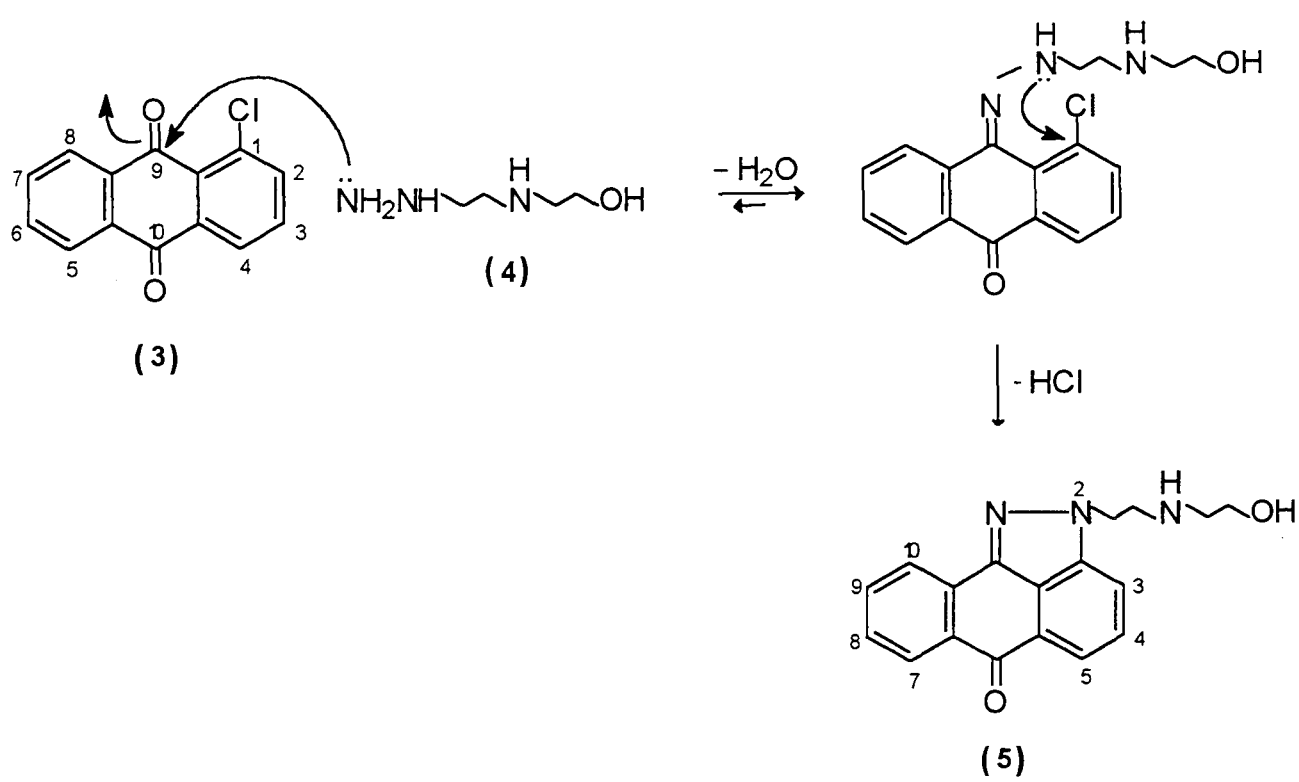

Figure 12: Mechanism of imine formation by reaction of ketone with primary amine.

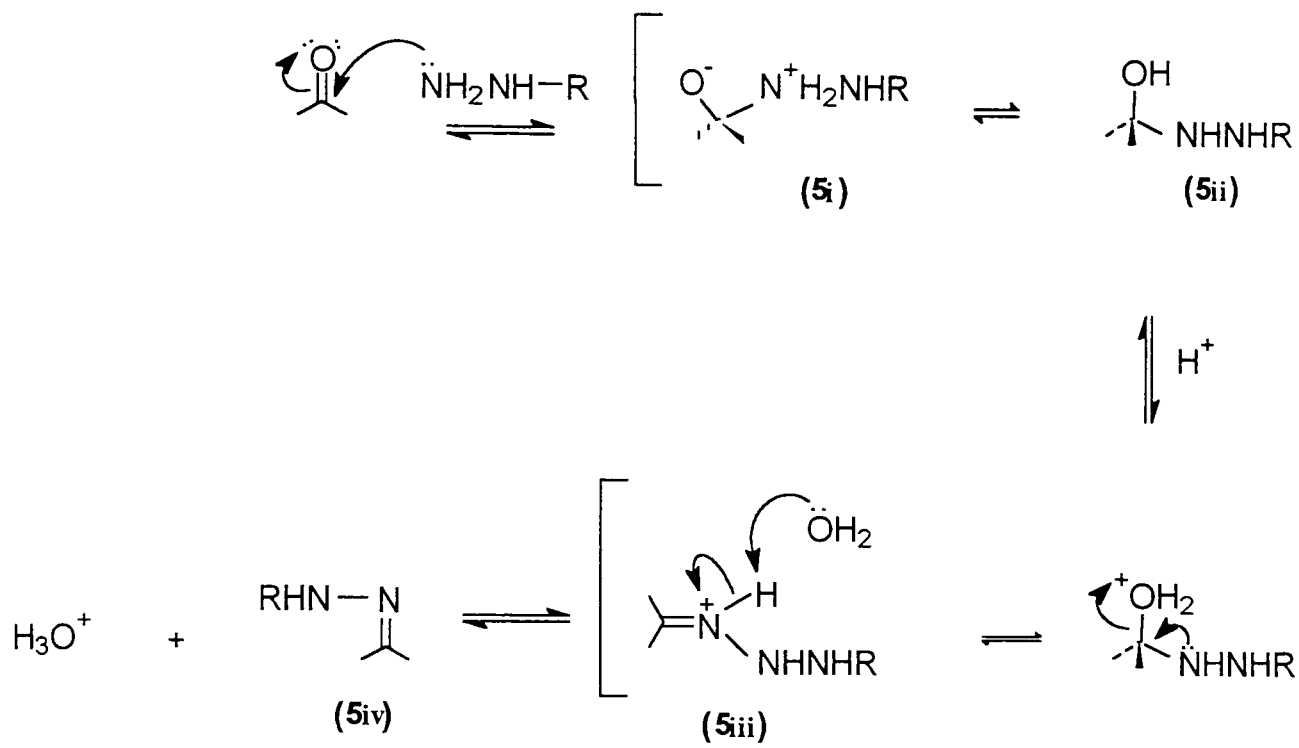

Figure 11 shows that the initial nucleophilic attack by **(4)** occurs favourably at the more electrophilic carbonyl carbon (see also figure 12) and not at the chloro substituted carbon. Figure 12 illustrates the nucleophilic attack by the primary amine on the ketone functionality resulting in a polarised tetrahedral intermediate **(5i)**, which then undergoes proton transfer to yield a neutral carbinolamine **(5ii)**. A proton picked up by the hydroxyl oxygen generates water as the leaving group. Iminium ion **(5iii)** was formed as a result of water lost to yield the product imine **(5iv)**. The electron sink effect facilitated the second nucleophilic attack at the chlorinated substituted carbon giving rise to the loss of hydrogen chloride. Triethylamine, a lewis base, was added to the reaction mixture to increase the pH.

After the reaction had completed, the product was isolated by cooling the reaction mixture to room temperature, and storing at 4°C overnight. The solid product was then filtered *in vacuo* with thorough cold methanol washes. The product was further purified by recrystalisation from hot methanol. The 6π

electron ring closure ensures that the reaction lies to the 'right hand side' of the equilibrium resulting in high yield.

2.3.2.1 Synthesis of 2-{2-[*N*-(2-Hydroxyethyl)-*N*-methylamino]ethyl}anthra[1,9 *c,d*]pyrazol-6(*2H*)-one (6) (Step 3).

The APZ derivative **(5)** synthesised during the last step contained a secondary amine in the side arm. An alkylation step was carried out to prevent acylation of this 'active' nitrogen (figure 13). This reaction required the refluxing of formaldehyde solution with formic acid as shown in figure 13.

The transfer of a proton from the formyl anion to the cationic intermediate resulted in the concomitant liberation of gaseous carbon dioxide detected as bubbles. The product initially, in the protonated form, was solubilised in the aqueous phase. In isolating this product, the reaction mixture was taken up in chloroform and the aqueous phase extracted. The aqueous phase was then basified to ~pH12 to give a fine precipitate, which was extracted using ethyl acetate. The combined organic phase was dried *in vacuo* to afford a dark viscous oil which on trituration with methanol and cooling overnight gave a lime green solid material **(6)**. This was further recrystallised to yield a very pure final product.

Figure 13: Mechanism for methylation of side-chain nitrogen.

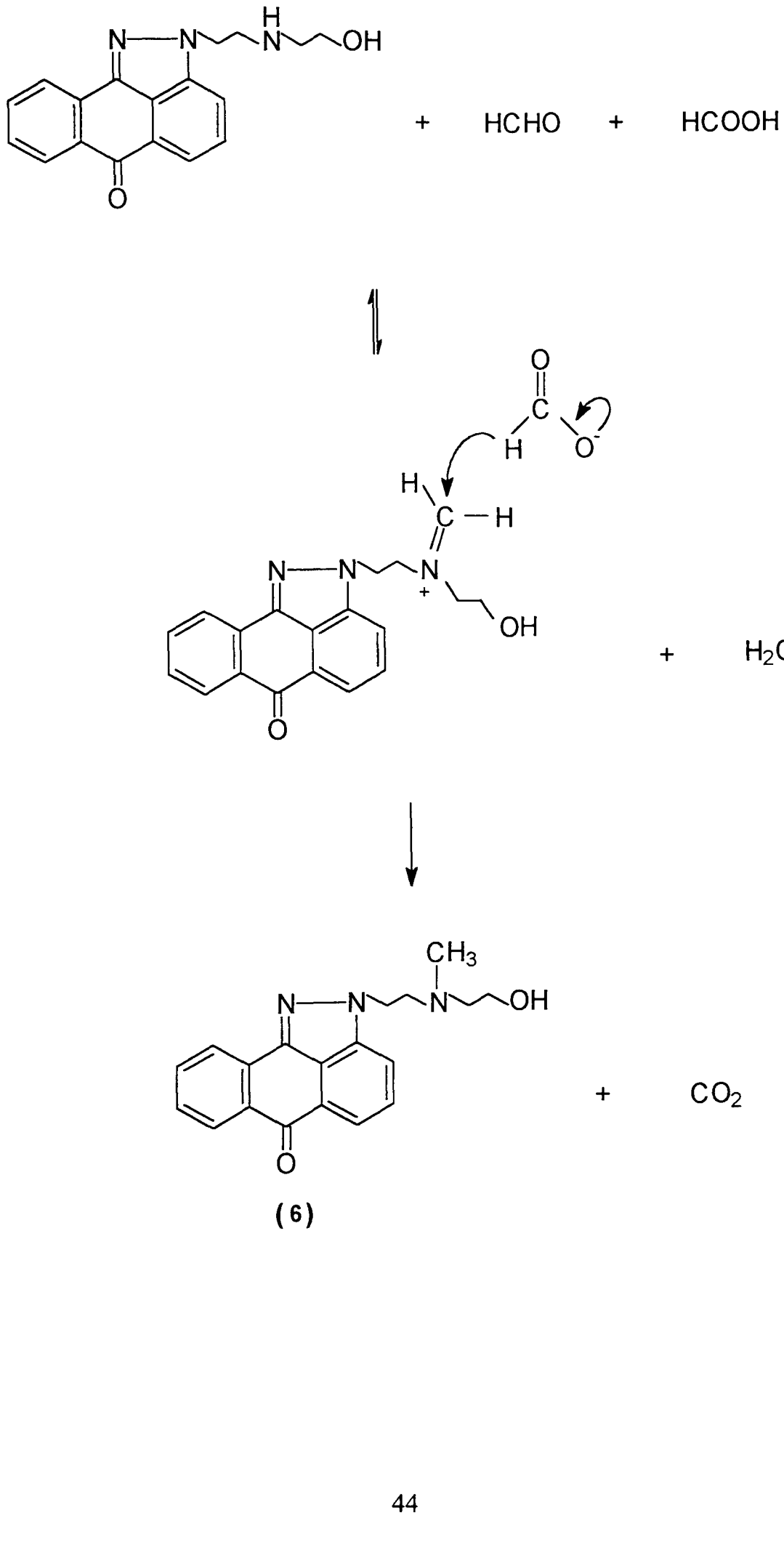

(6)

2.3.2.2 Synthesis of 2-{2-[*N*-(2-Chloroethyl)-*N*-methylamino]ethyl}anthra[1,9-*c,d*]pyrazol-6(*2H*)one (7) (Step 4).

The next stage was to consider ways of coupling the monosubstituted methylated anthrapyrazole to the peptide sequence (see chapter 4 for coupling and table 7 for the peptides used). One way of linking the two components was to convert the hydroxyl group to a chloride to afford an anthrapyrazole mustard hydrochloride derivative. In this reaction thionyl chloride reacted with the hydroxyl group making it readily expelled by SN_2 nucleophilic attack by the chloride ion (see figure 14).

On completion of the reaction, excess thionyl chloride was carefully removed *in vacuo* and the solid residue that remained was triturated with anhydrous ether. Crystallisation from methanol yielded a bright yellow product **(7)**. Coupling of the mustard anthrapyrazole to the amino terminus of the peptide took place via formation of a highly reactive aziridium ion (see session 4.1.1 on coupling).

Figure 14: Conversion of hydroxyl to chloride group.

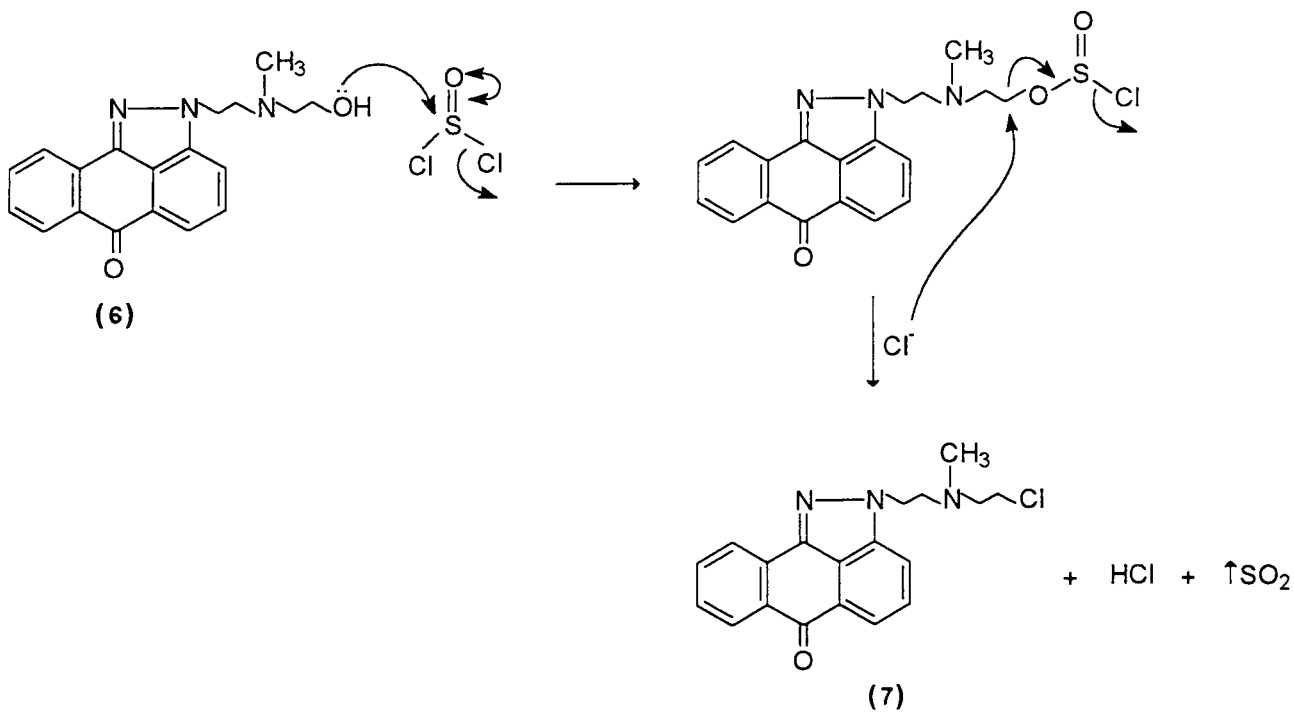

2.3.3 Synthesis of 7-Chloro-2-{2-[*N*-(2-hydroxyethyl)amino]ethyl}anthra[1,9-*c,d*] pyrazol-6(*2H*)-one (9) (Step 5).

The mechanism for coupling of the side chain **(4)** to 1,5-dichloroanthraquinone was exactly the same as that described in step 2 (Showalter *et al*, 1986c). However because the starting material, 1,5-dichloroanthraquinone has two possible attack sites, 1- and 5-, a side product in which two side chains were substituted was also produced (figure 15). This by-product **(9i)** was removed by washing the yellow product mixture thoroughly with cold methanol during filtration *under vacuo*. The absence of the carbonyl carbon signal in the IR range 1650-1750 cm^{-1} was indicative of the presence of this side-product in the mother liquor.

Figure 15: Two possible products.

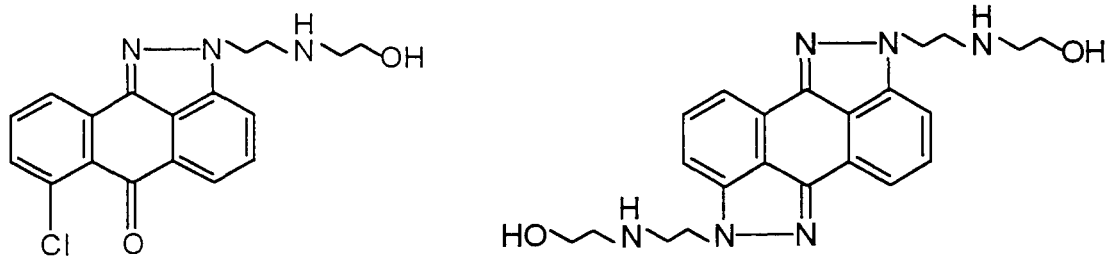

(9) **(9i)**

However, the second carbonyl is less susceptible to nucleophilic attack because of an increase in electron density in the aromatic chromophore following coupling of the first side-chain. As a result, the yield obtained for the desired mono-substituted product **(9)** was higher.

2.3.3.1 Synthesis of 7-Chloro-2-{2-[*N*-(2-hydroxyethyl)-*N*-methylamino]ethyl} anthra [1,9-*c,d*]pyrazol-6(*2H*)-one (10) (Step 6).

The procedure carried out for this reaction was as described for step 3. Except that in this case the final product **(10)** was a yellow rather than a lime green solid.

2.3.3.2 Synthesis of 7-(2-Aminoethyl)amino-2-{2-[*N*-(2-hydroxyethyl)-*N*-methyl amino]ethyl}anthra [1,9-*c,d*]pyrazol-6(*2H*)-one (11) (Step 7).

This next reaction involved making a substitution at the 7- position. To synthesise the title compound, excess ethylenediamine was refluxed for 4 hr or until all the APZ starting material had reacted. This was determined by t.l.c. The amine functionality in the new side arm helps to stabilise the binding of APZ to the DNA backbone by interacting with phosphate groups (Patterson and Newell, 1994). To avoid possible intramolecular nucleophilic attack by the primary amine on the ring to form a stabilised 6-membered ring (figure 16), the refluxing was kept to a minimum.

Figure 16: Ring closure

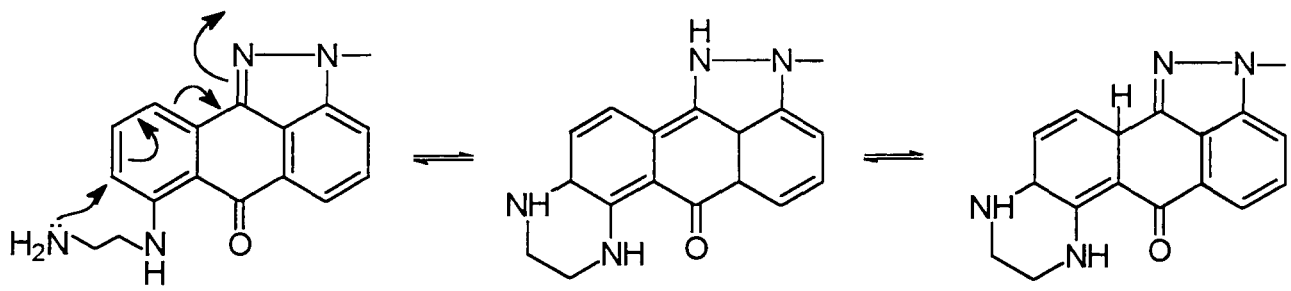

(11) **(11i)** **(11ii)**

However, this type of closure involves loss of aromaticity and is therefore unlikely to occur. Nevertheless, intramolecular attack of this nature could be possible at temperatures exceeding 250°C. The reaction mixture was then taken up in water and the crude product extracted with dichloromethane. The resulting red viscous oil formed upon evaporation of the solvent was triturated with hexane to remove any remaining ethylenediamine. The desired product **(11)** was isolated by column chromatography using dichloromethane : ethanol: ammonia (9:1:0.1) as the eluent.

2.3.3.4a Synthesis of 7-{2-[(methoxycarbonylmethyl)amino]ethylamino}-2-{2-[*N*-(2-hydroxyethyl)-*N*-methylamino]ethyl}anthra[1,9-*c,d*]pyrazol-6(*2H*)-one (13) (Step 9).

To further extend the side arm, methyl chloroacetate was made to react with **(11)** to give the APZ ester derivative **(13)**. This reaction was carried out under ambient conditions in the presence of dimethylformamide (DMF) for 24 hr. By using a one-to-one equivalent it was possible to avoid a second substitution at the same nitrogen. The product **(13)** was isolated by column chromatography using dichloromethane:methanol (8:2).

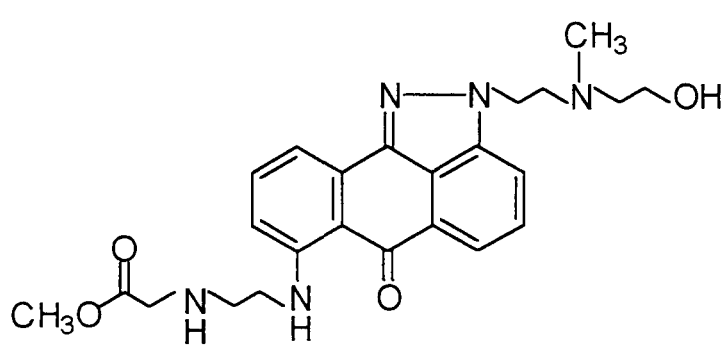

(13)

The following section outlines the dealkylation of this APZ ester to form the APZ acid derivative. Activation of this resulting carboxylic acid using PyBOP (section 4.1.2) will allow the direct coupling of the APZ intercalator with the amino terminus of the peptide, hence forming the desired intercalator-peptide complex (see chapter 4 for coupling).

2.3.3.5 Conversion of Ester to Acid.

An initial attempt at dealkylation of the APZ ester was carried out according to the method of Node *et al* (1991). The mechanism for this reaction is based on the principle of hard and soft acids and bases as shown below.

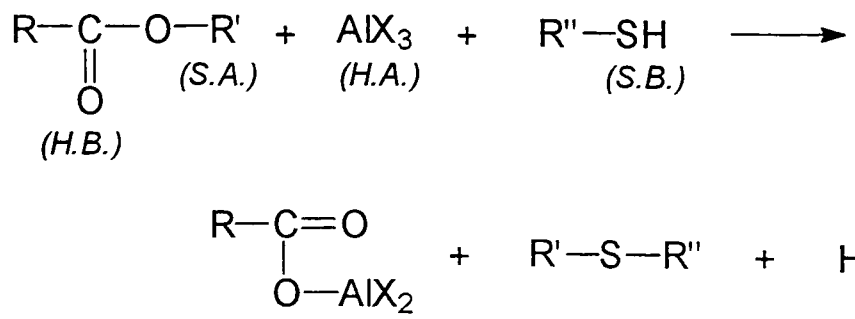

The following components, compound **(13)**, aluminum chloride and tetrahydrothiophene were dissolved in dichloromethane and left to stir overnight. Unfortunately, no reaction took place. This reaction was therefore abandoned, in favour of another procedure.

An alternative method involved refluxing **(13)** with lithium bromide and pyridine. After 9 hr the pyridine was evaporated under vacuum. Ethanol was added and heated and filtered while still hot to remove the remaining inorganic materials. The ethanol was removed and the final acid product **(14)** was obtained on acidification using hydrochloric acid. The yield was very low at this stage and therefore it could not be used in subsequent steps. The synthesis of **(14)** was again dismissed, and other acid containing APZ compounds were synthesised instead (see section 2.3.3.4b).

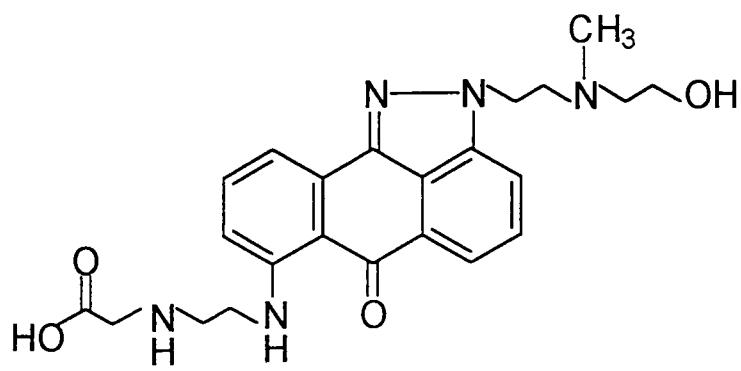

(14)

2.3.3.4b Synthesis of 7-(2-Succinamidoethyl)amino-2-{2-[*N*-(2-hydroxyethyl)-*N*-methylamino]ethyl} anthra[1,9-*c,d*]pyrazol-6(*2H*)-one (12) (Step 8).

Instead of methyl chloroacetate, succinic anhydride was used in extending the linker. The coupling onto the peptide could then occur via the resulting carboxyl group. Note however, this linker contained an amide functionality which is less

favourable than the amine in binding to the DNA backbone (Patterson and Newell, 1994).

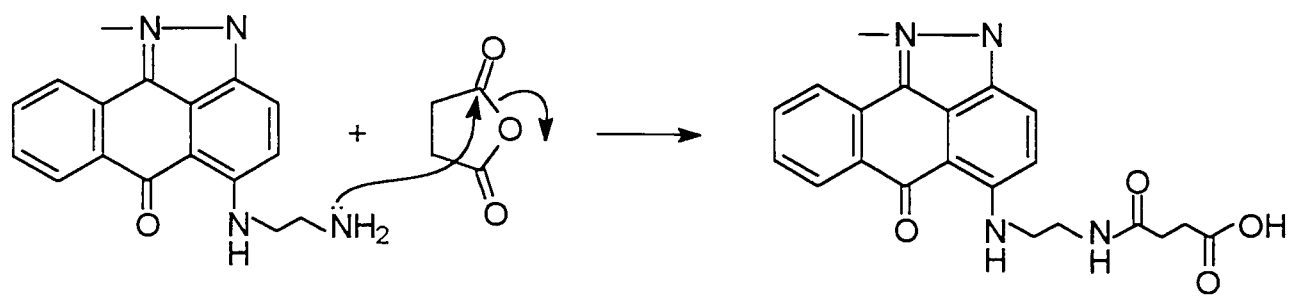

(11) **(12)**

For this reaction, 1.2eq of succinic anhydride and compound **(11)** were dissolved in DMF:methanol (1:1) and left to react at 40°C for 1.5 hr. The solvent was removed *in vacuo* and the product **12** isolated using column chromatography. Neat methanol was used to elute the desired component.

(12) was recrystallised using ethanol and dried over phosphorous pentoxide. A relatively good yield was obtained of the analytically pure acid APZ product.

2.3.4a Synthesis of 1,4-dichloroanthraquinone (15) via Friedel Craft's Acylation (Step 11).

Two very different methods have been employed for the preparation of 1,4-dichloroanthraquinone. The first of these involved the Friedel-Crafts acylation (Phillips, 1926).

Laboratory preparation was carried out according to Philips 1926. In this reaction p-dichlorobenzene, pthalic anhydride and anhydrous aluminium chloride were heated together at 140-160°C for 5 hr (figure 17).

The driving force in the first step of this reaction was ring opening of the anhydride by catalytic aluminium chloride. *p*-Dichlorobenzene was added in great excess effectively to compensate for the electron withdrawing effect of the two chloro-groups. These have the effect of reducing the nucleophilicity at the *O*-

carbon, the attacking site for the acylium ion. Formation of aluminium salts at this stage led to darkening of the reaction mixture.

Sublimation of the *p*-dichlorobenzene during heating resulted in blockage of the neck joint which was dislodged hourly using a strong metal rod. To obtain the product, benzophenone acid **(15i)**, water was added to the cooled black reaction mixture, followed by 50mL of concentrated hydrochloric acid. Excess *p*-dichlorobenzene was then removed by steam distillation rather than by temperature distillation. A combination of steam and *p*-dichlorobenzene gave rise to an azeotropic vapour mixture. This vapour on cooling deposited solidified *p*-dichlorobenzene on the inner surface of the cooling condenser. The solid starting material *p*-dichlorobenzene was then collected at the end of the condenser by continual and careful alteration of the rate at which water flowed through the condenser.

Figure 17: Friedel-Crafts Acylation.

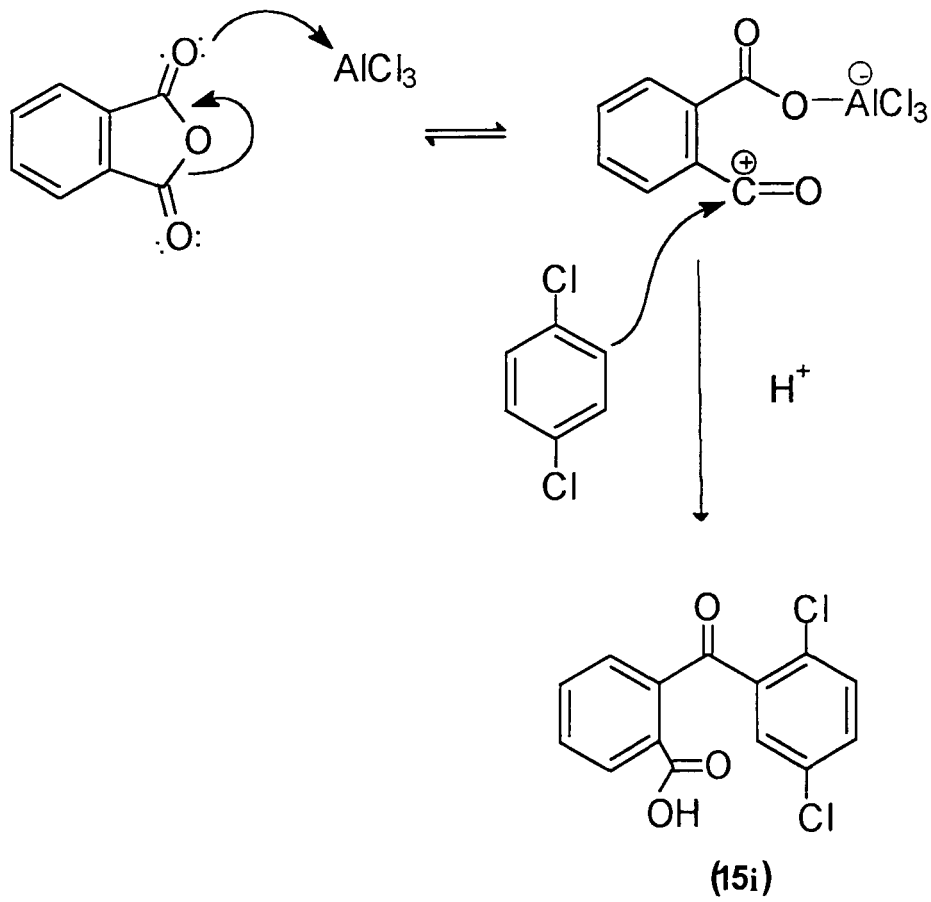

(15i)

The remaining content of the reaction mixture was then basified and filtered *under vacuo* to remove any precipitated aluminium salt. Decolourising charcoal was added before further acidification to yield the intermediate product benzophenone acid **(15i)**, as an off-white precipitate. This low yielding reaction was a direct result of the electron-induction effect mentioned above.

The second step of the reaction (figure 18), cyclisation of the benzophenone acid to 1,4-dichloroanthraquinone, takes place under extreme acidic conditions. Approximately 50 fold excess of concentrated sulphuric acid was added to the starting material, which was then heated for 5 hr at 150-160°C.

Figure 18: Cyclisation of benzophenone to 1,4-dichloroanthraquinone.

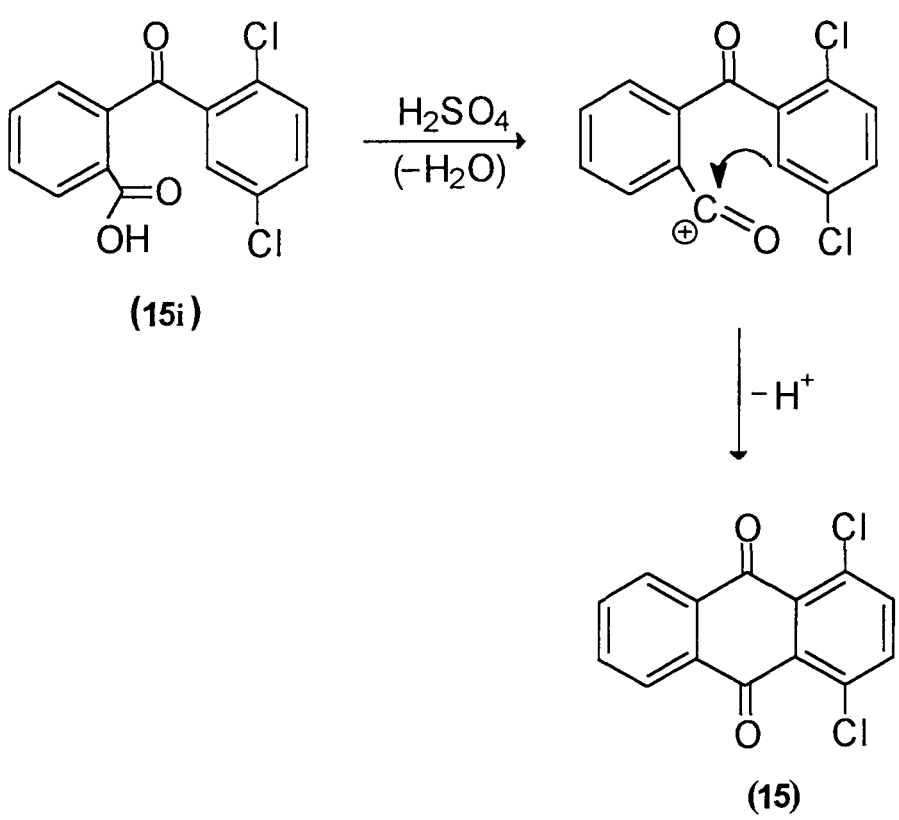

As shown in figure 18, formation of 1,4-dichloroanthraquinone takes place via a second acylium ion. After heating for ~5 hr, the reaction mixture was poured into ice cold water upon which a fine precipitate formed, which was extracted using ethyl acetate. The organic layer was then washed several times with aqueous sodium hydroxide and then with saturated brine. A brown-yellow precipitate was obtained on drying *in vacuo*. Purification by column

chromatography and further recrystallisation using methanol and chloroform gave a bright yellow solid material of melting point 128-129°C (cf lit. 129°C).

2.3.4b Synthesis of 1,4-Dichloroanthraquinone (15) via leucoquinizarin (Step 12).

An alternative method for the preparation of 1,4-dichloroanthracenedione-9,10-dione was carried out according to Krapcho and Gretahun (1985). This method makes use of the widely available leucoquinizarin (also called 1,4,9,10 hydroxyanthracene). This method of preparing 1,4-dichloroanthraquinone was favoured over the above mentioned Friedal Crafts because of the higher yield.

This reaction involved refluxing leucoquinizarin, phosphorous pentachloride and 1,1,2,2-tetrachloroethane for 24 hr (figure 19). The mixture was then allowed to cool to room temperature before excess methanol was added. Hydrogen chloride gas was vigorously produced at this stage and the mixture was then left to stir overnight. Upon further cooling to -20°C a brown-yellow solid appeared which was filtered with cold methanol and air dried to give **15**.

Figure 19: Two-step conversion of leucoquinizarin to 1,4-dichloroanthraquinone.

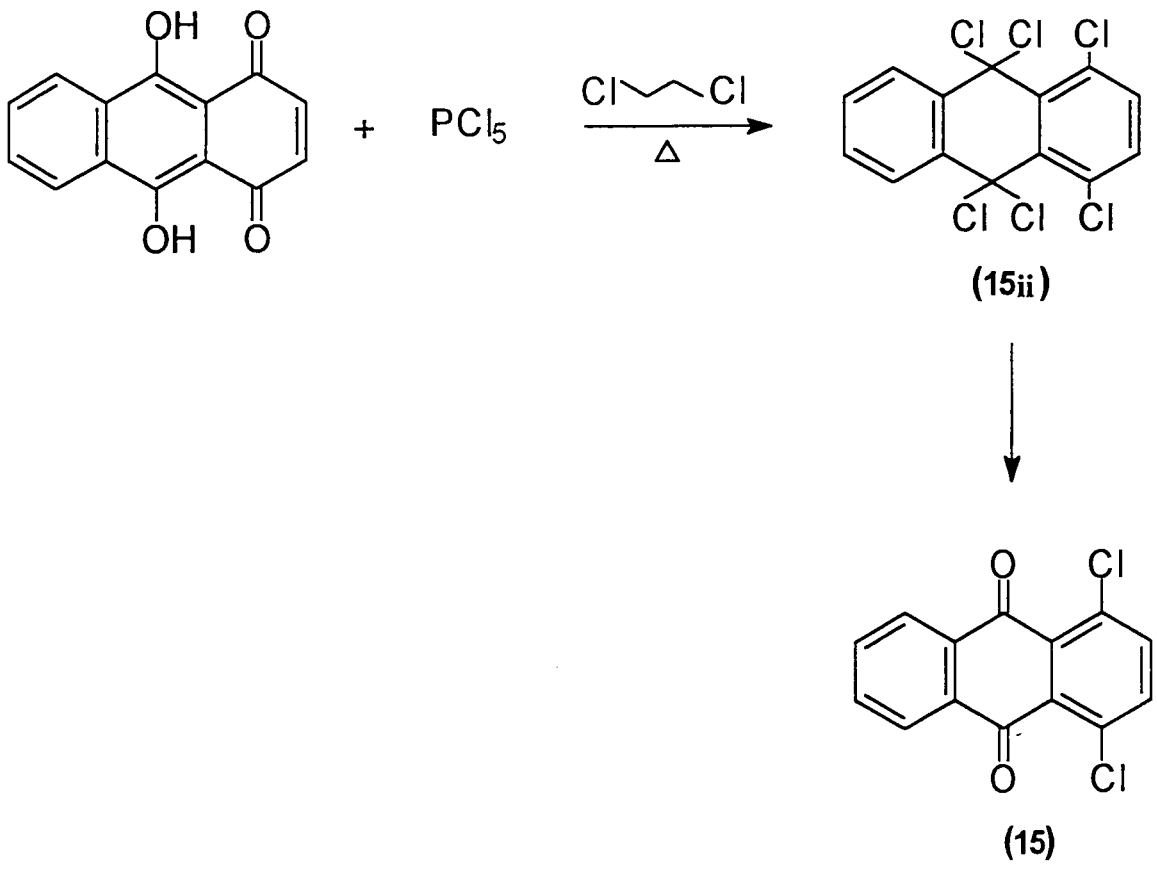

The next reaction step involved oxidation of the hexachloro compound **(15ii)** by refluxing in 1-pentanol for 18 hr. On completion, the reaction mixture was cooled to room temperature, then further cooled to -20°C before filtering to afford a yellow solid. T.L.C. showed a single UV spot and the analytical data was as expected.

2.3.4.1 Synthesis of 5-Chloro-2-{2-[N-(2-hydroxyethyl)amino]ethyl}anthra[1,9-*c,d*]pyrazol-6(*2H*)-one (16) (Step 13).

The coupling of the side chain (**4**) onto 1,4-dichloroanthraquinone is very similar to that described for the 1,5-dichloroanthraquinone (section 2.3.3) (Showalter *et al*, 1986b). However the yield obtained was different in each case, with the yield of the 1,5-dichloroanthraquinone being slightly lower. The reason being that the electron withdrawing effect of the chloride in the same ring destabilises the cationic intermediate and thus disfavours its formation. However, once formed, nucleophilic attack is rapid.

2.3.4.2 Synthesis of 5-Chloro-2-{2-[*N*-(2-hydroxyethyl)-*N*-methylamino]ethyl} anthra[1,9-*c,d*]pyrazol-6(*2H*)-one (17) (Step 14).

The procedure carried out was again the same as that for the synthesis of the 2,7-substituted APZ (section 2.3.2.1). However, because of the lower melting point of 2,5-*N*-methylated APZ, it was an oil at room temperature. It was possible to form the solid hydrochloride of the title compound by adding an equivalent number of moles of acetyl chloride/methanol at 0°C to a solution of the described compound.

2.3.4.3 Synthesis of 5-(2-Aminoethyl)amino-2-{2-[*N*-(2-hydroxyethyl)-*N*-methyl amino]ethyl}anthra [1,9-*c,d*]pyrazol-6(*2H*)-one (18) (Step 15).

Substitution at the 5-position was achieved by refluxing **(17)** with excess ethylenediamine for 4 hr. The reaction mixture was then taken up in water and the crude product extracted with dichloromethane and dried to give a viscous red oil. The product **(18)** was isolated by column chromatography using dichloromethane:ethanol:ammonia (9:1:0.1) as eluent.

Using similar synthetic routes, anthraquinone derivatives (refer to T. Ijaz (1998) for more experimental detail) were also synthesised (figure 20).

Figure 20: General synthetic routes for anthraquinone derivatives

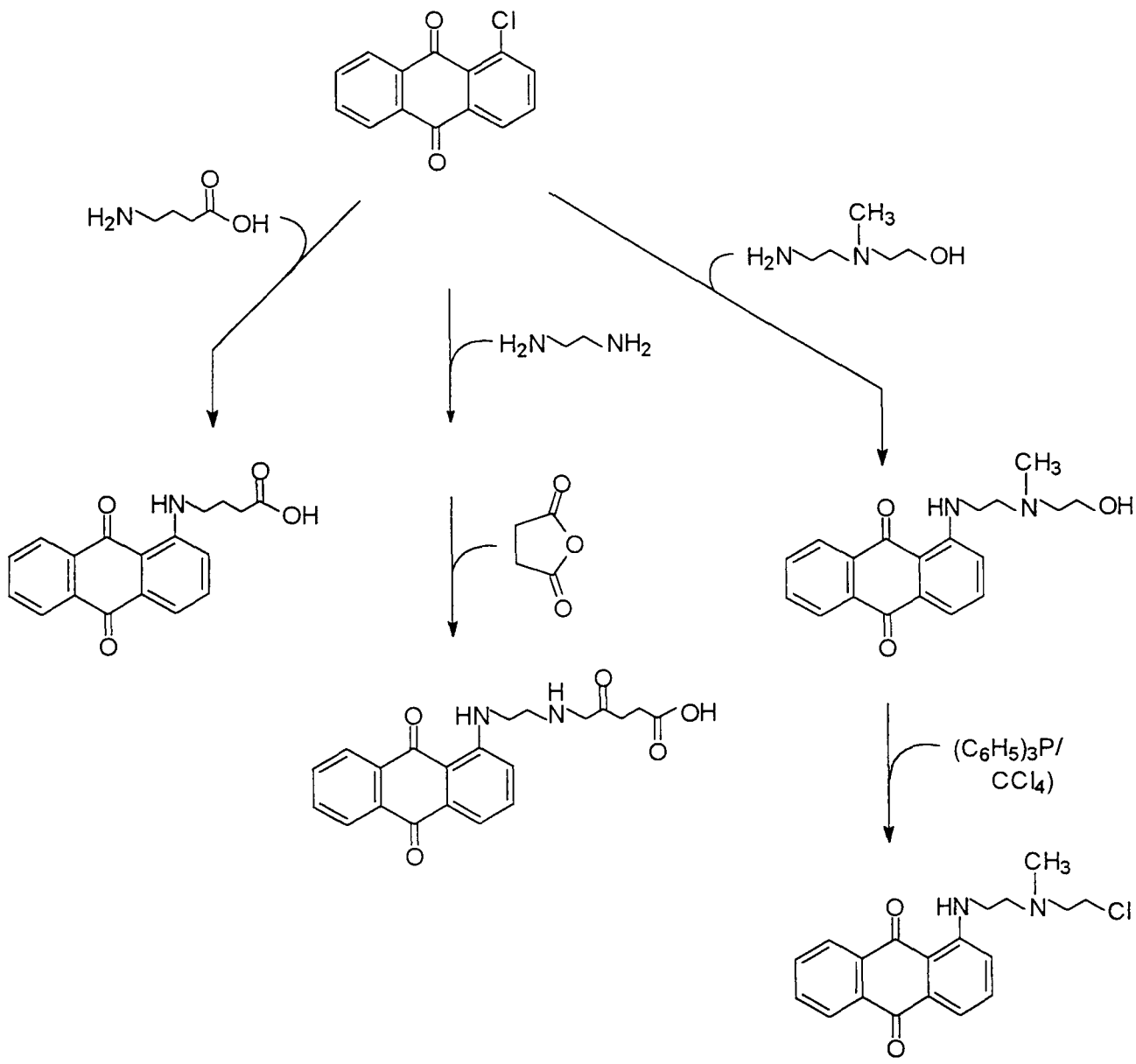

Anthraquinones are also well known intercalators (Kapuscinski and Darzynkiewicz, 1985), examples including mitoxantrone and ametantrone.

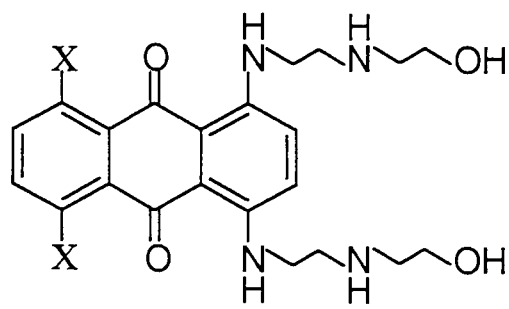

X = OH mitoxantrone

X = H ametantrone

The synthesised anthraquinone chromophores were coupled to the peptide chain to give a series of peptide-hybrid ligands. The cell free biological evaluation of the synthesised anthrapyrazole compounds along with the anthraquinones, and their respective peptide hybrid complexes can be found in chapter 5.

Chapter 3

The Synthesis, Isolation and Characterisation of Short Oligopeptides

The DNA sequence specificity of the intercalator-peptide complex is almost entirely dependent on the attached peptide sequence. Solid phase peptide synthesis (SPPS) used in the synthesis of short polypeptides is discussed. The final part of this chapter looks at three different methods used in the isolation, purification and characterisation of the synthesised peptides.

3.1 The Synthesis of the KCR containing Peptide using the Solid Phase Peptide Synthesizer.

In this work, two short polypeptide sequences (figure 21) were synthesised on a semi-automated solid phase peptide synthesiser. Additional peptides (table 7) were purchased from Novabiochem.

3.1.1 Solid Phase Peptide Synthesis (SPPS).

Solid Phase Peptide Synthesis (SPPS) is based on sequential addition of ∝-amino and side chain protected amino acid residues to an insoluble polymeric support (Merrifield 1963; Atherton *et al*, 1979).

The general procedure was (see also figure 22): Following the removal of the base-labile Fmoc group using 20% piperidine:DMF, the next protected amino acid was added using a pre-activated protected amino acid derivative. The resulting peptide attached to the resin, via a linker, through its C-terminus was cleaved to yield the peptide acid or amide, depending on the linking agent used. Cleavage of the side chain protecting groups and detachment of the peptide from the resin was simultaneously carried out in the presence of a strong acid, trifluoroacetic acid (TFA). Details of the practical approach can be found in "Solid Phase Peptide Synthesis" by Atherton and Sheppard (1989).

Figure 21: Two peptides synthesised on the solid phase peptide synthesizer.

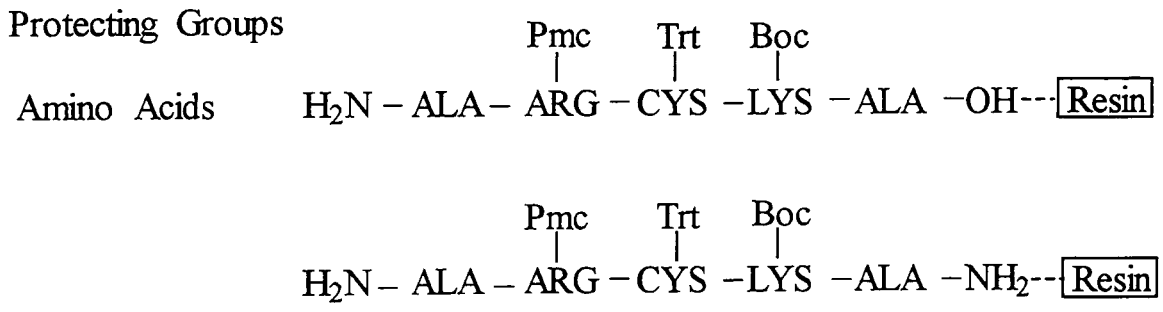

Figure 22: The strategy of solid phase peptide synthesis (Novabiochem catalog and Peptide Synthesis Handbook).

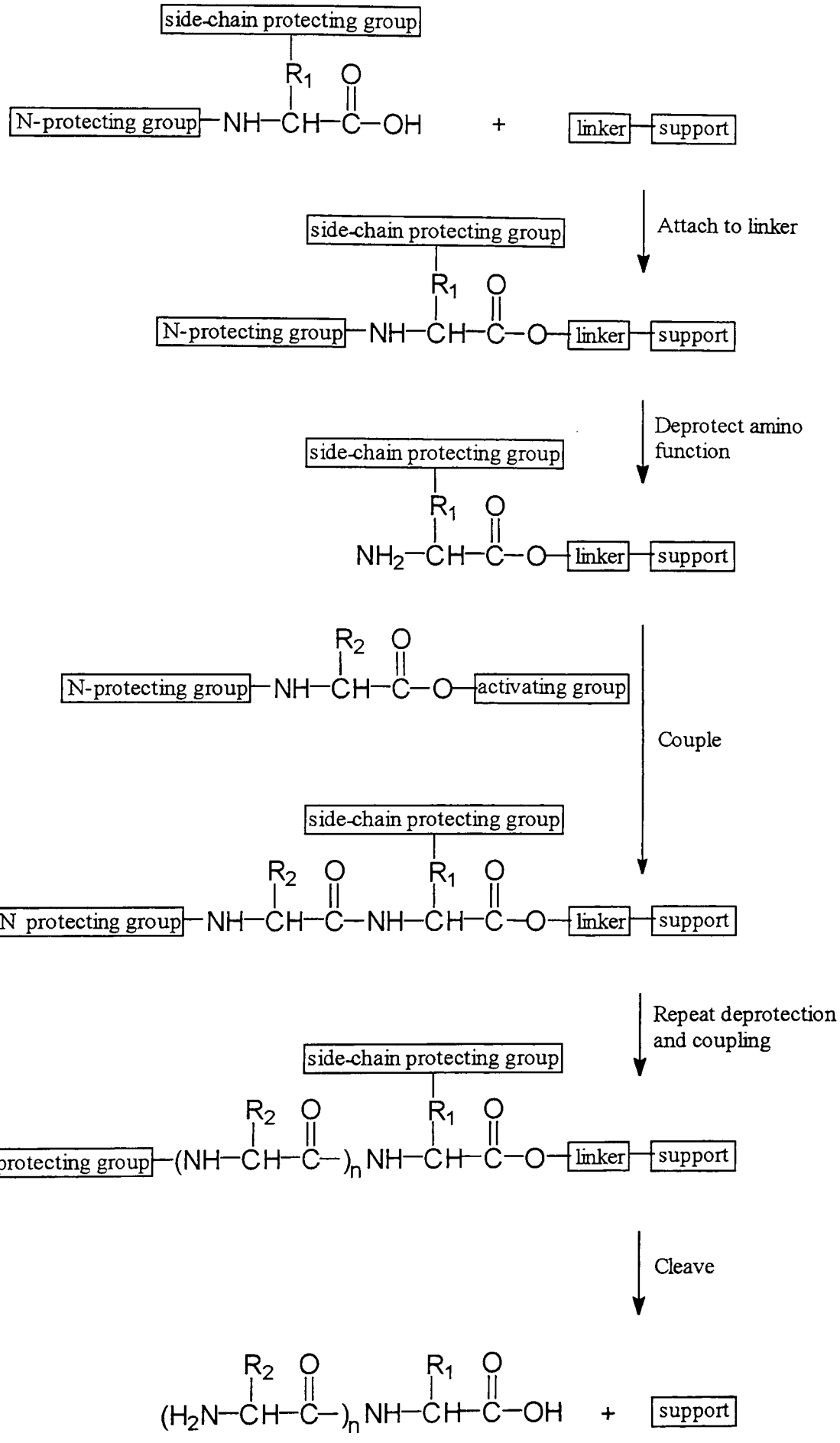

3.1.2 The Fmoc Strategy.

The Fmoc stategy (Dryland and Sheppard, 1986) was chosen over the Boc strategy for the synthesis of the peptides since with the Boc-group, deprotection by repetitive TFA acidolysis could lead to alteration of sensitive peptide bonds as well as acid catalysed side-reactions. With the Fmoc strategy, the growing peptide was subjected to mild base treatment using piperidine during Fmoc-group deprotection, and TFA (Albericio and Barany, 1990) was used in the final stage of cleavage and deprotection of the peptide-resin. By contrast however, cleavage and deprotection in the Boc strategy would require the use of highly acidic conditions such as hydrogen fluoride.

The cleavage of Fmoc was carried out with 20% (v/v) piperidine in DMF which allowed the dibenzofulvene olefin, produced by β-elimination, to be trapped as its piperidine adduct **(19)**, as shown in figure 23. Deprotection with piperidine took only a matter of seconds at room temperature. The mechanism of cleavage occurs via the stabilised dibenzocyclopentadienide anion; the dibenzofulvene produced reacted with piperidine, giving the adduct **(19)** as co-product.

3.1.3 Coupling Reagent.

In recent years, *in situ* activating reagents have become widely accepted because of their ease of use, fast reaction even between sterically hindered amino acids, and their general lack of side-reactions. Most coupling reagents are based on phosphonium or uranium salts which, in the presence of a tertiary base, can smoothly convert protected amino acids to a variety of activated species. The coupling reagent used as part of the Fmoc strategy, PyBOP allowed efficient, fast and racemisation-free coupling. The mechanism for this coupling can be found in section 4.1.2.

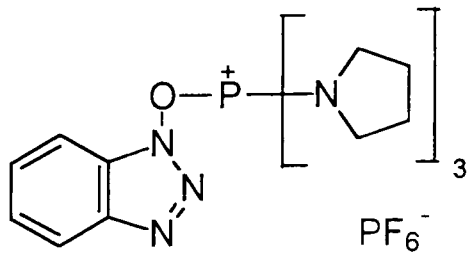

PyBOP

Figure 23: The cleavage of the Fmoc protecting group by piperidine.

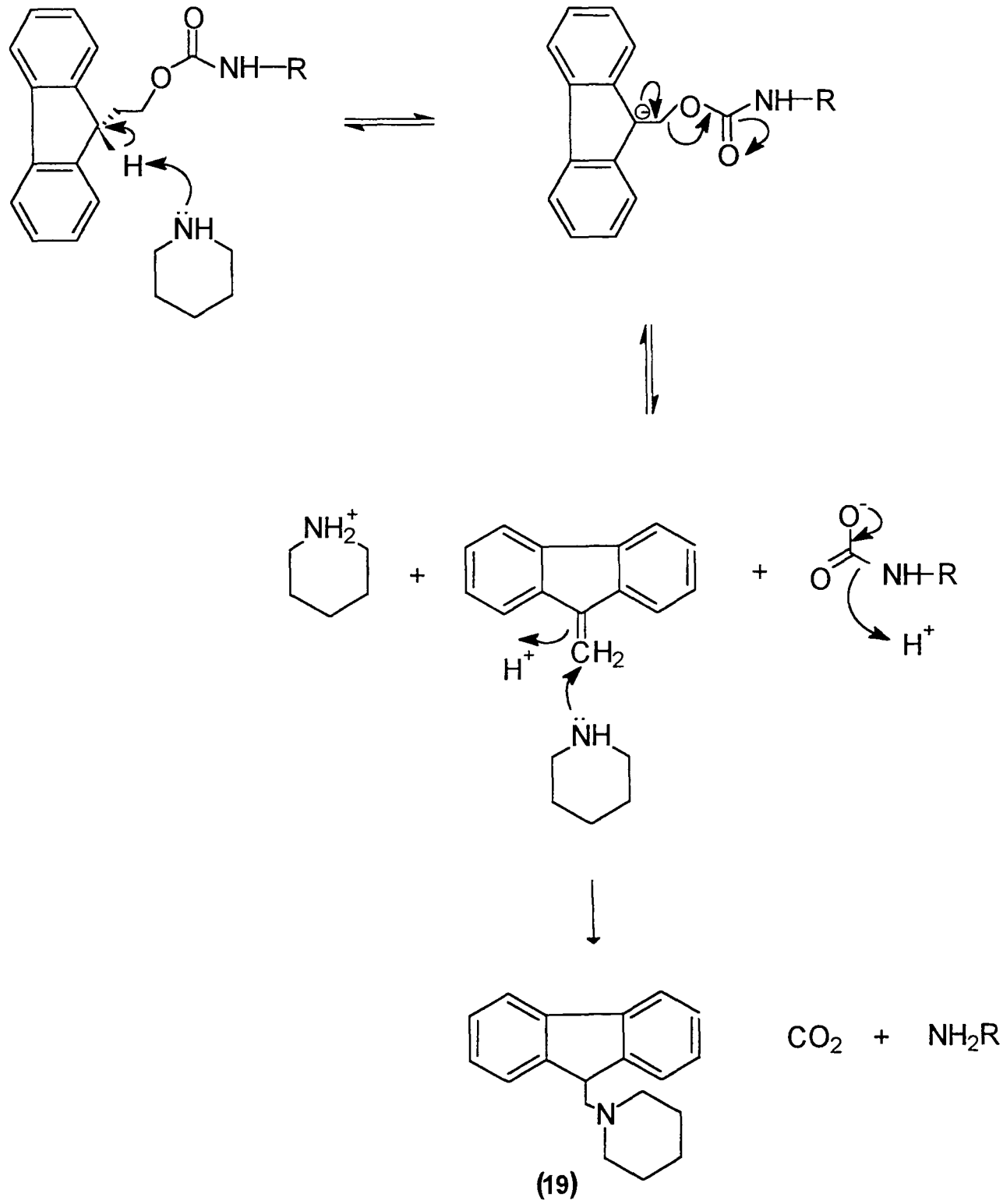

(19)

3.1.4 Amino Acid derivatives: problem species.

One of the residues that was considered a 'problem species' was the arginine residue. The tri-functional guanidino side chain group of Arg, being strongly nucleophilic, could become acylated during the peptide synthesis if not protected. Ideally all three side chain nitrogen atoms should be blocked, however, in practice, the majority of protecting groups only block the ϖ-nitrogen. The 2,2,5,7,8-pentamethylchroman-6-sulphonyl (Pmc) group is the preferred protecting group for arginine, as this gives superior acid lability over the other available protecting groups (such as Mtr) (Ramage and Green, 1987).

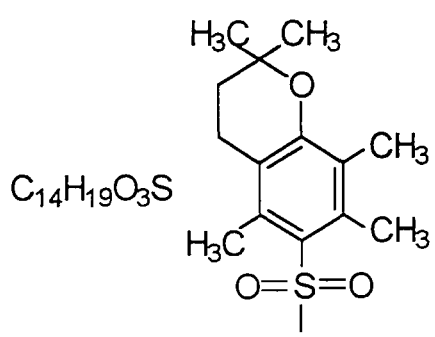

Pmc

Cysteine residues are both nucleophilic and susceptible to oxidation under basic conditions to form disulphide bridges (White, 1967), it was therefore imperative that the sulfhydryl (mercapto) moiety be protected. The triphenylmethyl (trt) (Atherton *et al*, 1985) group being acid labile was used for this purpose.

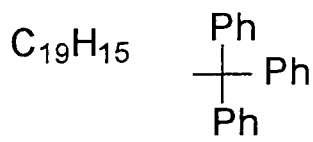

Trt

3.1.5 Spectrometric Monitoring in Continuous-Flow Synthesis.

Spectrometric monitoring of both acylation and deprotection reactions was possible because of the UV-absorbing Fmoc protecting group (Dryland and Sheppard, 1986). In the peptide-bond-forming step, the activated Fmoc-amino acid was taken out of solution and transferred to the solid phase. The introduction of the deprotection reagent caused an initial rapid release of the amine carbamate salt and dibenzofulvene; the latter then reacts further with excess reagent to form the piperidine adduct **(19)**. DMF was used at this stage to wash the resin of any remaining deprotection reagent. The corresponding changes in absorbance were taken as a direct measure of the efficiency of the two reactions (see figure 24).

3.1.6 Qualitative Colour Tests using Ninhydrin

The ninhydrin colour test for residual resin-bound amino groups was used to determine completion of the acylation reaction (Kaiser *et al*, 1970). It was easy and quick to carry out. Whilst some deprotected amino acids do not show the expected dark blue colour typical of free primary amino groups, it provided a seemingly reliable indication of the presence of free primary amino functions on the resin beads. A repeat acylation step was undertaken for any incomplete acylation. This proved necessary for the arginine and alanine residues in the target peptide. The test was only semiquantitative because the amount of amine present was estimated visually from the intensity of the blue colour found both in the solution and on the resin beads. Attempts made in the past (Sarin *et al*, 1981) to make this test quantitative have been generally unsatisfactory.

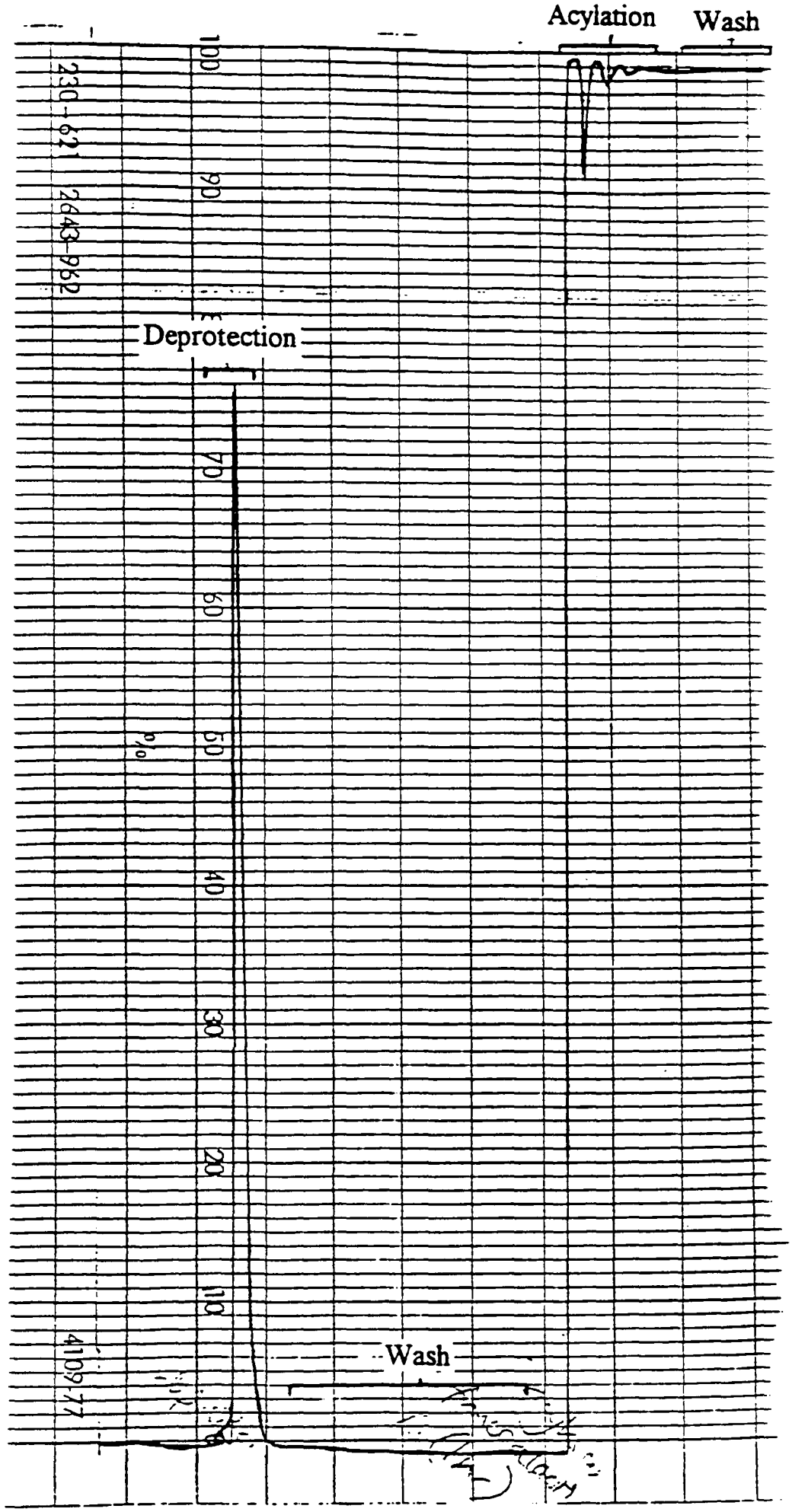

Figure 24: A complete cycle for the acylation of a single amino acid residue.

3.1.7 TFA Cleavage and Deprotection.

Optimum cleavage conditions were very much dependent on the individual amino acid residues present, their number and sequence, the side-chain protecting groups, and the amino acid residue attached to the handle. Both 1,2-ethanedithiol (EDT) and TIS (triisopropylsilane) (Pearson *et al*, 1989) were used as scavengers to trap reactive TFA liberated carbonium ions (figure 25) and thereby prevent them from undergoing deleterious side-reactions with sensitive amino acid residues i.e. cysteine.

Figure 25: Carbonium Ions

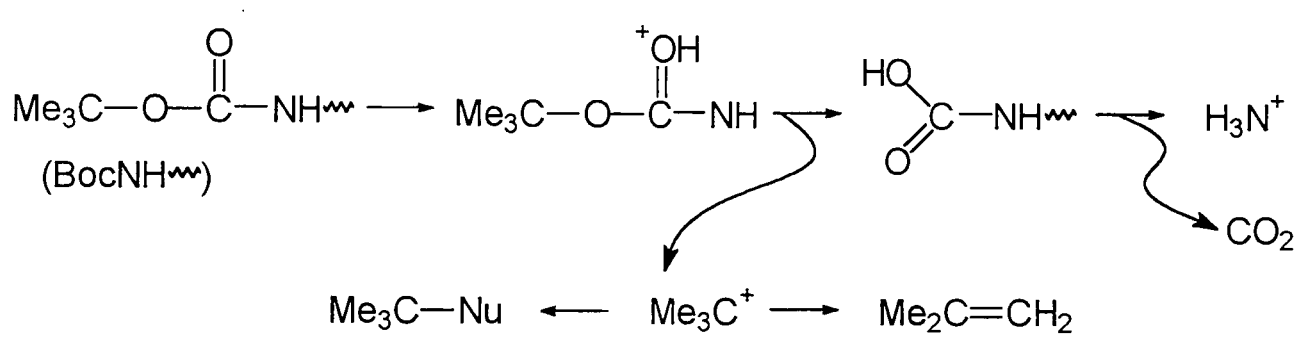

It was interesting to observed that with the thioanisole scavenger, the liberated carbonium ions reassociated with the amino acid side chains. This was evident from the rp-HPLC chromatograph, in which the signal for the peptide appeared significantly further along the chromatograph (non-polar region) then would normally be expected. This aspect of the work is discussed further in section 3.2.

The isolation and characterisation of the peptides and of the peptide-linked intercalators were performed using the following techniques, rp HPLC, MALDI-MS and 2D NMR. The results onbtained from applying these techniques are discussed below.

3.2 Isolation and Characterisation of the Synthesised Peptides.

The inherent complexity of peptide drug substances demands suitable analytical methodology for determining their structure, stability, and purity (and for correlating this information with biological activity). Three methods were employed for the analysis of the synthesised peptides in this work. The first was reversed phase HPLC (rp-HPLC) where fragments differing by a single residue can be isolated as separate components. The second method was mass spectroscopy. In particular, matrix assisted laser desorption ionisation (MALDI) was used for the characterisation of isolated peptides. This technique relies on a special matrix to absorb excess kinetic energy upon firing of the pulse. This effectively leaves the peptide fragment of interest intact allowing its entire molecular structure to be analysed. The third method, 2D NMR (COSY and NOESY), yielded information about the peptide structure, along with information relating to the conformation adopted by the peptide.

3.3 Isolation of the Synthesised Polypeptide using rp-HPLC.

After strong acid deprotection from the resin, the peptides were isolated using HPLC at λ_{max} 210nm (Rivier *et al*, 1984). A gradient made up of an aqueous mobile phase containing TFA (0.1%) and acetonitrile as the organic modifier was used to elute the peptide components. TFA was used throughout this work because of its volatility which enabled easy removal from collected fractions. Additionally, it had little UV adsorption (Winkler, 1987) at the set wavelength which therefore enhanced the sensitivity of detection. Acetonitrile was used as the organic modifier because of its low viscosity and hence reduced back pressure, compared with methanol (Winkler, 1987).

rp-HPLC can also be used to determine peptide homogeneity. In particular for peptides produced by synthetic methods (Rivier *et al*, 1984), since various chemical reactions (e.g., racemisation) can alter the desired biological activity of the final product.

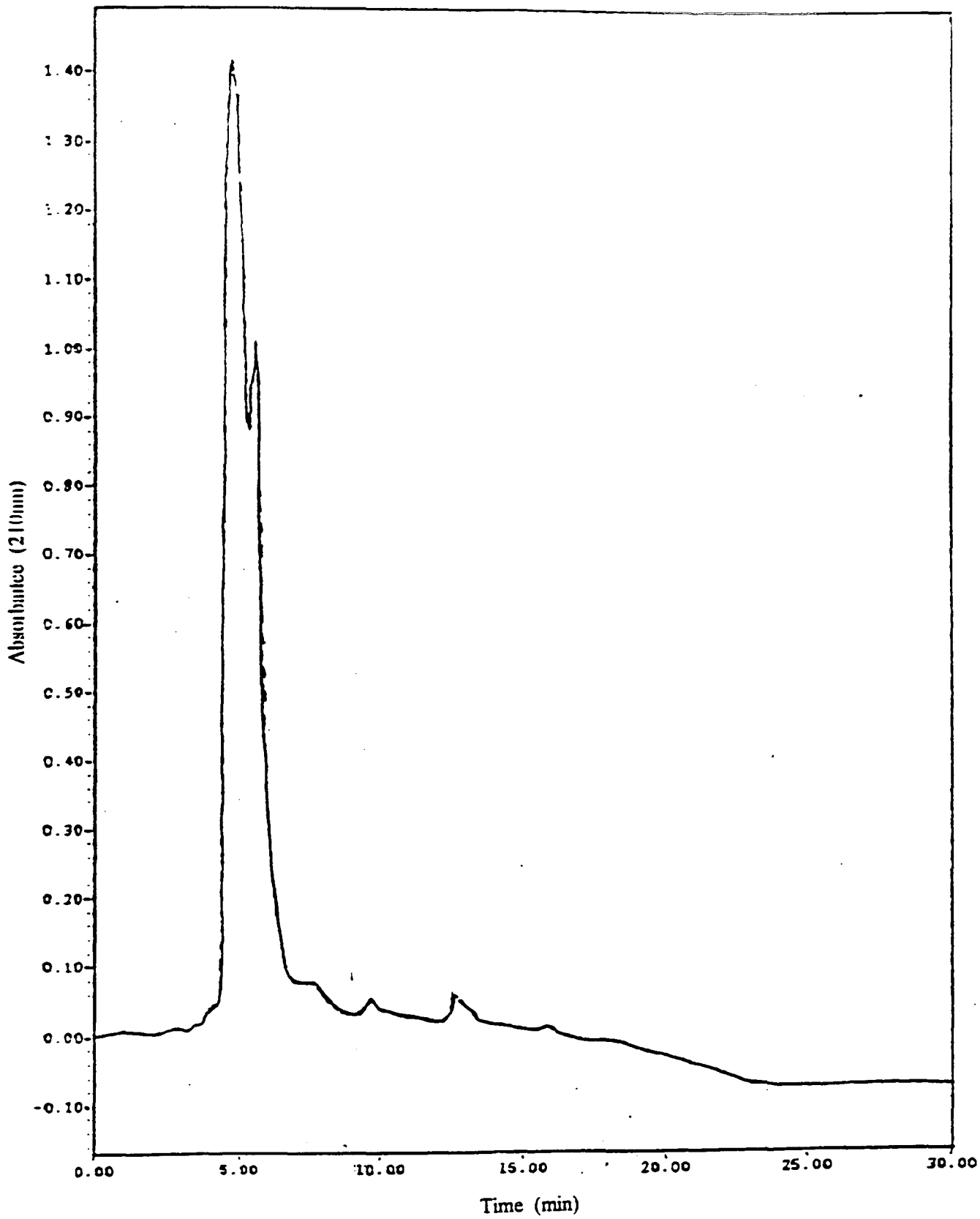

Figure 26: HPLC chromatograph of peptide acid after cleavage from resin using TFA. Reversed phase C_{18} column. Elution with linear gradient over 30 min of 0.1% TFA in CH_3CN and 0.1% TFA in H_2O from 40:60 to 100:0, flow rate 1.0mL/min.

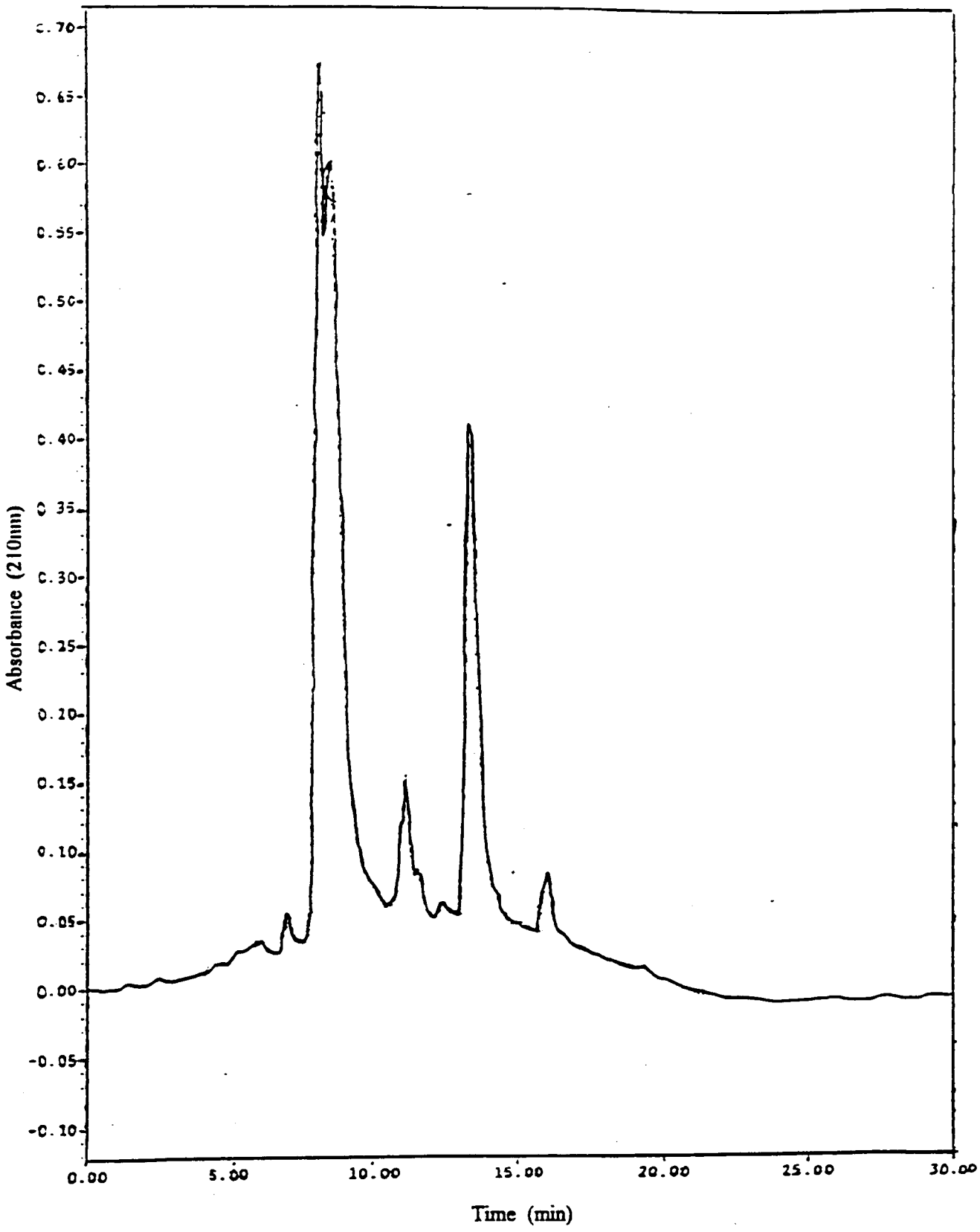

Figure 27: HPLC chromatograph of peptide acid after storage at 0°C in CH_3N/H_2O for three days. Reversed phase C_{18} column. Elution with linear gradient over 30 min of 0.1% TFA in CH_3CN and 0.1% TFA in H_2O from 0:100 to 100:0, flow rate 1.0mL/min.

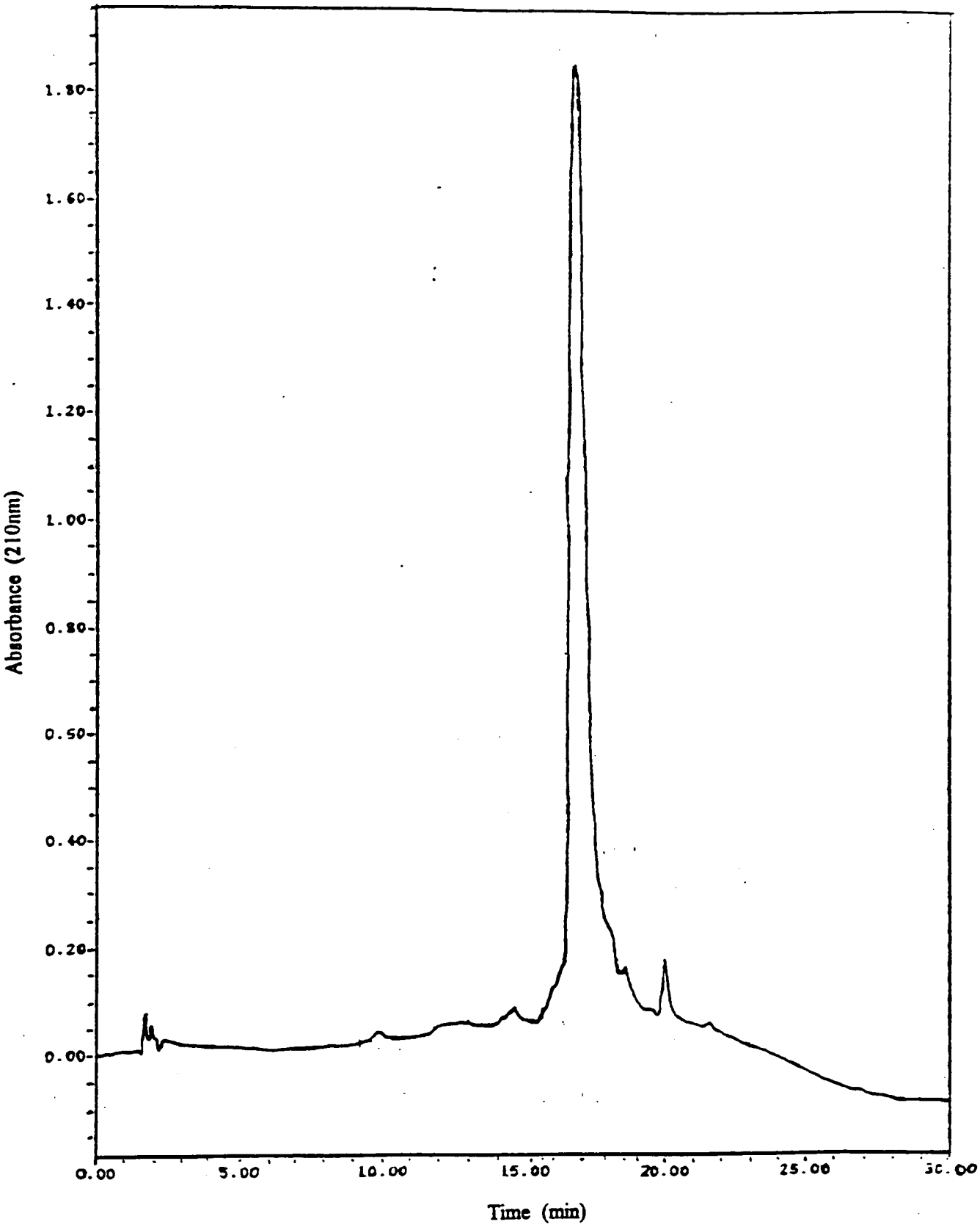

Figure 28: HPLC chromatograph of peptide acid after cleavage from resin using TFA. Reversed phase C_{18} column. Elution with linear gradient over 30 min of 0.1% TFA in CH_3CN and 0.1% TFA in H_2O from 0:100 to 100:0, flow rate 1.0mL/min.

In this work, the stability of the peptides were assessed by reinjecting the isolated peptide sample. Figures 26 and 27 clearly shows the appearance of additional peaks. There are several explanations for this occurring, (a) the peptide may undergo acid catalysed racemisation (b) thiol oxidation of the cysteine residue or (c) the peptide is unstable and undergoes gradual degradation above 4°C. It was found that when stored under nitrogen at -78°C the peptide remained intact hence this was the main method for storage of the synthesised peptides.

Below is a table outlining the results obtained from the HPLC of the two synthesised pentapeptides (also shown below). Figure 28 shows a typical chromatograph of the peptide amide.

H_2N-Ala-Lys-Cys-Arg-Ala-$CONH_2$ (amide)

H_2N-Ala-Lys-Cys-Arg-Ala-COOH (acid)

Table 4: Retention times, eluent and purity for both peptide acid and amide.

Peptide	Retention time /min	Eluent : Acetonitrile/water (%)	Approximate % purity
Amide	17 (total run time 30)	57/43	70
Acid	15.5 (total run time 30)	52/48	70

The retention times for both the acid and amide peptides were found to be very similar, the acid peptide being slightly more water soluble.

3.4 Mass Analysis of the Peptides using MALDI-MS.

The characterisation of the synthesised peptides were carried out using a matrix assisted laser desorption ionisation mass spectrometer (MALDI-MS) (Hillenkamp and Karas 1990; Karas *et al*, 1990). The mass analyzer used in this work was a Lasermat (Finnigan MAT Ltd., Hemel Hampstead, UK).

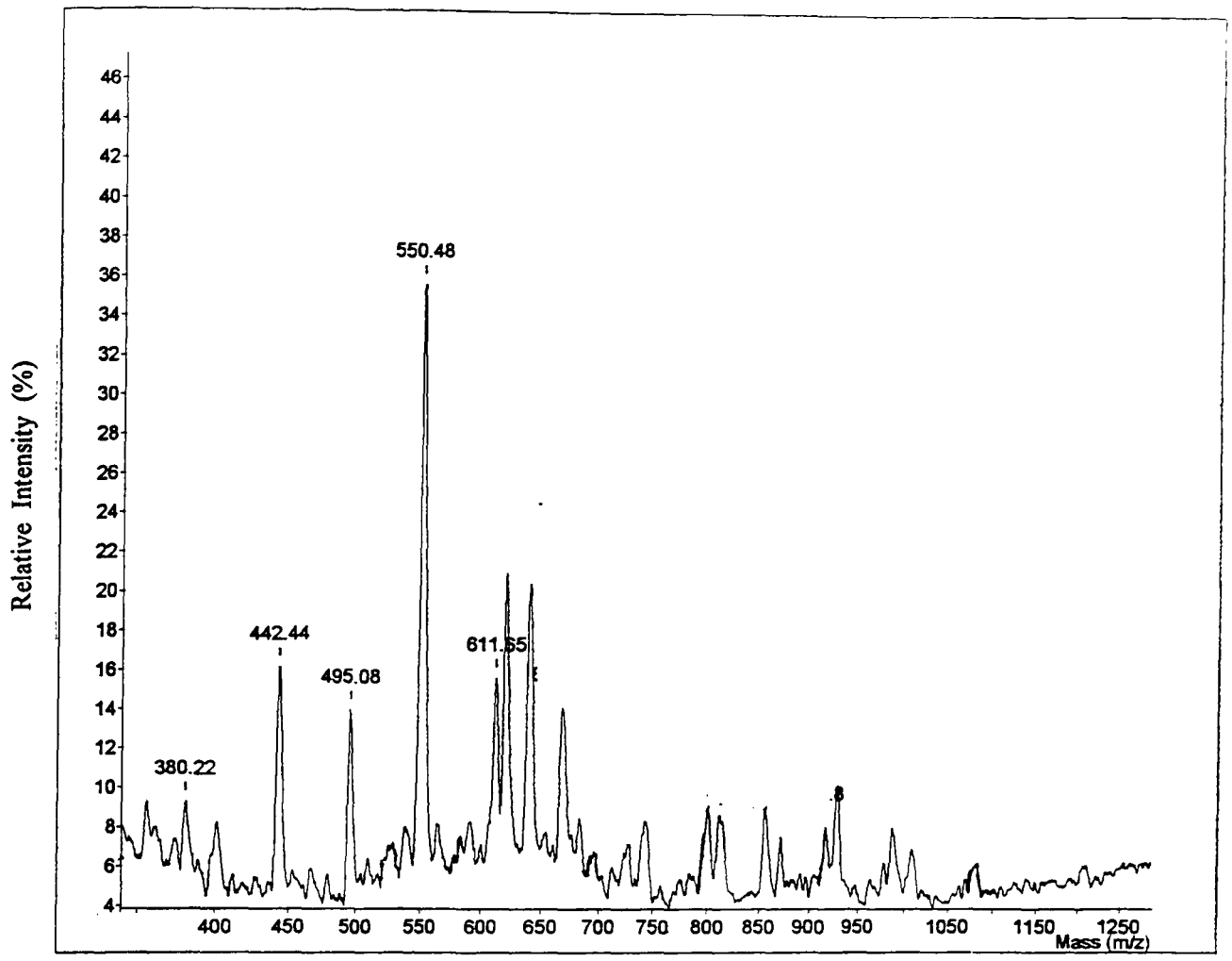

Figure 29: Positive-ion MALDI mass spectrum of peptide acid (H_2N-A-K-C-R-A-CO_2H). Molecular ion is seen as m/z 550.

Figure 29 shows a MALDI-MS spectrum of a peptide acid, following isolation by HPLC. Notice that signals below 442 MW correspond to those of the ACH matrix (Beavis *et al*, 1992), so consequently any peptide fragments occurring in this region will be indistinguishable from those of the matrix. Figure 29 shows a signal at m/z = 558.48 which coincides with the peptide fragment of interest. The smaller of the two signals has a molecular weight of 621.51, a difference greater of 71 D. Essentially, the 71D coincides with an alanine residue. One obvious explanation for a repeat addition of an alanine residue stems from following the cleavage of the Fmoc protecting group from the initial resin-attached alanine. The subsequent concentration and base strength of the primary amine resulting from the first Fmoc cleavage was therefore a problem. This was resolved by allowing the resin to swell in DMF (Pugh *et al*, 1992) for at least 45 minutes before coupling the first residue. The swelling of the amino-component reduced the strength of the base per unit volume on the resin hence preventing any unwanted Fmoc deprotection.

It was also noted that in the presence of low abundance of analyte and relatively high levels of contaminants, it was necessary to find "good spots" on the probe tip of the MALDI slide. In addition poor crystalline peptide samples could caused a combination of reduced signal intensity and peak broadening (Mock *et al*, 1992).

One disadvantage of using the dried-drop preparation method in preparing the slides for MALDI was the nonhomogeneous surfaces which led to signal variations over the surface of the target. And because of the nonhomogeneous crystallisation process, there was little correlation of the signal intensity with the amount of sample analysed (Hillenkamp and Karas, 1990). Consequently, because of the intra- and intersample heterogeneity, a slightly different laser irradiance was required to reach the thresthold of ion production on different spots of the same preparation or upon repetitive analysis of different preparations of the same sample.

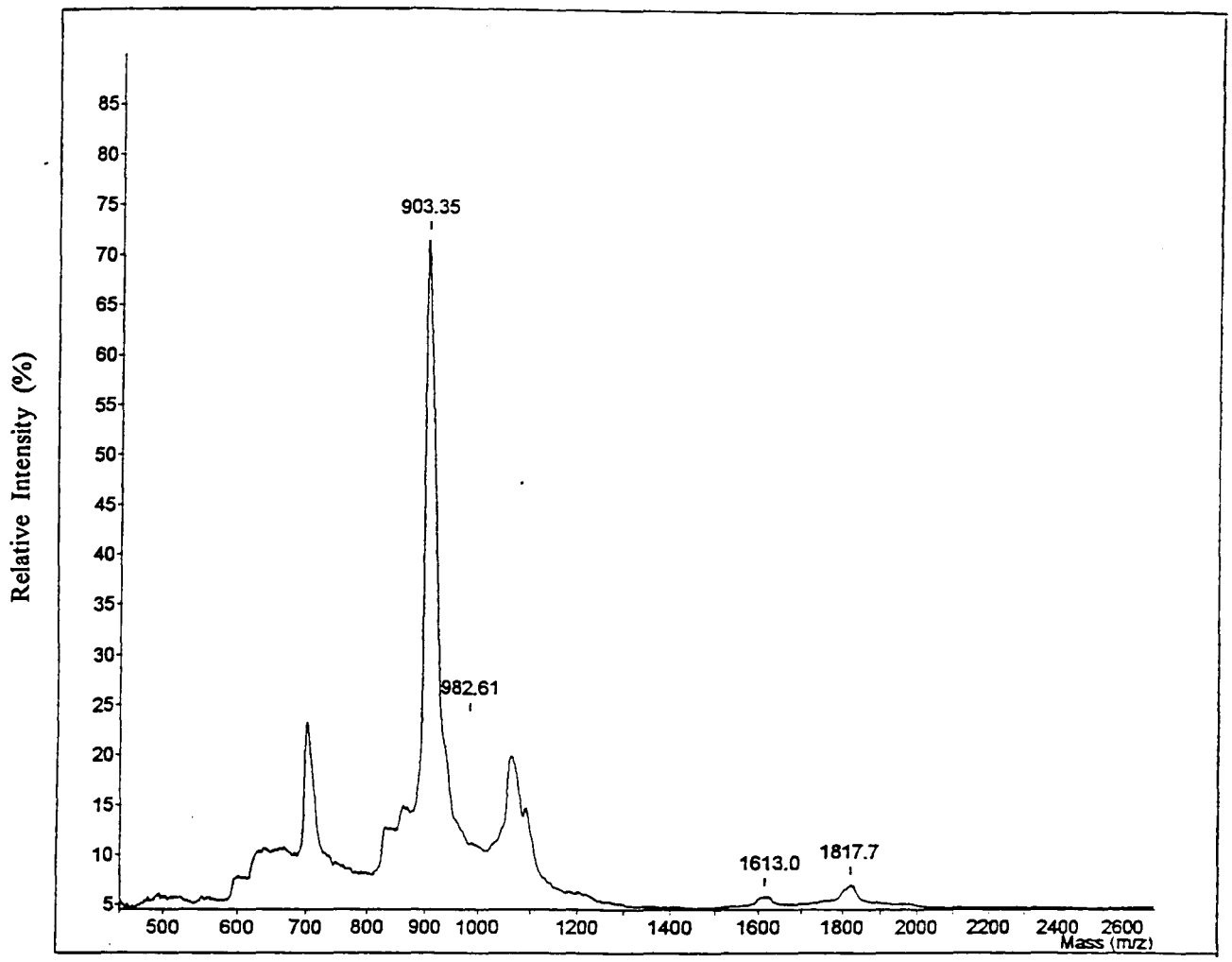

Conjugate **1D**

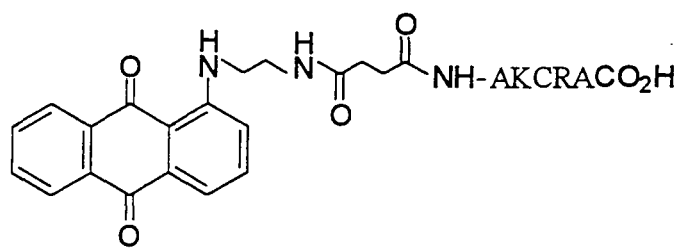

Figure 30: Positive-ion MALDI mass spectrum of intercalator (**D**)-linked peptide (**1**). Molecular ion is seen as m/z 903.

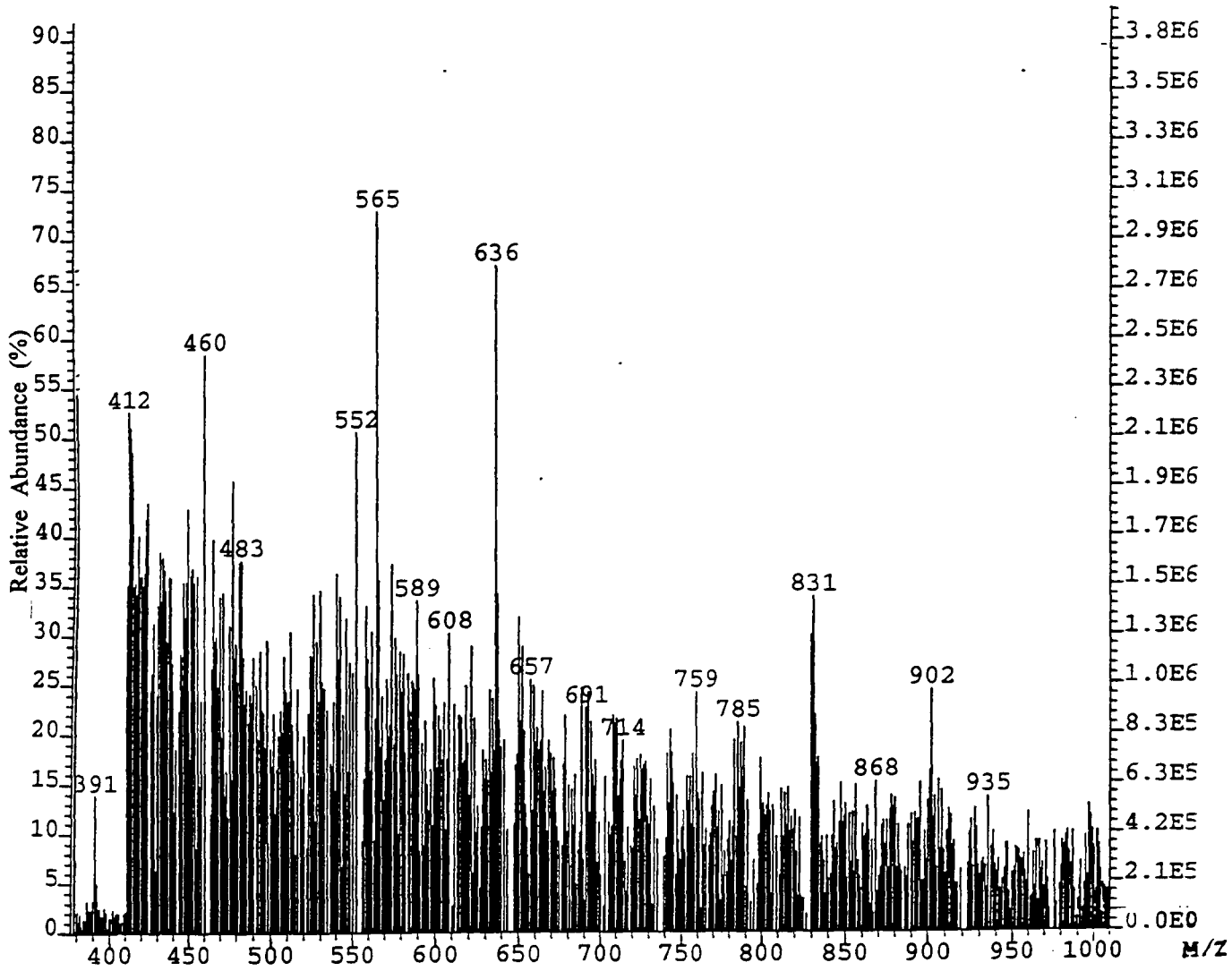

Figure 31: FAB mass spectrum of peptide amide (H_2N- A-K-C-R-A-$CONH_2$). Molecular ion seen as m/z 565.

Nevertheless, despite the poor shot to shot as well as sample to sample signal reproducibility and an ion production process which was strongly dependent on laser fluence, MALDI was a powerful tool for the analysis of the synthetic peptides.

Figure 30 shows a relatively 'clean' signal for one of the many synthesised intercalator-peptide molecules (intercalator **D** linked-peptide acid). It has been estimated from HPLC chromatographs and MALDI spectra that the purity of the hybrid ligands used in the biological evaluation (chapter 5) is within the 90-95% range (see also T. Ijaz, 1998).

For comparison, a FAB-MS of the same conjugate was also obtained (figure 31). Notice that with this technique extensive fragmentation was observed. So by using the matrix assisted technique, minimal fragmentation was obtained and hence a very high success rate in the characterisation of peptides and intercalator-linked peptide ligands was achieved.

3.5 2D NMR of the Peptide.

In order to record NMR spectra of sufficient quality for detailed NMR structural studies, sample concentrations of at least 1mM in 0.5ml solution were prepared (Wuthrich, 1990). The peptide was required to be stable for at least 24 hr at room temperature.

Figure 32 shows a small region of homonuclear 2D ^{1}H NMR COSY spectrum of the peptide amide. The NMR peaks are spread out along the two frequency axes and they are therefore quite well separated, CαH protons typically resonate between 3 and 5ppm and methyl groups between 0 and 2ppm. Differences in chemical shifts between two amide protons, for example, are caused by structural differences in their vicinity. However, no clear correlation between local structure and chemical shift has yet been shown (Pardi *et al*, 1983; Gross *et al* 1988).

The table below shows typical chemical shifts (ppm) observed with each of the residue present in the synthesised pentapeptide.

Table 5: Chemical shifts for the four amino acid residues.

Amino acid	H^N /ppm	H^α	H^β	H^γ	H^δ	H^ε
Ala (A)	8.3	4.5	1.6			
Arg (R)	8.1	4.5	1.9	1.8	3.6	
Cys (C)	8.4	4.8	3.2			
Lys (K)	8.5	4.5	1.9	1.5	1.8	3.0

3.5.1 Nuclear Overhauser Effect (NOE).

A second even more important source of structural information stems from the fact that the protons continuously exchange their nuclear magnetisation with one another, at rates that depend on the sixth power of their interspatial distance, r^6. This magnetisation exchanger is often refered to as the nuclear Overhauser effect (n.O.e) (Noggle and Schirmer, 1971) and the most convenient method for measuring it is called the NOESY (NOE spectroscopy) experiment (Jeener *et al*, 1979). In contrast to all other NMR parameters ^1H-^1H distance measurements by NOE experiments can be directly related to the peptide conformation. Short distances (<2.5 Å) always yield substantial NOEs, medium-range distances (2.5 - 3.5 A) yield weaker NOEs, whereas distances larger than 3.5Å are often two weak to be observed in the short mixing time NOESY spectra.

Figure 33 shows a NOESY spectrum of the hexapeptide amide. The presence of through space interactions were indicated by cross-peaks, a good indication of helicity formation. The amino acid residues that are considered to favour helical conformation are the alanine, lysine and cysteine all found in the peptide sequence, whereas arginine is indifferent. Tyrosine, threonine, glycine, serine and proline, absent from the hexapeptide amide sequence, all break up helical formation (Creighton, 1983).

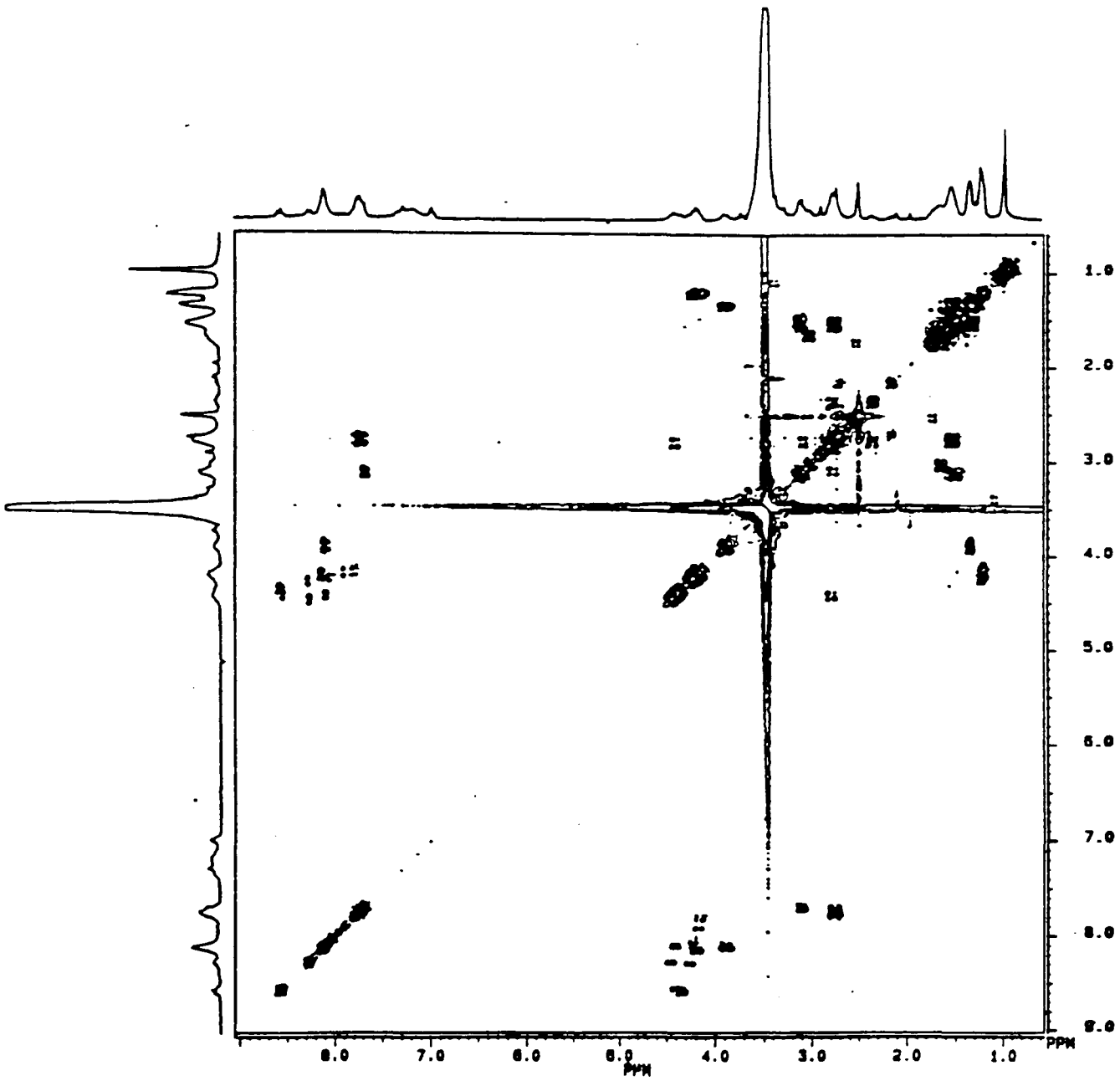

Figure 32: Partial ^{1}H-^{1}H COSY spectrum of NH_2-A-R-C-K-A-NH_2 in dimethylsulfoxide.

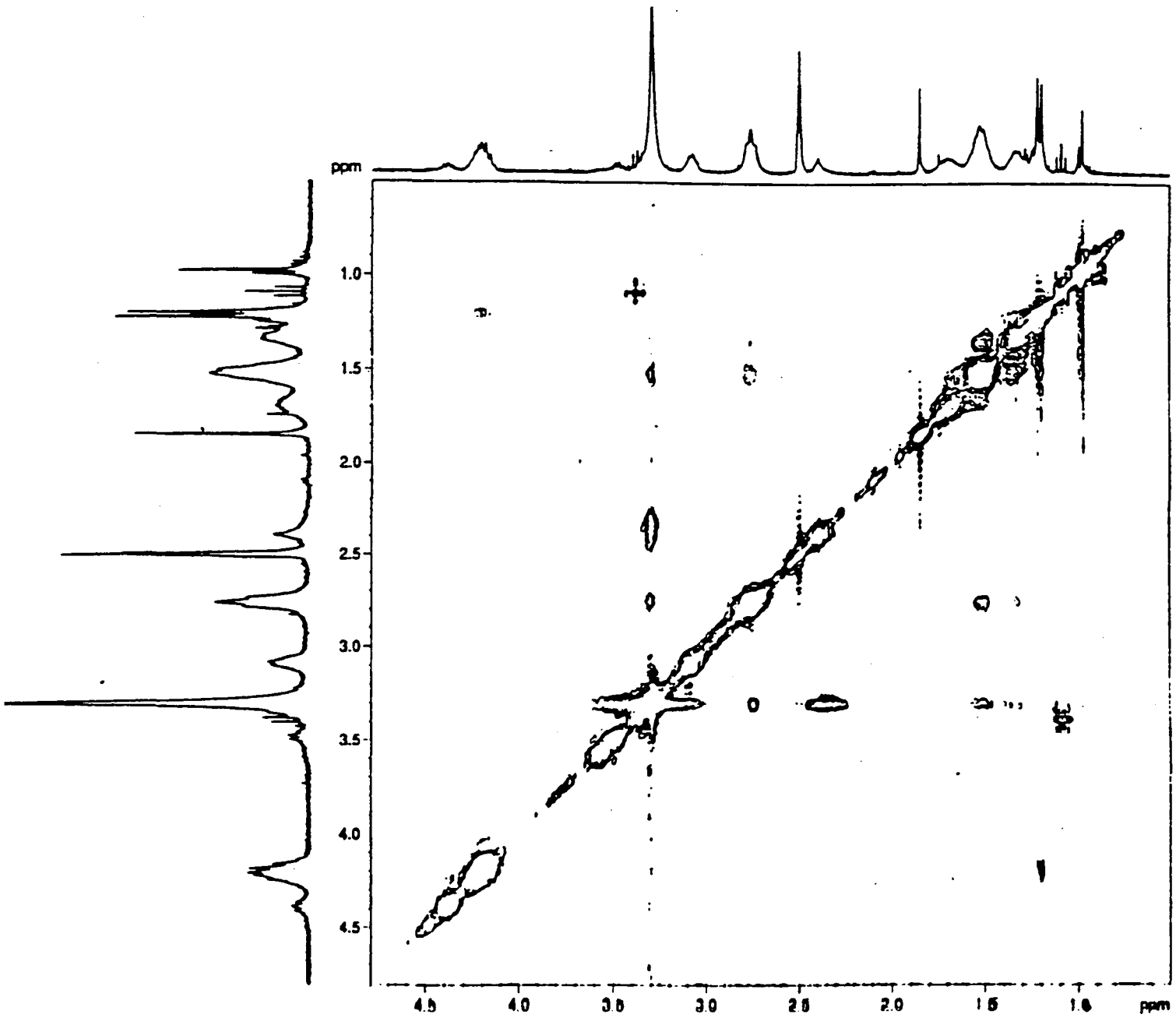

Figure 33: Partial ^{1}H-^{1}H NOESY spectrum of NH_2-A-R-C-K-A-NH_2 in dimethylsulfoxide.

Similar analysis for the other six peptides used in this work was observed (T. Ijaz, 1998). The remainder of this thesis focuses on the *in vitro* biological evaluation (Chapter 5) of the peptides and intercalator-linked peptide ligands.

Chapter 4

Synthesis of Intercalator-linked Peptide Complexes

This chapter describes how the intercalator is coupled onto the amino terminus of the peptide to form the intercalator-linked peptide molecule.

4.1 Synthesis of Intercalator-linked Peptide Ligands.

The sequence-specific recognition of double-stranded DNA has been the subject of extensive studies. The design of ligands specific to a given DNA sequence is an important area of research, as such ligands have the potential to control transcription (Chuang *et al*, 1984) and replication (Fox and Smith, 1990). Research to date has mainly focused on the recognition and modification of double-stranded DNA by oligonucleotides containing both natural and synthetic base pairs, these bind into the major groove of DNA by forming Hoogsteen hydrogen bonds, resulting in a triple helix structure (Mouscadet *et al*, 1994).

In this chapter, the synthesis of the AP-1 basic region-intercalator hybrid peptide is described. This molecule has been designed to combine the minimum features of the peptide necessary for recognition of the consensus site with the known binding enhancement of an interacting anthrapyrazole moiety. In this way it is hoped to achieve both tight binding and a high degree of molecular recognition with a comparatively small peptide.

In the section below, two different methods for the synthesis of novel peptide intercalator ligand have been described. Each route involves several reaction steps and of high yielding, and can easily be adapted to incorporate other linker/intercalator combinations.

4.1.1 Coupling via formation of a reactive Aziridinium Ion.

A model system, glycine methyl ester hydrochloride **(20)** was employed in place of the actual peptide in the first instance (figure 34). This model system successfully demonstrated that the coupling via the aziridinium was viable in the presence of a base, *N, N*-diisopropylethylamine (DIEA). The high reactivity of the aziridinium ion made it susceptible to even very weak nucleophiles such as methanol **(21)**.

Figure 34: Model system for coupling

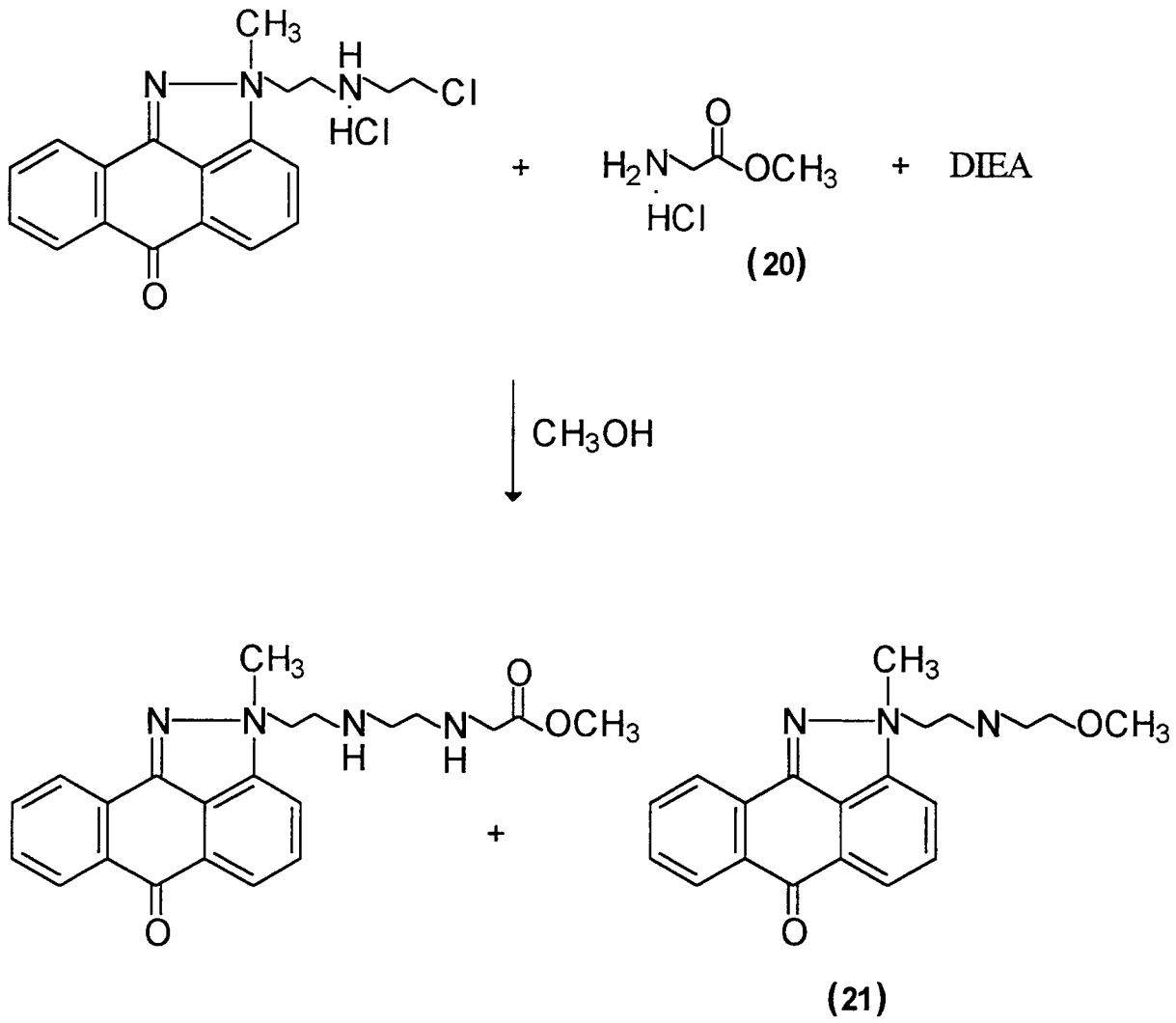

The coupling between the resulting aziridinium ion and the amino terminus of the peptide sequence was carried while the peptide was still attached to the resin (figure 35). Any excess drug and contaminants can then be filtered-off on washing the resin through a sintered glass funnel. Once formed the intercalator-peptide was cleaved from the resin-support using TFA, dried and analysed. HPLC and MALDI-MS techniques were then used to characterise the hybrid (chapter 3).

Figure 35: Coupling via a reactive aziridinium ion.

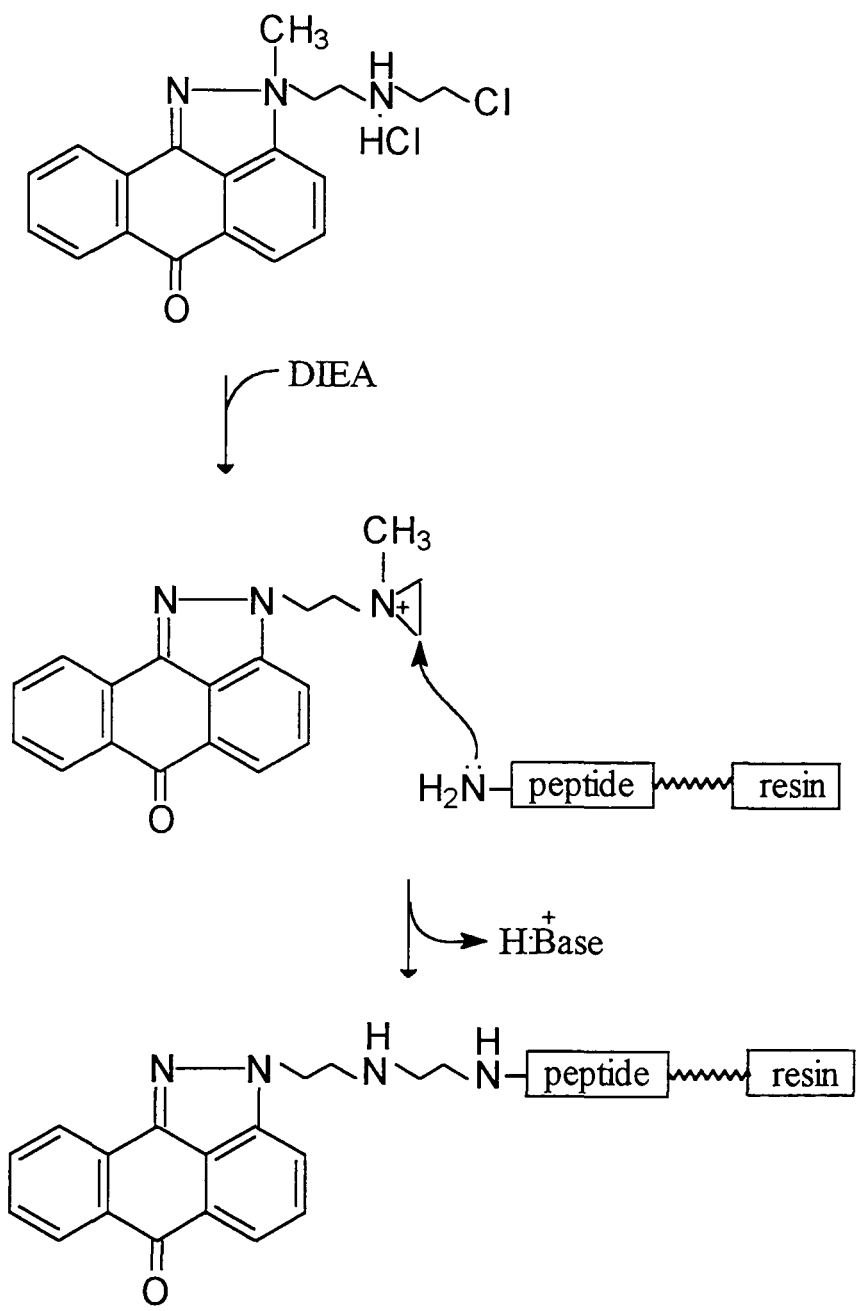

4.1.2 Coupling using a PyBOP Reagent.

The second method of peptide acylation makes use of benzotriazole-1-yl-oxy-tris-pyrrolidino-phosphonium hexafluorophosphate (PyBOP), the same coupling reagent used in solid phase peptide synthesis. The carboxylate group on the anthrapyrazole was pre-activated using PyBOP (figure 36) prior to contact with the amino functionality of the peptide sequence. This method proved to be highly successful, both in terms of yield and simplicity. As a result the majority of the intercalator-peptide complexes were synthesised using this latter method.

Figure 36: Mechanism for PyBOP coupling.

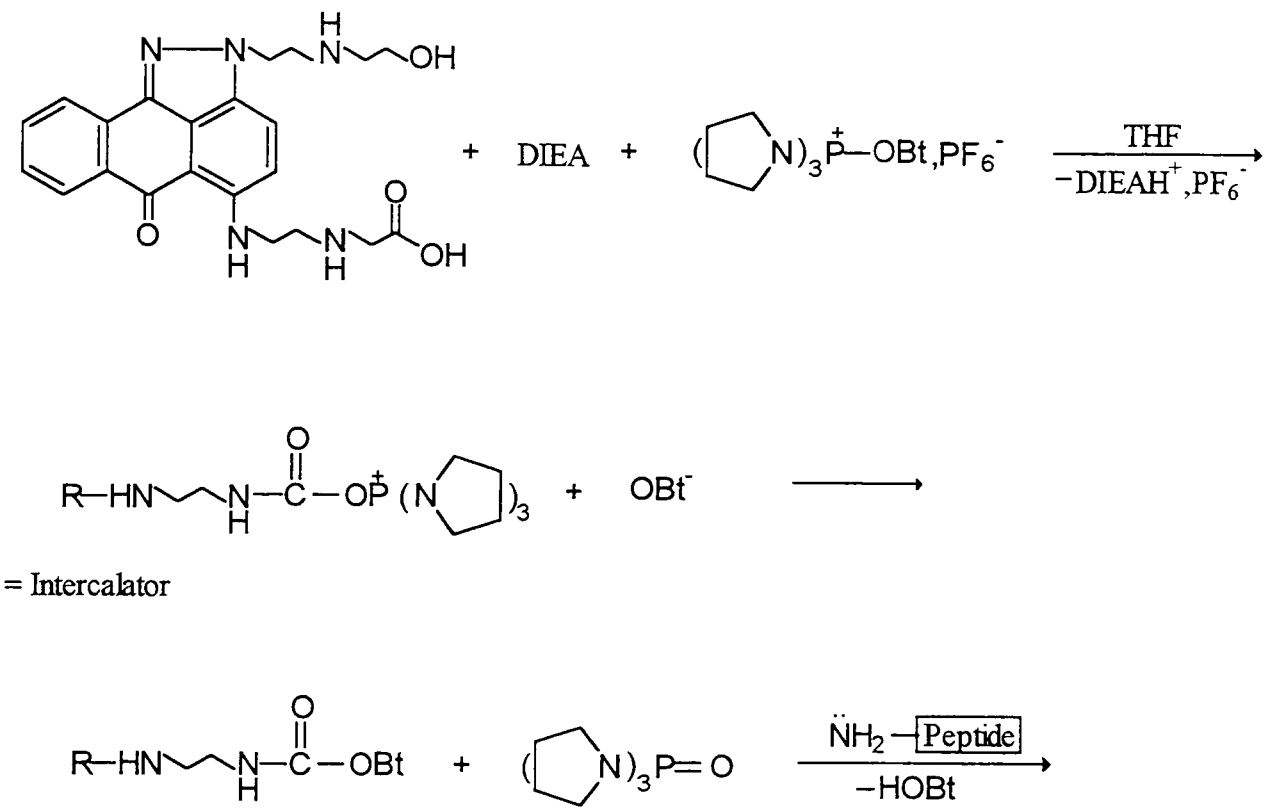

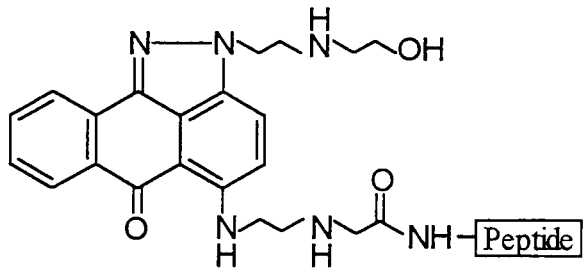

As well as synthesising a series of anthrapyrazole-linked peptide ligands, similar synthetic routes were used to produce a series of anthraquinone-peptide ligands (see figure 37 and T. Ijaz, 1998), these compounds were also tested for their biological activity. Both the anthrapyrazole and anthraquinone compounds together with their respective peptide complexes were tested *in vitro* for their inhibition of AP-1 transcription factor protein from binding to AP-1 DNA consensus sequence (chapter 5).

Figure 37: Shows two anthraquinone derivative-linked peptide complexes (see table 7 for the peptide sequences used).

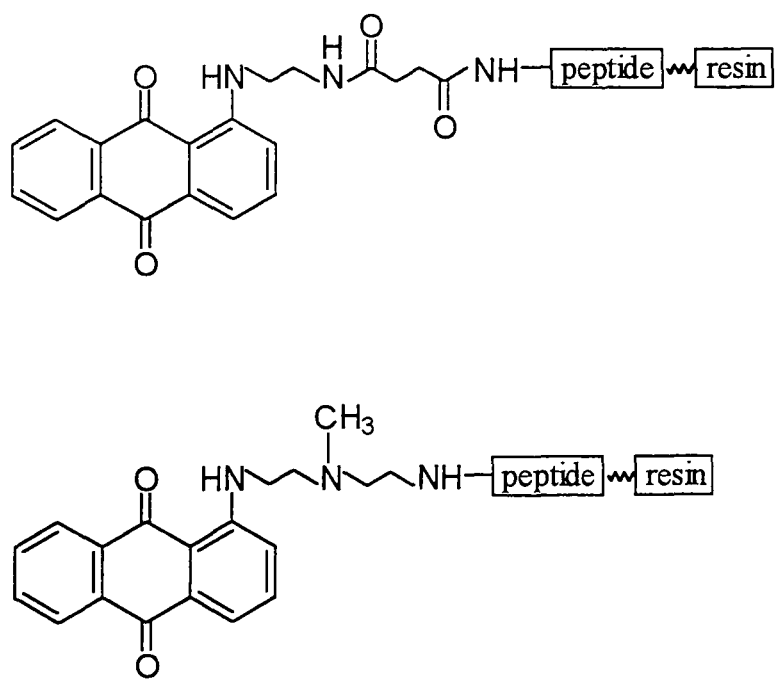

Chapter 5

Cell free Biological Evaluation and DNA Binding Studies

This chapter assesses the binding of the intercalator-peptide ligand to the AP-1 DNA consensus oligonucleotide *in vitro* using an electrophoretic mobility shift assay (EMSA). For assessing the nature and the binding affinity of the intercalator-peptide complex, two separate methodologies using UV/vis spectrophotometry and fluorimetry are used.

5.1 Introduction.

Recently many research efforts have been aimed at targeting specific sequences in DNA using synthetic ligands with the idea of designing both drugs and molecular probes for DNA polymorphism. The selective inhibition of transcription from particular sequences by the specific targeting of a ligand, in other words the control of gene expression, has become a very attractive and productive research area (Neilsen, 1991)

Many groups have described a strategy to reach this objective with the common and ultimate aim of designing agents which can effectively read DNA in a manner analogous to regulatory proteins. Among the various approaches, oligonucleotides capable of recognising DNA via the formation of triple helices are described (Mouscadet *et al*, 1994).

In this thesis, the synthesis of novel AP-1 base region-intercalator hybrid peptide molecules has been attempted. AP-1 was chosen in particular because of its very unique and specific mode of binding and because of the potential for redox control of its binding. The main features of this molecule combine the peptide necessary for the recognition of the AP-1 DNA consensus site with the DNA binding affinity of an intercalating moiety. In this work, the effect of the synthesised intercalator-peptide molecules on the binding of the AP-1 transcription factor protein to the AP-1 consensus was determined by an electrophoretic mobility shift assay. In support of this, the mode and binding affinity of the hybrid molecules for DNA was determined by spectrophotometry and fluorimetry. All three techniques are described below.

5.2 Binding of the Intercalator-Peptide to the AP-1 DNA consensus sequence as determined by PAGE.

The gel electrophoresis mobility shift assay (Fried, 1989; Revzin, 1989; Hendrickson, 1985) was chosen for the study of protein-DNA interactions. This assay provided electrophoretic resolution of protein-DNA complexes from each other and from free DNA. The advantages of the electrophoresis DNA-binding

assay include its speed, simplicity and flexibility. Binding of proteins that interact weakly with DNA, or of proteins that for other reasons fail to be detected in other assays (i.e. a filter-binding assay), can generally be detected by gel electrophoresis. One other major advantage is that highly purified protein or DNA samples are unnecessary (Strauss and Varshavsky, 1984; Varshavsky, 1987). For example, in this work, sequence-specific DNA binding of recombinant transcription factors as well as cell lysates were shown.

5.3 The affinity and mode of binding to DNA as determined by UV/vis Spectrophotometry and Fluorimetry.

In order to evaluate DNA-binding of the compounds prepared, two methods were selected. Both methods allowed the nature of binding and affinity of the ligand for DNA to be determined. Changes in the UV visible and fluorescence absorbance properties of the ligand can occur upon its binding to DNA (Neidle, 1978; Waring, 1981). Methods which monitor such changes were also used here.

5.3.1 Effect of Intercalator-Peptide on the thermal denaturation properties of DNA.

When double-stranded DNA molecules are subjected to an increase in temperature or extremes of pH, the DNA denatures to give two single-stranded molecules as a result of the rupturing of the hydrogen bonds in the double helix. On denaturation there is an increase in absorbance of the DNA solution, so the change in absorbance can be used to monitor denaturation (Marmur and Doty, 1962). The temperature at which half the total increase in absorbance has occurred is known as the melting (or transition) temperature (T_m).

By measuring the change in absorbance with temperature of the DNA solution at the DNA λ_{max} (260nm), in the presence and absence of the ligand, the ΔT_m (difference in T_m's) can be determined. This is a measure of the stability of the ligand/DNA complex. The increased stability imparted to the DNA helix by the ligand is a measure of the affinity of binding. Furthermore the stability of the DNA helix is also affected by changes in the base composition; DNAs with high

guanine-cytosine content have higher T_m's than DNAs with high adenine-thymine content (Marmur and Doty, 1962).

5.3.2 Effect of Intercalator-Peptides on the binding of ethidium to DNA.

By using a compound which is known to intercalate into DNA and which has a large change in quantum yield upon release from DNA (such as ethidium bromide), it was possible to examine the DNA binding of the compounds synthesised in this work using fluorescence spectroscopy by competition displacement of ethidium from DNA. This type of competitive study provides information on both the nature of interaction of ligands with DNA and the relative affinity of the drugs for DNA.

The interaction of ethidium bromide with DNA has been extensively reviewed, (Waring, 1981; Yielding *et al.*, 1983). Ethidium bromide has been shown to bind to DNA by intercalation. When binding to DNA the quantum yield of the fluorescence of ethidium is enhanced (Le pecq and Paoletti, 1967). Hence if a compound binds to the same site in the DNA helix as ethidium the drug will compete with ethidium for that site. Provided the compound, in the absence of DNA, has no effect on the fluorescence of ethidium, it is possible to monitor the effect of that compound on fluorescence enhancement.

RESULTS

5.4 Specificity and Redox Sensitivity of the c-Jun homodimer protein for AP-1 DNA consensus sequence.

Specificity of c-Jun homodimer protein for the AP-1 DNA consensus sequence was demonstrated by competition experiments. Two such experiments were performed, one with unlabelled target (AP-1) DNA consensus sequence as competitor (figure 38) the other with unlabelled (SP-1) DNA consensus sequence as the competitor (figure 39). Figure 39 showed that with increasing concentration of unlabelled SP-1 (0.11-0.86ng) the binding of the AP-1 protein to the labelled AP-1 DNA consensus sequence was unaffected. However, with increasing concentration of unlabelled AP-1 DNA consensus sequence a reduction in band intensity was observed.

Cell lines treated with phorbol diesters such as TPA (12-*O*-tetradecanoyl-phorbol-13-acetate) can express elevated levels of Fos and Jun proteins. Treatment of cultured cells with TPA was shown to lead to a rapid 3- to 4-fold increase in TRE binding activity by the AP-1 protein. This has been observed previously and it is suggested to be due to a post-translational modification (Angel *et al*, 1987). The exact mechanism responsible for the increase in TRE activity shortly after TPA treatment remains to be determined. Figure 40 shows that a TPA dissolved in DMSO as a vehicle, was responsible for elevating AP-1 binding, probably by an increase in both *fos* and *jun* expression as previously shown by Barber and Verma (1987).

In figure 40 it can be seen that cell lysates 2 and 4 (which were TPA treated cell lines) displayed elevated concentrations of AP-1 binding proteins compared with untreated equivalent cells not TRE treated. Both these cell lysates were used to investigate the specificity of the intercalator-peptide for the AP-1 DNA consensus sequence (see section 5.13).

Figure 41 shows that the binding of c-Jun homodimer recombinant protein was highly specific for AP-1 DNA wild type, and that no binding was observed with

mutant AP-1 DNA. The redox sensitivity of the AP-1 binding to its oligomer consensus sequence was subsequently demonstrated by direct oxidation of the protein. This was accomplished using oxygen which was allowed to pass through a sample containing the Fos/Jun proteins at 4°C. A similar set- up using nitrogen gas was investigated. It was clear from figure 43 that the oxygenated sample displayed a reduction in AP-1 protein-DNA complex formation.

Figure 43 indicates that binding of c-Jun homodimer protein to AP-1 oligonucleotide was very much enhanced by a reducing environment. This was consistent with the results described previously (Xanthoudakis and Curran, 1992). Dithiothreitol (DTT) was used as the reducing agent in this assay. It was observed that c-Jun protein was highly selective for the AP-1 DNA consensus sequence but not for the SP-1. The presence of a faint band corresponding to c-Jun-DNA complex even in the absence of DTT can be accounted for by the presence of some DTT in the storage buffer of the commercially available c-Jun protein. However, whether or not bands of DNA-protein complexes are observed can sometimes be dependent on many other factors including intrinsic stability of the complex itself, the salt concentration and temperature within the gel and the total time of electrophoresis. Any DNA from complexes which dissociate during analysis will trail behind the free DNA band, forming a 'smear' between the complex and the unbound DNA bands. For an example, see figure 40.

Figure 44 demonstrates that even in a crude lysate extract, specific binding of AP-1 heterodimer protein did still occur as has also been observed previously (Strauss and Varshavsky, 1984; Varshavsky, 1987). This was shown by a supershift in which HeLa cell extract was incubated with ^{32}P-labelled AP-1 DNA consensus sequence and AP-1 antibody. The presence of specific antibodies during binding reactions was used here as a form of identification of protein complexes (Kristie and Roizman, 1986). Notice that no supershift was observed with the ^{32}P-labelled SP-1 DNA consensus sequence, an indication of the lack of binding of AP-1 antibody for the SP-1 protein-DNA complex.

5.5 The effect of Anthrapyrazole and Anthraquinone derivatives on the binding of AP-1 protein to AP-1 DNA consensus sequence.

In this work ^{32}P-labelled DNA fragment containing the putative target site AP-1 DNA consensus sequence was incubated with a cell extract containing AP-1 proteins and was then subjected to the electrophoretic mobility shift assay (EMSA). The transcription factors used in *in vitro* systems were derived from extracts of HeLa cell nuclei as previously described by Shapiro *et al*, 1988; Dignam *et al*, 1983. However, because nuclear factors are likely to contain both sequence-specific transcription factors and sequence-independent DNA binding proteins, upon gel electrophoresis, high molecular weight complexes formed between the AP-1 DNA consensus sequence and specific as well as nonspecific binding proteins which were retained near the loading wells. This was subsequently resolved by preincubating the nuclear fractions with poly (dI-dC) DNA prior to adding the AP-1 DNA consensus sequence, which effectively removed the non-specific high molecular weight proteins. The highest practical concentration of protein used in this work was dictated by a combination of the availability of specific reagents, the detection limits of the assay and to some extent by the solubility of the intercalator-peptide conjugates.

For comparison and as a control, ethidium was also tested for its effect on the binding of AP-1 protein to the AP-1 DNA consensus sequence. It was observed that at 20:1 (ethidium:DNA) almost complete inhibition of AP-1 protein binding was accomplished, (see figure 45). In contrast, with some of the synthesised anthrapyrazole/anthraquinone intercalators, little or no inhibition of AP-1 protein from binding to AP-1 DNA was detected, even at concentration ratios of 800:1 (APZ:DNA). An example of such an intercalator is **A** (figure 46), see table 6 for other intercalators investigated. Figure 47 shows an example of an intercalator (**D**) which clearly does display some inhibition of AP-1 protein from binding to AP-1 DNA but only at a high (800:1) APZ:DNA ratio.

5.5.1 The effect of Peptide units on the binding of AP-1 protein to the AP-1 DNA consensus sequence.

It was observed that peptide **1** (figure 48) had no effect on the binding of AP-1 protein to AP-1 DNA consensus sequence even at concentration ratio of 8000:1 (peptide:DNA) (see table 7 for results of other peptides). This can be seen as a direct measure of the binding affinity of AP-1 protein for AP-1 DNA. However, inhibition was observed with peptides **4**, **5**, **6** and **7** all containing greater numbers of basic residues, such as Cys, Lys and Arg. For an example see figure 49.

5.5.2 The effect of Intercalator-Peptide conjugates on the binding of AP-1 protein to AP-1 DNA consensus sequence.

Table 8 contains a list of all the intercalator-peptide molecules tested and figures 50 and 51 show typical examples of results obtained. The extent of inhibition of AP-1 protein from binding to AP-1 DNA was found to be most significant with the intercalator-peptides and least with the peptide units alone (see also figures 54, 55 and 56 for data obtained). This is discussed in section 5.9.

5.6 The Specificity of Intercalator-Peptide for AP-1 DNA consensus sequence.

Specificity of the intercalator-peptide for AP-1 consensus oligonucleotide was investigated. This was achieved by measuring the extent of inhibition when ^{32}P-labelled AP-1 DNA consensus sequence was replaced by SP-1 DNA, and AP-1 protein replaced by SP-1 protein. The results showed (figure 52 and 53) that the intercalator-peptide molecules displaced the SP-1 protein from its consensus sequence. This is discussed further in section 5.13.

DNA binding assays

5.7 The effect of Intercalator-Peptide conjugates on the thermal denaturation properties of DNA.

The spectra of DNA plus drug were recorded against DNA alone at λmax 260nm; the concentrations of DNA in both reference and sample cuvette were

identical and therefore only the affect of the DNA on the absorbance spectrum of drug was recorded. The Tm of calf thymus DNA in the absence of the drug was shown to be $71.2 \pm 0.1°C$ at pH7.4. The Tm values obtained for DNA, DNA and drug (10:1 DNA/drug ratio) are shown in table 9. It was observed that **J** conjugates, containing an extra lysine moiety had higher ΔTm values than **D** containing conjugates. Higher ΔTm values were also observed with conjugates containing the more basic peptides (i.e. **4**, **5**, **6** and **7**). Typical melting curves for DNA and DNA in the presence of drug are shown in figure 57.

5.7.1 The effect of Intercalator-Peptide conjugates on fluorescence enhancement of ethidium bromide due to binding to DNA.

The ability of the intercalator linked peptide complexes to displace intercalated ethidium bromide was investigated. For each compound investigated fluorescence reading versus ethidium:DNA ratio was plotted (figures 58 and 59). These plots show the fluorescence enhancement, and hence DNA-binding, of ethidium is reduced when hybrid compounds are added to DNA. It is clear from the two plots that displacement of the ethidium does occur with the ligands and that substituted chromophores are able to displace ethidium from its binding (intercalation) site.

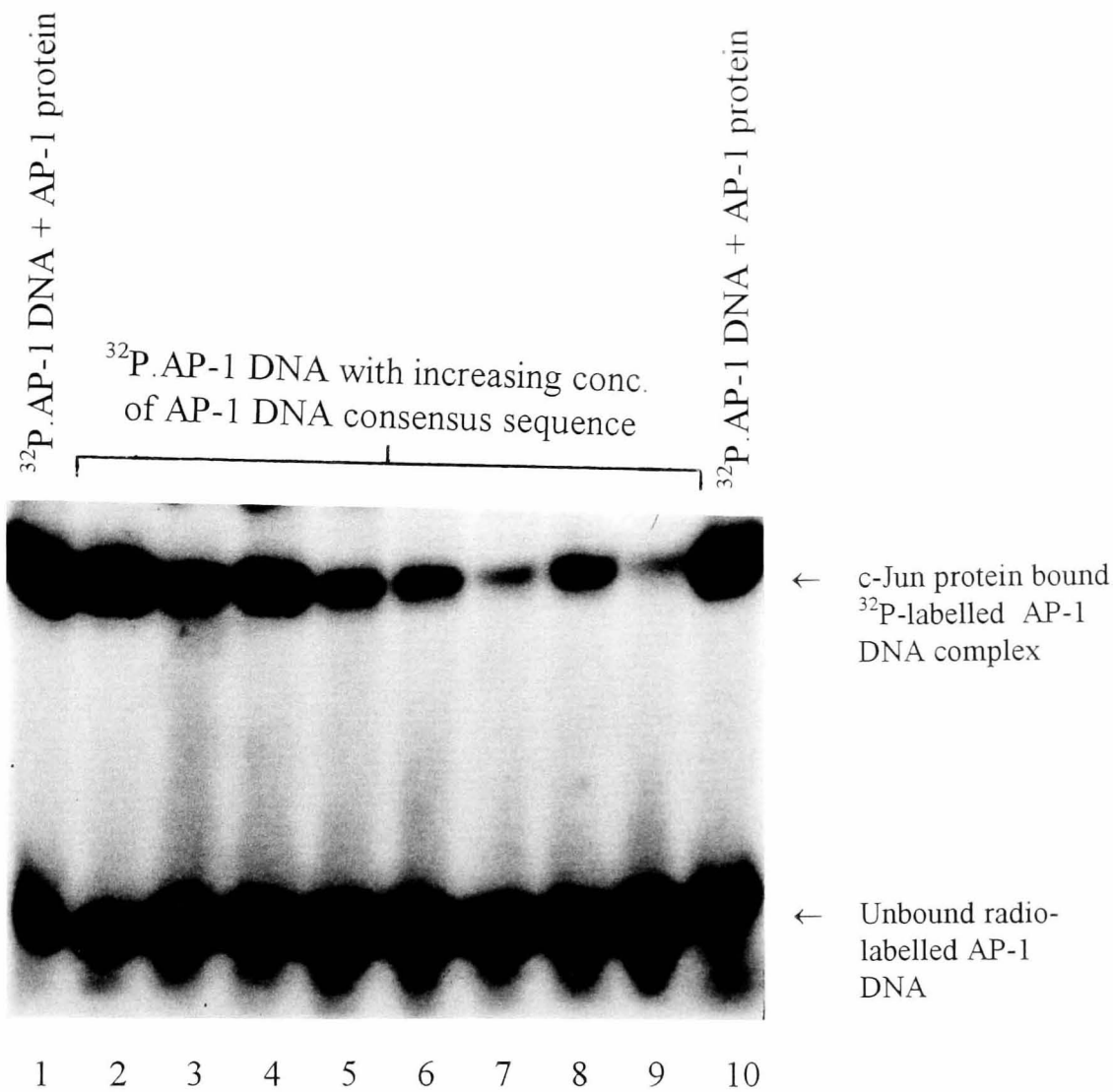

^{32}P.AP-1 DNA = ^{32}P-labelled AP-1 DNA consensus sequence

Figure 38: The effect of increasing concentration of unlabelled AP-1 DNA (lanes 2 to 9; 2: 0.011; 3: 0.022; 4: 0.032; 5: 0.043; 6: 0.054; 7: 0.065; 8: 0.076 and 9: 0.086 ng/μl) on the binding of c-Jun homodimer protein. Lanes 1 and 10 contain ^{32}P-labelled AP-1 DNA. The concentration of labelled AP-1 DNA and c-Jun protein used was 2.10nM and 0.055μg/μl, respectively. See section 6.11.3 for experimental detail.

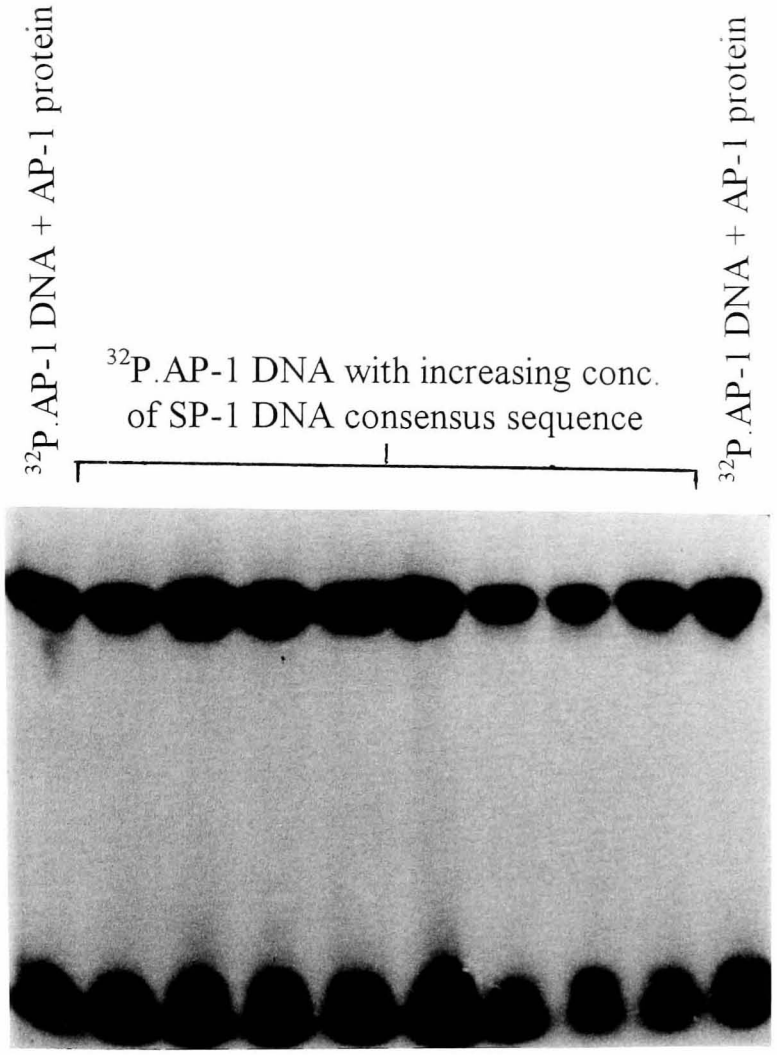

^{32}P.AP-1 DNA = ^{32}P-labelled AP-1 DNA consensus sequence

Figure 39: The effect of increasing concentration of unlabelled SP-1 DNA (lanes 2 to 9; 2: 0.011; 3: 0.022; 4: 0.032; 5: 0.043; 6: 0.054; 7: 0.065; 8: 0.076 and 9: 0.086 ng/μl) on the binding of c-Jun homodimer protein. Lanes 1 and 10 contain ^{32}P-labelled AP-1 DNA. The concentration of labelled AP-1 DNA and c-Jun protein used was 2.10nM and 0.055μg/μl, respectively. See section 6.11.3 for experimental detail.

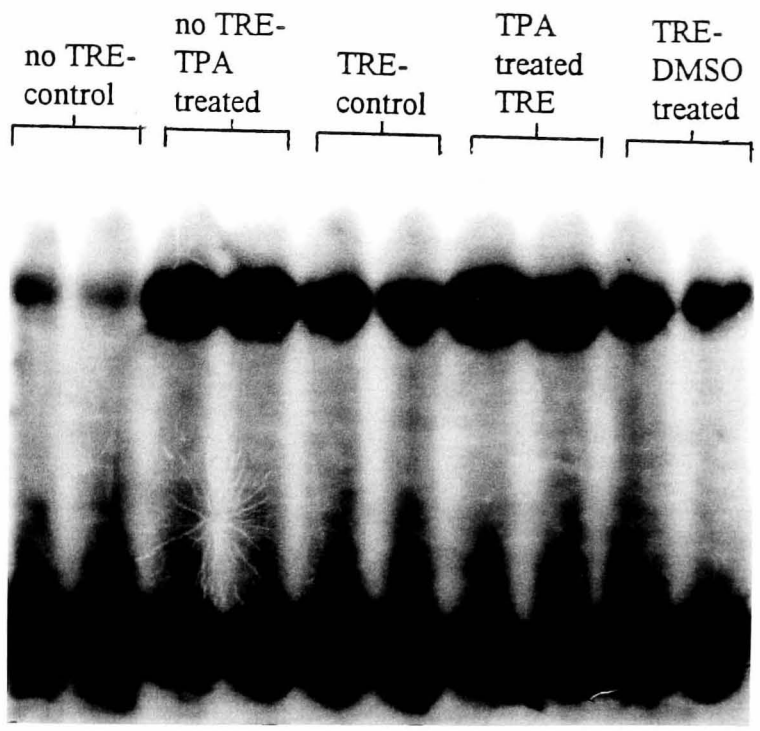

TPA = 12-*O*-Tetradecanoyl-phorbol-13-acetate

TRE = TPA responsive element

DMSO = Dimethylsulfoxide

Figure 40: Effect of TPA treated MDA-468 breast carcinoma cell line lysates on AP-1 protein binding to AP-1 consensus sequence. Lanes 3/4 and 7/8 are the TPA treated MDA-468 cell line variants whereas the remaining cell line variants were controlled experiments starved of TPA. The concentration of the radiolabelled AP-1 DNA and protein used was 2.10nM and 0.018µg/µl, respectively. See section 6.11.1 for experimental detail.

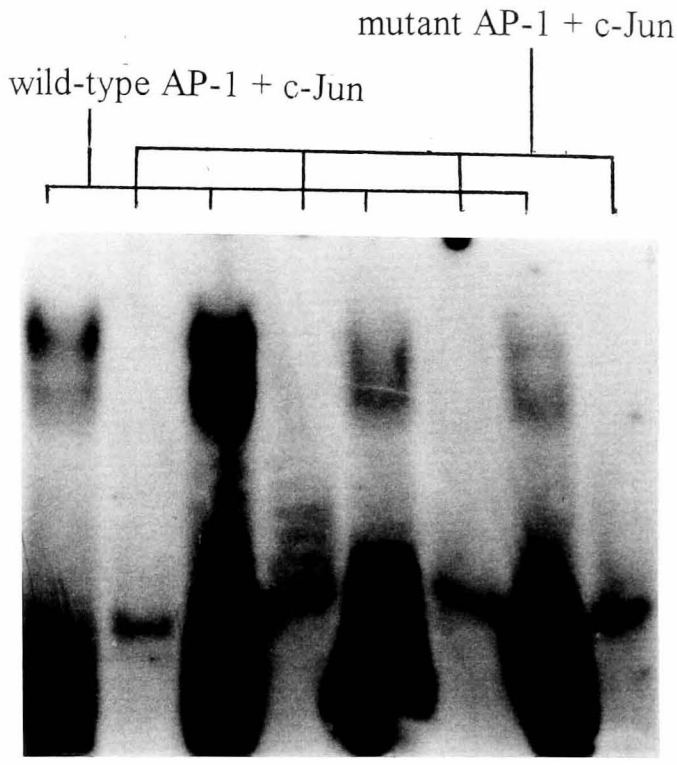

Wild-type AP-1 DNA = 5'-CGCTTGATGAGT**CA**GCCGGAA-3'

Mutant AP-1 DNA = 5'-CGCTTGATGAGT**TG**GCCGGAA-3'

c-Jun = c-Jun homodimer protein

Figure 41: Electrophoretic mobility shift assay of c-Jun homodimer with wild-type (lanes 1, 3, 5 & 7) and mutant (lanes 2, 4, 6 & 8) AP-1 oligonucleotide. The amount of c-Jun protein and oligonucleotide used was 0.055µg/µl and 2.10nM, respectively. See section 6.11.2 for experimental detail.

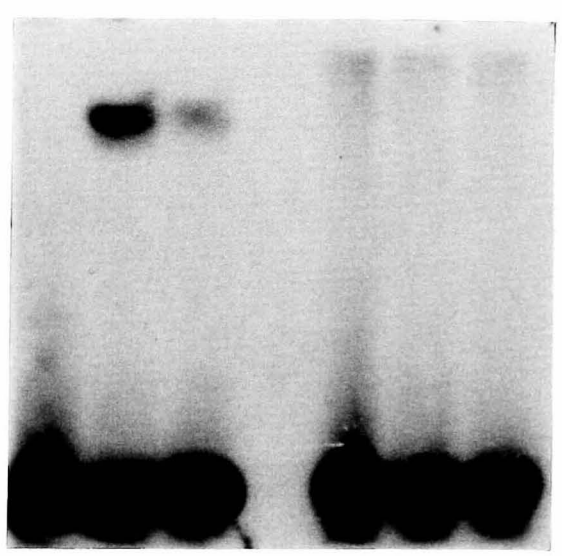

^{32}P.AP-1 DNA = ^{32}P-labelled AP-1 DNA consensus sequence

^{32}P.SP-1 DNA = ^{32}P-labelled SP-1 DNA consensus sequence

c-Jun = c-Jun homodimer protein

DTT = dithiothreitol

Figure 42: Electrophoretic mobility shift assay of c-Jun homodimer protein in the presence and absence of dithiothreitol (DTT). Lanes 1 & 4 are ^{32}P-labelled AP-1 and SP-1 consensus oligonucleotide, respectively. Lanes 2 & 3 consist of c-Jun protein incubated with ^{32}P-labelled AP-1 DNA in the presence and absence of dithiothreitol (DTT), respectively. Lanes 5 & 6 consist of c-Jun protein incubated with ^{32}P-labelled SP-1 DNA in the presence and absence of DTT, respectively. The amount of c-Jun protein, oligonucleotide and DTT used was 0.055μg/μl, 2.10nM and 0.5mM, respectively. See section 6.11 for experimental detail.

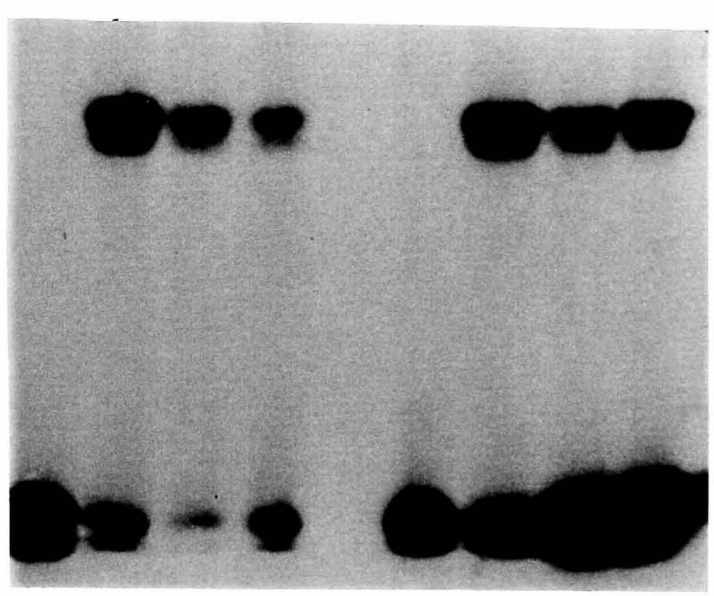

^{32}P.AP-1 DNA = ^{32}P-labelled AP-1 DNA consensus sequence

AP-1 protein = AP-1 (fos/jun) heterodimer protein (HeLa cell nuclear extract)

Figure 43: The effect of oxygenation on the binding of AP-1 heterodimer protein to AP-1 DNA consensus sequence. Lanes 1 & 5 contain ^{32}P-labelled AP-1 DNA. Lanes 2 & 6 are the controls with no addition of either oxygen or nitrogen. Lanes 3 & 4 are results from oxygenation for 3 and 6 hr, respectively. Lane 7 and 8 are AP-1 protein samples under nitrogen gas for 3 and 6 hr, respectively. The concentration of the AP-1 protein and labelled AP-1 DNA used was 0.073ng/μl and 2.10nM, respectively. See section 6.11.5 for experimental detail.

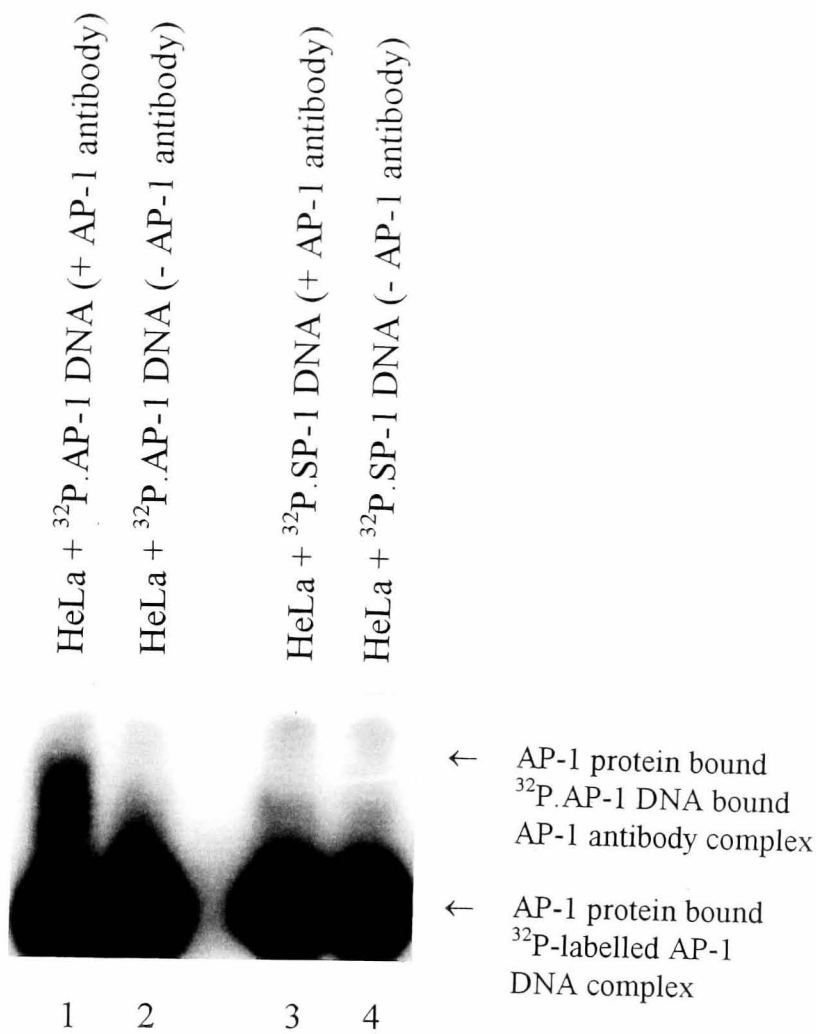

^{32}P.AP-1 DNA = ^{32}P-labelled AP-1 DNA consensus sequence

^{32}P.SP-1 DNA = ^{32}P-labelled SP-1 DNA consensus sequence

HeLa = HeLa cell nuclear extract

Figure 44: Electrophoretic mobility shift assay of AP-1 (fos/jun) heterodimer protein binding to AP-1 DNA consensus sequence in the presence of AP-1 antibody. The HeLa cell nuclear extract was incubated with the ^{32}P-labelled AP-1 DNA, with (lane 1) and without (lane 2) AP-1 antibody. As a control, HeLa nuclear extract was also incubated with ^{32}P-labelled SP-1 DNA, with (lane 3) and without (lane 4) AP-1 antibody. The concentration of AP-1 protein, AP-1 antibody and oligonucleotide used was 1.73ng/µl, 1.00ng/µl and 2.10nM, respectively. See section 6.11.4 for experimental detail.

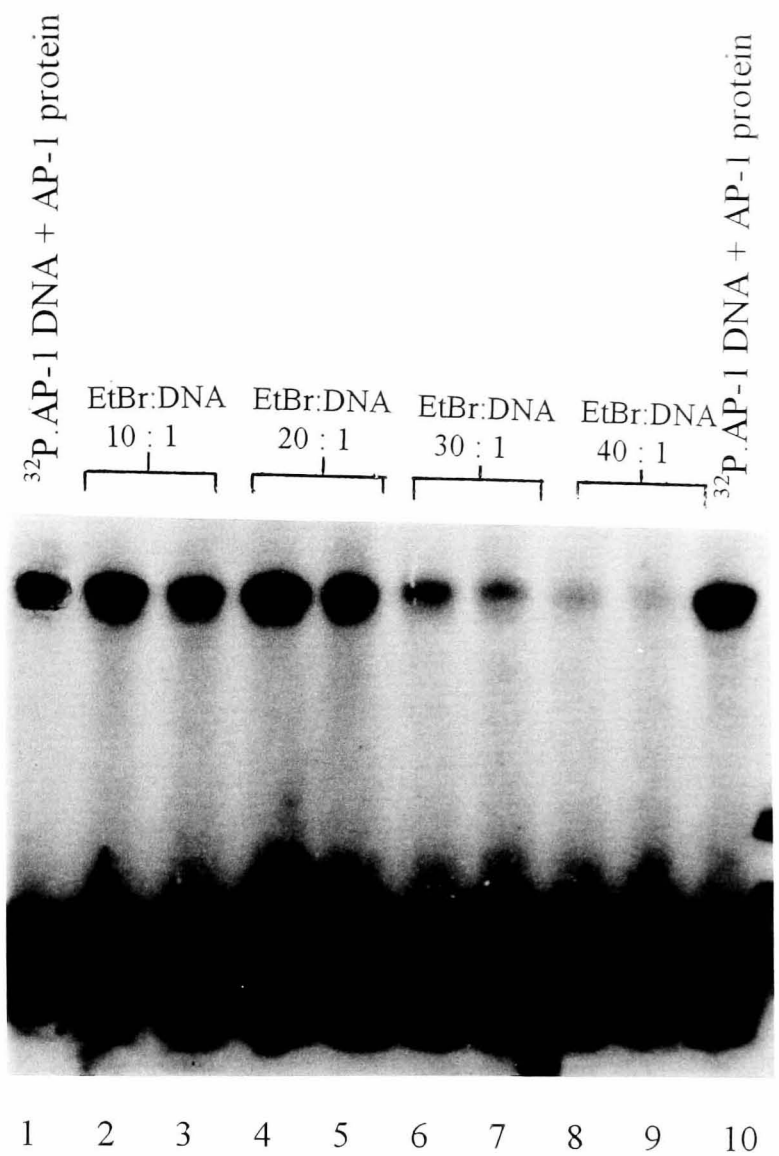

^{32}P.AP-1 DNA = ^{32}P-labelled AP-1 DNA consensus sequence

AP-1 protein = AP-1 (fos/jun) heterodimer protein (HeLa cell nuclear extract)

Ethidium Bromide =

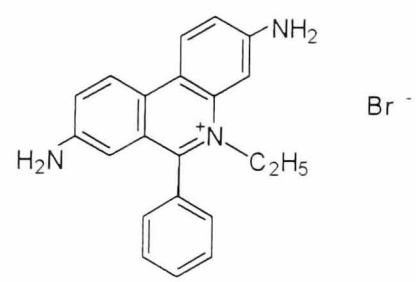

Figure 45: The effect on the binding of AP-1 protein to AP-1 DNA consensus sequence in the presence of a range of concentrations of ethidium (lanes 2 to 9; 2/3: 21; 4/5: 42; 6/7: 63; 8/9: 84 nM) and 2.10nM DNA. Lanes 1 & 10 contain no added ethidium.

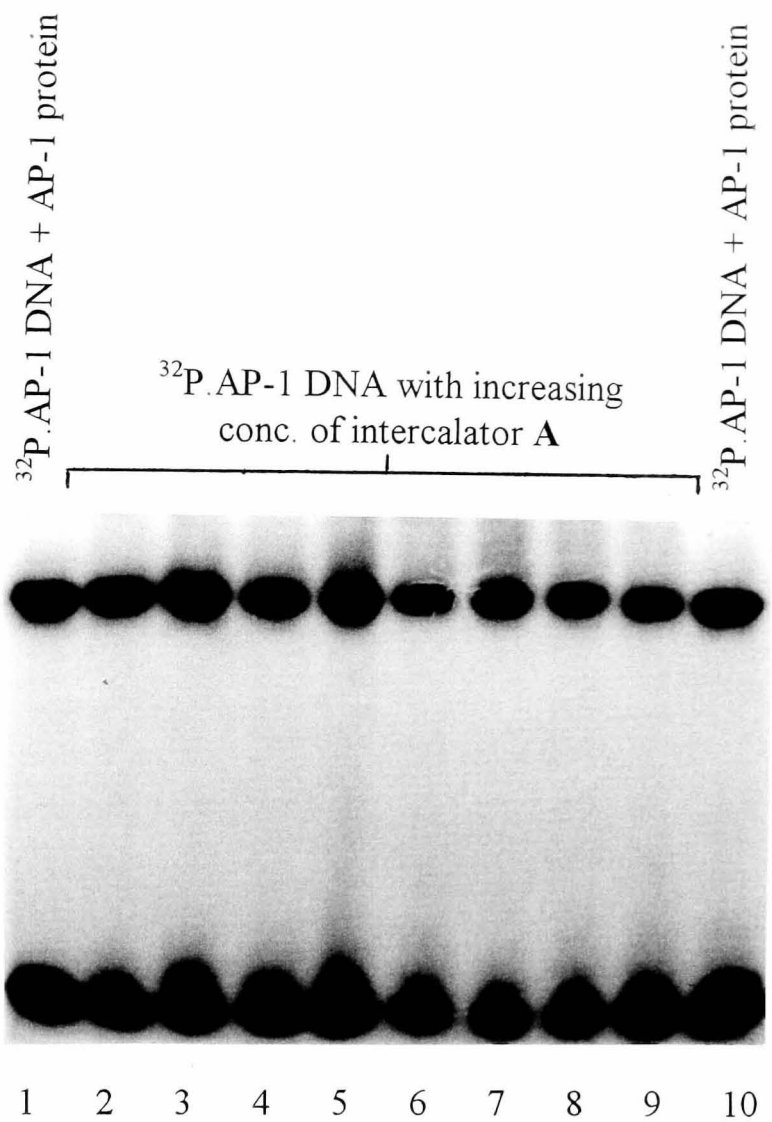

^{32}P.AP-1 DNA = ^{32}P-labelled AP-1 DNA consensus sequence

AP-1 protein = AP-1 (fos/jun) heterodimer protein (HeLa cell nuclear extract)

Intercalator **A** =

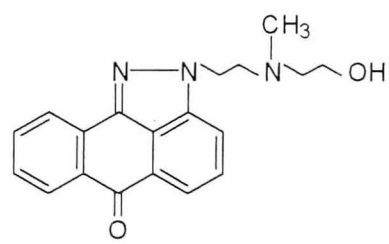

Figure 46: Electrophoretic mobility shift assay of AP-1 protein binding to ^{32}P-labelled AP-1 DNA consensus sequence in the presence of intercalator **A**. Lanes 2 to 9 contain increasing concentration of intercalator **A** (2: 0.21; 3: 0.42; 4: 0.63; 5: 0.84; 6: 1.05; 7: 1.26; 8: 1.47; 9: 1.68 μM) and 2.10nM DNA. Lanes 1 and 10 contain no added **A**. See section 6.12 for experimental detail.

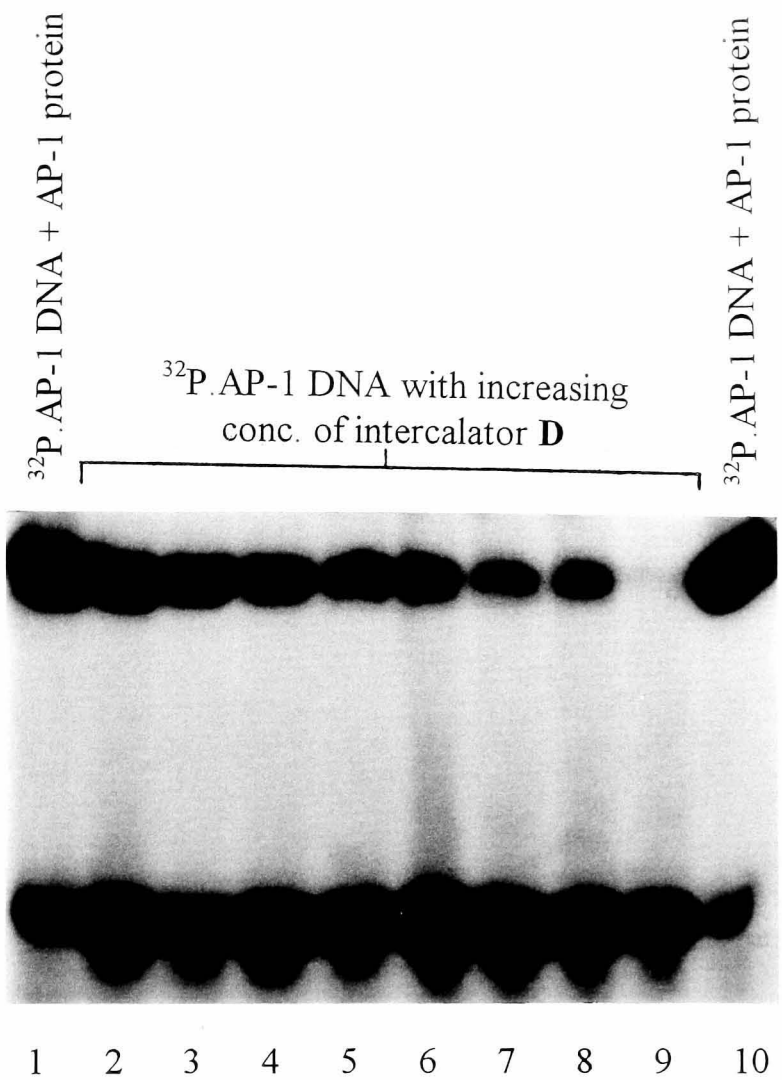

^{32}P.AP-1 DNA = ^{32}P-labelled AP-1 DNA consensus sequence

AP-1 protein = AP-1 (fos/jun) heterodimer protein (HeLa cell nuclear exract)

Intercalator **D** =

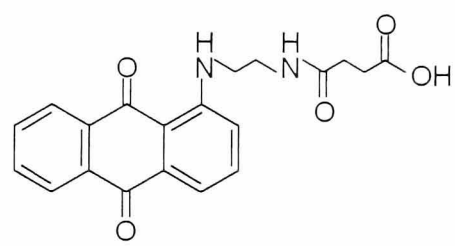

Figure 47: Electrophoretic mobility shift assay of AP-1 protein binding to ^{32}P-labelled AP-1 DNA consensus sequence in the presence of intercalator **D**. Lanes 2 to 9 contain increasing concentration of intercalator **D** (2: 0.21; 3: 0.42; 4: 0.63; 5: 0.84; 6: 1.05; 7: 1.26; 8: 1.47; 9: 1.68 μM) and 2.10nM DNA. Lanes 1 and 10 contain no added **D**. See section 6.12 for experimental detail.

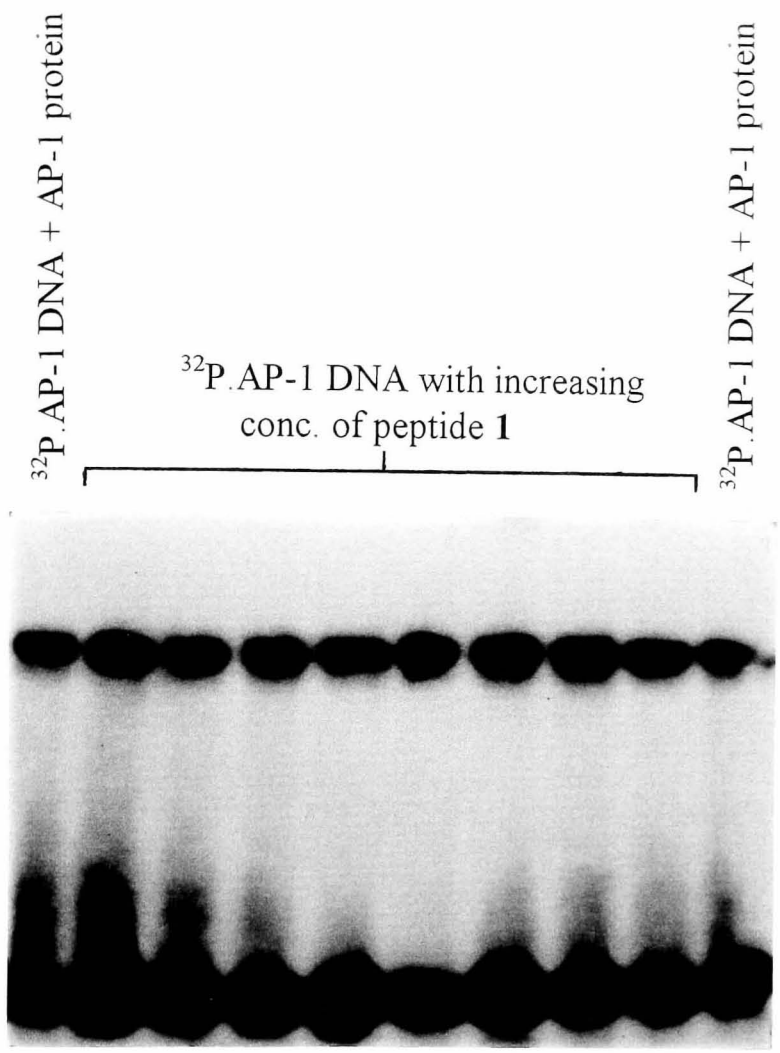

^{32}P.AP-1 DNA = ^{32}P-labelled AP-1 DNA consensus sequence

AP-1 protein = AP-1 (fos/jun) heterodimer protein (HeLa cell nuclear extract)

Peptide **1** = H_2N-A-K-C-R-A-CO_2H

Figure 48: Electrophoretic mobility shift assay of AP-1 protein binding to ^{32}P-labelled AP-1 DNA consensus sequence in the presence of peptide **1**. Lanes 1 and 10 contain no added peptide molecule. Lanes 2 to 9 consist of increasing concentration of peptide **1** (2: 2.1; 3: 4.2; 4: 6.3; 5: 8.4; 6: 10.5; 7: 12.6; 8: 14.7; 9: 16.8 μM) and 2.10nM DNA. The concentration of the AP-1 protein and labelled AP-1 DNA was 1.73ng/μl and 2.10nM, respectively. See section 6.12.1 for experimental detail.

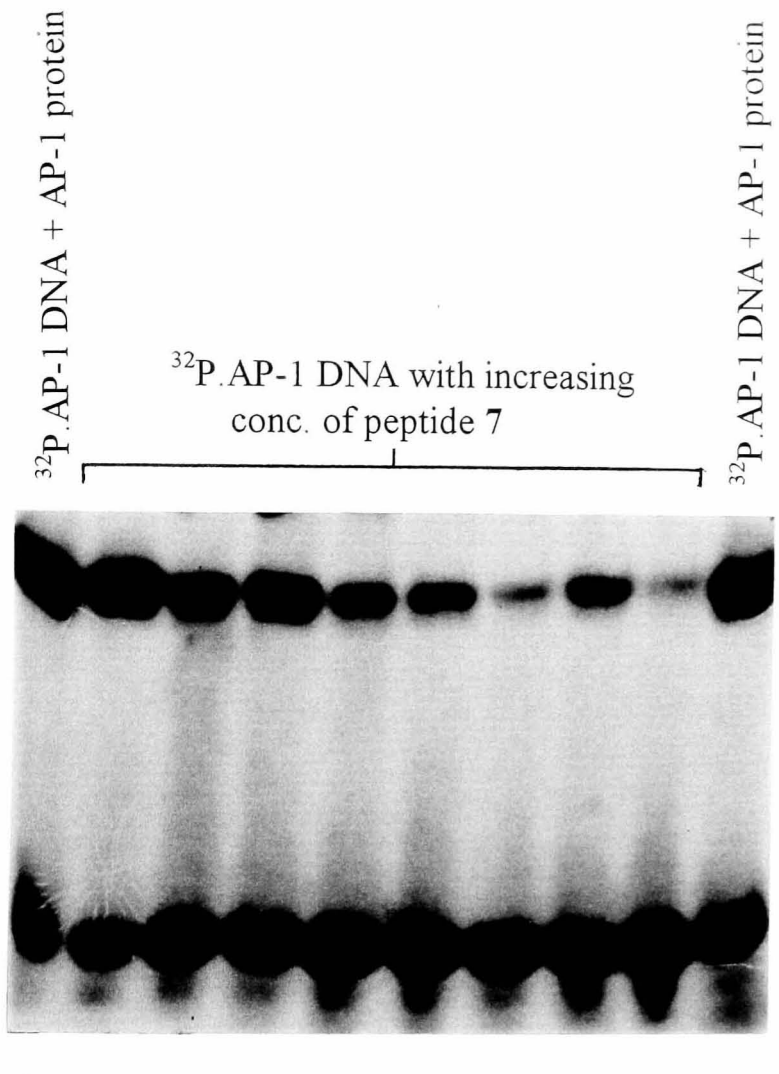

^{32}P.AP-1 DNA = ^{32}P-labelled AP-1 DNA consensus sequence

AP-1 protein = AP-1 (fos/jun) heterodimer protein (HeLa cell nuclear extract)

Peptide **7** = H_2N-A-K-C-R-K-R-A-$CONH_2$

Figure 49: Electrophoretic mobility shift assay of AP-1 protein binding to ^{32}P-labelled AP-1 DNA consensus sequence in the presence of peptide **7**. Lanes 1 and 10 contain no added peptide molecule. Lanes 2 to 9 consist of increasing concentration of peptide **7** (2: 2.1; 3: 4.2; 4: 6.3; 5: 8.4; 6: 10.5; 7: 12.6; 8: 14.7; 9: 16.8 μM) and 2.10nM DNA. The concentration of the AP-1 protein and labelled AP-1 DNA was 1.73ng/μl and 2.10nM, respectively. See section 6.12.1 for experimental detail.

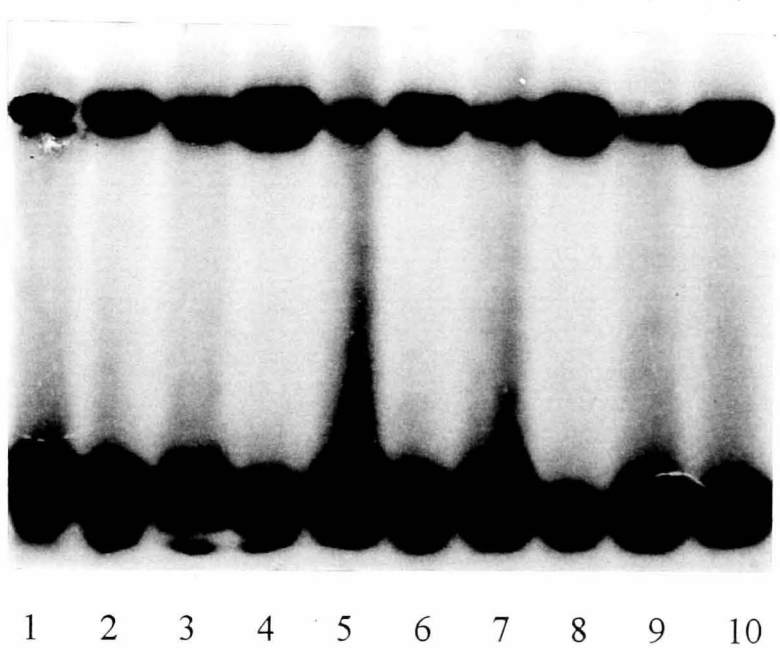

^{32}P.AP-1 DNA = ^{32}P-labelled AP-1 DNA consensus sequence

AP-1 protein = AP-1 (fos/jun) heterodimer protein (HeLa cell nuclear extract)

Conjugate **4D** =

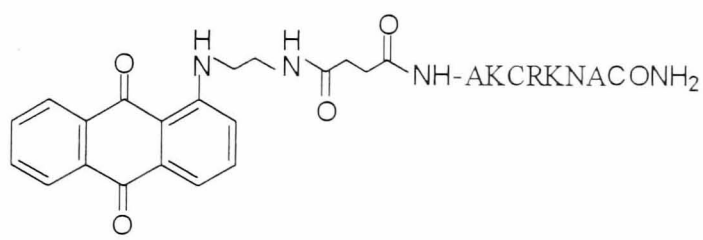

Figure 50: Electrophoretic mobility shift assay of AP-1 protein binding to ^{32}P-labelled AP-1 DNA consensus sequence in the presence of a range of concentrations of conjugate **4D**. Lanes 1, 3, 5, 7 and 9 contain increasing concentration of conjugate **4D** (0.21-1.68 μM : 2.1nM; **4D**:DNA). The remaining lanes (2, 4, 6, 8 and 10) contain no added conjugate. See section 6.12.2 for experimental detail.

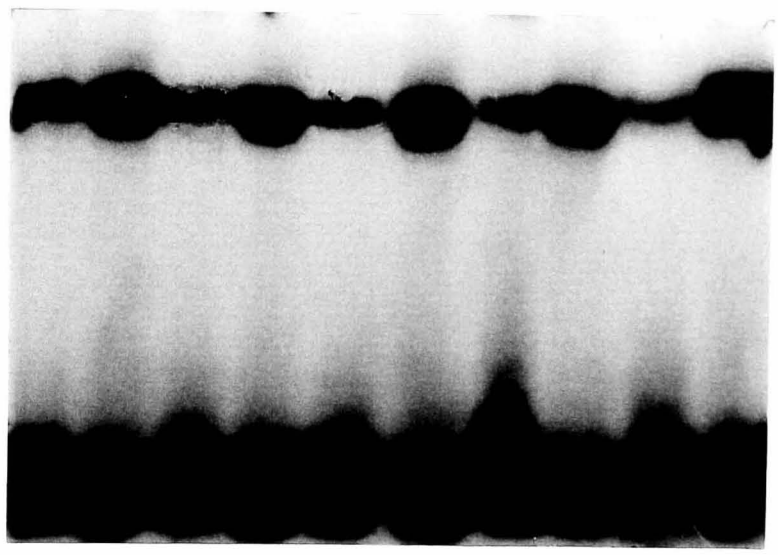

^{32}P.AP-1 DNA = ^{32}P-labelled AP-1 DNA consensus sequence

AP-1 protein = AP-1 (fos/jun) heterodimer protein (HeLa cell nuclear extract)

Conjugate **7D** =

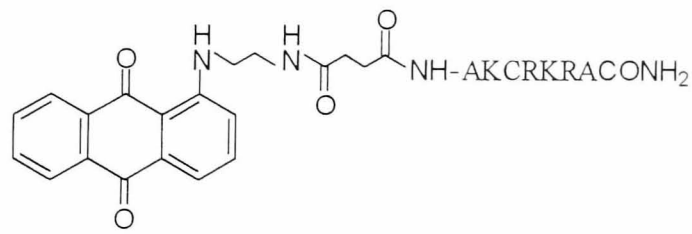

Figure 51: Electrophoretic mobility shift assay of AP-1 protein binding to ^{32}P-labelled AP-1 DNA consensus sequence in the presence of a range of concentrations of conjugate **7D**. Lanes 1, 3, 5, 7 and 9 contain increasing concentration of conjugate **7D** (0.21-1.68 μM : 2.1nM; **7D**:DNA). The remaining lanes (2, 4, 6, 8 and 10) contain no added conjugate. See section 6.12.2 for experimental detail.

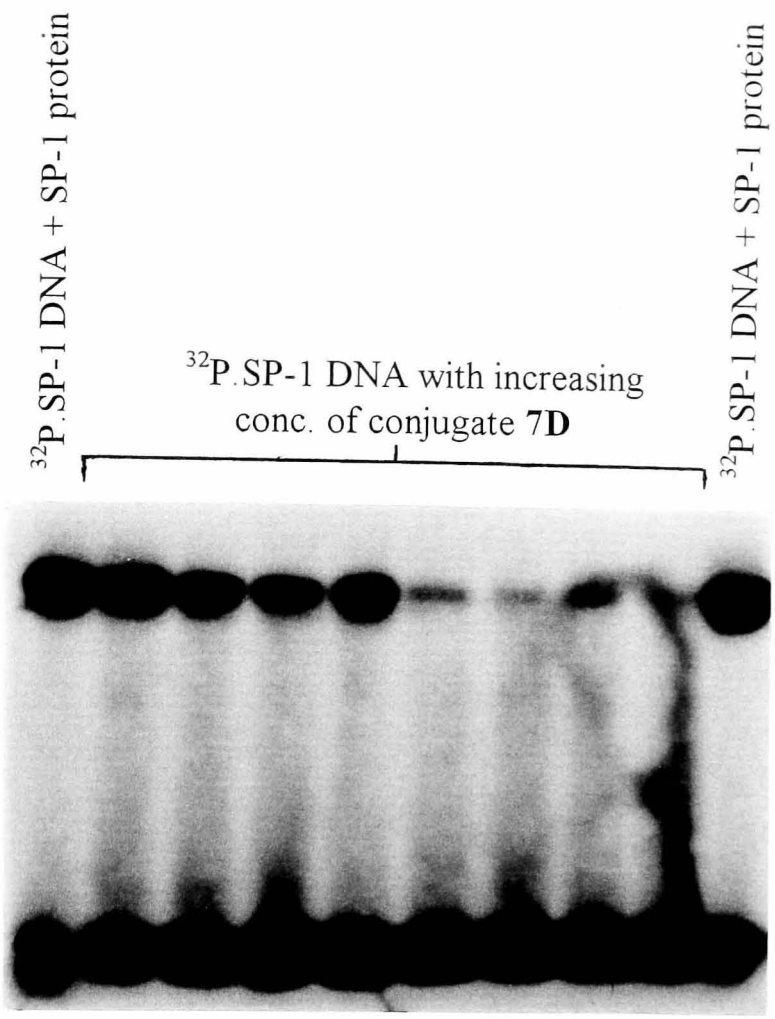

^{32}P.SP-1 DNA = ^{32}P-labelled SP-1 DNA consensus sequence

Conjugate **7D** =

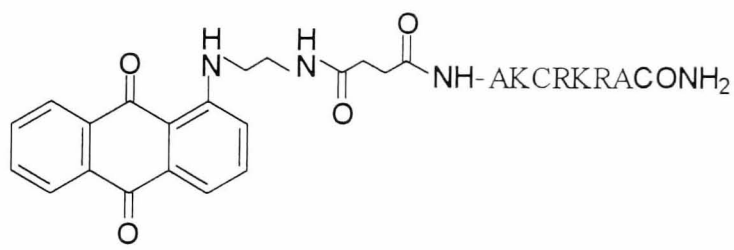

Figure 52: Electrophoretic mobility shift assay to show the effect of conjugate **7D** on the binding of SP-1 protein to ^{32}P-labelled SP-1 DNA consensus sequence. Lanes 1 & 10 contain no added **7D**. Lanes 2 to 9 contain increasing concentration of **7D** (2: 0.21; 3: 0.42; 4: 0.63; 5: 0.84; 6: 1.05; 7: 1.26; 8: 1.47; 9: 1.68 μM) and 2.10nM DNA. See section 6.13 for experimental detail.

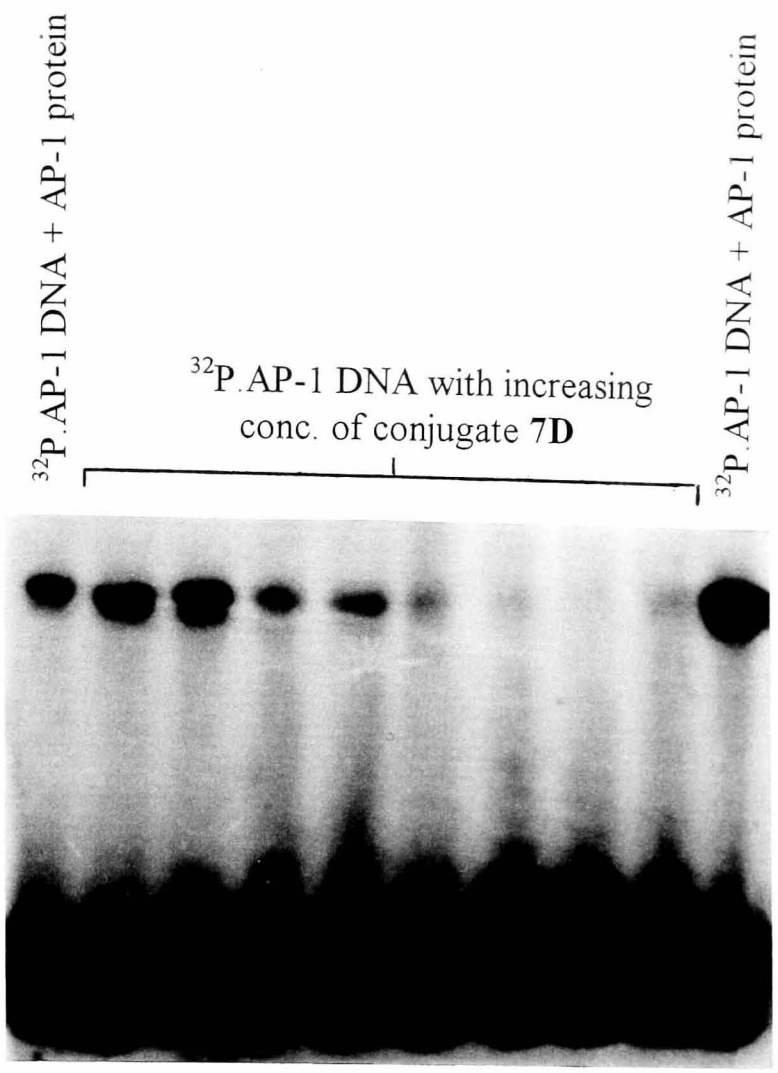

^{32}P.AP-1 DNA = ^{32}P-labelled AP-1 DNA consensus sequence

AP-1 protein = AP-1 (fos/jun) heterodimer protein (HeLa cell nuclear extract)

Conjugate **7D** =

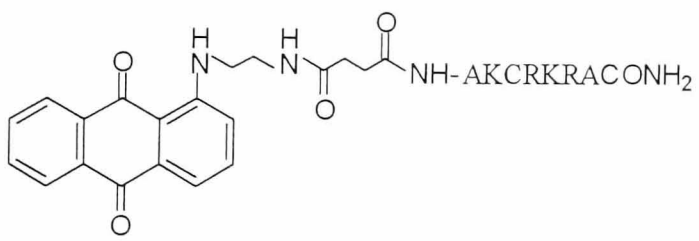

Figure 53: Electrophoretic mobility shift assay to show the effect of conjugate **7D** on the binding of AP-1 protein to ^{32}P-labelled AP-1 DNA consensus sequence. Lanes 1 & 10 contain no added **7D**. Lanes 2 to 9 contain increasing concentration of **7D** (2: 0.21; 3: 0.42; 4: 0.63; 5: 0.84; 6: 1.05; 7: 1.26; 8: 1.47; 9: 1.68 μM) and 2.10nM DNA. See section 6.13 for experimental detail.

Table 6: The effect of intercalators on the binding of AP-1 protein to AP-1 DNA consensus sequence.

Intercalators Tested	Abbreviation*	Mean Band Intensity ±10%**
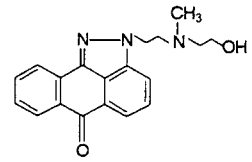	**A**	87
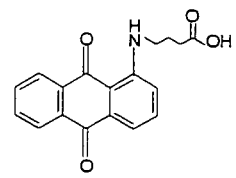	**B**	96
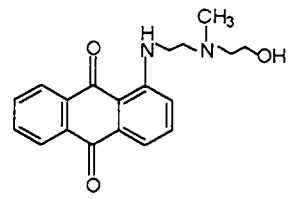	**C**	88
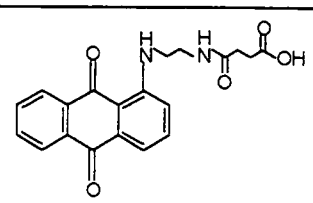	**D**	80
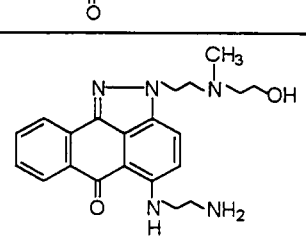	**E**	79
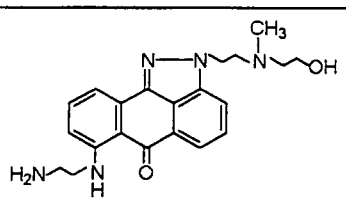	**F**	67
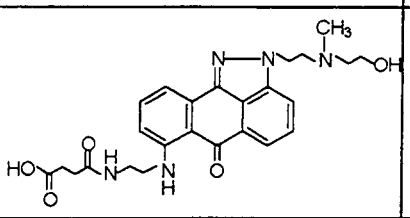	**G**	82
Ethidium bromide	**H**	26
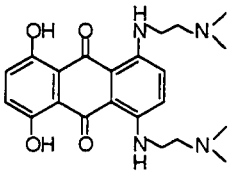 (AQ4)	**I**	38

* These abbreviations are consistently used throughout this thesis.

** The band intensity (i.e. the degree of inhibition of AP-1 protein binding) was recorded using a densitometer (arbitrary units). The results are the mean value of two separate EMSA for each compound (see section 6.9 for experimental detail). For raw data obtained see figure 55. The concentrations used were as follows: [AP-1] = 1.73ng/μl; [DNA] = 2.10nM; [intercalator] = 0.21-1.68μM.

Table 7: The effect of peptide units on the binding of AP-1 protein to AP-1 DNA consensus sequence.

Peptide Unit *	Abbreviation**	Mean Band Intensity ±10 %***
H_2N-A-K-C-R-A-CO_2H	**1**	98
H_2N-A-K-C-R-A-$CONH_2$	**2**	99
H_2N-A-K-S-R-A-$CONH_2$	**3**	99
H_2N-A-K-C-R-N-A-$CONH_2$	**4**	82
H_2N-A-K-C-R-K-A-$CONH_2$	**5**	83
H_2N-A-K-C-R-N-R-A-$CONH_2$	**6**	87
H_2N-A-K-C-R-K-R-A-$CONH_2$	7	86
H_2N-A-A-K-C-R-A-A-$CONH_2$	**8**	93

* A, alanine; K, Lysine; C, cysteine; R, arginine; N, asparagine; S, serine.

** These abbreviations are used consistently throughout this thesis.

*** The band intensity (i.e. the degree of inhibition of AP-1 protein binding) was recorded using a densitometer (arbitrary units). The results are the mean value of two separate EMSA for each compound (see section 6.9 for experimental detail). For raw data obtained see figure 54. The concentrations used were as follows: [AP-1] = 1.73ng/μl; [DNA] = 2.10nM; [peptide] = 2.1-16.8μM.

Table 8: The effect of intercalator-peptide conjugates on the binding of AP-1 protein to AP-1 site.

Intercalator-peptide Conjugate**	Mean Band Intensity ±10 % *	
	[Conjugate] 0.21-1.68μM	[Conjugate] 2.1-16.8μM
1D	79	51
2D	78	43
3D	73	41
4D	67	32
5D	68	39
6D	70	38
7D	61	26
8D	79	56
5J**	70	35
6J	69	34
7J	64	23
8J	78	53
5K**	68	42
6K	71	39

* The band intensity (i.e. the degree of inhibition of AP-1 protein binding) was recorded using a densitometer (arbitrary units). The results are the mean value of two separate EMSA for each compound (see section 6.9 for experimental detail). For raw data obtained see figure 56. The concentrations used were as follows: [AP-1] = 1.73ng/μl; [DNA] = 2.10nM.

** These abbreviations are used consistently throughout this thesis. **J** = **D**-Lysine; **K** = **D**-$(Lysine)_2$ (see table 6).

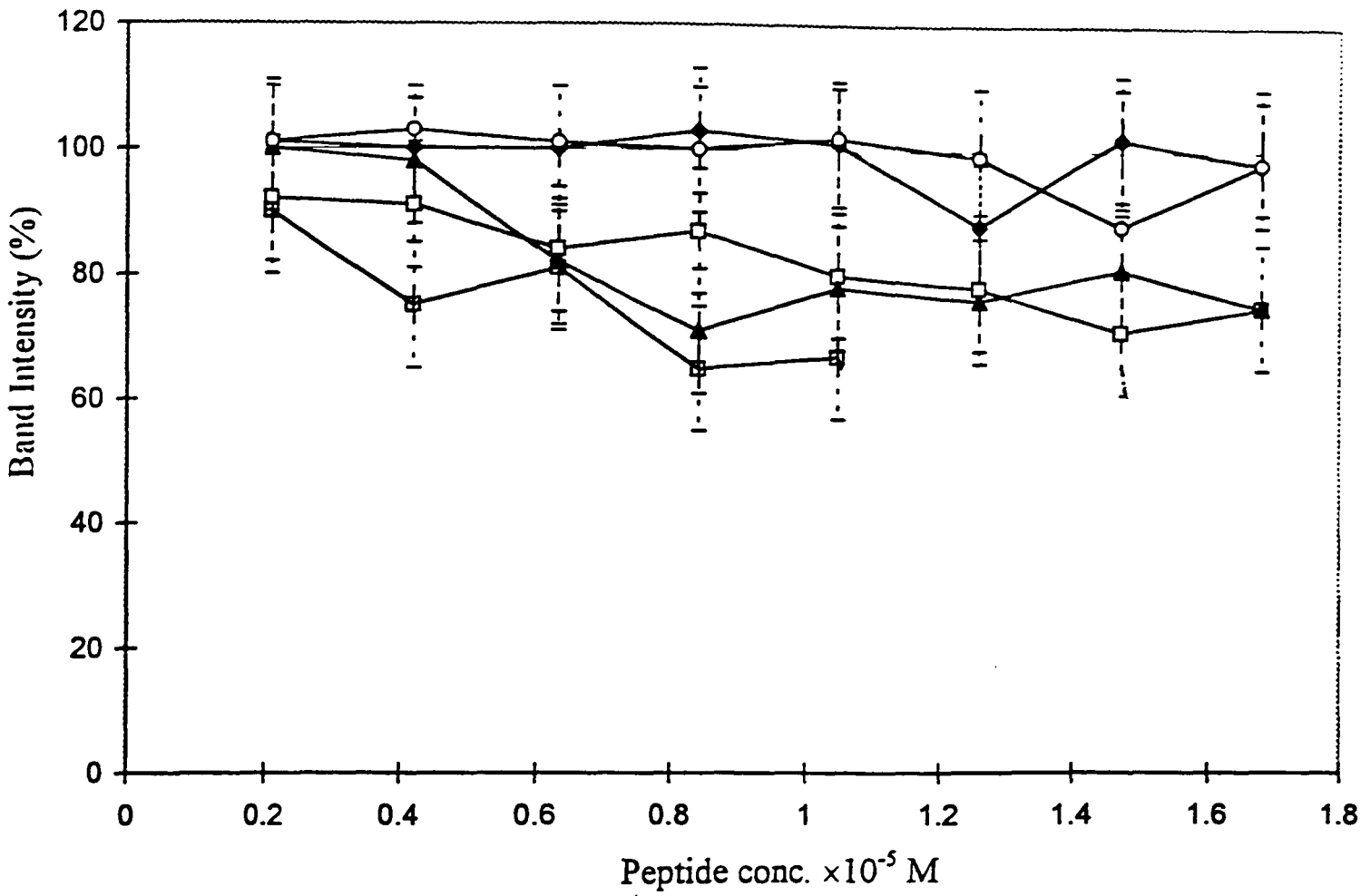

Peptide 1 = H_2N-A-K-C-R-C-CO_2H (♦)

2 = H_2N-A-K-C-R-C-$CONH_2$ (○)

4 = H_2N-A-K-C-R-C-$CONH_2$ (□)

5 = H_2N-A-K-C-R-C-$CONH_2$ (▲)

7 = H_2N-A-K-C-R-C-$CONH_2$ (■)

Figure 54: The effect of increasing concentration of peptides **1**, **2**, **4**, **5** and **7** on the binding of AP-1 protein to AP-1 DNA consensus sequence as measured by densitometry. See section 6.12.1 for experiment detail.

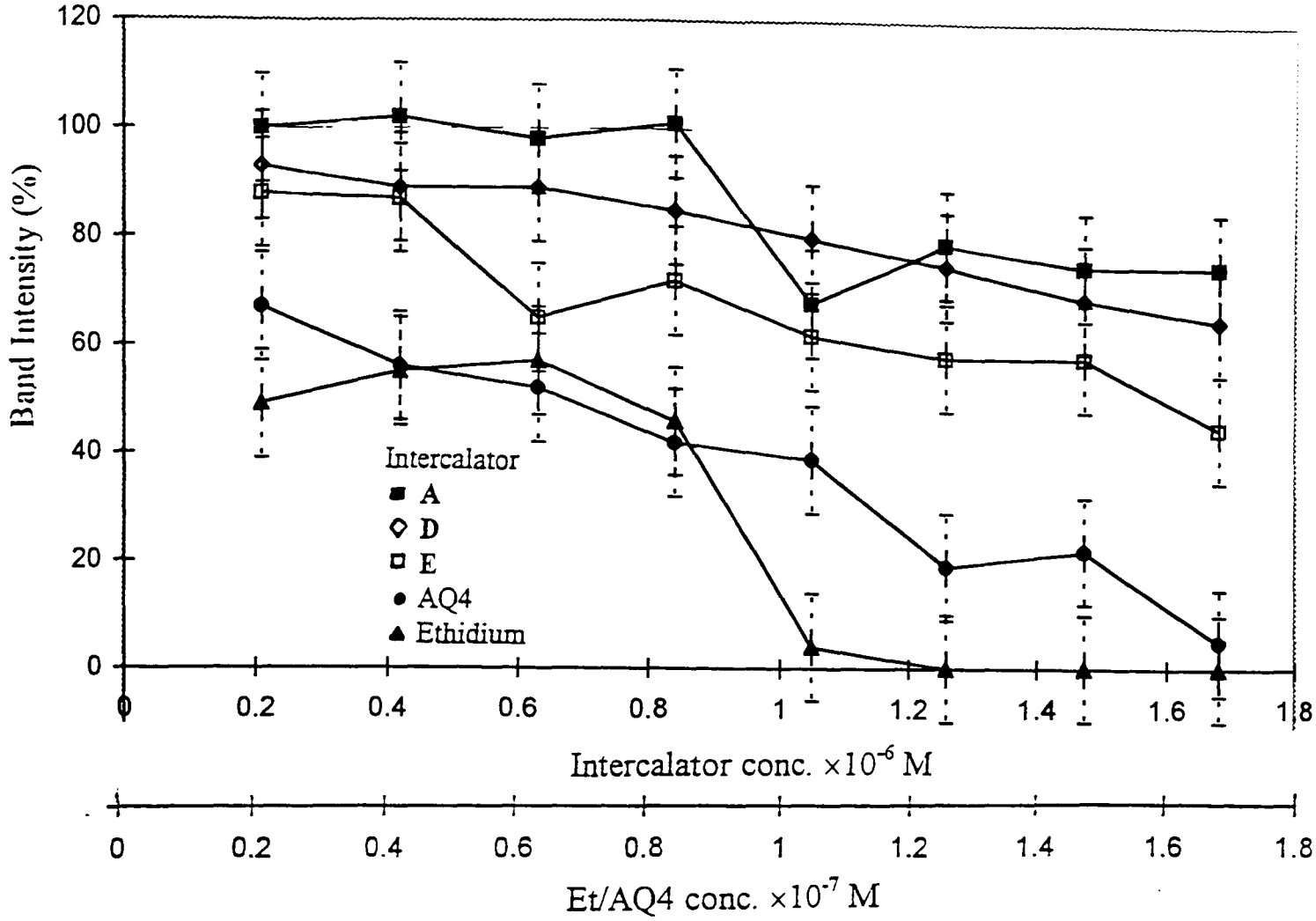

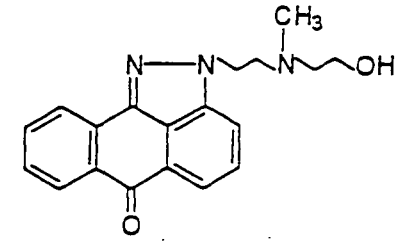

(A)

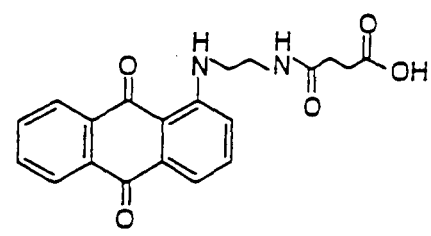

(D)

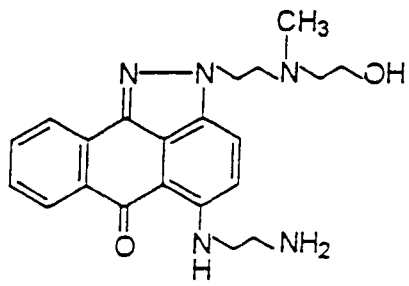

(E)

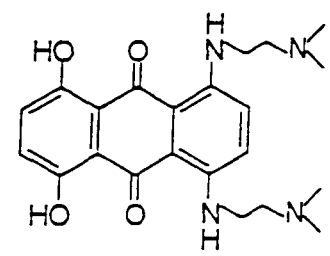

(AQ4)

Figure 55: The effect of increasing concentration of intercalators **A**, **D** and **E** on the binding of AP-1 protein to AP-1 DNA consensus sequence as measured by densitometry. Note that the concentration range of ethidium and AQ4 is 10^{-7} M. See section 6.12 for experimental detail.

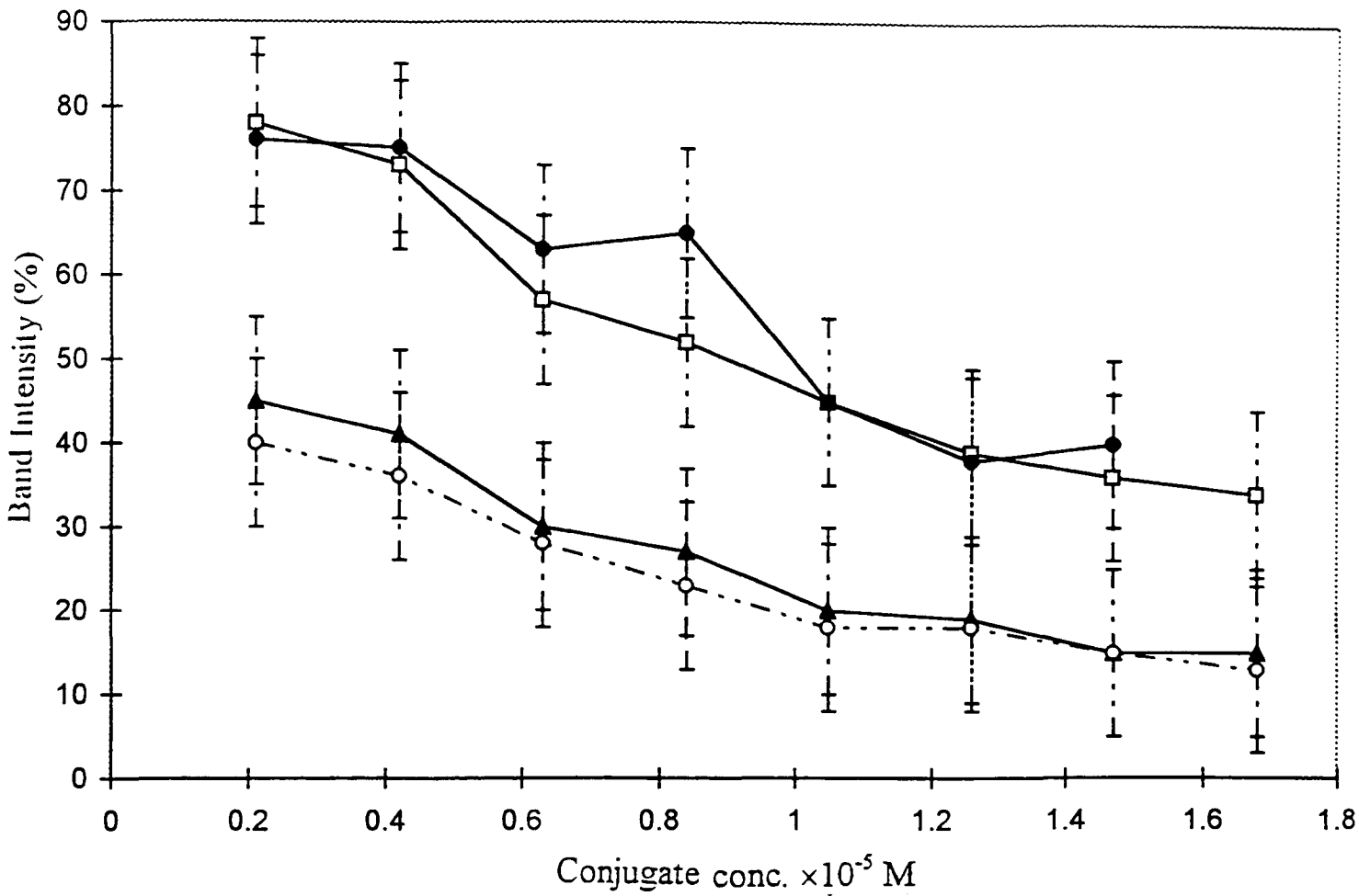

Conjugate **1D** = D-HN-A-K-C-R-C-CO_2H (□)

7D = D-HN-A-K-C-R-C-$CONH_2$ (○)

7J = J-HN-A-K-C-R-C-$CONH_2$ (▲)

8D = D-HN-A-A-K-C-R-A-A-$CONH_2$ (●)

Figure 56: The effect of increasing concentration of intercalator-peptide conjugates **1D**, **7D**, **7J** and **8D** on the binding of AP-1 protein to AP-1 DNA consensus sequence as measured by densitometry. See section 6.12.2 for experimental detail.

Table 9: ΔTm values for calf thymus DNA incubated with intercalator-peptide conjugates.

Intercalator-peptide Conjugate	Tm°C* (DNA+ligand)	ΔTm°C*
AQ4**	87.5	16.6
1D	73.5	2.6
2D	74.6	3.7
3D	70.9	0
4D	77.4	6.5
5D	76.0	5.1
6D	80.2	8.3
7D	79.4	8.5
8D	73.0	2.1
4J***	76.8	6.9
5J	75.1	5.8
6J	77.2	8.7
7J	79.5	9.6
8J	74.1	3.2
4G	76.2	4.6
7G	77.3	5.4
4L***	73.1	2.2
7L	74.0	3.1

* Mean Tm values ±0.1°C and are the mean of three replicates.
Tm of DNA = 70.9 ± 0.1°C; pH7.2, 0.05M NaCl, 0.008M tris buffer.

** See table 6 for structure.

*** **J** = **D**-Lysine; **L** = **D**-$NH(CH_2)_2NHCO(CH_2)_2CO_2H$.

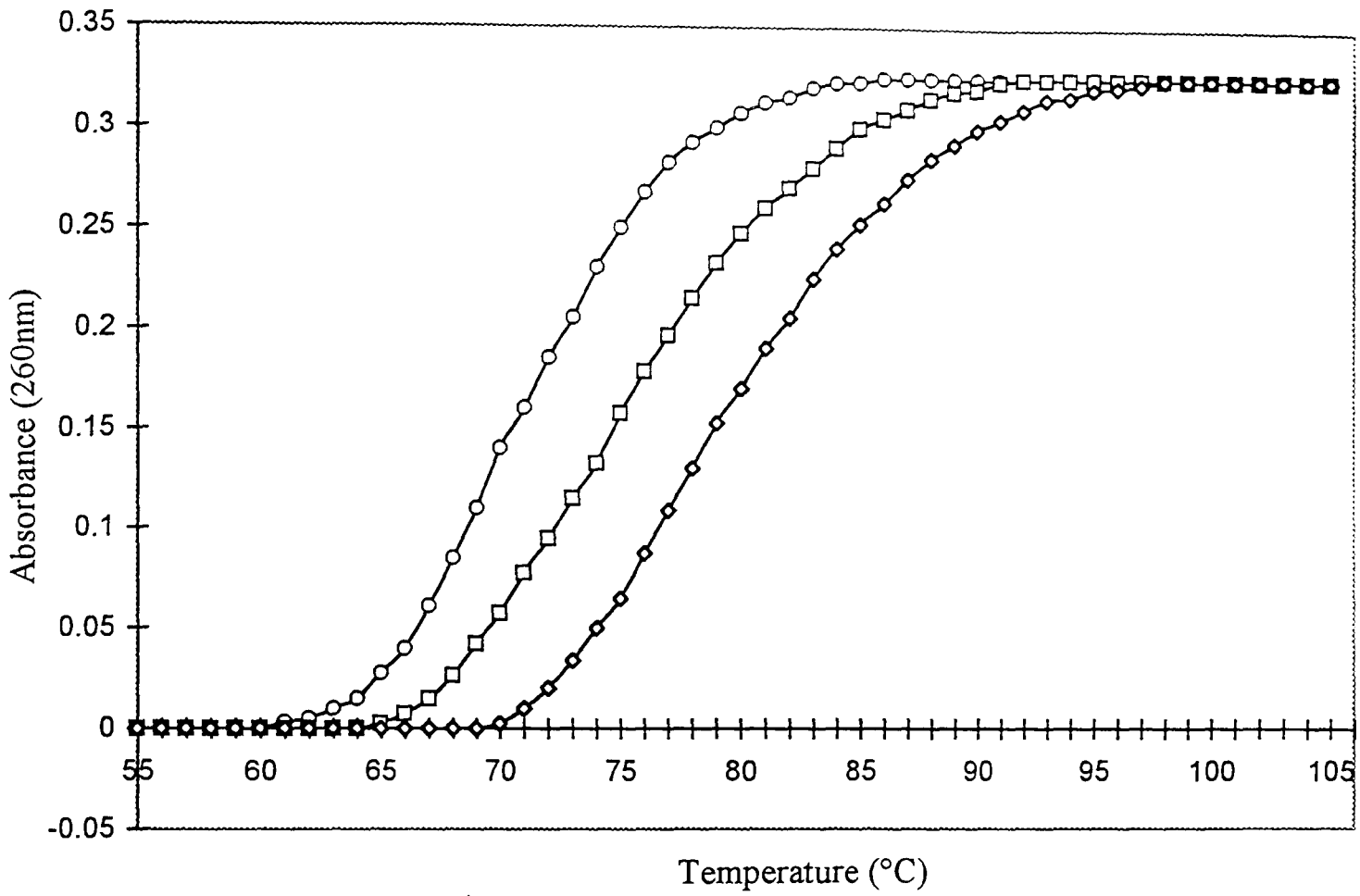

Conjugate **7D** =

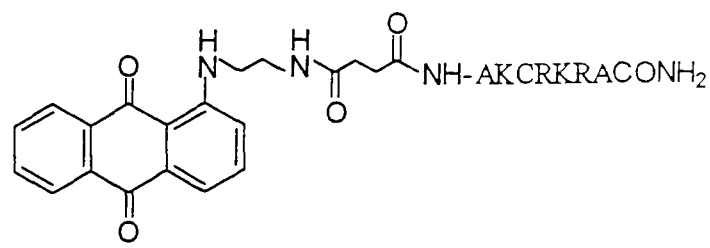

Conjugate **5J** = **D**-KAKCRKA-$CONH_2$

Figure 57: Melting curve of DNA (○), DNA + **5J** (□) and DNA + **7D** (◊), in the temperature range 58-94°C. The concentration of DNA and conjugate used was 2.5×10^{-3} M and 2.5×10^{-4} M, respectively. See section 6.14 for experimental detail.

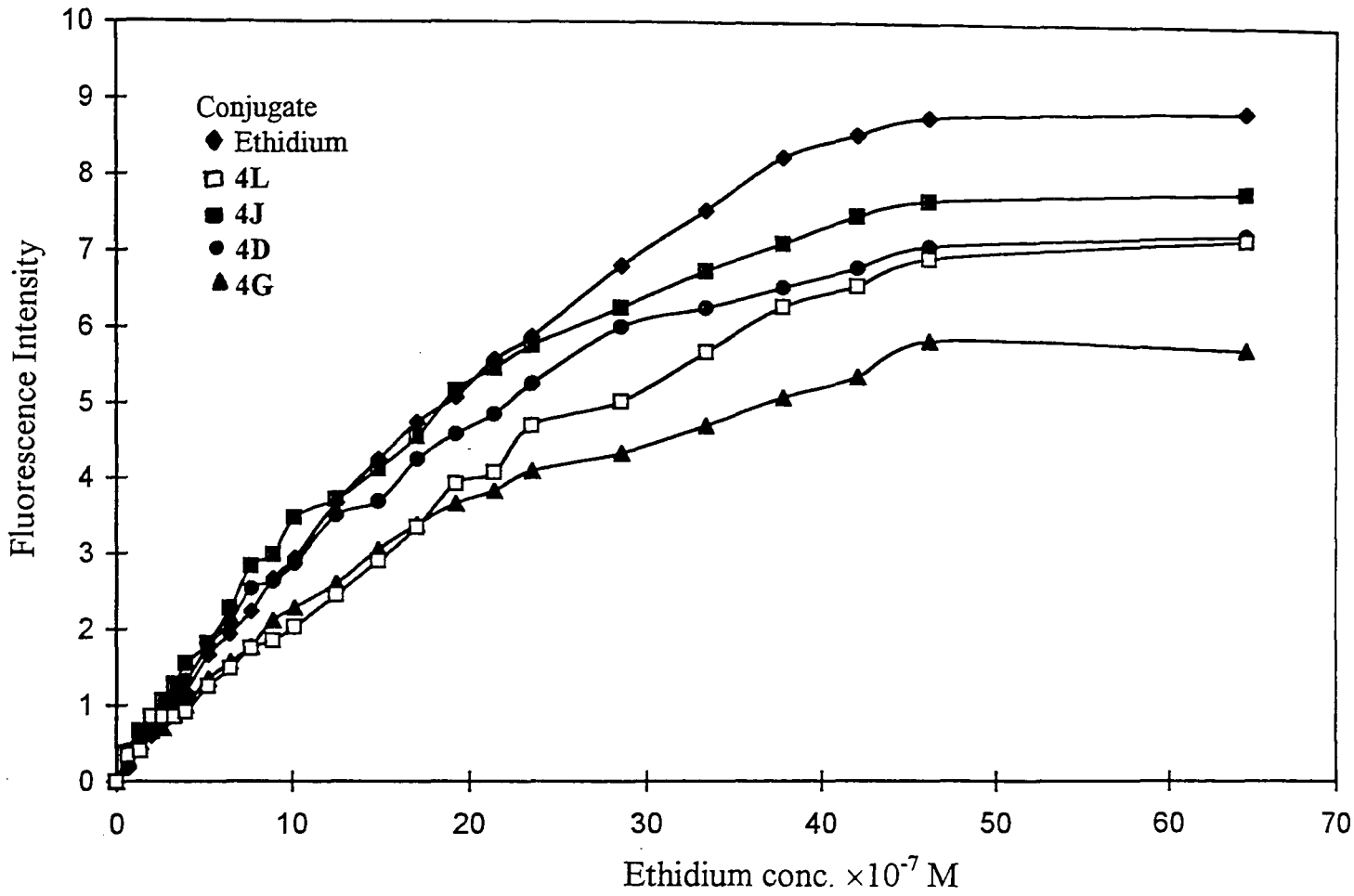

Conjugate **4D** =

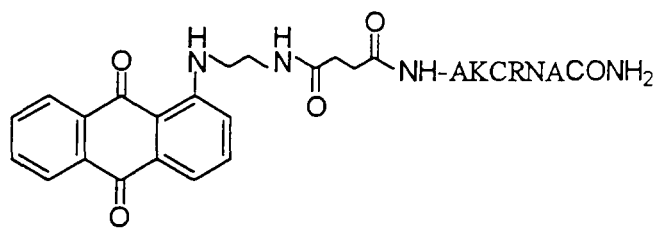

Conjugate **4G** = **G**-NH-AKCRNACONH$_2$

Conjugate **4J** = **D**-KAKCRNACONH$_2$

Conjugate **4L** = **D**-NH(CH$_2$)$_2$NHCO(CH$_2$)$_2$CONH-AKCRNACONH$_2$

Figure 58: The effect of **4D**, **4G**, **4J** and **4L** on the fluorescence enhancement of ethidium binding to DNA. The concentration of conjugate and DNA used was 2.0×10^{-6} M and 2.0×10^{-5} M, respectively. See section 6.14. 2 for experimental detail.

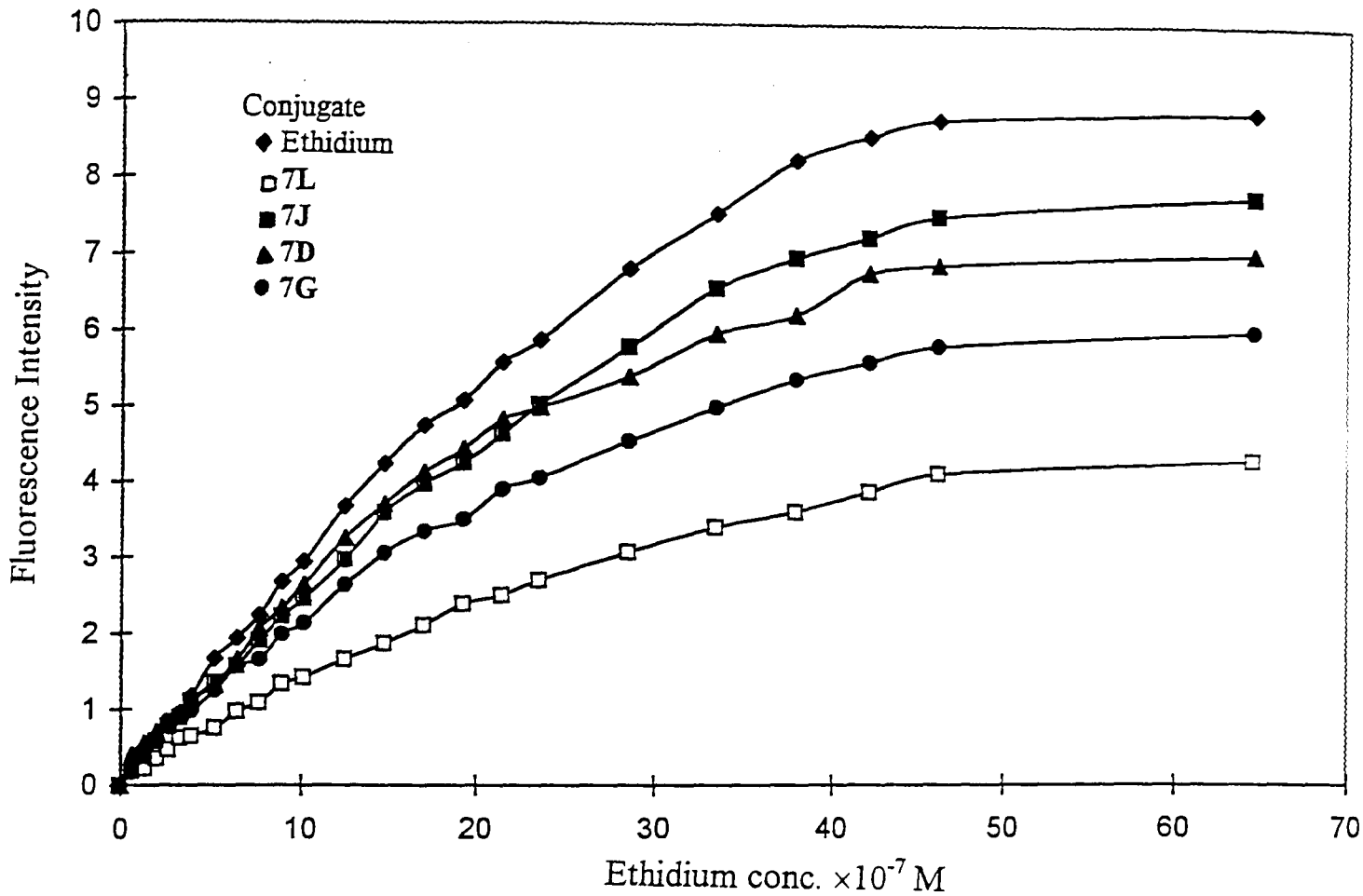

Conjugate **7D** =

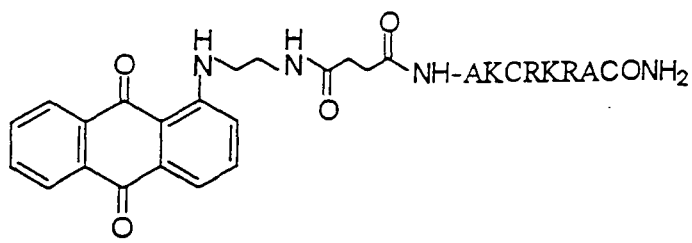

Conjugate **7G** = **G**- NH-AKCRKRACONH$_2$

Conjugate **7J** = **D**-KAKCRKRACONH$_2$

Conjugate **7L** = **D**-NH(CH$_2$)$_2$NHCO(CH$_2$)$_2$CONH-AKCRKRACONH$_2$

Figure 59: The effect of **7D**, **7G**, **7J** and **7L** on the fluorescence enhancement of ethidium binding to DNA. The concentration of conjugate and DNA used was 2.0×10^{-6} M and 2.0×10^{-5} M, respectively. See section 6.14.2 for experimental detail.

5.8 Discussion: DNA Binding Studies.

The aim of this section was to assess the relative affinity of the drugs for DNA and to investigate the nature of the drug-DNA interactions.

5.8.1 Effect of Intercalator-Peptide conjugates on thermal denaturation of DNA.

The intercalation of a drug molecule into the DNA helix stabilises the macromolecule such that more energy is required to separate the two strands. Thus the T_m of the DNA is increased due to a change in enthalpy (Zunino *et al*, 1972). However if the drug binds externally to the helix then there is generally no significant change in the T_m. The ΔT_m values obtained in this work gives some indication of binding ability of ligand to DNA. From these data it was observed that all the conjugates tested (table 9) were able to stabilise the DNA to thermal denaturation, though to varying degrees. It was however evident that the higher ΔT_m were observed with conjugates containing the more basic peptides (i.e. peptides **4**, **5**, **6** and **7**). This was consistent with the results obtained in the electrophoretic mobility shift assay and with the molecular modelling calculated for these peptides (section 5.14). EMSA and T_m data also showed that conjugates containing the **J** intercalator were slightly better than **D** containing conjugates. It was also interesting to observe that in general, conjugates which possessed the higher T_m values were most effective at displacing ethidium. The rank order of the T_m values relating to the conjugates was found to be **J>D>G>L**, where **J** conjugates were found to have the largest ΔT_m values. The conjugates which were most effective at displacing ethidium were **J>D>L>G**. Therefore, it seemed that the conjugates most able to stabilise the DNA duplex to thermal denaturation were also most effective at displacing ethidium and hence at intercalating. Thus mono-substituted anthraquinone chromophores such as **J** and **D** intercalators did display intercalation, especially in the case of **J**, where an extra lysine residue further enhanced binding. However, the di-substituted anthrapyrazole derivative **G** was shown to be less effective at displacing ethidium and also has a lower ΔT_m value when compared

with **J** and **D**. The unexpected weaker binding of **G** could be as a result of the amide moiety and the carboxyl functionality at the 7-substituted position.

5.8.2 Effect of Intercalator-Peptide conjugates on fluorescence enhancement of ethidium bromide due to binding to DNA.

The ability of the intercalator-peptides to displace ethidium bromide was investigated. The results showed that fluorescence enhancement, and hence DNA-binding, of ethidium was reduced when compounds **4/7(D, G, J** and **L)** were added to DNA. It was noted that of the two main peptides studied, **4** and 7, peptide 7 was observed to be the better of the two at displacing ethidium. The same conclusion was derived from T_m and EMSA assays. Molecular modelling also indicated that the binding energies upon interaction of peptides **4** and 7 were -499.27 and -495.12 kcal mol^{-1}, respectively (refer to section 5.14.1). Its believed that binding by peptide 7 was favoured because of the presence of an extra basic amino acid residue. Also, as mentioned above, the conjugates which had the most effect on ethidium displacement also displayed higher ΔT_m values. The results therefore showed that chromophores of the APZs and AQ conjugates intercalate with DNA as judged by displacement of ethidium from its binding site. Nevertheless, it must be highlighted that minor groove binders such as netropsin have been known to increase the melting temperature of DNA. Some intercalators (i.e. amsacrine see Baguley and LeBret, 1984) are also able to quench DNA-ethidium fluorescence without actually intercalating.

5.9 Biological Evaluation: Establishing the Specificity and Redox Sensitivity of c-Jun homodimer protein for AP-1 DNA consensus sequence.

Before any *in vitro* assays were carried out with the synthesised intercalator-peptide compounds, assays were performed to assess the specificity of the transcription factor protein used in this work and to optimise conditions for studying their binding to DNA. The specificity of the c-Jun homodimer protein was ascertained using wild-type and mutant AP-1 oligonucleotides, which differed by two base pairs, as shown below.

wild-type 5'-CGCTTGATGAGT**CA**GCCGGAA-3'
mutant 5'-CGCTTGATGAGT**TG**GCCGGAA-3'

The results showed that purified c-Jun homodimer protein was highly specific and can readily distinguish the mutant (has one inverted base pair) from the wild-type AP-1 oligomer (figure 41)

Subsequently it was demonstrated that binding of the c-Jun homodimer protein is required to be in the reduced state. Figure 42 clearly indicated that only when the reducing agent dithiothreitol, (DTT) was present did the c-Jun homodimer bind to the AP-1 consensus oligomer. This is consistent with reduction of the cysteine residue in the c-Jun homodimer being a prerequisite for binding to AP-1 site to occur (Abate *et al*, 1990a).

It was also observed that binding of the c-Jun homodimer protein does not occur with the SP-1 consensus oligomer. The SP-1 protein like the AP-1 binds to DNA via a redox regulated mechanism but interacts with the DNA structure via a zinc finger rather then via an ∝-helical conformation (Briggs *et al*, 1986). Both SP-1 and AP-1 proteins and their respective oligomers were used in later experiments to investigate the specificities of the synthesised intercalator-peptide conjugates (see figures 52 and 53).

SP-1 5'-ATTCGATCGGGGCGGGGCGAGC-3'
3'-TAAGCTAGCCCCGCCCCGCTCG-5'

AP-1 5'-CGCTTGATGAGTCAGCCGGAA-3'
3'-GCGAACTACTCAGTCGGCCTT-5'

Competition assays were also performed to detect the specificity of purified c-Jun protein. Competition assays can be seen as a way of assessing the stability of the interaction between the protein and its consensus oligonucleotide. The competing DNA acts as a catalyst causing the dissociation of preformed complexes in a DNA concentration-dependent and sequence-specific manner. The magnitude of the effect also depends on the particular protein under study. The

displacement of protein in direct transfer from one DNA site to another could be important in the search process for specific binding sites.

Two competition experiments were carried out. The first of these showed how the band intensity becomes diluted out with increasing concentration of unlabelled AP-1 oligomer. However the same effect was not observed with increasing concentration of unlabelled SP-1 oligomer. The unlabelled SP-1 oligomer in this case was unable to compete with the labelled AP-1 oligomer for the c-Jun protein. Essentially, the binding of the c-Jun homodimer protein to the labelled AP-1 DNA was not displaced in the presence of SP-1 DNA. This demonstrates the high specificity of the c-Jun homodimer protein for the AP-1 consensus oligomer.

In this work, the effect of the intercalator-peptide on the binding of the AP-1 protein to AP-1 site was investigated using HeLa nuclear extract. The extract is relevant to the complex cellular systems in which drug/DNA interactions would take place. It was important initially to show that the AP-1 heterodimer protein present in the HeLa extract was indeed responsible for binding to the AP-1 DNA consensus oligonucleotide and not by nonspecific proteins. One way in which this was achieved was by using AP-1 antibody. AP-1 antibody was incubated with the HeLa extract and AP-1 DNA consensus oligomer. The resulting ternary complex (antibody-protein-DNA) caused a 'supershift' to occur, this was seen as a second band above the existing protein-DNA band. This supershift was caused by an increased in molecular weight upon binding of the AP-1 antibody to AP-1 protein, and of the latter to DNA. It is therefore highly likely that the protein-DNA complex found in the existing HeLa extract corresponds to that of the AP-1 protein-AP-1 oligomer complex (see figure 44).

It was also successfully demonstrated that direct oxygenation of the AP-1 protein caused a reduction in binding to AP-1 DNA consensus sequence. The reversible oxidation product is thought to either be in the form of sulphenic (RSOH) or sulphonic (RSO_2H) acid (Abate *et al*, 1990a).

5.10 Effect of Anthrapyrazole and Anthraquinone derivatives on AP-1 protein binding to AP-1 DNA consensus sequence.

A ligand is accepted as an intercalator for several reasons including (a) it produces a helix extension corresponding to 3.4Å per drug chromophore, as measured by, say, viscosity changes (Wilson and Jones, 1981); (b) the chromophore is aligned parallel to these pairs, as indicated by electric dichroism or X-ray fibre diffraction (Neidle and Berman, 1983); or (c) DNA unwinding is produced (Wang, 1974). It is clear that planar drug molecules inserted between DNA base pairs can cause the DNA to unwind and hence show a somewhat smaller value of propeller twist. Propeller twist is defined as the angle (~12°) between two base planes when viewed along the axis joining them (Neidle and Berman, 1983).

Ethidium bromide (figure 45) is perhaps the best studied of the intercalators which along with 1,4-bis{[2-(dimethylamino-ethyl]amino}5,8-di-hydroxyanthracene-9,10-dione (AQ4) an analogue of mitoxantrone, both display good inhibition of AP-1 protein binding to AP-1 consensus sequence. Inhibition was observed with ethidium at ratio of 10:1 (ethidium:DNA), compared with some of the APZ and AQ derivatives synthesised in this thesis which showed inhibition at higher ratios (200:1).

Its been shown by previous workers that as a general principle following intercalation the base pairs remain perpendicular to the helix axis, but they are moved apart (by up to ~3.4Å) to accommodate the intercalator molecule. Van der Waals contact between the π-orbitals of the drug molecule and the base pairs would help to stabilise the complex via hydrophobic and charge-transfer forces. Local distortion of the helix occurs since it has to unwind in order to accommodate the drug molecule. Distortion of the helix due to local unwinding at intercalation sites would destroy the long-range regularity of the helix, as observed by X-ray diffraction studies. In principle, saturation of the DNA by intercalators causes the recognition site to become distorted (Chen *et al*, 1985).

This could explain the displacement of AP-1 and SP-1 transcription factors from binding to DNA.

A series of compounds (table 6) were tested for their intercalative activity, and compound **B** was found to display little or no inhibition of AP-1 protein binding to AP-1 DNA, even at concentrations of 800:1 (**B**:DNA). The lack of intercalation by **B** can be explained by considering its structure (see table 6), a very short side arm with no basic amino group and of mono-substituted configuration. Other mono-substituted intercalators that caused a slight inhibition of AP-1 binding were **A**, **C** and **D**. These structures differ from **B** in that they have a tertiary amine separated from N^2 by two methylene groups (in the cases of **A** and **C** intercalators). Nevertheless, it has also been shown (see review by Patterson and Newell, 1994) that the amine can either be primary or secondary to be active. The effect of extending beyond three methylene groups has not been reported. It has been suggested (Showalter *et al*, 1987) that for related anthraquinones there is a more rigid requirement for only two methylene groups separating the two nitrogens. Basic side chains will allow electrostatic attraction of the positively charged amino functionalities to the phosphate residues on the outside of the DNA duplex. An amide containing side chain as in the case of intercalator **D**, was also seen to cause some inhibition of the binding of AP-1 protein to AP-1 DNA consensus sequence.

The compounds that proved most effective at displacing AP-1 were the di-substituted intercalators, **E**, **F** and **G**. Intercalator **E** (2,5-disubstitution APZ) binds directly to the DNA by inserting between the base pairs in a conventional manner (Fry, 1991), however with intercalators **F** and **G** (2,7-disubstitution APZ) the intercalation process is more complex. Its been demonstrated on similar compounds that, in order for **F** and **G** to bind, DNA-breathing (transient base pair unstacking) (Tanious *et al*, 1992; Fry, 1991) has to occur to allow the docking of the drug molecule into the intercalation site. Once the intercalator has 'straddled' the DNA, DNA-breathing is required before dissociation can take place. The latter method of intercalation by **F** could explain why inhibition of

AP-1 protein from binding to AP-1 DNA was more significant than either **E** or **G**. The order of decreasing inhibition AP-1 protein binding to AP-1 site was found overall to be **F>E>G>D>A>C>B**.

The dissociation rate constant for DNA complexes with disubstituted anthraquinones was investigated by Gandecha (1985). He found that the order of dissociation was 1,4-bis-substituted anthraquinones followed by 1,5-bis-substituted anthraquinones, with the latter possessing the lower dissociation rate constant (i.e. 3.82 and 0.91 s^{-1}). Nevertheless both types of compounds were found to have similar DNA affinity constants.

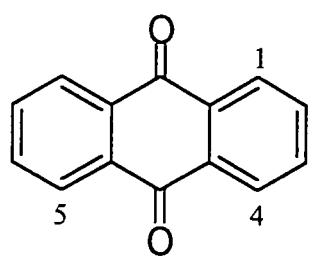

It was highly likely that the binding of **F** via straddling the **F**:DNA complex, could account for the higher activity. Disturbance of the DNA structure would be required in order to affect straddling/threading of a bulky polar side chain from one side of the DNA to the other. Two key features can therefore be summarised for such a mechanism: (i) both the association and dissociation rate constants should be decreased relative to classical intercalative DNA binding and (ii) threading of cationic side chains through the DNA duplex would require sequential formation and breakage of electrostatic interactions in the threading complex. In support of this Tanious *et al* (1992) shown that the binding modes for the anthracene-9,10-diones involved threading-type intercalation for the 1,5- or 2,6-disubstituted compounds and classical DNA intercalation for the 1,4- and 1,8-difunctionalised derivatives, where both side chains occupy the same groove.

In considering the ratio of intercalator used in this work to cause an inhibition (as high as 800:1), it was possible that the intercalator interacted directly with the transcription factor protein AP-1 rather then with the DNA. However

because very similar intercalators had very different degrees of inhibition, it can be concluded that interaction of the intercalator was predominately with DNA. However, it must be highlighted that in the presence of large excesses of intercalator material a different and unique mode of binding might arise. For example, ligands that are known to intercalate can also display self association. This 'stacking' process involve ligand molecules binding to the exterior of the DNA helix and stacking upon each other (Blake and Peacock 1968). This stacking is due to electrostatic interactions of the positive charges of drug with negatively charged phosphate groups. However, this interaction is unlikely to be of significance *in vivo*, where relatively low ligand concentrations, are found. It must be emphasised, however, that stacking, unlike intercalation, is a non-specific event and often occurs when the ratio of ligand to DNA is greater than one; and often with extended side chains on the chromophore, where incorporation of all parts of the molecule is precluded. This can effectively lead to different modes of binding (Foye *et al*, 1982) including exterior electrostatic binding as well as intercalation and stacking. The stronger binding is most likely associated with intercalation of the chromophore.

This work suggested that there was no clear preference/selectivity of any intercalator synthesised for the AP-1 site compared to the SP-1 site. This was not surprising since only a few of the intercalators are known to display any preferences for either GC or AT base pair sequences and these often have very well defined functional moieties that would enable them to behave as such. For example, actinomycin (Muller and Crothers, 1968) and mitoxantrone (Lown *et al*, 1985) are G-C specific, tilorone (Strum *et al*, 1981) and the neocarzinostatin chromophore (Dasgupta and Goldberg 1986) is A-T specific. Threading intercalators tend to be AT specific since the breathing of A-T rich DNA is facilitated by presence of two hydrogen bond per base pair compared to three hydrogen bonds in G-C rich regions. A more involved situation can occur as in the case of daunomycin and adriamycin (Chen *et al*, 1985) for which the actual sequence selectivity must be expressed at the level of a triplet of mixed base pairs.

5.11 Effect of Oligopeptide functionality on AP-1 protein binding to AP-1 DNA consensus sequence.

In this work eight short peptides (table 7) ranging from 5 to 7 amino acid residues in length, all containing the KCR motif were tested for their effect on binding to the AP-1 DNA consensus oligonucleotide. KCR is the centre for recognition of the AP-1 site and it is responsible for redox sensitive DNA binding of the AP-1 heterodimer (O'Neil *et al*, 1990). The mode of binding is very well documented and involves the formation of an α-helix upon binding to the DNA recognition site (see chapter 1). Note, however, that this design is not limited to AP-1. Any protein or other molecule that recognizes a specific DNA sequence by binding along the major groove could be a candidate.

The results from these assays showed that even when the peptide concentration used was 10-fold greater than that for the intercalator, only four of the eight peptides displayed any effect on the binding of AP-1 protein to the AP-1 DNA binding site. However, it was interesting to note that of the eight peptides, the four that did display inhibition of AP-1 binding were those considered to be most basic (i.e. peptides **4**, **5**, **6** and 7). It was also observed that conjugates containing these peptides (**4**, **5**, **6** and 7) displayed higher ΔT_m (table 9) than for conjugates coupled to the other four peptides (**1**, **2**, **3** and **8**). Peptide-dependent conjugates were seen for both **D** and **J** intercalators (see table 9). This observation highlights the significance and the influence that the peptide has on the binding nature of the intercalator. In addition the binding energies upon interaction of peptides **1** to **8** with the AP-1 DNA binding site were considered most favourable for peptides **4**, **5**, **6** and 7 (see table 10). Furthermore, the peptide sequences that most resembled the AP-1 basic binding domain were **4**, **5**, **6** and 7. The high concentration of peptide required to inhibit the binding of AP-1 protein (ranging from 2000 to 8000:1, peptide:DNA), effectively means that the affinity constant between the peptide unit and DNA AP-1 oligomer is relatively low. However, despite the low affinity of the peptide for DNA, it is considered to be the more selective half of the peptide-intercalator molecule. In principle, it was antipicated that by linking the peptide unit to an intercalator it

is possible to facilitate binding of the oligopeptide to DNA in a selective manner governed predominantly by the peptide unit used.

As mentioned before, it is possible that inhibition of AP-1 binding to the AP-1 site can be caused by formation of ligand-AP-1 protein complexes rather then drug-DNA. Nevertheless, this was unlikely since all eight peptides despite their similarity have very differing degrees of inhibition. It was therefore likely that the peptide units were bound to the DNA and not to the AP-1 protein. It appears that the interaction between the DNA and KCR containing peptide unit was selective and influenced by the sequence and nature of the peptide used. Talanian *et al* (1992) have addressed this area of peptide sequence-specific DNA binding. They showed from DNAase I footprinting experiments that dimers of peptides containing 20 residues of GCN4 (see chapter 1) bind DNA with a sequence specificity similar to that of the intact protein. Also circular dichroism experiments suggest that specific binding involves only 15 residues (corresponding to residues 231-245 of GCN4), in an ∝-helical conformation. Thus, the essential contribution of the leucine zipper to DNA binding appears to be dimerisation, and the basic domain of the peptide contains sufficient information for specific DNA binding (Talanian *et al*, 1990).

5.12 Effect of Intercalator-Peptide conjugates on AP-1 protein binding to AP-1 DNA consensus sequence.

The approach of ligands having mixed binding functions is complicated by drug-induced DNA conformational changes. Indeed, theoretical and experimental studies have both clearly shown that binding to DNA, whatever the nature of the implied process, results in an adoptation of the DNA conformation to that of the ligand rather than vice versa (Gilbert and Feigon, 1991).

In this work a series of intercalator-linked peptide compounds were synthesised, see table 8. Such hybrid ligands were designed with the rationale that an intercalating chromophore would provide DNA affinity whilst the appended peptide may encourage DNA sequence selectivity.

The intercalator **D** was selected as one of the main intercalators to be used in this work for several reasons. Firstly, **D** showed an appreciable degree of inhibition of AP-1 binding to AP-1 site. Secondly it was readily coupled onto the peptide using PyBOP. The relatively low affinity of intercalator **D** for DNA (deduced from EMSA data) was also considered advantageous in that the search for the AP-1 recognition site by the attached peptide unit would be facilitated. In contrast, intercalators with high DNA affinity constants would tend to inhibit sliding of the peptide along the DNA (see introduction). The role of the chromophore was seen therefore to anchor the peptide to DNA which has practically no affinity for DNA but nevertheless possesses higher specificity. Thus by conjugating the intercalator and peptide, the resulting molecule will be directly delivered to the DNA target.

A total of seventeen intercalator-peptide compounds were tested for their effect on the AP-1 binding to AP-1 DNA consensus sequence. The results obtained in this work clearly indicated that inhibition of protein-DNA complex formation was most significant with the intercalator-peptide. The relative activity was therefore in order of intercalator-peptide > intercalator >> peptide. From this it can be postulated that, in order for the intercalator-peptide to possess a greater inhibition/activity than the intercalator or peptide, both the intercalator unit and peptide unit must be bound simultaneously to the DNA (see Waring and Bailly, 1994; Bailly and Henichart, 1991) i.e. intercalation of the flat aromatic chromophore and major groove binding of the peptide part. It was observed that the most potent conjugates were those containing peptides **4**, **5**, **6** and 7, which was consistent with the fact that these peptides were most potent when tested as peptide units. This outcome further supports the concept of bimodal binding by the intercalator-peptide, in which conjugates containing peptides **4**, **5**, **6** and 7 have superior activity. Conjugates containing the more basic peptides also gave the largest ΔTm values. Furthermore, EMSA and T_m assays showed that conjugates containing **J** intercalator (with one extra lysine residue) were more active than the **D** intercalator containing conjugates. In addition, EMSA showed that peptide 7 containing conjugates were favoured over **4**, this was consistent

with the data obtained from molecular modelling (see section 5.14), Tm and ethidium displacement assays.

The choice of the linker connecting the recognition elements may also be a critical design feature with regard to simultaneous binding of all moieties (Dervan, 1986). The most suitable linkers are considered to be the alkylamino or aminoalkylamino, as these generally show greater activity. Conjugates **4J** to **8J** and **5K** and **6K** all contained one (**J**) and two (**K**) lysine residues in their linker group, respectively. It was anticipated that distortion of the double helical structure upon intercalation could alter the AP-1 recognition site thus preventing the peptide unit from binding. Therefore it seemed beneficial to increase the length of the linker between the two DNA-binding units in order to permit bimodal binding of the hybrid to DNA. The extended linker might allow proper placement of the peptide in the groove and the chromophore in between base pairs.

The results in table 8 indicated that conjugates with a lysine extended linker (conjugates **J** and **K**) were more effective at inhibiting AP-1 protein from binding to AP-1 DNA consensus sequence. However the enhanced activity may be as a result of the basicity of the lysine residue contributing to the DNA binding. In fact, the presence of basic peptides bearing as many as seven free amino groups supports the view that binding of the peptide moiety will be external as opposed to intercalative. Furthermore, electrostatic interactions may come to predominate over the expected specific hydrogen-bond formation in the major groove of DNA, just as observed with polyamines such as spermine and spermidine (Tabor and Tabor, 1984).

5.13 Specificity of Intercalator-Peptide conjugates for AP-1 DNA consensus sequence.

In this work the relative concentrations of oligomer transcription factor protein and drug was kept constant for both AP-1 and SP-1. In assessing the specificity, intercalator-peptide compound **7D** (and **4D**) was incubated with both AP-1 and SP-1 DNA oligomer along with their respective AP-1 and SP-1 proteins.

AP-1 5'-CGC TTG ATG AGT CAG CCG GAA-3'
3'-GCG AAC TAC TCA GTC GGC CTT-5'

SP-1 5'-ATT CGA TCG GGG CGG GGC GAG C-3'
3'-TAA GCT AGC CCC GCC CCG CTC G-5'

SP-1 is a sequence-specific transcription factor that recognises GGGGCGGGGC and closely related sequences, which are often referred to as GC boxes (Briggs *et al*, 1986; Kadonaga *et al*, 1987). The sequence specificity of SP-1 protein binding to DNA is conferred by Zn (II) fingers, whereas a different region of SP-1 appears to regulate the affinity of DNA binding.

Binding of AP-1 to AP-1 DNA binding site was inhibited by conjugates **7D** and **4D**. However, a similar extent of inhibition was observed for the SP-1 oligomer. It would therefore seem that the compounds lacked selectivity. However on evaluation, several contributory factors to the selectivity or specificity of the intercalator-peptide ligand should be considered. The concentration of intercalator-peptide used (200 to 800:1; hybrid:DNA) in order for an effect to be observed was very high. At this concentration it was possible that any specificity displayed by the conjugate was lost. However, one solution to this problem would be to use more sensitive detection methods. One approach that could be considered is DNA foot printing. However, this method requires the drug in question to have a high affinity for DNA. It is also now thought that although the leucine zipper region is not directly involved in DNA binding, results by Park *et al* (1992) indicate that its position relative to the basic region may play a role in

determining which target sequence of DNA the protein recognizes. Therefore it is possible that by replacing the leucine zipper with an intercalator the molecule has been "disabled".

It is also possible that because both the binding mechanism of AP-1 and SP-1 protein involves a redox mechanism, better comparisons would have been made using non-redox regulated transcription factors. Other widely commercially available transcription factors that could have been used include, TFIIB (Maldonado *et al*, 1990) and TFIID (Patterson *et al*, 1990). Furthermore, the GC boxes found in SP-1 DNA consensus sequence could invariably favour binding of both AQ and APZ intercalators (see section 5.10) whilst binding of the peptide moiety to AP-1 is preferred. Despite the lack in selectivity demonstrated by these intercalator-peptides, a novel approach in using EMSA to explore drug mediated displacement of transcription factors has been established. Moreover, future peptides can potentially be modelled around this concept of hybrid ligands and bimodel binding.

Recently Tabor (1996) described the synthesis of a peptide-intercalator hybrid based on the bZIP motif from GCN4. Like the target hybrid molecule presented in this thesis, the design of the hybrid ligand described by Tabor combined a peptide necessary for recognition of the consensus site with the known binding enhancement of an intercalating moiety specifically acridine.

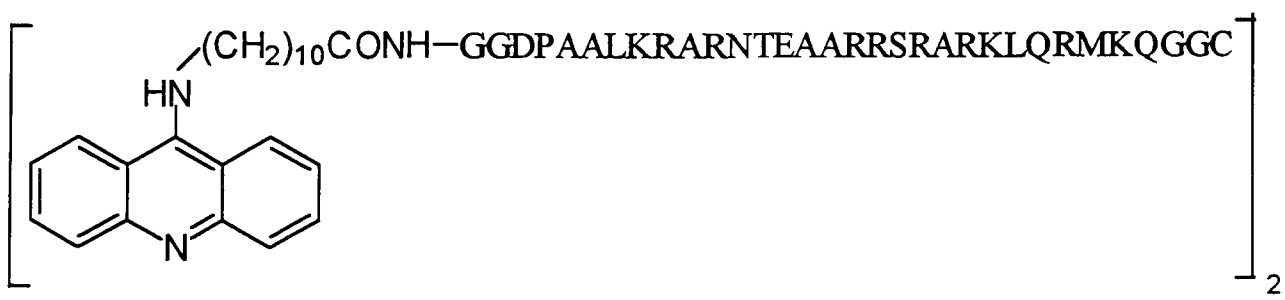

No biological evaluation was carried out on this hybrid ligand, although even if this hybrid had been selective for AP-1, the enormous length of the peptide moiety makes it an unlikely candidate for drug development. The *in vivo* situation is considerably more complicated due to problems of permeability

(particularly hybrids with longer ligands), solubility, competitive binding to proteins and/or lipids and metabolic breakdown of the conjugates. It is therefore important when designing future drugs that a balance is struck between activity and pharmacokinetics.

5.14 Molecular Modelling of the AP-1 Leucine Zipper - Oligopeptide-DNA Interaction.

As mentioned before in chapter 1, how much DNA sequence-information is available in the phosphate backbone in terms of interphosphate distances (groove widths), deoxyribose conformation, and electronegative potential and to what extent this is exploited by nature is still not clear. Nevertheless, most sequence information is considered to be on the 'floor' of the major groove.

Four recognition sites are present in the major groove of AT base pairs (figure 61). These are the adenine-N7 (hydrogen acceptor), the adenine amino group (N6) (hydrogen donor), the thymine-O4 (hydrogen acceptor), and the thymine methyl group (van der Waal interaction). Similarly, the recognition sites available at GC base pairs are two hydrogen acceptors (guanine-N7 and guanine-O6) and one hydrogen donor (the cytosine amino group at C4). Thus the DNA sequence can be unambiguously read from the major groove as a 'two-dimensional grid' of hydrogen-donor and -acceptor and van der Waals contact sites. In this respect ApT versus TpA (and GpC versus CpG) base pairs are readily distinguishable. Since the floor of the groove is not planar, the corresponding sites of the DNA binding ligand furthermore have to be positioned correctly in space in much the same way as the key-lock principle of the substrate-enzyme recognition.

5.14.1 Molecular Modelling of Peptides containing the AP-1 Leucine Zipper.

A series of binding energies (Horton and Lewis, 1992) were obtained for each of the eight peptides (table 10) using the molecular modelling software Insight II. Previously Niles and Brunger (1991) developed a largely automatic GCN4 leucine zipper. They first constructed an idealised C_α model, corresponding to parallel, straight, helices. The remaining atoms are then constructed automatically

Major groove

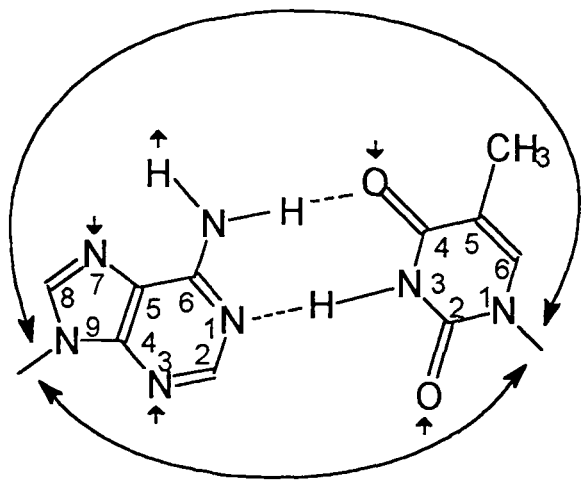

Minor groove

Adenine : Thymine

Major groove

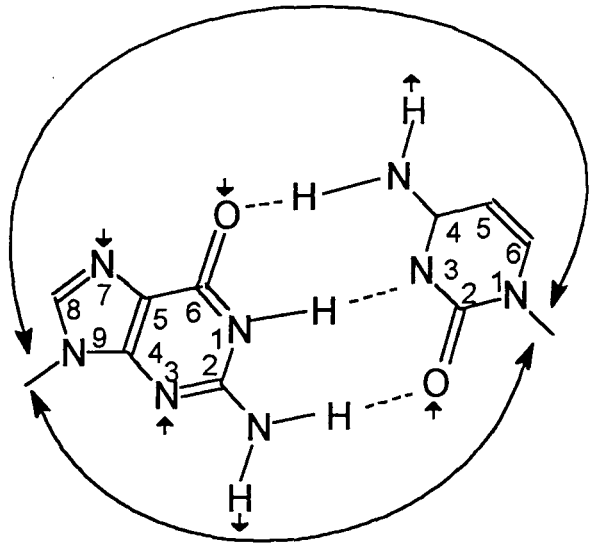

Minor groove

Guanine:Cytosine

Figure 60: Donor and acceptor groups in the grooves of A·T and G·C base pairs.

from the C_{α} coordinates. The model is refined with minimisation and molecular dynamics, with a final stage of unrestrained molecular dynamics simulation with explicit solvent. It is assumed the model is some kind of parallel coiled-coil, but the detailed parameters of the coiled-coil can vary.

Table 10: Binding energies upon interaction of peptides **1** to **8** with the AP-1 DNA binding site.

Peptide Unit	Binding Energies (kcal mol^{-1})
1	-474.65
2	-480.49
3	-477.51
4	-495.12
5	-480.70
6	-486.43
7	-499.27
8	-471.26

5.15 Discussion

From the data obtained in table 10 it was observed that binding to the major groove was favoured by peptides that were longer and more basic in nature i.e. peptides **4**, **5**, **6** and 7. This was consistent with the results obtained in EMSA in which peptides **4**, **5**, **6** and 7 were found to show the greatest degree of inhibition. Furthermore, conjugates containing these particular peptides were also most effective at inhibiting AP-1 protein from binding to AP-1 DNA consensus sequence. The same conjugates containing these four peptides were shown also to have higher ΔT_m values. Of the two peptides mainly investigated, peptide 7 was shown to have the greater binding constant compared to **4**. This was consistent with the EMSA data in which peptide 7 showed better inhibition of AP-1 protein binding than peptide **4**. Peptide 7-containing conjugates were also demonstrated to be both better inhibitors of AP-1 binding and have greater ΔT_m values than peptide **4**-containing conjugates.

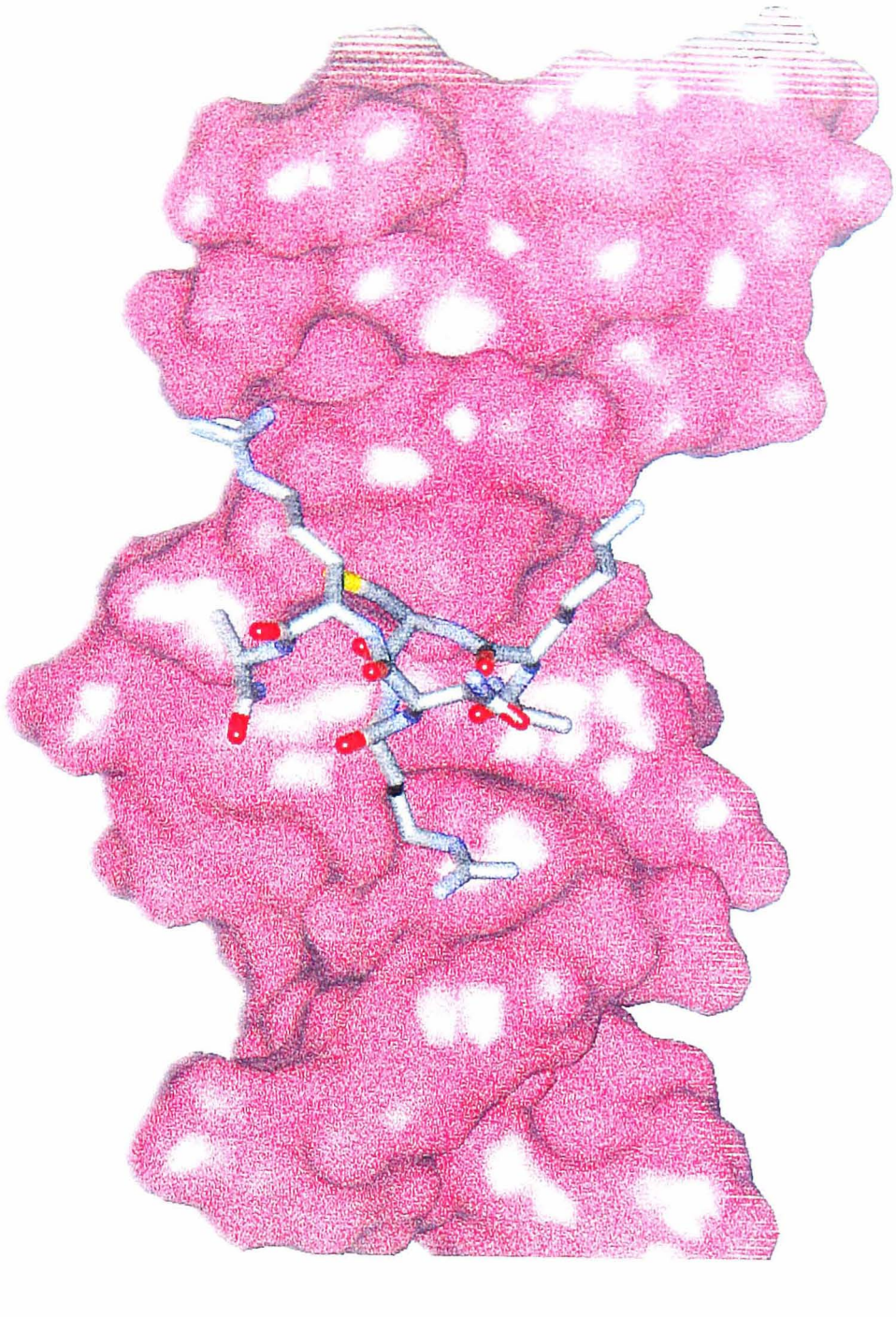

Figure 61: Peptide **6** (H_2N-A-K-C-R-N-R-A-$CONH_2$) bound to AP-1 DNA consensus sequence.

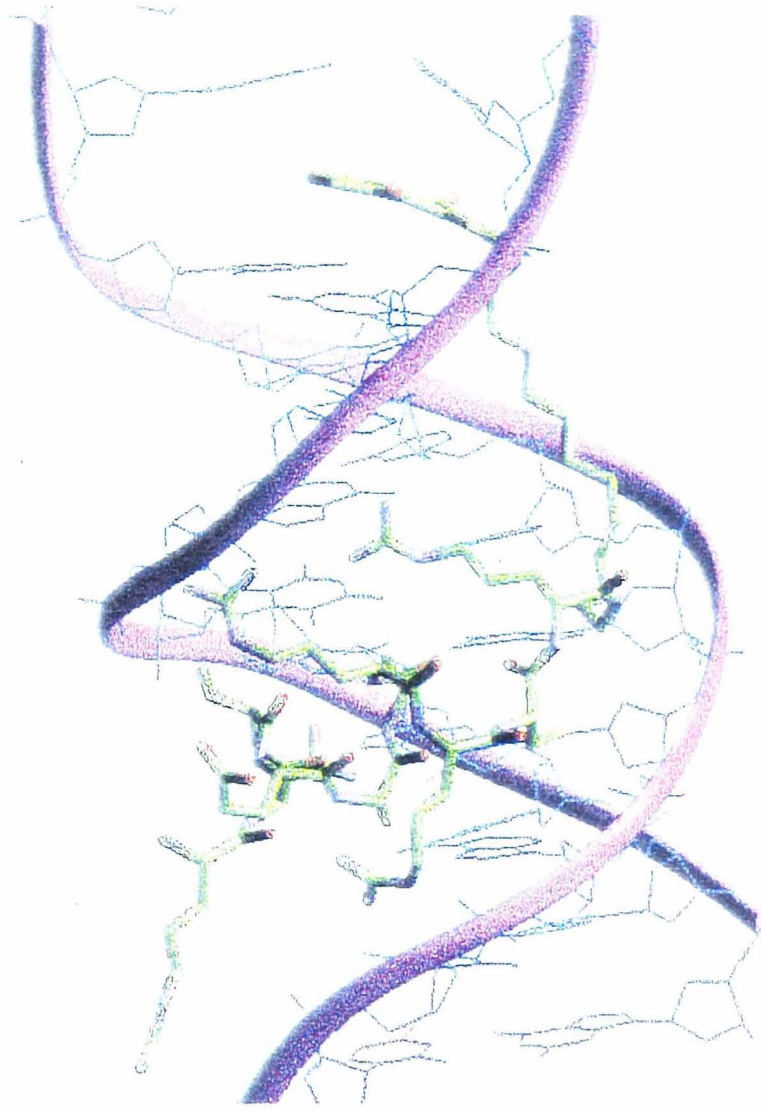

Conjugate **7D** =

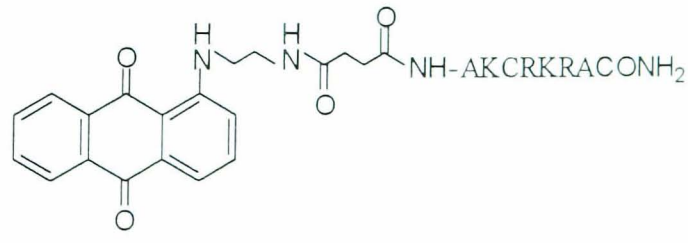

Figure 62: Intercalator **D**-linked peptide 7 bound to AP-1 DNA consensus sequence.

5.16 Summary

The aim of this investigation was to design and synthesise hybrid (intercalator-linked peptide) ligands combining a peptide necessary for recognition of the consensus site with the known binding enhancement of an intercalating moiety. Such a molecule was anticipated to inhibit transcription by preventing the binding of transcription factors such as AP-1 protein from binding to its consensus sequence. In this thesis, a series of intercalator-peptide conjugates were successfully synthesised, isolated and characterised using modern analytical techniques. It was also characterised using 2D nmr techniques such as NOESY to show that peptides prepared in this work exist in an ∝-helical conformation.

These intercalator-peptide compounds were then shown to bind to DNA via intercalation as demonstrated by their effect on the thermal denaturation of DNA and on their ability to displace ethidium. In addition, an electrophoretic mobility shift assay showed that binding of AP-1 protein to the AP-1 DNA consensus sequence was inhibited by these compounds, though not selectively. It is therefore worth while investigating how, by extending the peptide unit better selectivity could be achieved. Finally, the redox sensitivity of these peptide hybrids should be explored. The KCR motif central to all the compounds prepared is, in principle, hugely sensitive to oxidation. An oxidised cysteine residue should, by analogy with AP-1 proteins, prevent binding of the hybrid to DNA. In this way, redox control of binding could be achieved. This may have utility as a design feature in transcription factor inhibitors since it would ensure that the peptide hybrid is only active in cells under oxidative stress. This condition is often associated with cancer cells, and hence tumour selective therapy is possible by this approach.

So for future work, it would be worthwhile to synthesise longer peptide sequences and to vary the binding constant by using other intercalators. It is also possible to enhance bimodal binding by looking at different linker groups. Cleavage based assays such as affinity cleavage, strand cleavage and footprinting could then be used to investigate the specific location of binding on DNA.

Chapter 6

Experimental

(C=O), 1250 (C-N); δ_H (DMSO): 8.10 (7H, m, Ar*H*), 4.65 (2H, t, NNCH_2), 4.40 (1H, bt, O*H*), 4.00 (1H, s, N*H*), 3.40 (2H, q, CH_2OH), 3.15 (2H, t, CH_2NH), 2.65 (2H, t, HNCH_2); δ_C (DMSO): 182.6, 139.6, 137.5, 136.0, 133.8, 132.6, 131.4, 128.7, 128.5, 128.5, 125.3, 122.5, 120.5, 117.1, 60.2, 51.2, 49.7, 49.0; m/z (FAB) 308 $(M+H)^+$; (Found: C, 70.71, H, 5.76; N, 13.92. $C_{18}H_{17}N_3O_2$ requires C, 70.34; H, 5.57; N, 13.67%).

6.3.1 Synthesis of 2-{2-[*N*-(2-Hydroxyethyl)-*N*-methylamino]ethyl}anthra[1,9-*c,d*]pyrazol-6(*2H*)-one (6).

2-{2-[*N*-(-2-Hydroxyethylamino)ethyl}anthra[1,9-*cd*]pyrazol-6(*2H*)-one **(5)** (1.23g, 4.02mmol) was dissolved completely in formic acid (2.74mL, 72mmol) before addition of aqueous formaldehyde solution (37%, 0.71mL, 11mmol). The mixture was heated to 95-100°C on an oil-bath for 5 hr. The reaction mixture was cooled to room temperature before being taken up in chloroform (5mL), giving rise to an immisible solution. The isolated water phase was then basified to pH12 with (2% w/v) NaOH (40mL) to afford a fine green precipitate. This was extracted with chloroform (4×30mL) and the solvent removed *in vacuo* to obtain a dark viscous oil, then triturated with methanol (2mL) and left overnight at ≤5 °C. Lime green solid material was obtained by filtration and further recrystallised from methanol to obtain the analytically pure 2-{2-[*N*-(2-hydroxyethyl)-*N*-methylamino]ethyl}anthra[1,9-*cd*]pyrazol-6(*2H*)-one **(6)** (0.981g, 76.3%) m.p. 78-80°C, t.l.c R_f 0.5 (CH_2Cl_2/MeOH 1/1), ν_{max} (KBr) cm^{-1}: 3400 (OH), 1670 (C=O); δ_H (DMSO): 8.00 (7H, m, Ar*H*), 4.70 (2H, t, NNCH_2), 4.25 (1H, bt, O*H*), 3.40 (2H, q, CH_2OH), 3.00 (2H, t, CH_2NMe), 2.50 (2H, t, MeNCH_2), 2.25 (3H, s, Me); δ_C (DMSO): 182.9, 139.7, 137.5, 136.2, 134.1, 132.9, 131.7, 129.0, 128.8, 127.5, 125.6, 122.8, 120.8, 117.4, 59.6, 59.3, 57.4, 48.2, 42.9; m/z (FAB) 322 $(M+H)^+$; (Found: C, 71.32; H, 5.83; N, 13.25. $C_{19}H_{19}N_3O_2$ requires C, 71.01; H, 5.96; N, 13.07%).

6.3.2 Synthesis of 2-{2-[*N*-(2-Chloroethyl)-*N*-methylamino]ethyl}anthra[1,9-*c,d*] pyrazol-6(*2H*)-one (7).

Thionyl chloride (4mL) was added dropwise to a cooled (0°C) and stirred sample of **(6)** (1.42g, 4.43mmol) with no other solvent present. The reaction

mixture was then removed from the ice-bath and allowed to come to room temperature over the course of 15 hr with minimal stirring under anhydrous conditions. Excess thionyl chloride was then carefully removed *in vacuo* to afford a dark tar-like material which on trituration with dry ether (3×5mL) gave a browny yellow solid. Bright yellow crystals were obtained on crystallisation with hot methanol (~1mL) to yield the product (0.86g, 51.7%) m.p. 108-110°C, ν_{max} (KBr) cm^{-1}: 1670 (C=O), 1250 (C-N), 700 (C-Cl); δ_H (DMSO): 8.00 (7H, m, Ar*H*), 5.05 (2H, t, NNCH_2), 4.00 (2H, t, CH_2Cl), 3.85 (2H, t, CH_2NMe), 3.65 (2H, t, MeNCH_2), 2.20 (3H, s, Me); δ_C (DMSO): 182.2, 139.9, 137.5, 136.7, 133.9, 132.8, 131.5, 129.2, 129.0, 128.8, 125.5, 122.8, 121.0, 116.8, 56.6, 54.7, 53.5, 44.1, 37.9; m/z (FAB) 341 $(M+H)^+$; (Found: C, 67.33; H, 5.28; Cl, 10.62; N, 12.65. $C_{19}H_{18}ClN_3O$ requires C, 67.16; H, 5.34; Cl, 10.43; N, 12.36%).

6.4 Synthesis of 7-Chloro-2-{2-[*N*-(2-hydroxyethyl)amino]ethyl}anthra[1,9-*c*,*d*] pyrazol-6(*2H*)-one (9).

1,5-Dichloroanthraquinone (5.54g, 20mmol) and 2-[(2-(hydrazinoethyl)amino]ethanol **(4)** (5.14g, 38mmol) were suspended in acetonitrile:DMF (50:25mL). Triethylamine (3.0mL, 27mmol) was added and the stirred mixture heated to reflux for ~20 hr under positive nitrogen pressure. The mixture was then allowed to come to room temperature before further storage at ≤5°C overnight. A deep red solution was obtained in which a yellow precipitate was suspended. This was filtered under pressure using a generous volumn of cold methanol followed by recrystallisation with methanol to yield the product as a yellow crystalline solid (4.03g, 58.9%) m.p. 140-142°C, t.l.c R_f 0.2 (CH_2Cl_2/MeOH 1/1), ν_{max} (KBr) cm^{-1}: 3400 (OH), 1670 (C=O), 1250 (C-N); δ_H (DMSO): 8.00 (6H, m, ArH), 4.65 (2H, t, NNCH_2), 4.45 (1H, bt, O*H*), 4.00 (1H, s, N*H*), 3.40 (2H, q, CH_2OH), 3.15 (2H, t, CH_2NH), 2.65 (2H, t, HNCH_2); δ_C (DMSO): 181.7, 139.5, 137.0, 136.0, 134.6, 134.0, 132.5, 128.8, 128.4, 126.0, 122.0, 121.9, 120.7, 116.8, 60.7, 51.7, 50.2, 49.5; m/z (FAB) 342 $(M+H)^+$; (Found: C, 63.26; H, 4.68; Cl, 10.07; N, 12.62. $C_{18}H_{16}ClN_3O_2$ requires C, 63.25; H, 4.72; Cl, 10.37; N, 12.30%).

6.4.1 Synthesis of 7-Chloro-2-{2-[*N*-(2-hydroxyethyl)-*N*-methylamino] ethyl} anthra[1,9-*c,d*]pyrazol-6(*2H*)-one (10).

(9) (0.17g, 0.50mmol) readily dissolved in formic acid (0.38mL, 10mmol) and formaldehyde solution (37%, 0.11mL, 1.50mmol). The mixture was heated at 95-100°C on an oil bath for 4 hr. The reaction was then cooled to room temperature and dissolved in chloroform. The aqueous layer was separated and basified to pH12 with NaOH (2% w/v). The N-methylated product was extracted with chloroform (4×5mL). The chloroform was removed under vacuum to leave a viscous oil which on cooling formed a crystalline solid. This residue was redissolved in hot methanol and on cooling reformed as the pure product (0.085g, 48.0%) m.p. 119-121°C, t.l.c R_f 0.6 (CH_2Cl_2/MeOH 1/1), ν_{max} (KBr) cm^{-1}: 3400 (OH), 1670 (C=O), 1030 (C-N); δ_H (DMSO): 7.80 (6H, m, Ar*H*), 4.65 (2H, t, NNCH_2), 4.20 (1H, bt, O*H*), 3.25 (2H, q, CH_2OH), 2.95 (2H, t, CH_2NMe), 2.40 (2H, t, MeNCH_2), 2.25 (3H, s, Me); δ_C (DMSO): 181.5, 139.2, 136.9, 136.0, 134.4, 133.8, 132.3, 128.7, 128.3, 126.0, 121.9, 121.8, 120.6, 116.6, 59.6, 59.3, 57.3, 48.1, 42.9; m/z (FAB) 356 $(M+H)^+$; (Found: C, 64.30; H, 4.95; Cl, 10.08; N, 12.01. $C_{19}H_{18}ClN_3O_2$ requires C, 64.14; H, 5.10; Cl, 9.96; N, 11.81%).

6.4.2 Synthesis of 7-(2-Aminoethyl)amino-2-{2-[*N*-(2-hydroxyethyl)-*N*-methyl amino] ethyl}anthra[1,9-*c,d*]pyrazol-6(*2H*)-one (11).

(10) (0.322g, 0.90mmol) was suspended in ethylenediamine (5mL, excess) and refluxed with stirring for 4 hr at ~118°C. The reaction mixture was cooled to room temperature to which water (20mL) was added. The product was then extracted using dichloromethane (3×50mL) and concentrated under high vacuum. Trituration with hexane (2×10mL) removed any remaining ethylenediamine, the sample was again dried. The product was then isolated by column chromatography with dichloromethane:ethanol:ammonia (9:1:0.1) eluent. The product was redissolved in dichloromethane (5mL) and pet. ether (40:60) added dropwise until the product precipitated (~10 drops). This was left to stand at 4°C overnight and filtered with cold pet. ether (40:60) and dried to afford **(11)** (0.12g, 34.9%) m.p. 125-126°C, t.l.c R_f 0.2 (CH_2Cl_2/MeOH 4/1), ν_{max} (KBr) cm

[1]: 3400 (OH), 1670 (C=O), 1230 (C-N); δ_H ($CDCl_3$): 10.3 (1H, bt, N*H*Ar), 8.00 (6H, m, Ar*H*), 4.60 (2H, t, NNCH_2), 4.30 (1H, bs, O*H*), 3.45 (2H, q, CH_2OH), 3.40 (2H, q, CH_2NH), 3.10 (2H, t, CH_2NMe), 3.10 (2H, q, HNCH_2), 2.60 (2H, t, MeNCH_2), 2.25 (3H, s, Me); δ_C ($CDCl_3$): 187.1, 157.7, 140.0, 138.9, 135.0, 133.1, 128.4, 127.9, 122.9, 119.5, 114.6, 113.6, 111.9, 109.8, 59.1, 58.9, 57.3, 48.0, 45.9, 42.3, 41.3; m/z (FAB) 380 $(M+H)^+$; (Found: C, 66.87; H, 6.87; N, 18.18. $C_{21}H_{25}N_5O_2$ requires C, 66.48; H, 6.64; N, 18.46%).

6.4.3a Synthesis of 7-{2-[(methoxycarbonylmethyl)amino]ethylamino}-2-{2-[*N*-(2-hydroxyethyl)-*N*-methylamino]ethyl}anthra[1,9-*c,d*]pyrazol-6(*2H*)-one (13).

(11) (0.42g, 1.11mmol) and methyl chloroacetate (0.14g, 1.33mmol) was dissolved in DMF (1.0mL) and stirred at room temperature for 24 hr under nitrogen. After which DMF was removed *in vacuo*. Column chromatography was carried out using dichloromethane:methanol (9.5:0.5 → 8:2) to elute the purified product derivative **(13)** (0.15g, 28.6%) m.p. 80-81°C, t.l.c R_f 0.3 (CH_2Cl_2/MeOH/NH_3 9/1/2drops), ν_{max} (KBr) cm^{-1}: 3400 (OH), 1670 (C=O), 1230 (C-N), 1050 (C-O); δ_H (DMSO): 10.2 (1H, bt, *H*NAr), 8.00 (6H, m, Ar*H*), 4.55 (2H, t, NNCH_2), 4.30 (1H, bs, O*H*), 4.10(2H, s, COCH_2NH), 3.60 (3H, s, OCH_3), 3.40 (2H, q, CH_2OH), 3.35 (2H, q, CH_2NH), 3.10 (2H, t, CH_2NMe), 3.15 (2H, q, HNCH_2), 2.60 (2H, t, MeNCH_2), 2.30 (3H, s, Me); δ_C (DMSO): 186.2, 166.9, 152.4, 139.6, 138.7, 135.6, 132.1, 129.4, 126.4, 121.9, 120.2, 115.6, 114.1, 112.4, 110.5, 65.3, 57.3, 54.7, 54.4, 54.3, 52.9, 46.9, 45.4, 43.6; m/z (FAB) 452 $(M+H)^+$; (Found: C, 63.56; H, 6.51; N, 15.90. $C_{24}H_{29}N_5O_4$ requires C, 63.84; H, 6.47; N, 15.51%).

6.4.4 Synthesis of 7-{2-(carboxymethylamino)ethylamino}-2-{2-[*N*-(2-hydroxy ethyl)-*N*-methylamino] ethyl}anthra[1,9-*c,d*]pyrazol-6(*2H*)-one (14).

For the dealkylation of ester, **(13)** (0.02g, 0.044mmol), lithium bromide (0.012g, 0.13mmol) and sodium iodide (6.64mg, 0.044mmol) were dissolved in pyridine (10mL) and refluxed for 9 hr. The pyridine was evaporated and ethanol was added and heated and filtered to remove remaining inorganic material. The residue was further dried leaving behind a crude sample of the title compound.

Analytical data suggested a possible 10% yield. t.l.c R_f 0.3 (CH_2Cl_2/MeOH/NH_3 9/1/2 drops),

6.4.3b Synthesis of 7-(2-Succinamidoethyl)amino-2-{2-[*N*-(2-hydroxyethyl)-*N*-methylamino]ethyl} anthra[1,9-*c,d*]pyrazol-6(*2H*)-one (12).

(11) (0.20g, 0.53mmol) and succinic anhydride (0.063g, 0.63mmol) were suspended in DMF (10mL) and heated to 80°C with stirring for 3 hr. On completion of the reaction DMF was evaporated under vacuum. The solid residue was then taken up in methanol (1mL) and chromatographed with neat methanol (0.12g, 47.5%); m.p. 101-102°C, t.l.c R_f 0.6 (CH_2Cl_2/MeOH/NH_3 9/1/2drops), ν_{max} (KBr) cm^{-1}: 3400 (OH), 1670 (C=O), 1230 (C-N); δ_H (DMSO): 8.50 (1H, bt, *H*NAr), 7.50 (6H, m, Ar*H*), 4.60 (2H, t, NNC*H*2), 4.40 (1H, bs, O*H*), 3.60 (2H, q, CH_2OH), 3.30 (2H, t, CH_2NHAr), 3.20 (2H, t, CH_2CO), 3.0 (2H, t, CH_2CO_2H), 2.90 (2H, t, CH_2NMe), 2.45 (2H, t, HNCH_2), 2.40 (2H, t, MeNCH_2), 2.30 (3H, s, Me); δ_C (DMSO): 186.1, 176.5, 173.8, 153.1, 138.9, 138.5, 135.2, 132.6, 128.4, 126.6, 121.9, 119.4, 115.7, 113.6, 111.9, 109.1, 59.1, 58.8, 57.0, 47.7, 42.5, 41.4, 37.9, 33.8, 33.1; m/z (FAB) 480 $(M+H)^+$; (Found: C, 63.00; H, 5.90; N, 14.58. $C_{25}H_{29}N_5O_5$ requires C, 62.62; H, 6.10, N, 14.60%).

6.5a 1,4-Dichloroanthraquinone (15) via Friedel Craft's Acylation - Synthesis of 2,5- Dichloro-2-benzoylbenzoic Acid.

Phthalic anhydride (7.4g 50mmol), *p*-dichlorobenzene (36.7g, 250mmol) and anhydrous aluminum chloride (20g, 75mmol) were placed in a flask provided with an air condenser at the end of which was attached a calcium chloride tube. It was heated in an oil-bath maintained at 110-120°C until there was no further evolution of hydrogen chloride (4 hr). The black, viscous reaction product, after being cooled to room temperature, was poured into ice water. Concentrated hydrochloric acid (50mL) was added and the mixture was steam distilled to remove excess *p*-dichlorobenzene. The residue in the flask was washed with hot water and digested on the steam-bath with sodium hydroxide 15% (v/w). The digestion mixture was then boiled with charcoal and filtered. The filtrate was made acid with dilute hydrochloric acid. The dichlorobenzoylbenozoic acid was

extracted with ethyl acetate (4×30mL) and dried to afford (3.82g, 27.2%) m.p. 157-159°C, ν_{max} (KBr) cm^{-1}: 3100 (CO_2H), 1670 (C=O), 1500 (Ar), 1230 (C-N); δ_H (DMSO): 7.2-7.8 (7H, m, Ar*H*); δ_C (DMSO): 181.2, 169.0, 155.6, 150.2, 147.9, 147.5, 130.2, 129.8, 128.7, 127.4, 127.0, 125.8, 124.3, 123.7; m/z (FAB) 295 $(M+H)^+$; (Found: C, 56.92; H, 2.35; Cl, 24.46. $C_{14}H_8Cl_2O_3$ requires C, 57.17; H, 2.40; Cl, 24.11%).

6.5b 1,4-Dichloroanthraquinone (15).

2',5'-Dichloro-2-benzylbenoic acid (0.70g, 2.5mmol) and concentrated sulphuric acid (8mL, in excess) were heated together in an oil-bath at 150°C for 4 hr. The reaction mixture, after cooling to room temperature was poured into ice water (200mL) and washed with sodium hydroxide (1M, 600mL) and saturated brine (600mL). It was recrystallised from methanol to give orange-coloured needles (0.51g, 78.5%) m.p. 187-189°C, ν_{max} (KBr) cm^{-1}: 1670 (C=O), 1600 (Ar); δ_H (DMSO): 8.28-8.20 (2H, m, Ar*H*), 7.87-7.80 (2H, m, Ar*H*), 7.53-7.45 (2H, m, Ar*H*); δ_C (DMSO): 159.0, 154.3, 150.9, 148.4, 147.5, 128.9, 127.6; m/z (FAB) 277 $(M+H)^+$; (Found: C, 60.29; H, 2.19; Cl, 25.95. $C_{14}H_6Cl_2O_2$ requires C, 60.68; H, 2.18; Cl, 25.59%).

6.6 Synthesis of 1,4-Dichloroanthraquinone (15) from Leucoquinizarin.

To phosphorous pentachloride (100g, 0.48mol) suspended in 1,1,2,2-tetrachloroethane (65ml) was added leucoquinizarin (20g, 0.083mol). The mixture was heated to reflux with stirring for 27 hr. The mixture was cooled to room temperature using a water-bath. Methanol (50mL) was added slowly in 1-2mL aliquots. Further methanol (25mL) was added in 5mL aliquots. The mixture was allowed to stir overnight and then cooled to -20°C. The yellow solid was filtered, washed with cold methanol, and dried under vacuum to give the hexachloro intermediate product (19.75g, 61.3%). This (9.25g, 0.024mol) was refluxed in 1-pentanol (100ml) for 18 hr with stirring and the solid which separated upon cooling (-20°C) was filtered and washed with ethanol. The ethanol was dried to afford a yellow solid (5.39g, 81.4%). (Found: C, 60.71; H, 2.22; Cl, 25.87. $C_{14}H_6Cl_2O_2$ requires C, 60.68; H, 2.18; Cl, 25.59%).

6.6.1 Synthesis of 5-Chloro-2-{2-[N-(2-hydroxyethyl)amino]ethyl}anthra[1,9-*c,d*]pyrazol-6(*2H*)-one (16).

A mixture of 1,4-dichloroanthraquinone (0.55mg, 2.0mmol), 2-[(2(hydrazinoethyl)amino] ethanol (300mg, 2.5mmol) and triethylamine (0.3mL, 2.67mmol) in acetonitrile-DMF (10mL, 0.6mL) were heated to reflux under positive nitrogen pressure for 15 hr. The reaction mixture was initially cooled to room temperature then stored at ≤5°C overnight. The solid precipitate was collected by filtration with thorough cold methanol washes. Recrystallisation with methanol was carried out to afford analytically pure bright yellow crystals (0.37mg, 55.3%) m.p. 129-130°C, t.l.c R_f 0.2 (CH_2Cl_2/MeOH 1/1), ν_{max} (KBr) cm^{-1}: 3400 (OH), 1670 (C=O), 1250 (C-N); δ_H (DMSO): 8.00 (6H, m, Ar*H*), 4.70 (2H, t, NNCH_2), 4.40 (1H, bt, O*H*), 4.00 (1H, s, N*H*), 3.35 (2H, q, CH_2OH), 3.10 (2H, t, CH_2NH), 2.60 (2H, t, HNCH_2); δ_C (DMSO): 180.8, 137.8, 137.7, 133.7, 132.5, 131.3, 130.1, 128.9, 128.6, 127.7, 123.4, 122.3, 120.6, 117.8, 57.3, 55.2, 53.9, 44.1; m/z (FAB) 342 $(M+H)^+$; (Found: C, 63.01; H, 4.71; Cl, 10.70; N, 11.98. $C_{18}H_{16}ClN_3O_2$ requires C, 63.25; H, 4.72; Cl, 10.37; N, 12.29%).

6.6.2 Synthesis of 5-Chloro-2-{2-[*N*-(2-hydroxyethyl)-*N*-methylamino] ethyl} anthra[1,9-*c,d*]pyrazol-6(*2H*)-one (17).

(16) (0.78g, 2.28mmol) was dissolved in formic acid (2.5mL, excess) and aqueous formaldehyde solution (37%, 1.1mL) and the mixture heated to 100°C for 3.5 hr. The reaction was cooled to room temperature and extracted with chloroform (6mL). The organic layer was discarded. The aqueous phase was basified to pH 12 with NaOH (2% w/v), then extracted with chloroform (4×25mL). The combined chloroform extracts were washed with brine (300mL) and dried to afford an orange oil (0.75g, 92.4%). To obtain the solid hydrochloride form, acetyl chloride (0.2mL, 2.8mmol) was added dropwise to methanol (2.5mL) at 0°C. The resulting solution was added to a solution of the N-methylated APZ derivative (0.75g, 2.11mmol) dissolved in methanol (15mL). A bright yellow precipitate was formed after a few minutes of stirring. Filtration of the reaction afforded bright yellow crystals which were dried under vacuum (0.64g, 77.2%), m.p. 263-265°C, t.l.c R_f 0.6 (CH_2Cl_2/MeOH 1/1), ν_{max} (KBr) cm^{-1}:

3400 (OH), 1670 (C=O), 1030 (C-N); δ_H (DMSO): 8.00 (6H, m, Ar*H*), 4.60 (2H, t, NNCH_2), 3.35 (2H, t, CH_2OH), 2.90 (2H, t, CH_2NMe), 2.40 (2H, t, MeNCH_2), 2.20 (3H, s, Me); δ_C (DMSO): 180.4, 138.0, 136.8, 133.6., 132.5, 130.8, 130.5, 128.6, 128.5, 127.4, 123.1, 122.1, 120.5, 117.9, 59.4, 59.1, 57.1, 48.1, 42.7; m/z (FAB) 356 $(M+H)^+$; (Found: C, 64.50; H, 5.18; Cl, 10.21; N, 11.52. $C_{19}H_{18}ClN_3O_2$ requires C, 64.14; H, 5.10; Cl, 9.96; N, 11.81%).

6.6.3 Synthesis of 5-(2-Aminoethyl)amino-2-{2-[*N*-(2-hydroxyethyl)-*N*-methyl amino]ethyl}anthra[1,9-*c,d*]pyrazol-6(*2H*)-one (18).

The yellow oily product was isolated by column chromatography using dichloromethane:methanol:ammonia (9:1:2 drops). Yield 0.098g, (28%), t.l.c R_f 0.2 (CH_2Cl_2/MeOH 4/1), ν_{max} (KBr) cm^{-1}: 3400 (OH), 1670 (C=O), 1220 (C-N); δ_H ($CDCl_3$): 9.80 (1H, bt, N*H*Ar), 8.00 (6H, m, Ar*H*), 4.50 (2H, t, NNCH_2), 4.10 (1H, bs, O*H*), 3.45 (2H, q, CH_2OH), 3.35 (2H, q, CH_2NH), 3.15 (2H, t, CH_2NMe), 3.00 (2H, q, HNCH_2), 2.55 (2H, t, MeNCH_2), 2.30 (3H, s, Me); δ_C ($CDCl_3$): 183.3, 161.6, 151.0, 138.4, 133.4, 132.1, 130.2, 128.0, 127.5, 123.6, 122.5, 122.7, 118.1, 115.1, 60.2, 58.0, 56.8, 47.5, 45.7, 43.9, 42.5; m/z (FAB) 380 $(M+H)^+$; (Found: C, 66.82; H, 6.50; N, 18.63. $C_{21}H_{25}N_5O_2$ requires C, 66.48; H, 6.64; N, 18.46%).

6.7 Solid Phase Peptide Synthesis.

All the protected amino acid derivative, PyBOP and the resin used were purchased from Novabiochem. Solvents used were of HPLC grade.

Resin:	NovaSyn® P 500 (polyhipe SU)	01-64-0019 (I)
	NovaSyn® TGA	01-64-0040 (II)

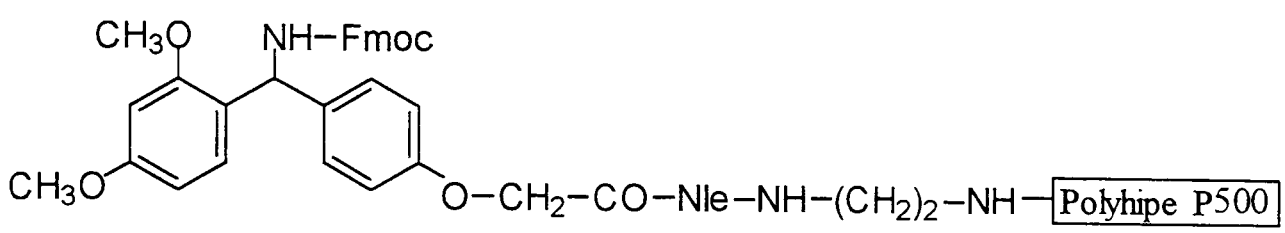

(I)

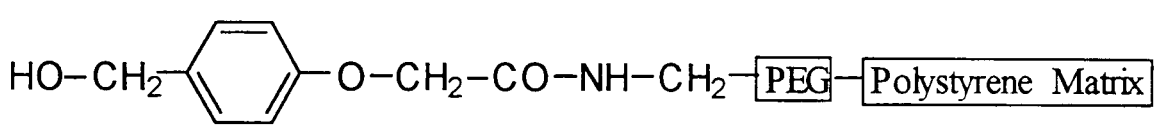

(II)

Protected Amino Acids:	Fmoc-Ala-OH	04-12-1006
	Fmoc-Arg(Pmc)-OH	04-12-1073
	Fmoc-Cys(Trt)-OH	04-12-1018
	Fmoc-Lys(Boc)-OH	04-12-1026

Peptide synthesis was carried out on a Pharmacia-LKB Model 4175.

Ninhydrin (Kaiser) colour Test:

Reagents: ninhydrin (1g) dissolved in ethanol (10mL)

phenol (5g) dissolved in ethanol (1.25mL)

KCN, 2mL of a stock 0.001M solution diluted to 100mL with pyridine

6.8 Preparing the Resin.

The dried resin (1g) was weighed and placed in a column along with enough DMF to swell the resin, this took 30 min. Mixing of the DMF with the resin was carried out using a pipette and any 'fines' was allowed to come to the surface and removed using a pipette.

6.8.1 Assembling the Peptide.

The resin (loading potential of 0.14mmol/g) was made ready for acylation by cleaving the initial Fmoc by introducing the resin to 20% (v/v) piperidine:DMF. Each amino acid derivative (4 molar eqv.) was weighed and placed in separate glass vial along with the PyBOP (4 molar eqv.) dissolved in 3 mL DMF and *N,N*-diisopropylethylamine (8 molar eqv.) added to this mixture. This cocktail was then immediately loaded onto the waiting column containing the free primary amine. The acylation reaction was left for between 2 to 5 hr (see table 11) depending on the amino acid residue. Complete acylation was determined by carrying out the Kaiser test.

Table 11: Reactants and times for peptide assembly.

Acyl Amino acid	Amount (mg)	PyBOC (mg)	N, N-DIPA (μL)	Acylation (hr)
Fmoc-Lys(Boc)-OH	262.4	291.4	195	2
Fmoc-Cys(Trt)-OH	328.0	291.4	195	2
Fmoc-Arg(Pmc)-OH	340.9	291.4	195	3
Fmoc-Ala-OH	174.4	291.4	195	4

6.8.2 Ninhydrin (Kaiser) Colour Test.

A sample (5-10 mg) was removed at the end of the wash period following deprotection, and transferred to a small sintered glass funnel. The resin was then washed with DMF, ethanol, acetic acid, ethanol, DMF and ether, the resin being agitated throughout with a spatula. Some resin beads (10-20) from the funnel was transferred to a test tube and 2-3 drops of the above reagents (section 7.7) were added. The tube was then heated to 120°C for 5 min. Complete acylation was indicated by the test solution remaining a straw-yellow colour with no colouration of the beads.

For the second pentapeptide the resin used was of polyhipe with an amine instead of an acid terminus. Table 12 shows the quantity used for each acyl amino acid residue. The ratio of the components present was 1:4:4:8 (resin:amino acid residue:PyBOP:base). The loading potential of the resin being 0.36mmol/g.

Table 12: Reactants and times of peptide assembly.

Acyl Amino acid	Amount (mg)	PyBOP (mg)	N, N-DIPA (μL)	Acylation (hr)
Fmoc-Lys(Boc)-OH	674.6	749.2	501.7	2
Fmoc-Cys(Trt)-OH	843.4	749.2	501.7	2
Fmoc-Arg(Pmc)-OH	876.5	749.2	501.7	3
Fmoc-Ala-OH	448.3	749.2	501.7	4

The peptide resin was stored at -80°C ready for coupling onto the intercalator.

6.8.3 Coupling of the Peptide to the Intercalator - Removal of N-terminal Fmoc-group.

The peptide resin was placed in a round-bottom-flask with sufficient 20% (v/v) piperidine in DMF to cover the resin. This was stirred at room temperature for 30 min. The peptide resin was then placed in a sintered glass funnel *in vacuo* and washed with DMF, dichloromethane and ether. The resin was removed and dry under high vacuum for 4 hr.

6.8.4 Attaching the Intercalator to the Peptide.

The resin was placed in a r.b.f with DMF along with the drug mixture (the ratio of each component being resin:intercalator:PyBOP:base ; 1:4:4:8). This was stirred under nitrogen for 3-4 hr. On completion, the resin was transferred to a glass sintered funnel under reduced pressure and washed as before, and then dried *under vacuo*.

6.8.5 Cleavage from the Resin.

An appropriate cleavage cocktail was prepared as listed below.

92.5 % Trifluoroacetic acid (TFA)

2.5% 1,2-Ethanediothiol (EDT)

2.5% Triisopropylsylane (TIS)

2.5% Water

The amount added to the resin was 10-25 mL/g and allowed to stand at room temperature with occasional stirring for 2-4 hr. The peptide-intercalator complex was then filtered through a sintered funnel under reduced pressure, and washing twice with small volumes of TFA. Dropwise addition of 8-10 fold volume of cold ether caused precipitation to occur overnight at 4°C. The precipitated peptide/intercalator was filtered using a fine sintered glass funnel under low vacuum. The intercalator-peptide compound was further washed with cold ether and dried *in vacuo*.

6.9 Biological Evaluation.

Materials and Methods

Preparation of (mini) polyacrylamide gels

A 40% stock solution of acrylamide was made up as follows:

acrylamide	38g
N,N'-methylenebisacylamide	2g
Water	100ml

TBE buffer (see below) was made up and stored as a 10× stock solution. The pH of the buffer was approximately 8.3.

10× TBE:

890mM Tris-borate

890mM boric acid

20mM EDTA (pH8.0)

10% Ammonium persulphate was also prepared

ammonium persulphate 1g

H_2O to 10ml

The solution was stored at 4°C for no more than a week.

The glass plates, inner (11cm×7cm) and outer (11cm×9cm) were prepared by washing with water then ethanol and allowed to air dry. The two spacers (0.5mm) were held in place by plastic holders and held in the vertical position by aid of a gel caster.

In all cases mini gels were prepared using the following components indicated below;

10× TBE	2ml
40% (19:1) acylamide mix	3ml
TEMED	8µl
ammonium persulphate (10%)	200µl
water	to 20ml

TEMED (*N,N,N',N'*-tetramethylethylenediamine) acts as a catalyst for the polymerisation of polyacrylamide gels.

The gel constituents were mixed gently and poured between the glass plates. An appropriate comb was quickly inserted, being careful not to allow air bubbles to become trapped under the teeth. The acrylamide was then allowed to polymerise for 60 minutes at room temperature, after which a schlieren pattern was visible just beneath the teeth of the comb. The comb was carefully removed and the wells immediately rinsed out with the 0.5× TBE buffer already present in the reservoirs of the electrophoretic tank. This prevented small amounts of acrylamide solution trapped by the comb from polymerising in the wells, producing irregularly shaped surfaces that would give rise to distorted bands of DNA.

The gel was pre-electrophoresed (30 minutes) in order to remove any poorly polymerised acrylamide monomer and avoid the formation of a "salt-front". For the mini gels a constant voltage of 100V was supplied giving a current of 25mA.

6.10 DNA "end-labelling" using γ-[^{32}P]ATP - Phosphorylation Reaction.

The following reaction mixture was assembled in a sterile microcentrifuge tube:

consensus oligonucleotide	2µl
T4 Polynucleotide Kinase 10× buffer	1µl
[γ-^{32}P]ATP (3 000Ci/mmol at 10mCi/ml)	1µl
Nuclease-free water	5µl
T4 Polynucleotide Kinase (5-10u/µl)	1µl
total volume	10µl

The combined mixture was then incubated at 37°C for 10 minutes, and 1µl of 0.5M EDTA was added to stop the reaction.

6.10.1 Removal of Unincorporated label fragments by using "spin"-columns.

The labelling reaction from above was added to the top of a G50-Sephadex - packed 1ml syringe 'spin - column' along with 100µl of 1×TE. The tip of spin-

column was then placed within a microcentrifuge tube. Both the column and microcentrifuge tube were placed in a Red-cap and centrifuged at 400×g for 2 minutes. Depending on the amount of incorporated DNA eluted, a further 100µl 1×TE was added to the top of the spin-column and repeat centrifugation as in the previous step.

1×TE

1mM EDTA

0.06% PEG

10mM Tris

6.10.2 Determination of Percentage Incorporation.

1µl of the labelled primer was spotted onto each of four Whatmann DE812.3cm circular filter. Two filters were dried under a heat lamp. The other two were used for the direct determination of total cpm in the sample. The first of the dried set of two was then washed in 50ml of 0.5M Na_2HPO_4, pH6.8, twice for 5 minutes each, to remove the unincorporated label. These were dried under a heat lamp. All four filters were placed into individual vials, followed by the addition of scintillation fluid (5ml). These were then counted in a scintillation counter.

The average cpm for the total and incorporated filters was calculated as follows

$$\text{Percentage incorporation} = \frac{\text{cpm incorporated}}{\text{cpm total}} \times 100$$

Typically, 30-50% or more of the radioactivity was incorporated in the 5' end-labelling reaction.

6.10.3 Ethanol precipitation.

DNA precipitation was carried out by the addition of one-quarter volume ammonium acetate (5M, pH5.6) and two volumes of 100% ethanol. The mixture was stored at -20°C overnight. After centrifugation at 12 000 ×g for 20 minutes, the supernatant was discarded and the pellet washed with 70% ethanol and then dried *in vacuo* for 2-3 hr. The DNA pellet was then resuspended in 100µl of

water. A repeat scintillation count on 1µl of the oligonucleotide solution was undertaken (counts of 50 000-200 000cpm/µl were typically obtained). Labelled oligonucleotide probes were stored at -20°C.

Gel Shift Retardation Assays -

6.11 Effect of Dithiothreitol (DTT).

The following reaction components were assembled in a sterile microcentrifuge tube:

Nuclease-Free Water	5µl
Gel Shift Binding (×5) Buffer*	2µl
C-Jun Homodimer (0.55µg/µl)	1µl
DTT (0.5mM)	1µl
^{32}P-labelled DNA (SP-1/AP-1 consensus oligo) (typically 0.0011MBq/0.03µCi)*	1µl
total volume	10µl

* GSB contained the following; glycerol 20%, MgCl2 5mM, EDTA 2.5mM, NaCl 250mM, Tris-HCl, pH 7.5, 0.05mM, poly(dI-dC)·poly(dI-dC) 0.05mg/ml.

* this represents 50 000 - 200 000cpm/µl

Each reaction was incubated at room temperature for 10 minutes before adding 1µl of ^{32}P-labelled DNA probe followed by a further incubation at room temperature for 20 minutes. Loading-dye (×5) 2µl (two parts 50% glycerol: one part 0.1% bromophenol blue) was added to the binding assay. Loaded on to designated wells on gel. Electrophoresed (100V, 25mA), typically until lower-band of loading-dye reached the bottom of the gel.

On completion (60-90 minutes) the gel-kit was dis-assembled, and the glass plates sandwiching the gel carefully separated, leaving the gel on a single glass plate. The exposed gel was then overlaid with Whatmann 3MM paper tailored to fit the gel, ensuring an even contact between gel and paper. The paper was then

peeled off to which the gel adhered. Saranwrap was then overlaid on the exposed side of the gel. The paper/gel/saranwrap sandwich was transfered to the gel-dryer with the saranwrap side up and vacuum dried at 80°C for upto 2 hr.

The dried gel was then subjected to autoradiography at -70°C with an intensifying screen.

6.11.1 Effect of TPA on AP-1 Protein.

The following reaction components were assembled in a sterile microcentrifuge tube:

Nuclease-Free Water	5µl
Gel Shift Binding (×5) Buffer	2µl
Protein Cell Extract* (0.18µg/µl)*	1µl
DTT (0.5mM)	1µl
^{32}P-labelled AP-1 Consensus Oligo	1µl
total volume	10µl

* five MDA 468 breast cancer cell lines prepared as described by Dignam *et al*, 1983 at Nottingham University by Dr. S. Wrigley.

* total protein concentration was estimated by the Bradford assay to be 0.18µg/µl. The actual Fos and Jun protein present was estimated to be 0.204mg/ml using SDS-page.

The procedure for running this gel was similar to that described above.

6.11.2 Determination of AP-1 binding to wild-type and mutant AP-1 DNA consensus sequence.

The following reaction components were assembled in a sterile microcentrifuge tube:

Nuclease-Free Water	5µl
Gel Shift Binding (×5) Buffer	2µl
C-Jun Homodimer (0.55µg/µl)	1µl

DTT (0.5mM)	1µl
^{32}P-labelled DNA (wild type/mutant AP-1 consensus oligo)	1µl
total volume	10µl

The remaining procedure was as described in section 6.11.

6.11.3 Specificity of c-Jun homodimer protein for AP-1 DNA consensus sequence as demonstrated by Competition assay.

The following reaction components were assembled in sterile microcentrifuge tubes as outlined in the table below:

Lane on gel	1	2	3	4	5	6	7	8	9	10
Nuclease-Free Water	8	7	6	5	4	3	2	1	0	8
Gel Shift Binding Buffer (×5)	2	2	2	2	2	2	2	2	2	2
C-Jun Homodimer (0.55µg/µl)	1	1	1	1	1	1	1	1	1	1
DTT (0.5mM)	1	1	1	1	1	1	1	1	1	1
^{32}P-labelled AP1 oligo	1	1	1	1	1	1	1	1	1	1
unlabelled AP-1 or SP-1 oligo*	0	1	2	3	4	5	6	7	8	0
total volume	13	13	13	13	13	13	13	13	13	13

* depending on which competition assay (either with increasing concentration of unlabelled AP-1 or SP-1), the unlabelled oligomer was added and then incubated for 20 min before subsequent addition of the ^{32}P-labelled AP-1 DNA.

The gel was dried and developed as described in section 6.11.

6.11.4 Supershift assay for AP-1 in HeLa nuclear extract.

The following reaction components were assembled in a sterile microcentrifuge tube:

Nuclease-Free Water	4μl
Gel Shift Binding (×5) Buffer	2μl
Nuclear HeLa Extract (1.67μg/μl)	1μl
DTT (0.5mM)	1μl
AP1 Antibody/IGg (100ng/μl)	1μl
^{32}P-labelled DNA (AP-1 oligo)	1μl
total volume	10μl

AP-1 antibody (1μl) was added subsequent to the addition of ^{32}P-laballed AP-1 DNA. The incubation was for 40 minutes at room temperature. The running of the gel was also extended to 3 hr. The procedure for developing the gel was as described in section 6.11.

6.11.5 Effect of Oxygenation on the binding of AP-1 Protein to AP-1 DNA consensus sequence.

AP-1 (Fos/Jun) heterodimer protein (100μl) was placed in two separate sterile microcentrifuge tubes in which two fine glass capillaries were submerged into the liquid. Oxygen or nitrogen gas was then passed through the glass capillary to gas the respective samples while keeping the temperature at 4°C. 3μl of each sample was removed after 3 or 6 hr.

The following was then assembled in sterile microcentrifuge tubes;

Nuclease-Free Water	6μl
Gel Shift Binding (×5) Buffer	2μl
AP-1 (Fos/Jun) heterodimer	1μl
^{32}P-labelled DNA (AP-1 oligo)	1μl
total volume	10μl

The protein samples were then loaded onto the gel and electrophoresed. The gel was dried and exposed to film.

6.12 The Effect of Intercalators on the binding of AP-1 protein to AP-1 DNA consensus sequence.

For each intercalator tested (see table 6) a stock solution was made up using nuclease-free water or in some cases with 5-10% methanol to aid solubility, in a volumetric flask. The final methanol concentration in the reaction was between 0.5-1%.

The following reaction components were assembled in sterile microcentrifuge tubes as outlined in the table below:

Lane on gel	1	2	3	4	5	6	7	8	9	10
Nuclease-Free Water	6.0	4.75	4.5	4.25	4.0	3.75	3.50	3.25	3.0	6.0
Gel Shift Binding Buffer (×5)	2.0	2.0	2.0	2.0	2.0	2.0	2.0	2.0	2.0	2.0
Nuclear HeLa Extract (1.67μg/μl)	1.0	1.0	1.0	1.0	1.0	1.0	1.0	1.0	1.0	1.0
DTT (0.5mM	1.0	1.0	1.0	1.0	1.0	1.0	1.0	1.0	1.0	1.0
^{32}P-labelled AP-1 DNA	1.0	1.0	1.0	1.0	1.0	1.0	1.0	1.0	1.0	1.0
Intercalator*	0	0.25	0.5	0.75	1.0	1.25	1.5	1.75	2.0	0
total volume	10.0	10.0	10.0	10.0	10.0	10.0	10.0	10.0	10.0	10.(

* a stock solution was made up for each intercalator at 8.4×10^{-6} M so that by adding the amount shown in the table, a ratio ranging from 100:1 through to 800:1 (increasing by 100-fold intercalator:DNA) was achieved.

6.12.1 The Effect of Peptides on the binding AP-1 protein to AP-1 DNA consensus sequence.

The procedure carried out here was exactly the same as that with the intercalator.

The following reaction components were assembled in sterile microcentrifuge tubes as outlined in the table below:

Lane on gel	1	2	3	4	5	6	7	8	9	
Nuclease-Free Water	6.0	4.75	4.5	4.25	4.0	3.75	3.50	3.25	3.0	
Gel Shift Binding Buffer (×5)	2.0	2.0	2.0	2.0	2.0	2.0	2.0	2.0	2.0	
Nuclear HeLa Extract (1.67μg/μl)	1.0	1.0	1.0	1.0	1.0	1.0	1.0	1.0	1.0	
DTT (×10)	1.0	1.0	1.0	1.0	1.0	1.0	1.0	1.0	1.0	
^{32}P-labelled AP-1 DNA	1.0	1.0	1.0	1.0	1.0	1.0	1.0	1.0	1.0	
Peptide Fragment*	0	0.25	0.5	0.75	1.0	1.25	1.5	1.75	2.0	
total volume	10.0	10.0	10.0	10.0	10.0	10.0	10.0	10.0	10.0	

*methanol was also used to aid in the solubility of the peptide. Stock solution of concentration 8.4×10^{-5} M was prepared and so by adding the amount shown in the table of the peptide solution a ratio of peptide:DNA ranging from 1000:1 - 8000:1 (increasing by 1000-fold) was achieved.

6.12.2 The Effect of Intercalator-peptide Conjugates on the binding of AP-1 protein to AP-1 DNA consensus sequence.

Again a similar procedure to the two described above for the intercalator and peptide was carried out. However with the hybrid compounds, two separate stocks were prepared for each hybrid molecule giving a lower and an upper range of drug concentration, i.e. 8.4×10^{-6} M and 8.4×10^{-5} M respectively. (see table below and figure 50 and 51).

Lane on gel	1	2	3	4	5	6	7	8	9	10
Nuclease-Free Water	4.5	5.0	4.0	5.0	3.5	5.0	3.0	5.0	2.5	5.(
Gel Shift Binding Buffer (×5)	2.0	2.0	2.0	2.0	2.0	2.0	2.0	2.0	2.0	2.(
Nuclear HeLa Extract (1.67μg/μl)	1.0	1.0	1.0	1.0	1.0	1.0	1.0	1.0	1.0	1.(
DTT	1.0	1.0	1.0	1.0	1.0	1.0	1.0	1.0	1.0	1.(
^{32}P-labelled AP-1 DNA	1.0	1.0	1.0	1.0	1.0	1.0	1.0	1.0	1.0	1.(
Intercalator	0.5	0	1.0	0	1.5	0	2.0	0	2.5	0

linked Peptide*										
total volume	10.0	10.0	10.0	10.0	10.0	10.0	10.0	10.0	10.0	10

* two separate stocks were prepared one at the lower drug concentration range of 200-800:1 (conjugate:DNA) increasing by 200-fold. And at an upper concentration range of 2000-8000:1 (conjugate:DNA) increasing by 2000-fold.

The gels were developed as described before.

6.13 Specificity of Intercalator-Peptide Conjugates for the AP-1 DNA consensus sequence.

Reaction components were assembled in sterile microcentrifuge tubes as outlined in the table below:

Lane on gel	1	2	3	4	5	6	7	8	9
Nuclease-Free Water	6.0	4.75	4.5	4.25	4.0	3.75	3.50	3.25	3.0
Gel Shift Binding Buffer (×5)	2.0	2.0	2.0	2.0	2.0	2.0	2.0	2.0	2.0
Protein*	1.0	1.0	1.0	1.0	1.0	1.0	1.0	1.0	1.0
DTT (0.5mM)	1.0	1.0	1.0	1.0	1.0	1.0	1.0	1.0	1.0
^{32}P-labelled AP-1 or SP-1 DNA	1.0	1.0	1.0	1.0	1.0	1.0	1.0	1.0	1.0
Conjugate **4a***	0	0.25	0.5	0.75	1.0	1.25	1.5	1.75	2.0
total volume	10.0	10.0	10.0	10.0	10.0	10.0	10.0	10.0	10.0

* The relative molecular weights of AP-1 (94 kDa, 0.204mg/ml) and SP-1 (201 kDa, 0.035mg/ml) and c-Jun homodimer (78 kDa, 0.155mg/ml) were used to calculate the concentrations of proteins added. The AP-1 heterodimer protein was diluted 12.5 fold using a lysis buffer provided. c-Jun homodimer protein was diluted by ~11 fold.

* a stock solution of each conjugate at 8.4×10^{-6} M was prepared.

The reaction mixtures were then loaded onto the gel and electrophoresed.

6.13.1 Protein estimation using the Bradford Method.

Bradford reagent: Coomassie Brillant Blue G-250 (10mg) dissolved in 5ml of 95% ethanol. Add 10ml of 85% (w/v) phosphoric acid. Dilute to 500ml with water. Bovine serum albumin (BSA) was used as the protein standard. A stock solution of the BSA was prepared using the same storage buffer as the protein sample being tested. The concentration of the BSA protein was so that it 0.1-1mg/ml (total volume 20µl). The protein samples being analysed were then added to separate wells to which 180µl of the Bradford reagent was then added. The absorbance was measured at 630nm using a spectrophotometer. The concentration of the protein sample was determined from the plot of [BSA] against the absorbance.

6.13.2 Quantitating the [Fos] and [Jun] proteins in cell lysates using SDS-Page - Preparing the gel.

The gel used for this particular purpose was a discontinuous gel. The bottom half of the gel, the resolving gel (12%) was prepared as follows:

acrylamide:bis (30:0.8)	4.00ml
Tris-HCl pH8.8 3M	1.25ml
Water	4.55ml

To which the following was then added 100µl of 10% SDS, 100µl of fresh 10% ammonium persulphate and 5µl of TEMED. The gel was then gently mixed and poured between to glass plates and overlayed with propanol/water. The gel was allowed to polymerise for 20 minutes.

The stacking gel (the top half of the gel) was prepared as follows:

acrylamide:bis (30:0.8)	0.40ml
Tris-HCl pH6.8 0.5M	0.75ml
Water	1.80ml

To which, 30µl of 10% SDS, 30µl of fresh 10% ammonium persulphate and 3µl of TEMED was then added. The propanol/water layer was removed and the gel rinsed 2-3 times with water. The stacking gel was then poured on top to which a comb was then fixed. The gel was then allowed to set (1 hr).

6.13.3 Preparing the protein molecular weight markers.

The following components were found in each vial of protein standard.

	µg/vial	Subunit MW
Phosphorylase b	64	94 000
Bovine Serum Albumin	83	67 000
Ovalbumin	147	43 000
Carbonic Anhydrase	83	30 000
Soybean Trypsin Inhibitor	88	20 000
α-Lactalbumin	121	14 400
Sucrose	27mg	

The protein standards were then dissolved in 100µl water:100µl sample buffer (2×) and boiled for 2 minutes.

Sample buffer (2×): Tris-HCl pH6.8 0.125M
SDS 4%
glycerol 20%
2-mercaptoethanol 10%

5µl of the above protein solution was then further diluted by ten fold using sample buffer (1×). This was then pipetted into four microcentrifuge tube to give 2, 5, 10 and 15µl all of which were then diluted to 15µl, again with the sample buffer (1×). Next 5µl of each of the five different cell extracts (containing the Fos and Jun proteins) were placed in five microcentrifuge tubes to which 5µl of the sample buffer (2×) was added. All ten tubes were then placed in boiling water for 5 minutes.

6.13.4 Running the SDS gel.

Loading buffer (2×) was added to each of the ten samples before loading onto the gel. The gel was allow to run in Tris, glycine and SDS for ~1 hr at 150V. The run was stopped when the blue band (loading dye) reached the bottom of the gel. The apparatus was then disassembled and the isolated gel was submerged in coomassie blue for 5 minutes on a shaker. The excess dye was

then removed by placing the gel in a destain (10% methanol:10% acetic acid) for 1-2 hr on a shaker. Clearer bands were obtained on leaving it overnight.

The intensity of the Fos and Jun bands were then compared with the that of the protein standard. An estimate of the concentration of Fos and Jun protein was calculated.

6.14 DNA Binding Assays.

Materials

Calf thymus DNA was obtained from Sigma Chemical Company, London. All glass apparatus used in this work was silanised with Repelcote (Hopkins and Williams), washed twice with methanol (Fisons, HPLC grade) and dried overnight at room temperature before use. All volumetric glassware was of grade A specification. Volumes between ≤ 1ml were measured using Hamilton precision glass syringes. All drugs solutions were protected from light and stored at 4°C prior to use. Unless otherwise stated Tris buffer (pH 7.40, Tris Cl 0.008M, NaCl, 0.05M) was used throughout this next part of the work.

Methods

6.14.1 Effect of Intercalator-Peptide Conjugates on Thermal Denaturation properties of DNA.

A solution of an appropriate concentration of drug in buffer, and water (6.0mL) were added to a 10mL volumetric flask and the solution sonicated for 15mins to remove dissolved air.

DNA solution (Calf thymus), approximately 2.5×10^{-3} M in buffer, (precisely 0.2mL), was added to the contents of the flask, the solution made to volume with water, and mixed gently (final DNA:drug ratio of exactly 10:1). The solution (2.0mL) was placed in a quartz cuvette with a ground glass stopper. The cuvette was placed in an Peltier cell holder of a Perkin Elmer 552S Spectrophotometer fitted with a temperature programmer. The absorbance of the

solution at 260nm was recorded as the temperature was raised from 55 to 105°C (0.5°C/min). This was duplicated and the mean Tm calculated.

The mean Tm of DNA in the absence of drug in the same buffer was subtracted to give the ΔTm value.

6.14.2 Effect of Intercalator-Peptide Conjugates on the Fluorescence Enhancement of ethidium bromide bound to DNA.

A solution of drug (2.0×10^{-6} M) in tris buffer was prepared, two further solutions containing DNA (2.0×10^{-5}M) and DNA and drug (2.0×10^{-5} M and 2.0×10^{-6} M respectively) were prepared. Buffer (precisely 3ml) was places in one cuvette and the same volume of each of the above solutions were placed in three separate cuvettes; buffer and drug solutions acting as controls. The cuvettes were placed in a thermostatted cell holder of a Perkin Elmer LS5 spectrofluorimeter and fluorescence intensities, (λ excitation, 476nm, λ emission, 596nm), of solutions were determined at 25°C. Aliquots, (6×10μl, 5×20μl, 6×40μl, and 6×100μl), of ethidium solution (2.0×10^{-5} M) were sequentially added to each of the four cuvettes and readings taken after mixing and allowing to stand for 1 min. Fluorescence intensities were corrected for changes in volume.

REFERENCES

Abate, C. *et al* (1990a). *Science* **249**:1157-1161.
Redox regulation of fos and jun DNA-binding activity *in vitro*.

Abate, C. *et al* (1990b). *Cell Growth Differ.* **1**:455-462.
A ubiquitous nuclear protein stimulates the DNA-binding activity of fos and jun indirectly.

Agre, P. *et al* (1989). *Science* **246**:922-926.
Cognate DNA binding specificity retained after leucine zipper exchange between GCN4 and C/EBP.

Albericio, F. and Barany, G. (1990). *Int. J. Pept. Prot. Res.* **30**:206-216.
An acid-labile anchoring linkage for solid-phase synthesis of C-terminal peptide amides under mild conditions.

Angel, P. *et al* (1987). *Cell* **49**:729-739.
Phorbol ester-inducible genes contain a common *cis* element recognised by a TPA-modulated transacting factor.

Atherton, E. and Sheppard, R. C. (1989). In *Solid phase peptide synthesis: a practical approach.* IRL Press, Oxford, England.

Atherton, E. *et al* (1979). *Bioorg. Chem.* **8**:351-370.
The polyamide method of solid phase peptide and oligonucleotide synthesis.

Atherton, E. *et al* (1985). *J. Chem. Soc., Perkin Trans. 1*, 2057.
Peptide synthesis. Part 6. Protection of the sulphydryl groups of cysteine in solid-phase synthesis using Nα-fluorenylmethoxycarbonylamino acids. Linear oxytocin derivatives.

Aukerman, M. L. *et al* (1991). *Genes Dev.* **5**:310-320.
An arginine to lysine substitution in the bZIP domain of an *opaque*-2 mutant in maize abolishes specific DNA binding.

Ausserer, W. A. *et al* (1994). *Mol. Cell. Biol.* **14**:5032-5042.
Regulation of *c-jun* expression during hypoxic and low-glucose stress.

Bailly, C. and Henichart, J.-P. (1991). *Bioconjugate Chem.* **2**(6):379-393.
DNA recognition by intercalator-minor-groove binder hybrid molecules.

Barber, J. R. and Verma, I. M. (1987). *Mol. Cell. Biol.* 7(6):2201-2211.
Modification of *fos* proteins: Phosphorylation of *c-fos*, but not *v-fos*, is stimulated by 12-tetradecanoyl-phorbol-13-acetate and serum.

Beavis, R. C. *et al* (1992). *Org. Mass Spectrom.* **27**:156-158.
α-Cyano-4-hydroxycinnamic acid as a matrix for matrix-assisted laser desorption mass spectrometry.

Berge, J. M. (1990). *J. Biol. chem.* **265**(12):6513-6516.
Zinc fingers and other metal-binding domains. Elements for interactions between macromolecules.

Beylin, V. G. *et al* (1989). *J. Heterocyclic Chem.* **26**:85-94.
Anticancer anthrapyrazoles. Improved synthesis of clinical agents CI-939, CI-941, and piroxantrone hydrochloride.

Blake, A. and Peacock, A. R. (1968). *Biopolymers* **6**:1225-1229.
The interaction of amino acridines with nucleic acids.

Bohmann, D. *et al* (1987). *Science* **238**:1386-1392.
Human proto-oncogene *c-jun* encodes a DNA binding protein with structural and functional properties of transcription factor AP-1.

Bos, T. J. *et al* (1988). *Cell* **52**:705-712.

v-jun encodes a nuclear protein with enhancer binding properties of AP-1.
Bresloff, J. L. and Crothers, D. M. (1981). *Biochemistry* **20**:3547-3555.
Equilibrium studies of ethidium-polynucleotide interactions.
Briggs, M. R. *et al* (1986). *Science* **234**:47-52.
Purification and biochemical characterisation of the promoter-specific transcription factor, SP-1.
Brindle, P. K. and Montminy, M. R. (1992). *Curr. Opin. Genet. Deve.* **2**:199-204.
The CREB family of transcription activators.
Bush, S. J. and Sassone-Corsi, P. (1990). *Trends Genet.* **6**(2):36-40.
Dimers, leucine zippers and DNA-binding domains.
Chen, K.-X. *et al* (1987). *Anti-cancer Drug Des.* **2**:79-84.
Theoretical study of the intercalative binding of the antitumour drug anthrapyrazole to double-stranded oligonucleotides.
Chen, K.-X. *et al* (1985). *J. Biomolecular Struct. Dyns.* **3**(3):445-466.
A theoretical investigation on the sequence selective binding of daunomycin to double-stranded polynucleotides.
Chuang, L. F. *et al* (1984). *J. Biol. Chem.* **259**(18):11391-11395.
Inhibition of the initiation of leukaemic transcription by *N*-trifluoroacetyladriamycin-14-*O*-hemiadipate *in vitro*.
Chui, R. *et al* (1988). *Cell* **54**:552.
The c-FOS protein interacts with c-Jun/AP-1 to stimulate transrciption of AP-1 responsive genes.
Chothia, C. (1984). *Ann. Rev. Biochem.* **53**:537-572.
Principles that determine the structure of proteins.
Chothia, C. and Finkelstein, A. V. (1990). *Ann. Rev. Biochem.* **59**:1007-1039.
The classification and origins of protein folding patterns.
Cohen, D. R. and Curran, T. (1988). *Mol. Cell. Biol.* **8**:2063-2069.
fra-1: a serum-inducible, cellular immediate-early gene that encodes a fos-related antigen.
Cohen, D. R. and Curran, T. (1990). *Oncogene* **5**:929-939.
Analysis of dimerisation and DNA binding functions Fos and Jun by domain-swapping; involvement of residues outside the leucine zipper/basic region.
Creighton, T. E. (1983). In *Proteins: structure and molecular properties*. Edited by Freeman, W. H.
Curran, T. and Teich, N. M. (1982). *Virology* **116**:221-235.
Viral and cellular *fos* proteins are complexed with a 39,000-dalton cellular protein.
Curran, T. *et al* (1985). *Mol. Cell. Biol.* **5**:167-172.
Identification of a 39,000-dalton in cells tranformed by the FBJ murine osteosarcoma virus.
Curran, T. *et al* (1987). *Oncogene* **2**:79-84.
Isolation and characterisation of the *c-fos* (rat) c-DNA and analysis of post-translational modification *in vitro*.
Dasgupta, D. and Goldberg, I. H. (1986) *Nucleic Acids Res.* **14**:1089-1105.
Mode of reversible binding of neocarzinostatin chromophore to DNA-base sequence dependency of binding.
Dervan, P. B. (1986). *Science* **232**:464-471.
Design of sequence-specific DNA-binding molecules.
Dignam, J. D. *et al* (1983). *Nucleic Acids Res.* **11**:1475-1489.

Accurate transcription initiation by RNA polymerase II in a soluble extract from isolated mammalian nuclei.

Distel, R. J. *et al* (1987). *Cell* **49**:835-844.
Nucleoprotein complexes that regulate gene expression in adipocyte differentiation: direct participation of c-Fos.

Doglia, S. *et al* (1983). *Eur. J. Biochem.* **133**:179-186.
Binding of ethidium bromide of self-complementary deoxydinucleotides.

Dryland, A. and Sheppard, R. C. (1986). *J. Chem. Soc. Perkin Trans.*, 1. 125-137.
Peptide synthesis. Part 8. A system for solid-phase synthesis under low pressure continuous flow conditions.

Farrell, P. J. *et al* (1989). *EMBO. J.* **8**(1):127-132.
Epstein-Barr virus BZF1 *trans*-activator specifically binds to a consensus AP-1 site and is related to fos.

Fersht, A. R. (1987). *Trends biochem. Sci.* **12**:301-304.
The hydrogen bond in molecular recognition.

Flock, S. *et al* (1994). *J. Biomolecular Struct. Dyns.* **11**(4):881-900.
Interaction of two peptide-acridine conjugates containing the SPKK motif with DNA and chromatin.

Foye, W. O. *et al* (1982). *J. Pharm. Sci.* **71**:253-257.
DNA-binding specificity and RNA polymerase inhibiting activity of bis(aminoalkyl)anthraquinones and bis(methylthio)vinylquinolinium iodides.

Fox, M. E. and Smith, P.J. (1990). *Can. Res.* **50**:5813-5818.
Long-term inhibition of DNA synthesis and persistence of trapped topoisomerase II complexes in determining the toxicity of the antitumour DNA intercalators mAMSA and mitoxantrone.

Franza Jr, B. R. J. *et al* (1988). *Science* **239**:1150-1153.
The Fos complex and Fos-related antigens recognise sequence elements that contain AP-1 binding sites.

Franza Jr. B. R. J. *et al* (1987). *Oncogene* **1**:213-221.
Analysis of Fos protein complexes and Fos-related antigens by high-resolution two-dimensional gel electrophoresis.

Frederick, C. A. *et al* (1990). *Biochemistry* **29**:2538-2549.
Structural comparison of anticancer drug-DNA complexes: adriamycin and daunomycin.

Freemont, P. S. *et al* (1991). *Biochem. J.* **278**:1-23.
Structural aspects of protein-DNA recognition.

Fried, M. G. (1989). *Electrophoresis* **10**:366-376.
Measurement of protein-DNA interaction parameters by electrophoresis mobility shift assay.

Fry, D. W. (1991). *Pharmac. Ther.* **52**:109-125.
Biochemical pharmacology of anthracenediones and anthrapyrazoles.

Gandecha, B. M. 1985 Thesis.
Development of potential antitumour agents based on a consideration of the mode of action and pharmacokinetics of daunomycin and adriamycin.

Gartenberg, M. R. (1990). *Pro. Natl. Acad. Sci. USA.* **87**:6034-6038.
Molecular characterisation of the GCN4-DNA complex.

Gentz, R. *et al* (1989). *Science* **243**:1695-1699.
Parallel association of Fos and Jun leucine zippers juxtaposes DNA binding domains.

Gilbert, D. E. and Feigon, J. (1991). *Curr. Opinion Struct. Biol.* **2**:439-445.
Structural analysis of drug-DNA interactions.
Gonzalez, G. A. *et al* (1989). *Nature* **337**:749-752.
A cluster of phosphorylation sites on the cyclic AMP-regulated nuclear factor CREB predicted by its sequence.
Gross, K. H. and Kalbitzer, H. R. (1988). *J. Magn. Reson.* **76**:87-99.
Distribution of chemical-shift in H^1 nuclear magnetic-resonance spectra of proteins.
Hai, T. and curran, T. (1991). *Proc. Natl. Acad. Sci. USA* **88:**3720-3724.
Cross-family dimerisation of transcription factors Fos/Jun and ATF/CREB alters DNA binding specificity.
Halazonetis, T. D. *et al* (1988), *Cell* **55**:917-924.
c-Jun dimerises with itself and with c-Fos, forming complexes of different DNA binding affinities.
Hartley, J. A. *et al* (1988). *Mol. Pharmacol.* **33**:265-271.
Characterisation of the interaction of anthrapyrazole anticancer agents with deoxyribonucleotide acids: Structural requirements for DNA binding, intercalation and photosensitisation.
Hattori, K. *et al* (1988). *Proc. Natl. Acad. Sci. USA* 85:9148-9152.
Structure and chromosomal location of the functional intronless human *JUN* protocogene.
Hendrickson, W. (1985). *BioTechniques* **3**:198-207.
Protein-DNA interactions studied by gel electrophoresis-DNA binding assay.
Hennighausen, L. and Lubon, H. (1987). *Methods. Enyzmol.* **152**:721-735.
Interaction of protein with DNA *in vivo*.
Hill, D. E. *et al* (1986). *Science* **234**:451-457.
Saturation mutagensis of the yeast *his3* regulatory site: requirements for transcriptional induction and for binding by GCN4 activator protein.
Hillenkamp, F. and Karas, M. (1990). *Methods Enzymol.* **193**:280-295.
Spectrometry of peptides and proteins by matrix-assisted ultraviolet laser desorption/ionisation.
Hinnebusch, A. G. (1986). *Crit. Rev. Biochem.* **21**(3):277-317.
The general control of amino acid biosynthesis genes in the yeast *Saccharomyces cerevisae*.
Hoeffler, J. P. *et al* (1988). *Science* **242**:1430-1433.
Cyclic AMP-responsive DNA-binding protein: structure based on a cloned pacental cDNA.
Hoeffier, J. P. *et al* (1991). *Mol. Endocrinol.* **5**:256-266.
identification of multiple nuclear factors that interact with cyclic adenosine 3',5'-monophosphate response element-binding protein and activating transcription factor-2 by protein-protein interactions.
Hope, I. A. and Struhl, K. (1986). *Cell* **46**:885-894.
Functional activation of eukaryotic transcriptiona; activator protein, GCN4 of yeast.
Hope, I. A. and Struhl, K. (1987). *EMBO J.* **6**(9):2781-2784.
GCN4, a eukaryotic transcriptional activator protein, binds as a dimer to target DNA.
Horton, N. and Lewis, M. (1992). *Protein Science* **1**:169-181.
Calculation of the free energy of association for protein complexes.
Hurst, H. C. *et al* (1990). *Mol. Cell. biol.* **10**(12):6192-6203.

The cellular transcription factor CREB corrsponds to activating transcription factor 47 (ATF-47) and forms complexes with a group of polypeptides related to ATF-43.

T. Ijaz (1998). PhD Thesis DeMontfort University, Leicester.
Anthraquinone cysteinyl peptides as inhibitors of AP-1 transcription factor binding.

Johnson, P. F. and Mcknight, S. L. (1989). *Annu. Rev. Biochem.* **58**:799-839.
Eukaryotic transcriptional regulatory proteins.

Jones, N. (1990). *Cell* **61**:9-11.
Transcriptional regulation by dimerisation: two sides to an incestuous relationship.

Jones, N. C. *et al* (1988). *Genes Dev.* **2**:267-281.
Trans-acting protein factors and the regulation of eukaryotic gene expression: lessons from studies on DNA tumour viruses.

Kadonaga, J. T. *et al* (1987). *Cell* **51**:1079-1090.
Isolation of cDNA encoding transcription factor SP-1 and functional analysis of the DNA binding domain.

Kaiser, E. *et al* (1970). *Analyst. Biochem.* **84**:595-601.
Monitoring of solid-phase peptide synthesis by the ninhydrin reaction.

Kapuscinski, J. and Darzynkiewicz, Z. (1985). *Biochem. Pharmacol.* **34**:4203-4213.
Interactions of antitumour agents ametantrone and mitoxantrone (Novatrone) with double-stranded DNA.

Karas, M. *et al* (1990). *Anal. Chim. Acta* **241**:175-185.
Principles and applications of matrix-assisted UV-laser desorption/ionisation mass specrometry.

Katagiri, F. *et al* (1989). *Nature* **340**:727-730.
Two tobacco DNA-binding proteins with homology to the nuclear factor CREB.

Kerpolla, T. K. and Curran, T. (1991). *Curr. Opin. Struct. Biol.* **1**(1):71-79.
Transcription factor interactions: basics on zipper.

Kim, B. and Little, J. W. (1992). *Science* **255**:203-206.
Dimerisation of a specific DNA-binding protein on the DNA.

Kouzarides, T. and Ziff, E. (1988). *Nature* **366**:646-651.
The role of leucine zipper in the fos-jun interaction.

Kouzarides, T. and Ziff, E. (1989a). *Nature* **340**:568-571.
Leucine zippers of fos, jun and GCN4 dictate dimerisation specificity and thereby control DNA binding.

Krapcho, P.A. and Gretahun, Z. (1985). *Syn. Commun.* **15**(10):907-910.
Convenient synthetic routes to 1,4-difluoroanthracene-9,10-dione.

Kristie, T. M. and Roizman, B. (1986) *Pro. Natl. Acad. Sci. USA* **83**:3218-32222.
α4, the major regulatory protein of herpes simplex virus type 1, is stably and specifically associated with promoter-regulatory domains of α genes and of selected other viral genes.

Lamph, W. W. *et al* (1988) *Nature* **334**:629-631.
Induction of proto-oncogene Jun/AP-1 by serum and TPA.

Landschulz, W. H. *et al* (1988). *Genes Dev.* **2**:786-800.
Isolating a recombinant copy of the gene encoding C/EBP.

Landschulz, W. H. *et al* (1989). *Science* **243**: 1681-1688.
The DNA binding domain of the rat liver nuclear protein C/EBP is bipartite.

Laughton, A. (1991). *Biochemistry* **30**(48):11357-11367.

DNA binding specificity of homodomains.
Lee, W. (1987). *Cell* **49**: 741-752.
Purified transcription factor AP-1 interacts with TPA-inducible enhancer elements.
Le Pecq, J. B. and Paoletti, C. (1967). *J. Mol. Biol.* **27**:87-106.
A fluorescence complex between ethidium bromide and nucleic acids.
Lerman, L. S. (1961). *J. Mol. Biol.* **3**:18-25.
Structural considerations in the interaction of DNA and acridines.
Liaw, Y. C. *et al* (1989). *Biochemistry* **28**:9913.
Antitumour drug nogalamycin binds DNA in both grooves simultaneously: molecular structure of nogalamycin-DNA complex.
Lown, J. W. *et al* (1985). *J. Biomolecular Struct. Dyns.* **2**(6):1097-1106.
High field ^{1}H-NMR analysis of the 1:1 interaction complex of the antitumour agent mitoxantrone and the DNA duplex $[d(CpGpCpGp)]_2$.
Lucibello, F. C. *et al* (1988). *Oncogene* **3**: 43-51.
Transactivation of gene expression by fos protein: involvement of a binding site for the transcription factor AP-1.
Maekawa, T. *et al* (1991). *EMBO. J.* **8**(9):2032-2028
Leucine zipper structure of the protein CRE-BP1 binding to the cyclic AMP response element in brain.
Maki, Y. *et al* (1987). *Proc. Natl. Acad. Sci. USA* **84**:2848-2852.
Avian sarcoma virus 17 carries the *jun* oncogene.
Maldonado, E. *et al* (1990). *Molec. Cell. Biol.* **10**:6335-6347.
Factors involved in specific transcription by mammalian RNA polymerase-II.
Merrifield, R. B. (1963). *J. Am. Chem. Soc.* **85**:2149-2154.
Solid phase peptide synthesis. 1. The synthesis of a tetrapeptide.
Mock, K. K. *et al* (1992). *Rapid Commun. Mass Spectrom.* **6**:233-238.
Sample immobilsation protocols for matrix-assisted laser-desorption mass spectrometry.
Moye-Rowley, W. S. *et al* (1989) *Genes Dev.* **3**:283-292.
Yeast *YAP1* encodes a novel form of the Jun family of transcriptional activator proteins.
Molder, H. *et al* (1987) *Oncogene* **1**:377-383.
Isolation and strucural analysis of a biologically active chicken *c-fos* cDNA: identification of evolutionarily conserved domains in fos protein.
Mouscadet, J.-F. *et al* (1994). *Biochemistry* **33**:4187-4196.
Triple helix formation with short oligonucleotide-intercalator conjugates matching the HIV-1 U3 LTR end sequence.
Muller, R. (1986). *Biochem. Biophys. Acta* **823**:207-255.
Cellular and viral *fos* genes ; structure, regulation of expression and biological properties of their encoded products.
Muller, W. and Crothers, D. M. (1968). *J. Mol. Biol.* **35**:251-290.
Studies on the binding of actinomycin and related compounds to DNA.
Nakabeppu, Y. *et al* (1988). *Cell* **55**:907-915.
DNA binding activities of three murine Jun protein: stimulation by fos.
Neidle, S. and Berman, H. M. (1983). *Prog. Biophys. Mol. Biol.* **41**:43-49.
X-ray crystallographic studies of nucleic acids and nucleic acid-DNA complexes.

Neidle, S. *et al* (1987). *Biochem. J.* **243**:1-13.
DNA structure and perturbation by drug binding.
Neidle, S. (1978). In *Topics in Antibiotic Chemistry*, p240.
Edited Sammes, P. G., pulished by Horwood, E, Chichester.
Neilsen, P. E. (1991). *Bioconjugate Chem.* **2**(1):1-12.
Sequence-selective DNA recognition by synthetic ligands.
Neuberg, M. *et al* (1989). *Nature* **338**:589-590.
A Fos protein containing a Jun leucine zipper forms a homodimer which binds to the AP1 binding site.
Niles, M. and Brunger, A. T. (1991). *Protein Eng.* **4**(6):649-659.
Automated modelling of coiled-coils: application to the GCN4 dimerisation region.
Nishimura, T. and Vogt, P. K. (1989). *Oncogene* **3**:659-663.
The avian cellular homolog of the oncogene *jun*.
Node, M. *et al* (1981). *J. Org. Chem.* **46**:1991-1993.
Hard acid and soft nucleophile systems. 3. Dealkylation of esters with aluminium halide-thiol and aluminium halide-sulfide systems.
Noggle, J. H. and Schirmer R.H. (1971). In *The nuclear overhauser effect, chemical application*. New York:Academic.
Oakley, M. G. *et al* (1992). *Biochemistry* **31**:10969-10975.
Evident that a minor groove-binding peptide and a major groove-binding protein can simultaneously occupy a common site on DNA.
O'Neil, K. T. *et al* (1990). *Science* **249**:774-778.
Design of DNA-binding peptides based on the leucine zipper motif.
O'Neil, K. T. *et al* (1991). *Biochemistry* **30**:9030-9034.
DNA-induced increase in the α-helical content of C/EBP and GCN4.
O'Shea, E. K. *et al* (1989a). *Science* **243**:538-542.
Evidence that the leucine zipper is a coiled-coil.
O'Shea, E. K. *et al* (1989b). *Science* **245**: 646-648.
Preferential heterodimer formation by isolated leucine zippers from Fos and Jun.
Paluh, J. L. *et al* (1988). *Pro. Natl. Acad. Sci. USA* **85**:3728-3732.
The cross-pathway control gene of *Neurospora crassa*, cpc-1, encodes a protein similar to GCN4 of yeast and the DNA binding domain of the oncogene *v-jun* encoded protein.
Pardi, A *et al* (1983) *Eur. J. Biochem.* **137**:445-454.
Protein conformation and proton nuclear-magnetic-resonance chemical shift.
Park, C. *et al* (1992). *Pro. Natl. Acad. Sci. USA* **89**:9094-9096.
Protein stitchery: design of a protein for selective binding to a specific DNA sequence.
Patel, L. *et al* (1990). *Nature* **347**:572-575.
Altered conformation on DNA binding by Fos and Jun.
Patterson, L. H. and Newell, D. R. (1994). *Anticancer Drug-DNA interactions*, vol. **2**, p96-129. Editors Neidle, S. and Waring, J. "Cellular and molecular pharmacology of anthrapyrazole antitumour agents."
Pearson, D. A. *et al* (1989). *Tetrahedron Letters* **30**(21):2739-2742.
Trialkysilanes as scavengers for the trifluoroacetate acid deblocking of protecting groups in peptide synthesis.
Peterson, M. G. *et al* (1990). *Science* **248**:1625-1630.

Functional domains and upstream activation properties of cloned human TATA binding protein.

Phillips, M. (1926). *J. Am. Chem. Soc.* **48**:3198-3199.
The preparation of 1,4-dichloroanthraquinone from phthalic anhydride and para-dichlorobenzene.

Piette, J. and Yaniv, M. (1987). *EMBO J.* **6**:1331-1337.
Two different factors bind to the α-domains of the polyoma virus enhancer, one of which also interacts with the SV40 and *c-fos* enhancers.

Puge, K. *et al* (1992). *Int. J. Pept. Prot. Res.* **40**:208-213.
Effects of resin swelling and substitution on solid-phase synthesis.

Pu, W. T. and Struhl, K. (1991). *Proc. Natl. Acad. Sci. USA* **88**:6901-6905.
The leucine zipper symmetrically positions adjacent basic regions for DNA binding.

Quigley, G. J. *et al* (1980). *Pro. Natl. Acad. Sci.USA* 77:7204-7208.
Molecular structure of an anticancer drug-DNA complex: Daunomycin plus d(CpGpTpApCpG).

Ramage, R. and Green, J. (1987). *Tetrahedron Letters* **28**(20):2287-2290.
N_G-2,2,5,7,8-pentamethylchroman-6-sulphonyl-L-arginine: A new acid labile derivative for peptide synthesis.

Ransone, L. J. *et al* (1989). *Genes Dev.* **3**:770-781.
Fos-Jun interaction: mutational analysis of the leucine zipper domain of both proteins.

Ransone, L. J. *et al* (1990). *Mol. Cell. Biol.* **10**:4565-4573.
Domain swapping reveals the modular nature of fos, jun and CREB proteins.

Rauscher III, R. F. *et al* (1988a). *Genes Dev.* **2**:1687-1699.
Fos and Jun bind cooperatively to the AP-1 site: reconstitution *in vitro*.

Rauscher III, R. F. *et al* (1988b). *Science* **240**:1010-1016.
Fos associated protein p39 is the product of the *jun* proto-oncogene.

Rauscher III, R. F. *et al* (1988c). *Cell* **52**:471-480.
Common DNA binding site for Fos protein complexes and transcription factor AP-1.

Renz, M. *et al* (1987). *Nuc. Acids Res.* **15**:277-292.
Chromatin association and DNA binding properties of the *c-fos* proto-oncogene product.

Risse, G. *et al* (1989).*EMBO J.* **8**:3825-3832.
Asymmetrical recognition of the palindromic AP-1 binding site (TRE) by fos protein complexes.

Rivier, J. *et al* (1984). *J. Chrom.* **288**:303-328.
Reversed-phase high performance liquid chromatography: preparative purification of synthetic peptides.

Ryder, K.*et al* (1988). *Proc. Natl. Acad. Sci. USA* **85**:1487-1491.
A gene activated by growth factors is related to the oncogene *v-jun*.

Ryder, K.*et al* (1989). *Proc. Natl. Acad. Sci. USA* **86**:1500-1503.
Jun-D: a third member of the *Jun* family.

Ryseck, R.-P. *et al* (1988). *Nature* **334**:535-537.
Transcriptional activation of *c-jun* during the G_0/G_1 transition in mouse fibroblasts.

Seanger, W. (1984). *Principles of Nucleic Acid Structure*.

Edited by Cantor, C. R. Springer Advanced Texts in Chemistry. Springer- Verlag, New York, Berlin, Heidelberg, Tokyo.

Sambucetti, L. C. and Curran, T. (1986). *Science* **234**:1417-1419.
The fos protein complex is associated with DNA in isolated nuclei and binds to DNA cellulose.

Sarin, V. K. *et al* (1981). *Anal. Biochem.* **117**:147-157.
Quantitative monitoring of solid-phase peptide synthesis by the ninhydrin reaction.

Sassone-Corsi, P. *et al* (1988a). *Cell* **54**:553-560.
fos-associated cellular p39 is related to nuclear transcription factor AP-1

Sassone-Corsi, P. *et al* (1988b). *Nature* **334**:314-319.
Transcriptional autoregulation of the proto-oncogene *fos*.

Saudek, V. *et al* (1991a). *Protein Eng.* **4**(5):519-529.
The solution structure of a leucine-zipper motif peptide.

Saudek, V. *et al* (1991b). *Biochemistry* **30**:1310-1317.
Solution structure of the basic region from the transcriptional activator GCN4.

Schena, M. and Davis, R. W. (1992). *Proc. Natl. Acad. Sci. USA* **89**:3894-3898.
HD-Zip protiens: Members of an *Arabodopis* homeodomain protein superfamily.

Schleif, R. (1988). *Science* **241**:1182-1187.
DNA binding by proteins.

Schmid, R. M. *et al* (1991) *Nature* **352**:733-739.
Cloning of a NF-κB subunit which stimulates HIV transcription in synergy with p65.

Schonthal, A. *et al* (1988). *Cell* **54**:325-334.
Requirement for *fos* gene expression in the transcriptional activation of collagenase by other oncogenes and phorbal esters.

Serfling, E. (1989). *Trends Genet.* **5**(5):131-133.
Autoregulation - a common property of eukaryotic transcription factors.

Setoyama, C. *et al* (1986a). *Proc. Natl. Acad. Sci. USA* **83**:3213-3217.
Transcriptional activation encoded by the *c-fos* gene.

Setoyama, C. *et al* (1986b). *Biochem. Biophys. Res. Commun.* **136**:1042-1048.
Transcriptional activation encoded by *c-fos* gene.

Shapiro, D. J. *et al* (1988). *DNA* 7(1):47-55.
Laboratory methods: A high-efficiency HeLa cell nuclear transcription extract.

Showalter, H. D. H. *et al* (1986a). *Anti-cancer Drug Des.* **1**:73-85.
Design, biochemical pharmacology, electron chemistry and tumour biology of antitumour anthrapyrazoles.

Showalter, H. D. H. *et al* (1986c). *J. Heterocyclic Chem.* **23**:1491-1501.
Heteroannalated-9-10-anthracenediones. The synthesis of substituted 5- and 7-chloro-anthra[1,9-*cd*]pyrazol-6(*2H*)-ones, precursors to anticancer anthrapyrazoles.

Showalter, H. D. H. *et al* (1984). *J. Med. Chem.* **27**:253-255.
5-[(Alkylamino)amino]-substituted anthra[1,9-*cd*]pyrazol-6(*2H*)-ones as novel anticancer agents. Synthesis and biological evaluation.

Showalter, H. D. H. *et al* (1987). *J. Med. Chem.* **30**:121-131.
Anthrapyrazole anticancer agents. Synthesis and structure-activity relationships against murine leukemias.

Showalter, H. D. H. *et al* (1986b). *J. Med. Chem.* **30**:121-131.
Anthrapyrazole anticancer agents. Synthesis and structure-activity relationships against murine leukaemias.
Steitz, T. A. (1990). *Quart. Rev. Biophys.* **23**(3):205-208.
Structural studies of protein-nucleic acid interaction: the source of sequence-specific binding.
Strauss, F. and Varshafsky, F. (1984). *Cell* **37**:889-901.
A protein binds to a satellite DNA repeat at three specific sites that would be brought into mutual proximity by DNA folding in the nucleosome.
Struhl, K. (1987). *Cell* **50**:841-846.
The DNA binding domains of the Jun oncoprotein and the yeast GCN4 transcriptional activator protein are functionally homologous.
Suzuki, M. *et al* (1996). *Adv. Biophys.* **32**:53-72.
DNA conformation and its changes upon binding transcription factors.
Tabor, A. B. (1996). *Tetrahedron* **52**:2229-2234.
Synthesis of a peptide-intercalator hybrid based on the bZIP motif from GCN4.
Tabor, C. W. and Tabor, H. (1984). *Ann. Rev. Biochem.* **53**:749-790.
Polyamines.
Talanian, R. V. *et al* (1992). *Biochemistry* **31**:6871-6875.
Minimum length of a sequence-specific DNA binding peptide.
Talanian, R. V. *et al* (1990). *Science* **249**:769-771.
Sequence specific DNA binding by a short peptide dimer.
Tanious, F. A. (1992). *Biochemistry* **31**:11632-11640.
Substituent position dictates the intercalative DNA-binding mode for anthracene-9,10-dione antitumour drugs.
Takusagawa, F. *et al* (1982). *Nature* **296**:466-469.
The structure of a pseudo intercalated complex between actinomycin and the DNA binding sequence d(GpC).
Thireos, G. *et al* (1984). *Pro. Natl. Acad. Sci. USA* **81**:5096-5100.
5'untranslated regions are required for the translational control of a yeast regulatory gene.
Tong, G. L. *et al* (1979). *J. Med. Chem.* **22**:36-39
5-Iminodaunorubicin. Reduced cardiotoxic properties in an antitumour anthracycline.
Tonrud, D. E. *et al* (1987). *Science* **235**:571-574.
Structures of two thermolysin-inhibitor complexes that differ by a single hydrogen bnd.
Travers, A. A. (1988). "Protein-induced DNA bending" *in* Nucleic Acids and Molecular Biology. Edited by Eckstein, F. and Lilly, D. M. J. Springer-Verlag, Berlin, Heidelberg.
Travers, A. A. (1989). *Ann. Rev. Biochem.* **58**:427-452.
DNA conformation and protein binding.
Travers, A. A. (1990). *Cell* **60**:177-180.
Why bend DNA?
Turner, R. and Tjian, R. (1989). *Science* **243**:1689-1694.
Leucine repeats and an adjacent DNA binding domain mediate the formation of functional cFos-cJun heterodimers.
Ughetto, G. *et al* (1985). *Nucleic Acid Res.* **13**:2305-2323.

A comparison of the structure of echinomycin and triostin A complexed to a DNA fragement.

Van Beveren, C. *et al* (1983). *Cell* **32**:1241-1255.
Analysis of FBJ-MuS provirus and *c-fos* (mouse) gene reveals that viral and cellular *fos* gene products have different carboxy termini.

Van Straaten, F. *et al* (1983). *Pro. Natl. Acad. Sci. USA* **80**:3183-3187.
Complete nucleotide sequence of a human *c-onc* gene: Deduced amino acid sequence of the human *c-fos* gene.

Varshavsky, A. (1987). *Methods Enyzmol.* **151**:551-565.
Electrophoretic assay for DNA-binding proteins.

Verma, I. M. (1986). *Trends Genet.* **2**:92-96.
Proto-oncogene fos: a multifaceted gene.

Vinson, C. R. *et al* (1989). *Science* **246**:911-916.
Scissors-grip model for DNA recognition by a family of leucine zipper proteins.

Vogt, P. K. *et al* (1987). *Proc. Natl. Acad. Sci. USA* **84**:3316-3319.
Homology between the DNA-binding domains of the GCN4 regulatory protein of yeast and the carboyxl-terminal region of a protein coded for by the oncogene *jun*.

von Hippel, P. H. and Berg, O. G. (1989). "DNA-protein interactions in the regulation of gene expression" pp.1-18 *in* Protein-Nucleic Acid Interactions.

Wang, A. H. J. *et al* (1984). *Science* **225**:1115-1121.
The molecular structure of a DNA-triostin A complex.

Wang, J.C. (1974). *J. Mol. Biol.* **89**:783-789.
The degree of unwinding of the DNA helix by ethidium.

Waring, M. J. and Bailly, C. (1994). *J. Mol. Recognition* 7:109:122.
DNA recognition by intercalators and hybrid molecules.

Waring, M. J. (1981). In *Molecular Basis of Drug Action*, p258.
Edited Gale, E. F., Cundcliffe, E., Reynolds, P. E., Richmond, M. H. R. and Waring, M. J. Pulished by John Wiley and Sons (London).

Weiss, M. (1990). *Biochemistry* **29**:8020-8024.
Thermal unfolding studies of a leucine zipper domain and its specific DNA complex: implication for scissor's grip recognition.

White, F. H. (1967). *Methods Enzymol.* **11**:481-485.
Reduction and reoxidation of disulfide bonds.

Widom, J. (1985). *Bioassays* **2**(1):11-14.
Bent DNA for gene regulation and DNA packaging.

Wilson, W. D. and Jones, R. L. (1981). *Adv. Pharmacol. Chemother.* **18**:177-182.
Intercalating drugs: DNA binding and molecular pharmacology.

Winkler, G. (1987). LC/GC 5(12):1044-1045.
Increasing the senitivity of UV detection in protein and peptide separations when using TFA-acetonitrile gradients.

Wuthrich, K. (1990). *J. Biol. Chem.* **265**(36):22059-22062.
Protein structure determination in solution by NMR spectroscopy.

Xanthoudakis, S. and Curran, T. (1992a). *Methods Enzymol.* **234**:163-174.
Analysis of c-fos and c-jun redox-dependent DNA binding activity.

Xanthoudakis, S. *et al* (1992b).*EMBO J.* **11**:3323-3335.
Redox activation of fos-jun DNA binding activity is mediated by a DNA repair enzyme.

Xanthoudakis, S. and Curran, T. (1992c).*EMBO J.* **11**:653-665.

Identification and characterisation of ref-1, a nuclear protein that facilitates AP-1 DNA-binding avtivity.

Xanthoudakis, S. *et al* (1994). *Pro. Natl. Acad. Sci. USA* **91**:23-27.
The redox activation and DNA-repair activaties of ref-1 are encoded ny non-overlapping domains.

Yao,K.-S. *et al* (1994). *Mol. Cell. Biol.* **14**:5997-6003.
Activation of AP-1 and of a nuclear redox factor, ref-1, in the response of HT29 colon cancer cells to hypoxia.

Yielding, L.W. *et al* (1984) *Biopolymers* **23**:83-110.
Ethidium binding to deoxyribonucleotide acid: Spectrophotometric analysis of analogs with amino, azido, and hydrogen substituents.

Zerial, M. *et al* (1989). *EMBO. J.* **8**(3):805-813.
The product of a novel growth factor activated gene, *fos B*, interacts with JUN enhancing their DNA binding activity.

Zunino, F. *et al* (1972). *Biochim. Biophys. Acta.* **277**:489-498.
Interaction of daunomycin and its derivatives with DNA.